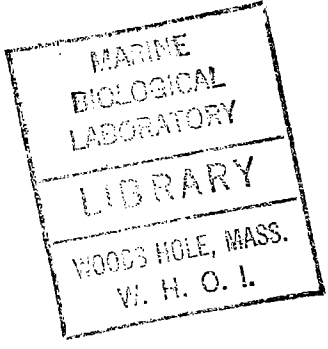


GC
7.4
B54
1977

1.



THE CHEMISTRY, BIOLOGY, AND
VERTICAL FLUX OF OCEANIC
PARTICULATE MATTER

by

JAMES KENNETH BRANSON BISHOP

B.Sc., University of British Columbia, CANADA

(1971)

SUBMITTED IN PARTIAL FULFILLMENT OF THE
REQUIREMENTS FOR THE DEGREE OF
DOCTOR OF SCIENCE

at the

MASSACHUSETTS INSTITUTE OF TECHNOLOGY

AND THE

WOODS HOLE OCEANOGRAPHIC INSTITUTION

January, 1977

Signature of Author..... *Jim Bishop*
Joint Program in Oceanography, Massachusetts
Institute of Technology - Woods Hole Oceanographic
Institution, and Department of Earth and Planetary
Sciences, Massachusetts Institute of Technology
January, 1977
Certified by..... *McDonald*
Thesis Supervisor
Accepted by..... *McDonald*
Chairman, Joint Oceanography Committee in the
Earth Sciences, Massachusetts Institute of
Technology - Woods Hole Oceanographic Institution

THE CHEMISTRY, BIOLOGY, AND VERTICAL FLUX OF OCEANIC PARTICULATE MATTER

by

JAMES KENNETH BRANSON BISHOP

Submitted to the Massachusetts Institute of
Technology - Woods Hole Oceanographic Institution
Joint Program in Oceanography on January 13, 1977,
in partial fulfillment of the requirements
for the degree of Doctor of Science.

ABSTRACT

Particulate matter samples, split into $<1 \mu\text{m}$, $1-53 \mu\text{m}$, and $>53 \mu\text{m}$ size fractions have been obtained using a Large Volume in situ Filtration System (LVFS) during the SOUTHLANT expedition, R/V CHAIN 115. Profiles to 400 m are reported for LVFS Stns. 2 and 4-8. Stns. 4, 5, and 8 (S.E. Atlantic, coastal waters near Walvis Bay and Cape Town, high biological productivity); Stns. 6 and 2 (S.E. Atlantic, Walvis Bay region and equatorial Atlantic, moderate productivity; and Sta. 7 (S.E. Atlantic, edge of central gyre, low productivity) formed a suite of samples for the study of the chemical, biological, morphological distributions and of the vertical mass flux of particulate matter as a function of biological productivity.

All samples were analysed for Na, K, Mg, Ca, carbonate, opal, Sr, C and N and those from Sta. 2 were further analysed for P, Fe, $\delta^{13}\text{C}$, ^7Be , ^{214}Bi , ^{214}Pb , (^{226}Ra), ^{210}Po , and ^{210}Pb . Biological distributions of Acantharia, dinoflagellates, coccolithophorids, Foraminifera, diatoms, silicoflagellates, Radiolaria, and tintinnids were made by light microscopy (LM) and augmented by scanning electron microscopy (SEM). Size and morphological distributions of the $>53 \mu\text{m}$ particles, especially Foraminifera, Acantharia, fecal pellets, and fecal matter have been determined by LM and SEM.

The particle distributions were controlled at all stations by processes of production, consumption, fragmentation, and aggregation. Maxima in organism abundance and particulate mass were generally coincident. They were found nearest the surface when the mixed layer was absent or poorly developed, and at the base of the mixed layer at the other stations.

Organism vertical distributions showed consistent features: Acantharia, and dinoflagellates were always nearest the surface; Foraminifera and diatoms were shallower than or at the base of the mixed layer; Radiolaria and tintinnids were found in the upper thermocline. Coccolithophorids and diatoms were the dominant sources of particulate carbonate and opal in the near surface waters, coccoliths and diatom fragments, deeper.

Features of the distributions of particulate matter attributed to the feeding activities of zooplankton were: strong concentration gradients in organisms, mass, and organic matter; enrichment of the $>53 \mu\text{m}$ fraction with coccoliths causing the steady decrease in $>53 \mu\text{m}$ Si/carbonate ratio with depth from values as high as 45 to values near 1.0 at 400 m; the decrease in organic content with depth from values near 100 % near the surface to 50 and 60 % at 400 m for the <53 and $>53 \mu\text{m}$ size fractions;

the fragmentation of most material below 100 m; and the production of fecal pellets and fecal matter which are carriers of fine material to the sea floor.

Other features were: the nearly constant organic C/N ratios ($7.3 \pm 0.5 \sigma$) found for the 1-53 μ m fractions at Stns. 4, 5, 6, and 8 compared with the steady increase observed at Stns. 2 and 7 with depth; particulate carbon was rather uniformly distributed below 200 m with concentrations showing a mild reflection of surface productivity; the $<1 \mu$ m C/N and $\delta^{13}\text{C}$ values are lower and lighter than the 1-53 μ m fraction, perhaps indicative of the presence of marine bacteria; the Ca/carbonate ratios in most samples significantly exceeded 1.0, values as high as 2.5 were observed at Sta. 8; the xs Ca and K have shallow regenerative cycles and contrast with Mg which is bound to a refractory component of organic matter; based on a organic C/ xs Ca ratio of 100-200:1 for surface samples, the cycling of xs Ca was calculated to be $1-2 \times 10^{13} \text{ mol/cm}^2/\text{y}$ compared with the production of carbonate, $7 \pm 2 \times 10^{13} \text{ mol/cm}^2/\text{y}$.

Chemical effects noted were: organic matter had both binding capabilities and ion-exchange capacity for major and minor ions present in seawater. Acantharia (SrSO_4) dissolve most significantly below 200 m at Sta. 2.

The vertical mass fluxes through 400 m at Stas. 2, 5, 6, and 7 were calculated from size distributions measured in 1 m^3 in seawater for Foraminifera, fecal pellets, and fecal matter. Two flux models were used together with Junge distributions for these calculations. Fecal matter and Foraminifera transported most mass at Stns. 2 and 5 where the fluxes were between 2 and 3, and 5 and 6 $\text{gm/cm}^2/1000\text{y}$ respectively; fecal matter, Foraminifera, and fecal pellets contributed equally to the .9-1.3 $\text{gm/cm}^2/1000\text{y}$ flux at Sta. 6; and fecal pellets and Foraminifera were the carriers of 0.1-0.3 $\text{gm/cm}^2/1000\text{y}$ to the sea floor. Corresponding chemical fluxes of organic carbon, carbonate, and opal were: 80-90, 11-24, and 10 $\text{mmol/cm}^2/1000\text{y}$ at Sta. 5; 15-20, 2.7-5.0 and 1.7-2.5 $\text{mmol/cm}^2/1000\text{y}$ at Sta. 6; 1-4, 0.6-1.5, and 0.1-0.3 $\text{mmol/cm}^2/1000\text{y}$ at Sta. 7, and 40-65, 4.6-7.4, and 4.9-7.9 $\text{mmol/cm}^2/1000\text{y}$ at station 2. Over 90% of the organic matter produced in the euphotic zone is recycled in the upper 400 m. The efficiency is nearly 99% in areas of low productivity; the organic to carbonate carbon ratios are highest at locations where the flux is greatest as are the Si/carbonate ratios. Besides carbonate, opal, celestite, and other mineral phases, organic matter may be a significant carrier of minor and trace elements to the deep ocean.

THESIS SUPERVISOR: Professor John M. Edmond, M.I.T.

1979-10-10

DEDICATION

To my father and my mother

ACKNOWLEDGEMENTS

Above all I would like to thank John Edmond for his energy and patient guidance during my tenure as a graduate student. I greatly appreciate the substantial resources made available to me for this research.

Derek Spencer, Susumo Honjo and Pierre Biscaye are thanked for being constructive and encouraging advisors.

Peter Brewer and Werner Deuser have both generously provided comments, assistance, and the use of their laboratories at Woods Hole.

Michael Bacon and Wyatt Silker analysed Station 2 samples for ^{210}Pb and ^{210}Po and for ^7Be , ^{214}Bi and ^{214}Pb . They are thanked for their important contribution to Chapter 2.

Special thanks are due to Darlene Ketten who has done much of the biological analyses reported throughout this thesis. She has maintained her enthusiasm in the face of a collection of physical and inorganic chemists.

I have benefited from discussions with Ed Boyle, Michael Bender and Fred Sayles. Robert Stallard, Amy Ng, David Drummond, Bob and Pat Collier, and Russ McDuff are thanked for being friends and for their assistance while at sea.

Many people have helped with the development, construction and deployment of the LVFS. Special thanks

are due to Cliff Winget of the Alvin group; Don LeBlank and Charlie Peterson of the instrument shop; Bobbie Weeks of the marine facility at W.H.O.I.; and Drs. Geoffrey Thompson, Colin Summerhayes, and Jack Corliss (Chief Scientists); Captains Babbit, Palmeri, and Phinney and the crews and scientific parties of the research vessels Atlantis II, Chain, and Melville.

Pam Thompson drafted most of the figures in Chapter 2 and Ruth Christensian of M.I.T. Graphic Arts did the figures in Chapters 3 and 4.

Dorothy Frank did a superb job of typing this thesis. Mary Lou LeClair and Maureen Hayes have kindly parted with their typewriters at crucial times during the preparation of this thesis.

The good spirits and friendship of Vincent Korkus, Bobby Ciccarello, and Charles Wainwright were especially appreciated during the 11 to 7 shift in the Green Building.

My friends Theodore Kuklinski, Doris Taam, John Willet, Mark Kurz, Don Levinstone, Julie Crowley, and Fung have greatly helped either directly or indirectly in the production of this thesis and have helped make life at M.I.T. an enjoyable experience.

This work was supported by contract N00014-75-C0291 from the Office of Naval Research and by the Doherty Foundation.

TABLE OF CONTENTS

	page no.
TITLE PAGE	1.
ABSTRACT	2.
DEDICATION	4.
ACKNOWLEDGEMENTS	5.
TABLE OF CONTENTS	7.
LIST OF FIGURES	8.
LIST OF PLATES	13.
LIST OF TABLES	14.
NOTE ON REFERENCES	16.
CHAPTER 1 - Introduction	17.
CHAPTER 2 - The Chemistry, Biology, and Vertical Flux of Particulate Matter from the Upper 400 m of the Atlantic Ocean	21.
CHAPTER 3 - The Chemistry, Biology, and Vertical Flux of Particulate Matter from the Upper 400 m of the Cape Basin in the S.E. Atlantic Ocean	134.
CHAPTER 4 The Distribution of Particulate Matter collected by Large Volume in situ Filtration to 1500 m in the Equatorial Pacific Ocean	237.
APPENDIX 0 Particulate data for LVFS Stn. 1	251.
APPENDIX 1 Particulate data for LVFS Stns. 4-8	254.
APPENDIX 2 Hydrographic Data from Chain 115 leg 2	278.
BIOGRAPHICAL NOTE	292.

LIST OF FIGURES

	page no.
Figure 2-1. Hydrography of upper 500 m at CHAIN 115-2 LVFS Station 2.	38
Figure 2-2. Graphic reproduction of 12 KHz PGR record obtained during the station.	40
Figure 2-3. Upper: Particulate dry weight profiles of <53 μ m and >53 μ m size fractions. Lower: Plankton distributions showing maxima at the depth of the particle maximum.	44
Figure 2-4. Upper: C _{org} , N, P profiles for the <1 μ m, 1-53 μ m, and >53 μ m size fractions. Lower: Organic C/N and C/P ratios showing size and depth dependent behavior.	56
Figure 2-5. $\delta^{13}\text{C}_{\text{PDB}}$ profiles for the organic carbon in the three size fractions.	60
Figure 2-6. Upper: Calcium and carbonate in the 1-53 μ m and >53 μ m size fractions showing excess calcium. Lower: Excess magnesium, calcium, and potassium in the two size fractions.	65
Figure 2-7. Ion exchange experiments for calcium, strontium, and potassium.	71
Figure 2-8. Upper: Silicate in >53 μ m fraction and from 0.4 μ m Nuclepore filter samples; total strontium and noncarbonate strontium (Sr*) in >53 μ m and <53 μ m fractions.	80

Lower: Strontium (Sr*), carbonate and silicate ratios in >53 μ m size fraction.

- Figure 2-9. Upper: Particulate iron showing strong correlation with ^{210}Pb . 91.
 Lower: Particulate ^{210}Pb and ^{210}Po , ^{214}Pb and ^{214}Bi , and ^7Be , activities in the three size fractions.
- Figure 2-10. Carbonate per Foraminifera, silicate per Radiolaria and per diatom, non-carbonate strontium per Acantharia, ratios in the >53 μ m size fraction. 104.
- Figure 2-11. Left: Size-frequency distribution of Foraminifera and Foraminifera fragments. 107.
 Right: Size-frequency distribution of fecal matter and fecal pellets.
- Figure 3-1. Station locations for LVFS and hydrographic profiles taken within the Cape Basin. 138.
- Figure 3-2. Bathythermograph records obtained near LVFS Stations 4 and 8. 141.
- Figure 3-3. Temperature and salinity sections for stations near Walvis Bay. 143.
- Figure 3-4. Dissolved oxygen and phosphate sections for stations near Walvis Bay. 144.
- Figure 3-5. Silicate section for the stations near Walvis Bay; Hydrographic data for stations near LVFS Station 8. 145.

Figure 3-6. T-S and Si-S plots for all stations in the Cape Basin.	147.
Figure 3-7. O ₂ -S and PO ₄ -S plots for all stations in the Cape Basin.	148.
Figure 3-8. Distributions of Foraminifera, Acantharia, and Radiolaria for stations near Walvis Bay.	155.
Figure 3-9. Distributions of centrate and solenoid diatoms at LVFS Stns 4-7, >53µm fraction.	157.
Figure 3-10. Distributions of silioflagellates, dinoflagellates and tintinnids at LVFS Stations 4-7.	158.
Figure 3-11. Distributions of organisms at LVFS Stn. 8, near Cape Town.	160.
Figure 3-12. >53 and <53µm particulate dry weight section for LVFS Stns. 4-7.	163.
Figure 3-13. Total dry weight distributions determined by LVFS and Niskin sampling methods.	165.
Figure 3-14. Particulate organic carbon distributions for Stations 4-7.	169.
Figure 3-15. Particulate nitrogen distributions for Stations 4-7.	170.
Figure 3-16. Particulate organic carbon and nitrogen at LVFS Stn. 8.	171.
Figure 3-17. Particulate C _{org} /N ratios for the <1 and 1-53 µm size fractions at LVFS Stns. 2, 4-8.	173.
Figure 3-18. Percentage of dry weight attributable to organic matter in the >53 and <53 m fractions.	175.

- Figure 3-19. >53 μ m particulate excess Ca, K, and Mg sections at LVFS Stns. 4-7. 177.
- Figure 3-20. >53 and <53 μ m particulate carbonate, Si, Sr*, excess Ca, K, and Mg at LVFS Stn.8. 178.
- Figure 3-21. <53 μ m particulate excess Ca and Mg for Stations 4-7. 180.
- Figure 3-22. >53 and <53 μ m ratios of particulate excess cation charge to nitrogen at LVFS Stns. 2 and 4-8. 181.
- Figure 3-23. >53 and <53 μ m particulate carbonate distributions at LVFS Stns. 4-7. 183.
- Figure 3-24. >53 and <53 μ m particulate carbonate distributions at LVFS Stns. 4-7. 186.
- Figure 3-25. >53 μ m total carbonate to total Foraminifera ratio indicating the enrichment of the large particles with coccoliths. (*) indicates the significant contributions of Orbulina Universa to the >53 μ m carbonate. 187.
- Figure 3-26. >53 μ m and Niskin particulate silicate distributions at LVFS Stns. 4-7. The Niskin method is seen to have missed the 52 m maximum at Stn. 6. 192.
- Figure 3-27. >53 and <53 μ m particulate Si/carbonate ratios for Stations 2 and 4-8. 197.
- Figure 3-28. >53 and <53 μ m particulate non-carbonate Sr* distributions. 199.

- Figure 3-29. Foraminifera size and Junge distributions 203.
in 1 m³ samples from 400 m at LVFS Stns. 2, 5-7.
Solid circles indicate Pteropods. >53 μm fraction.
- Figure 3-30. Size and Junge distributions for 204.
fecal pellets in the >53 μm fraction at
LVFS Stns. 2, 5, 6, and 7.
- Figure 3-31. Junge distributions of fecal matter 205.
at LVFS Stns. 2, 5, 6 and 7; result of sinking
experiments with fecal matter.
- Figure 3-32. Cumulative mass fluxes through 400 m 215.
at Stns. 2, 5, 6 and 7 for Foraminifera,
fecal pellets, and fecal matter.
- Figure 3-33. Model settling behavior as a function 216.
of size for Foraminifera, fecal pellets,
and fecal matter.
- Figure 3-34. Mass flux through 400 m as a function 223.
of integrated >53 μm mass ("productivity")
at LVFS Stns. 2, 5, 6 and 7.
- Figure 4-1. Four-filter Large Volume in situ 241.
Filtration System (LVFS-4).
- Figure 4-2. Flow rate versus time for samples to 249.
1500 m.
- Figure 4-3. Particulate mass profile taken by the 250.
LVFS-4.

LIST OF PLATES

- | | |
|---|------|
| Plate 1. Scanning electron micrographs of plankton
sampled by LVFS | 48. |
| Plate 2. Scanning electron micrographs of Acantharia
on 53 μ m filters from 32, 50 and 113 m
showing effects of dissolution | 84. |
| Plate 3. Scanning electron micrographs of Acantharia
on 53 μ m filters from 188, 294 and 388 m
showing effects of dissolution | 86. |
| Plate 4. Scanning electron micrographs of biogenic
debris on 53 μ m filters from various depths | 98. |
| Plate 5. Scanning electron micrographs of biogenic
material on 53 μ m filters from various depths | 100. |

LIST OF TABLES

table no.		Page no.
2-1	Major ion blank levels in Mead 935-BJ glass fiber filters.	26.
2-2	Carbon and Nitrogen uptake by Mead 935-BJ glass fiber filter from Rockport seawater	30.
2-3	Chemical data CHAIN 115-2 LVFS Stn. 2. Upper: >53 μm size fraction analyses Lower: <53 μm size fraction analyses	33.
2-4	Particulate Mass Concentration LVFS Stn. 2 Upper: >53 μm fraction Lower: <53 μm fraction	42.
2-5	Plankton abundances at LVFS Stn. 2. Upper: >53 μm fraction Lower: <53 μm fraction	46.
2-6	Particulate organic C, N, P, and $\delta^{13}\text{C}$ data	52.
2-7	Particulate Ca, carbonate, Mg, K, Si, and Sr at LVFS Stn.2	63.
2-8	Ion Exchange Experiments using 294 m 1-53 μm sample; results for Ca, K, Sr, and Mg.	73.
2-9	Organic C, N, P, cation relationships in particles normalized to 106 atoms of C.	77.
2-10	Particulate Fe and Radioisotope Data for LVFS Stn. 2	89.
2-11	Lead-210 and Polonium-210 contents of particulate matter from Stn. 2. compared with those of plankton.	94.
2-12	Mass and element fluxes of fecal pellets through 388 m.	113.
2-13	Mass and element fluxes of fecal matter through 388 m.	114.
2-14	Flux summary for >53 μm particles at Stn. 2	115.
2-15	Suspended particulate concentration-mass concentration summary at LVFS Stn. 2, >53 μm fraction	118.

3-1	Organism distributions in >53 μm fractions at LVFS stations 4-8.	151.
3-2	Particulate silicate concentrations from 0.4 μm Nuclepore filters	190.
3-3	Junge distribution parameters of >53 μm particles at LVFS stations 2, 5, 6, and 7.	207.
3-4	Particle flux through 400 m at stations 2, 5, 6, and 7.	217.
3-5	Major component analysis of >53 μm fecal material from 400 m at Stns. 2, 5, 6, and 7.	220.
3-6	Total chemical flux of >53 μm particles through 400 m at stations 2, 5, 6, and 7.	221.
3-7	Suspended mass concentration summary for sinking material at 400 m at Stns. 2, 5, 6, and 7.	224.
4-1	Flow meter data from LVFS-4 cast to 1500 m in the equatorial Pacific.	246.
4-2	Cast data for the 1500 m profile.	248.

NOTE ON REFERENCES

To facilitate publication, the references for a given chapter are listed at the end of each chapter rather than at the end of the entire thesis.

CHAPTER 1

INTRODUCTION

Oceanic particulate matter is known to be important in controlling the distributions of many non-conservative elements in the ocean. Furthermore, particulate matter is incorporated into the sediments and is an important source of information regarding past oceanic circulation and climate. For these reasons, it is crucial to study the processes operating in the water column that are responsible for particle production, degradation, and transportation to the sediment - seawater interface.

To begin such a study it is necessary to have sufficient material for a variety of chemical analyses and for the measurement of the size distribution and morphology of the particles contributing to the vertical mass flux. Particulate matter (defined as that material retained by a filter of a particular pore size) is sampled conventionally by filtering 10 - 20 liters of seawater through membrane filters (Spencer and Sachs, 1970). Although such a method has recently yielded the first reliable picture of the concentration of particulate matter in the Atlantic Ocean (Brewer, Spencer, Biscaye, Hanley, Sachs, Smith, Kadar, and Fredericks, 1976) it has been shown inadequate for studies of the vertical mass flux by virtue of the fact that the volume of water sampled is too small to include most particles contributing to the flux (McCave, 1975). To best satisfy the above

criteria a Large Volume in situ Filtration System (LVFS) was developed and deployed in a variety of oceanographic regimes in the Atlantic Ocean (Bishop and Edmond, 1976). Instead of reiterating already published work in this thesis, important points from this paper will be brought forth in the text where necessary.

The following chapters progress chronologically as would be expected of publications reporting the progress of a project lasting several years. Chapter 2, dealing with the chemistry, biology, and vertical flux of particulate matter from the upper 400 m at one LVFS station in the equatorial Atlantic, is therefore intended as an example of the application of the chemical and microscopic methods of analysis used for the LVFS samples from other stations. It is used to develop ideas that will be later applied and improved upon in Chapter 3 where the particulate distributions at five LVFS stations from the Cape Basin of the S.E. Atlantic Ocean are reported. Chapter 4 presents the preliminary results from the first LVFS profile to 1500 m obtained in the equatorial Pacific during July 1976. Because the chapters of this thesis are written in publishable format, each chapter has a summary rather than being summarized in a concluding chapter.

The emphasis of this thesis is on the understanding of the processes controlling the chemical and morphological distributions and the vertical flux of particulate matter within the upper 400 m of the Atlantic Ocean.

References

- Bishop J.K.B. and J.M. Edmond (1976), A New Large Volume in situ Filtration System for the sampling of Oceanic Particulate Matter, *Journal of Marine Research*, 34, 181 - 198.
- Brewer P.G., D.W. Spencer, P.E. Biscaye, A. Hanley, P.L. Sachs, C.L. Smith, S. Kadar, and J. Fredericks (1976), The distribution of Particulate Matter in the Atlantic Ocean, *Earth and Planetary Science Letters*, 32, 393 - 402.
- McCave I.N. (1975), Vertical Flux of Particles in the Ocean, *Deep-Sea Research*, 22, 491 - 502.
- Spencer D.W. and P.L. Sachs (1970), Some aspects of the distribution, chemistry, and mineralogy of suspended matter in the Gulf of Maine, *Marine Geology*, 9, 117 - 136.

CHAPTER 2

THE CHEMISTRY, BIOLOGY, AND VERTICAL
FLUX OF PARTICULATE MATTER
FROM THE UPPER 400 M
OF THE EQUATORIAL ATLANTIC OCEAN

Introduction

The study of the chemistry and settling behavior of particulate matter is of great importance in the fields of marine chemistry, geology, and biology. The bulk of the observed particulate matter has biological origin within the surface layer of the ocean. It sinks through the thermocline resulting in such phenomena as the familiar nutrient depletion of the surface layers and enrichment of the deep water column. The nutrient elements are largely recycled within the upper 1000m of the water column; however, the complex nature of thermocline processes precludes the calculation of rates of recycling using dissolved nutrient data. Inefficiency in the recycling mechanisms operating in the water column allows the deposition of particulate matter. Bottom dwelling organisms metabolize most of the organic constituents leaving the mineral components to form the geological record of the oceanic conditions prevailing at the time of sediment deposition. Understanding the mechanisms important in the deposition of nannofossils (such as coccoliths) is extremely important in paleoceanography. Determining the important processes operating within the water column to change the character of the particulate matter will contribute to the knowledge of such basic processes as nutrient recycling and sediment formation.

The vertical flux of any chemical element in particulate matter is dependent on the production, size distribution, density, and settling behavior of the particles carrying that element. Ideally, one would want to determine the vertical chemical flux as a function of depth. Any changes in flux would be interpreted in terms of interaction of the particles with the water column. The flux of chemical elements to the bottom would give rates of material deposition. Towards these ends the Large Volume in situ Filtration System (LVFS) was constructed to collect samples of particulate matter amounting to several hundred milligrams dry weight from the upper 400 m of the water column in the open ocean.

Bishop and Edmond (1976) reported the preliminary results from the particulate matter samples (split in situ into greater than and less than 53 μ m size fractions) resulting from the filtration of up to 30 cubic meters of seawater using the LVFS. They showed that particles smaller than 53 μ m accounted for most of the mass concentration, while, compared with this fraction, the >53 μ m particles carried 3 and 12 times the mass towards the sediments in areas of low and high biological productivity respectively. These authors observed that a particle maximum frequently occurred in the upper thermocline near the base of the mixed layer; in upwelling situations (Southeast Atlantic) the mixed layer was poorly developed and the maximum particulate concentrations were found nearest the sea surface. This chapter reports

the results from a variety of chemical and radio-chemical analyses as well as from light and scanning electron microscopic studies performed on the samples collected at LVFS Stn. 2 (2°47'N, 8°51'W, Dec. 19-20 1973, R/V CHAIN 115-2 Dakar-Capetown). This station was typical of those exhibiting a particle maximum in the upper thermocline. By studying one profile in great detail we hope to provide a basis for understanding the important chemical, biological, and physical mechanisms operating to change the character of the particulate matter in the upper 400 m of the open ocean.

METHODS

Bishop and Edmond (1976) described the LVFS, its filters, and filter handling technique prior to chemical analysis. 5 to 30 m³ of seawater are pumped in situ at a rate of about 6 m³ hr⁻¹ (maximum flow velocity 6 cm/sec) through 53µm Nitex mesh (25.4 cm effective diameter), and then through a pair of acid-leached precombusted Mead 935-BJ glass fiber (g-f) filters in series (each with pore size 1.25µm at 98% efficiency, 0.8µm at 75% efficiency; together they have a pore size of 0.8µm at 96% efficiency at zero loading). The resulting particulate matter sample is split into 3 size fractions defined as: >53µm, Nitex filter; 1-53µm, top g-f filter; and <1µm, bottom g-f filter.

The dry weight particulate matter concentrations for this station have already been reported (Bishop and Edmond,

1976). All chemical analyses were made on subsamples of the filters, either by weight or by area fraction. Subsampling by area was both faster and more accurate; specially machined and polished brass cork borers were used. A scalpel and a glass template were used to subsample the Nitex prefilters. The accuracy of the chemical analyses, of the blank corrections, and of the subsampling procedure was established by replicate analyses.

Major constituents

Na, K, Mg, Ca, and Sr were analyzed by leaching the filter subsamples (1/80 and 1/40 of each glass fiber (g-f) filter and Nitex prefilter respectively) in 0.6N HCl for 24 hours or in 2.2 M acetic acid for 70 hours. K was not measured in g-f samples as blank levels were too high (4 mgs). The leach solutions were filtered (0.6 μ m Nuclepore filter), made up to 50 ml, and analyzed by flame atomic absorption (P.E. 403). Samples, standards, and blanks were treated identically.

Na, Mg, K and Ca in the acid-leach solutions had three sources: filter blank, sea salt, and particulate matter.

The appreciable Na, Mg, and Ca blank levels in the untreated glass fiber filters (Table 1, line 1) were reduced by leaching batches of 15-20 filters with 300-500 mls of concentrated HCl for 12 hours and then washing them with

TABLE 1

MAJOR ION BLANK LEVELS* IN
MEAD 935- BJ GLASS FIBER FILTERS

Sample description	n [†]	Na/ σ_{Na}	Mg/ σ_{Mg}	Ca/ σ_{Ca}
Untreated Mead 935-BJ(1)	37.	/ -	2.7 / -	4.8 / -
JB - 91 unused blank L.V.F.S. Stn. 2	(4)	10.0 /1.56	0.697/0.073	2.74/0.059
JB - 91 Rockport blanks	(5)	5.00/0.46	0.586/0.066	2.27/0.23
JB - 108 Rockport blank (Batch 9)	(4)	5.75/0.77	0.603/0.068	2.79/0.27
JB - 121 Rockport blank (Batch 9)	(4)	6.46/0.95	0.823/0.065	3.77/0.49
All Rockport blank filters	(16)	5.63/0.85	0.632/0.107	2.62/0.66
L.V.F.S. Stn. 2** bottom filters (388m data omitted ?)	(5)	5.00assumed	0.654/0.153	2.78/0.79

* acid leachable blanks (0.6 N HCl), numbers reported in mgs.

** the Na analyses of these filters were corrected assuming a 5 mg Na blank (JB-91 Rockport blank). The residual Na was assumed to be due to sea salt and was used to correct the Mg and Ca analyses of these filters resulting in the filter blank estimate for both Ca and Mg.

† n = number of subsamples analysed

double distilled deionized water until neutral pH was measured in the effluent. The filters were then dried for 24 hours at 100°C and combusted, separated by Pyrex glass rods, at 450°C for 2.5 hours. The top and bottom filters from the stack were discarded, and the others weighed and placed in numbered poly bags in the same order as they were in the stack. Consequently, the top and bottom filters for each LVFS sample were next to each other throughout their whole history, from pretreatment to analysis. Generally, one batch of filters was used at each station with one filter being reserved for blank purposes.

In order to determine whether or not the unused blank filters were true blanks for those filters used in the LVFS (exposed to seawater and distilled water washed), 47mm diameter subsamples of unused blank filters from different batches were dipped in surface seawater at Rockport, Massachusetts for periods up to 3 hours. They were then treated in exactly the same fashion as the LVFS filters. Subsamples were leached with 0.6N HCl to determine the Na, Ca, Mg blank values and also were analyzed for C and N to investigate the possibility of adsorption of these elements from seawater onto the glass filters. Compared to unused JB-91 (LVFS Stn. 2 blank; Table 1, line 2) the subsamples of this blank filter, after exposure to Rockport seawater and treatment as the other LVFS samples, had lower and more

reproducible acid-leachable sodium content (Table 1, line 3). This was true for all batches and so the "Rockport" blanks were considered better than unused blanks for the correction of the LVFS data.

Replicate analyses of the Rockport blank filters indicated that individual filters had more uniform blank levels than all filters (Table 1, lines 3-6). Rockport blank filters JB-108 and JB-121 were the top and bottom filters of one batch and had different blank levels. The use of one blank to correct the analyses of filters from its batch results in a 0.7 mg maximum uncertainty for Na; 0.22 mg, for Mg; and 1.0 mg, for Ca.

Since the top and bottom glass fiber filters for each LVFS sample were next to each other in their batch, they are assumed to have similar blank levels. Consequently, each sodium analysis was corrected by subtracting 5.0 mgs (JB-91, Rockport) and the remaining Na was assumed to be from sea salt (Bishop and Edmond, 1976). The Mg and Ca analyses of each bottom filter were corrected for sea salt (using the Na data) and the residuals (calculated blanks) were subtracted from the analyses of the corresponding top filter. Blank values for Mg and Ca calculated in this fashion were comparable to the Rockport blank values (Table 1). The Sr analyses were corrected in the same fashion (typical blank = 0.01 mg). Major-ion blanks of the Nitex mesh were an order of magnitude lower and presented little problem when correcting the analyses

of the prefilters.

Carbon and nitrogen analyses were performed directly on subsamples of the g-f filters ($1/80^{\text{th}}$ of the filter, P.E. 240 CHN analyser, Culmo, 1969). Since Nitex mesh ($>53\mu\text{m}$ fraction) has a C/N ratio of about 6, particles were removed prior to analysis using a stiff nylon brush and sucked onto a pre-weighed, precombusted Whatman GFF filter in a 13 mm in-line Millipore filter holder. The procedure was monitored at 12X on a Wild M5 Stereomicroscope. After examination at 50x, Nitex fibers were removed, and the filters were reweighed (P.E. AD-2 autobalance). Particle recovery was calculated as the product of mass of particles recovered and the area factor divided by the total dry weight of particles on the Nitex filter, and was approximately 50%. Bias introduced by this technique is probably small but would favor the larger particles. Carbonate was removed prior to analysis by exposing the subsamples to fuming HCl in a closed container for 24 hours and then drying at 60°C for 8 hours.

The C, N analyses of JB-91 (Table 2) showed lower levels of C and similar levels of N compared to subsamples of the unused blank filter; in addition there was no evidence of uptake of C or N by the g-f filters from the surface seawater with time (Table 2). Analyses of C and N were therefore corrected using Rockport JB-91 as blank (questionable N data omitted).

TABLE 2

CARBON AND NITROGEN UPTAKE BY MEAD[†] 935-BJ GLASS FIBER FILTER
FROM "ROCKPORT" SEAWATER

Sample	C	N	Hours:Min Exposure Time
JB-91 Unused	4.94	0.27	0:00
" "	5.02	1.07 (?)	0:00
JB-91 Rockport	2.64	0.23	0:01
JB-91 Rockport	2.22	0.22	0:30
JB-91 Rockport	2.26	0.31	1:22
JB-91 Rockport	1.76	0.60 (?)	2:52
Avg. Rockport	2.22 ± .36	0.25 ± .05	

[†] results expressed as mg. C and N per 25.4 cm diameter
g-f filter area.

$\delta^{13}\text{C}$ in the organic material was determined by the method of Degens (1969). Prior to analysis, the subsamples of the g-f filters and the particles removed from the Nitex were flooded with 6N HCl in precombusted ceramic boats and taken to dryness (70°C) three times to remove carbonate.

Particulate carbonate was analyzed in a closed recirculation system using a Beckman 215 IR analyser and calcite standards (Menzel and Vaccaro 1964). Carbon dioxide was generated using 20% phosphoric acid in a Y-tube (Craig 1953). The residual phosphoric acid solutions from the >53 μm fraction were retained for analysis of Na, K, Mg and Ca.

Particulate Fe was analyzed by autoclaving subsamples of the filters in the presence of 0.2 M hydroxylamine hydrochloride and 0.6N hydrochloric acid for 18 hours. The resulting solution was filtered and analyzed using the method of Stookey (1970). The blank values for g-f filters were significant (1.12 mg), accounting for 50% of the measured iron in some samples, but replicate blanks agreed within 1%.

Phosphate was released from the particles by repeated treatment with saturated potassium persulphate solution followed by autoclaving for 30 minutes (three times). The particles were completely bleached by this treatment and the Nitex virtually destroyed. The samples, standards and blanks were processed identically, filtered and analyzed following

Murphy and Riley (1962). The rate of color development was lower than for normal seawater, stabilizing only after six hours.

Silica was leached from the $>53 \mu\text{m}$ fraction for one day at 60°C using either $0.4 \text{ M Na}_2\text{CO}_3$ or 1 N NaOH solutions. After filtration, and neutralization with HCl the solutions were analysed using the method of Mullin and Riley (1955).

It was not practical to analyse the material on the g-f filters for silica. However samples had been collected from 30 l Niskins on $0.4 \mu\text{m}$ Nuclepore filters for mass intercalibration (Bishop and Edmond, 1976). These were digested at 120°C in 10 N NaOH for 2 hours in Teflon beakers. After neutralization with 6N HCl the granular precipitate was removed by filtration and the sample analysed as above. Standards were treated identically; no interference from the Nuclepore filters was found.

Table 3 lists the analytical results and filter blanks for the various elements discussed above. For the purposes of material balance in the particulate matter, the results are tabulated in milligrams of element per sample. Chemical units (nanomoles kg^{-1}) are used in the discussions of the elemental relationships and distributions, and in the calculations of the vertical fluxes of particles in the water column. Precision of the various analyses is established by the analysis of multiple filter subsamples. Typical blank levels (g-f filters) and actual blank levels (Nitex filters) are also indicated in the table.

TABLE 3 : CHEMICAL DATA CHAIN 115-2
LVFS STN. 2

> 53 m SIZE FRACTION

z	Na	xs	Mg	xs	K	Ca	Sr	C _{inorg}	Si	Fe	C _{org}	N	P	$\delta^{13}\text{C}_{\text{PDB}}$	mass	vol.	weight
(m)	(mg)	(mg)	(mg)	(mg)	(mg)	(mg)	(mg)	(mg)	(mg)	(mg)	(mg)	(mg)	(mg)	($^{\circ}/_{\text{‰}}$)	(gm)	(m ³)	(10 ³ kg)
32 a	3.59	0.13	0.13	0.13	1.39		a 0.357	d 0.788	f 0.344	15.2	2.25	0.239		-23.16	0.042	4.57	4.67
a	4.36	0.12			1.55	0.276	a 0.408	e 0.889			15.7 (3.7?)	0.145				± 1.5	
b	2.81	0.148	0.10		1.83	0.276											
c																	
50 a	0.90	0.242	0.09		2.11		a 0.511	d 3.17	f 0.271	36.4	lost	0.512		-22.72	0.105	4.47	4.58
a	2.01	0.264	0.15		2.26		a 0.594	e 3.25		36.7	5.17	0.680				± 1.5	
b	1.87	0.25			2.24	0.419											
c	1.53	0.236	0.15		2.42	0.483											
113 a	1.05	0.130	0.02		4.01		a 1.181	d 3.861	f 0.320	17.8	2.04	0.151		-23.32	0.070	12.79	13.13
a	0.36	0.12			3.78	0.122	a >.9	e 3.69		19.1	2.23	0.180				± 3	
b	0.61	0.201	0.01		4.37	0.160											
c																	
188 a	1.17	0.143	0.01		2.99		a 0.887	d 2.88	f 0.337	14.0	1.68	0.097		-23.62	0.060	17.82	18.30
a	1.27	0.137	0.02		3.06		a 0.942	e 4.15		14.3	1.70	0.104				± 4	
b	1.48	0.19			3.60	0.158											
c	2.43	0.189	0.00		3.28	0.093											
294 a	1.03	0.198	0.01		3.63		a 1.076	d 3.03	f 0.473	12.5	1.58	0.056		-23.30	0.063	21.14	21.71
a	2.15	0.238	0.08		4.44		a 1.357	e 3.10		15.9	1.97	0.094				± 6	
b	1.00	0.14			4.27	0.100											
c	0.82	0.196	0.02		2.12	0.061											
388 a	0.57	0.157	-0.01		3.10		a 0.910	d 2.42	f 0.489	4.64	0.549	0.049		-23.72	0.019	23.70	24.34
a	0.49	0.163	-0.02		2.76		a 0.834	e 3.05				0.061				± 6	
b	1.66	0.15			3.22	0.097											
c	1.02	0.153	0.03		4.04	0.087											
BLANK	0.34	0.058	0.07		0.105	0.001	0.0007	0.05	0.040	0.4	0.031	0.014					

0+.026

33

< 53 μm SIZE FRACTIONS

z (m)	Na (mg)	xs Mg (mg)	Ca (mg)	Sr (mg)	C _{inorg} (mg)	Fe (mg)	ΣC (mg)	N (mg)	P/σ _P (mg)	δ ¹³ C _{PDB} (‰)	mass (gm)	vol. (m ³)	weight (10 ⁻³ kg)
32 b	11.2	0.03	2.62	0.144	a 0.82	FT 0.99	T 32.9	4.83	0.476/.026	-19.95	0.128	4.57	4.67
c	12.6	0.53	2.39	0.101	a 0.73	FB 0.44	B 9.1	1.45	0.155/.011	-21.98	0.159	±.15	
50 b	14.0	0.17	3.47	0.128	a 0.87	FT 0.52	T 37.6	5.40	0.639/.107	-23.05	0.140	4.47	4.58
c	13.8	0.44	3.19	0.115		FT 0.53	T 38.3	5.39		-24.12	0.174	±.15	
						FB 0.53	B 12.8	2.14	0.239/.069	-26.41			
113 b	6.34	0.69	30.80	0.448	a 8.06	FT 1.36	T 50.6	5.89	0.454/.015	-23.25	0.208	12.79	13.13
c	6.31	0.68	27.69	0.468	a 7.88	FT 1.30	T			-22.69	0.217	±.3	
					a 7.84	FB 0.63	B 10.0	1.67	0.135/.025	-23.10			
					a 7.85	FB 0.64							
188 b	16.0	0.75	29.03	0.362	a 7.79	FT 2.00	T 56.9	6.20	0.495/.008	-22.27	0.234	17.82	18.30
b	14.0	0.60	25.26	0.342	a 7.86	FT 0.36	T 56.7	5.95		-21.65	0.232	±.4	
c	14.3	1.13	27.52	0.345		FB 0.36	B 9.8	1.22	0.096/.003	-21.06	0.222		
294 b	10.62	2.31	37.03	0.351	a 9.22	FT 3.88	T 63.3	6.62	0.527/.006	-20.79	0.285	21.14	21.71
c	7.02	1.46	33.27	0.370	a 9.03	FT 4.22	T 59.6	6.08			0.273	±.6	
						FB 0.54	B 8.8	0.82	0.166/.006	-21.05			
						FB 0.54	B 8.8	0.81					
388 b	73.9	0.70	31.48	0.248	a 8.90	FT 4.53	T 57.6	5.66	0.525/.010	-20.98	0.368	23.70	24.34
b	85.5	0.90	31.98	0.225	a 8.91	FB 0.64	B 14.3	2.81	0.220/.002	-21.13	0.330	±.6	
c	38.6	-0.86	33.38	0.226		FB 0.64	B 14.3	2.81			0.541		
BLANK	5.0	0.58	2.5	0.01	0.12	1.10	2.2	0.24	0.006	-21.53	0.000		
	±.7				±.03	±.01	±.7	±.11			±.013		

a: 20% H₃PO₄ ; b: 2.0 M HAC ; c: 0.6 N HCl ; d: 1 N NaOH ; e: 0.4 M Na₂CO₃ ; f: 0.6 N HCl/0.2M NH₂OH·HCl
T: Top glass fiber filter = 1 ~ 53 μm size fraction ; B: Bottom glass fiber filter = <1 μm size fraction
mass : particulate dry weight= <1 μm + 1-53μm size fractions according to Bishop and Edmond (1976)
xs: residual after analysis has been corrected for filter blank and seasalt.

Radio isotopes

One half of each filter was analysed non-destructively by gamma-ray spectroscopy for the cosmic ray produced isotope Be-7 ($t_{1/2} = 53$ days) and the Ra-226 daughters Bi-214 and Pb-214 using a Ge(Li) detector at Battelle N.W.

1/90 to 1/30 of each filter was analysed for Pb-210 and Po-210 activity using the method of Bacon (1975). The only modification of the analytical procedure was the use of HF to destroy the g-f filter.

Microscopy

The samples of particulate matter either on g-f filter or on the Nitex mesh were prepared for scanning electron microscopy (SEM) by coating them with carbon and gold. Routine examination of the samples was made at 2500X using a J.E.O.L. Mod. J.S.M.-U3 scanning electron microscope at W.H.O.I.

For light microscopy, the 1-53 μ m (g-f) filter samples (0.92 cm diameter) were placed on a glass slide, wetted with Cargille's Type B Immersion Oil ($n_d^{25} = 1.5150$), degassed in a vacuum dessicator for several hours and permanently affixed with a No. 1 cover slip and sealed with silicone rubber cement. Preparation of the >53 μ m samples involved the use of saturated phenol-toluene solution to dissolve the Nitex mesh and deposit the particles onto a Whatman GFF g-f filter. The filter was then rinsed with toluene to remove the phenol and dried at 60°C on a hot plate for 30 minutes. The removal of the Nitex grid was necessary as this

material is strongly birefringent under polarized light and masks the presence of some organisms. Mounting of the samples onto glass slides followed the procedure outlined above.

The slides were examined at magnifications of 150 x to 800 x on a phase-contrast Olympus POM microscope and at magnifications of 50 x to 200 x on a Wild M-5 Stereomicroscope to determine the depth distributions of organisms and large aggregate particles. Identifications were completed to genera whenever possible. When this was not possible, organisms were listed by order or by similar appropriate classifications; i.e. Coccolithophoridae; Foraminiferida; centrate, pennate, solenoid, or gonioid diatoms; Radiolaria; Acantharia; gymnodinial or peridinal dinoflagellates; and such macroinvertebrate structures as poriferan spicules and portions of crustacean carapaces and appendages. The more general designations were considered sufficient for the context of this paper as they included most organisms encountered and adequately distinguished their chemical composition. Values for the concentration of organisms at each depth are computed on the basis of these classifications.

RESULTS AND DISCUSSION

A hydrographic profile was made to 550m (Fig. 1) in order to provide an oceanographic context for the LVFS samples and as an aid in choosing sampling depths. There

FIG. 2 - 1

Hydrography of the upper 500m at CHAIN 115-2
LVFS Station 2. LVFS depths are indicated
by the letter P.

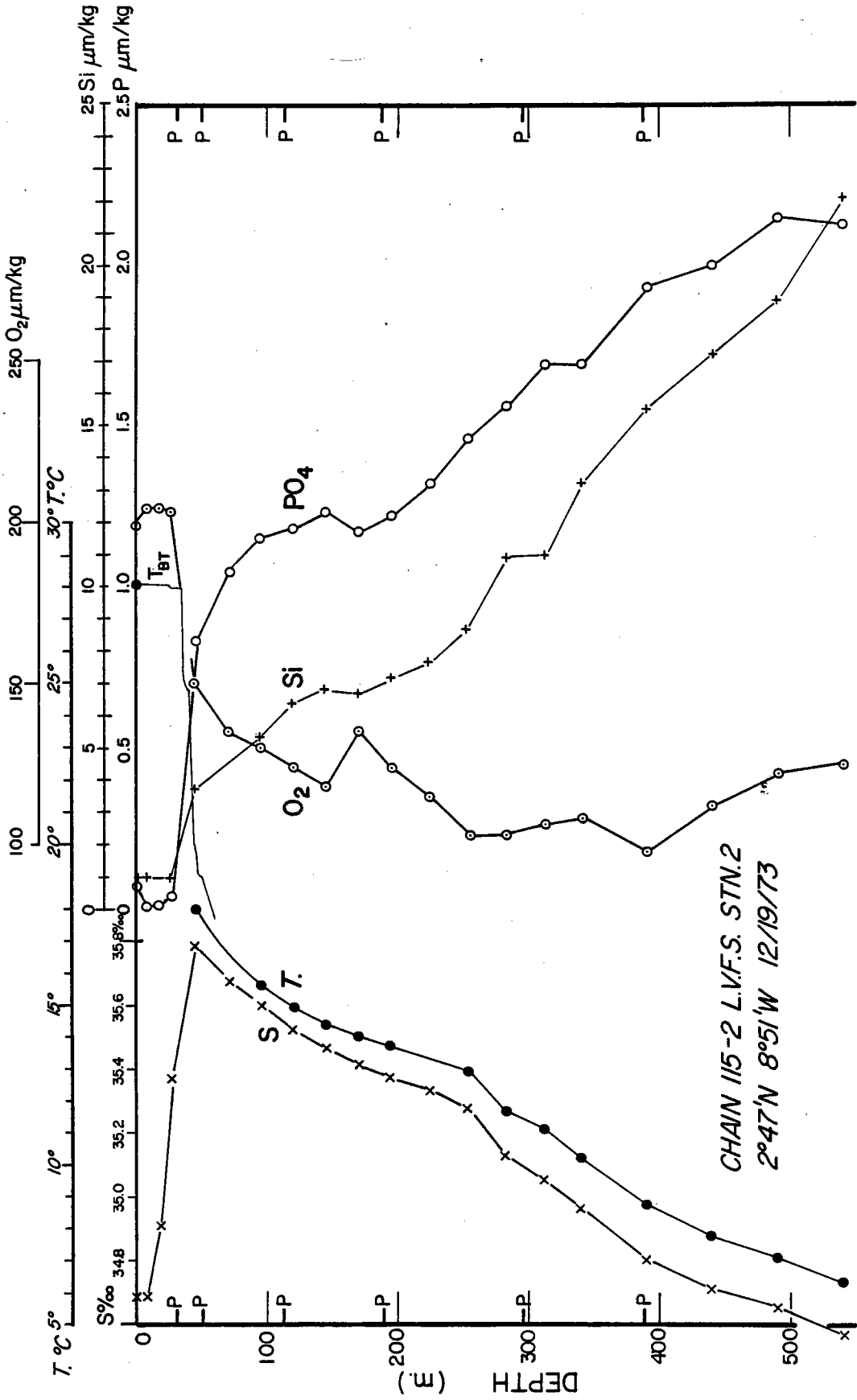
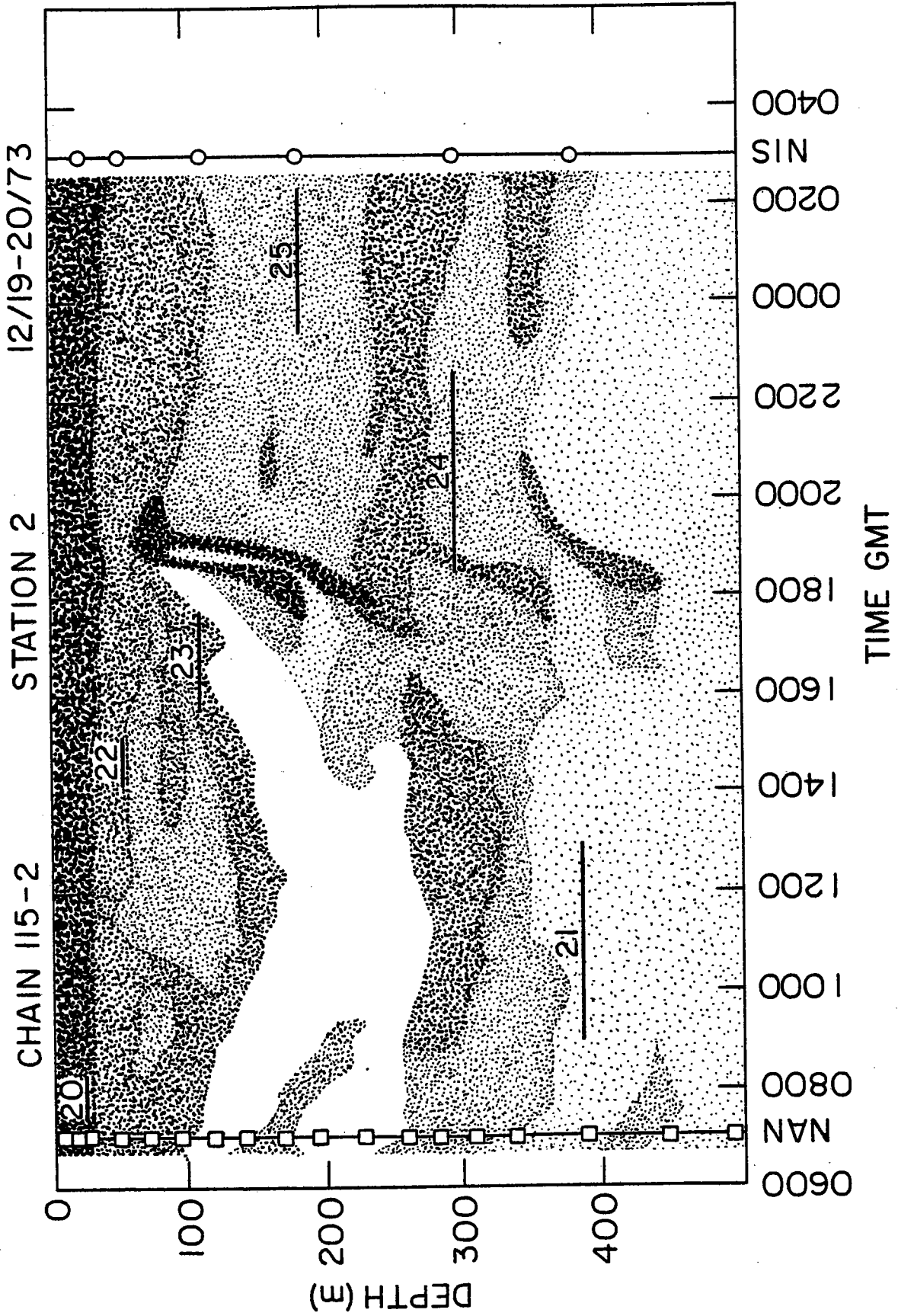


FIG. 2 - 2

Graphic reproduction of the 12 KHz PGR record obtained during the station. Shading is proportional to back scattering of sound by the deep scattering layer organisms. LVFS, Nansen, and 30 litre Niskin sample depths and times are shown. Time zone -1.



was a 40 meter mixed layer with the salinity maximum of the sub-tropical underwater being located at 46 m. The TS relation between 50 and 500 m falls in the field of South Atlantic Central Water. There is a maximum in oxygen and minimum in phosphate in the mixed layer and sharp vertical gradients in the thermocline. Below 200 meters the phosphate and silicate increase regularly with depth; the oxygen concentrations are quite uniform. During the station the ship drifted 25 km to the northeast at an average of 30 cm sec⁻¹ although the winds were light. A 12 KHz P.G.R. was used to monitor the depth of the LVFS as well as to observe the vertical migration of the deep scattering layer during the station (Fig. 2).

Gravimetric Results

The weights of suspended material on the filter calculated using the analytical data (taking organic carbon as CH₂O) agree well with the measured value (Table 4, Fig. 3) save for the deepest and two shallowest <53 μ m LVFS samples. The replicate sodium analyses on the deep sample were very poor and hence the computed gravimetric weight has a high uncertainty. It is possible that there is an appreciable contribution of non-biogenic material to the surface weights although this has not been verified directly.

TABLE 4 : PARTICULATE MASS CONCENTRATION

> 53 μm SIZE FRACTION

z (m)	Chemical* dry weight concentration ($\mu\text{g kg}^{-1}$)	Gravimetric dry weight concentration ($\mu\text{g kg}^{-1}$)	σ_{Grav} ($\mu\text{g kg}^{-1}$)
32	10.26	9.0	5.6
50	24.67	22.9	5.7
113	5.24	5.3	2.0
188	2.99	3.3	1.4
294	2.58	2.9	1.2
388	1.12	0.8	1.1

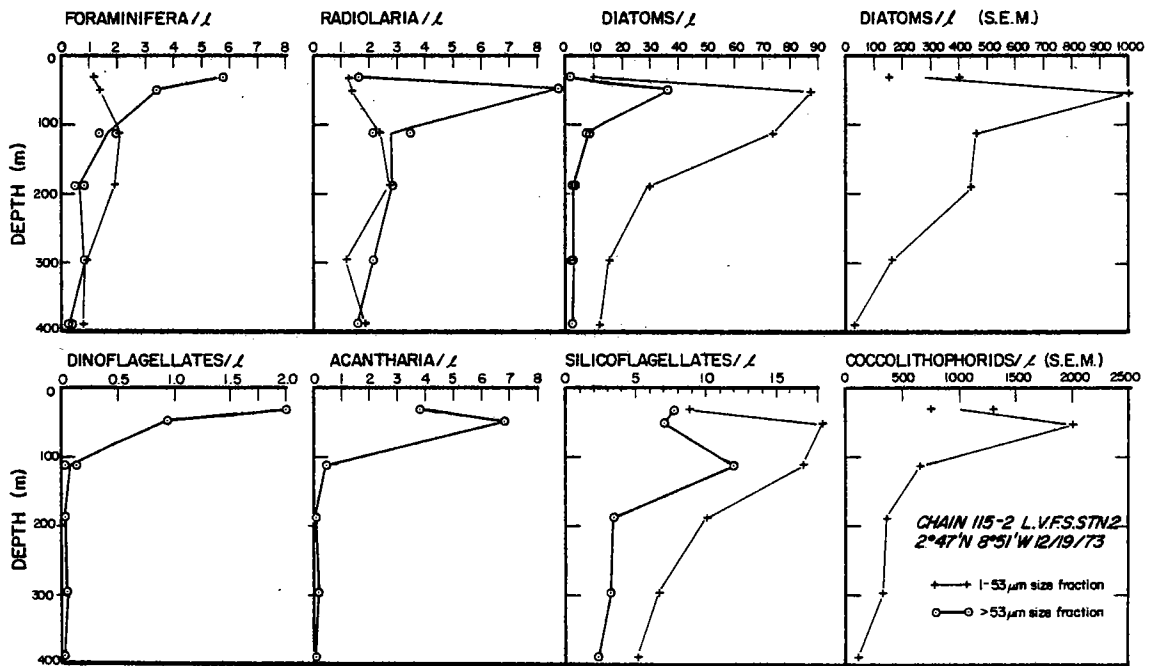
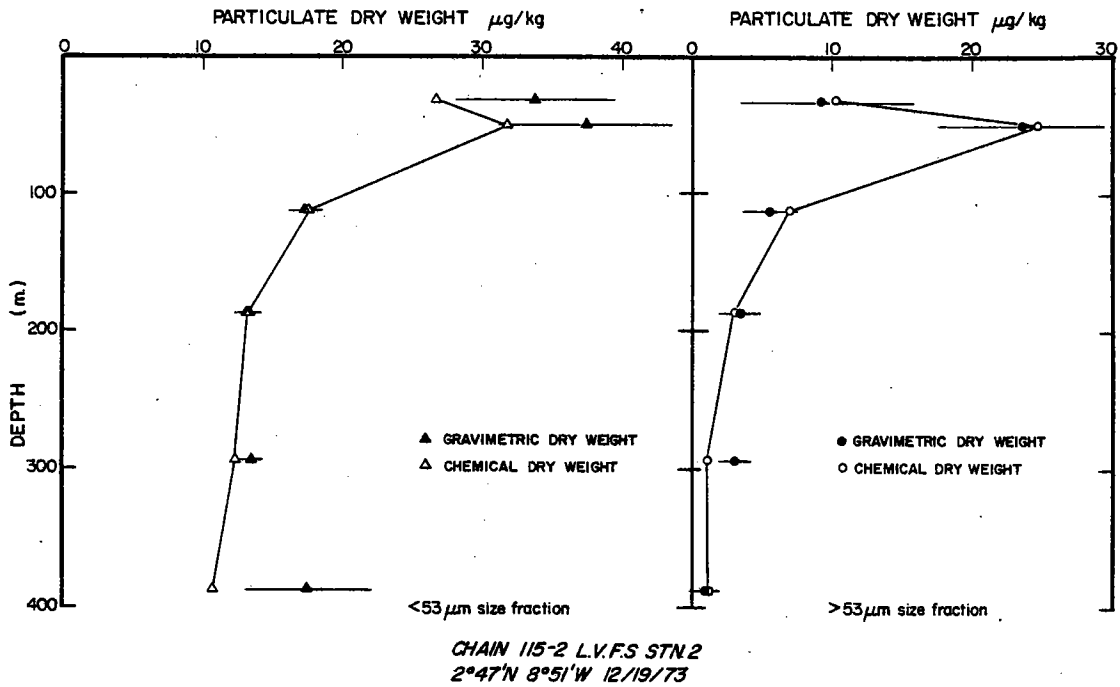
< 53 μm SIZE FRACTION

32	26.25	30.7	5.6
50	31.55	35.1	6.1
113	17.54	16.2	0.4
188	12.96	12.5	0.9
294	12.54	12.9	0.8
388	10.68	17.0	4.7

* calculated as the sum of weights of organic carbon (as CH_2O)+N+ PO_4 + CaCO_3 +excess Ca+excess Mg+excess K+Sr SO_4 +carbonate Sr+opal.

Figure 2-3. Upper: Particulate dry weight profiles of $<53\mu\text{m}$ and $>53\mu\text{m}$ size fractions. Open symbols are computed from the sum of $\text{CH}_2\text{O} + \text{N} + \text{P} + \text{CaCO}_3 + \text{SiO}_2 + \text{xs Ca} + \text{xs Mg} + \text{K} + \text{Sr}$ (in CaCO_3); closed symbols are total dry weight measurements. Comparison of the two sets of data shows that most particles in the upper 400 m are biogenic.

Lower: Plankton distributions showing maxima at the depth of the particle maximum. Abundances shown here are much higher than previously reported (e.g. Foraminifera) but are typical of other LVFS stations. This is primarily due to the fact that the LVFS acts like a $1\mu\text{m}$ plankton net and catches organisms usually missed in plankton tows. Two points indicate counts of different subsamples of the same filter.



Biological Observations

Both the large and small particle size fractions exhibit a dry weight concentration maximum at 50 m, just below the base of the mixed layer in the upper thermocline.

Microscopic examination of the filters showed that many phytoplanktonic and microzooplanktonic organisms have maximum population densities at this depth.

The most abundant organisms in the $>53\mu\text{m}$ size fraction are seen to be Foraminifera, Radiolaria, diatoms, and Acantharia (Table 5, Fig. 3). The density of 3-6 Foraminifera per liter of near surface waters is much higher than previously reported values of approximately 10 per cubic meter (Berger, 1968; Bottazzi, Schreiber and Bowen, 1971) obtained from $250\mu\text{m}$ mesh plankton net tows in the tropical Atlantic. Foraminifera in the $>53\mu\text{m}$ fraction ranged in size from $20\mu\text{m}$ to approximately $200\mu\text{m}$; they averaged $20\mu\text{m}$ in size in the $<53\mu\text{m}$ fraction. Our foraminifera counts at this station are representative of those obtained at other LVFS stations and so the increased number of foraminifera sampled by the LVFS can only be explained by the difference in its filtration efficiency compared to plankton nets. Counts of foraminifera $>100\mu\text{m}$ are comparable to those obtained from plankton tows.

The Foraminifera, primarily belonging to the Globigerinidae, reach their maximum density at 32 m. At

TABLE 5 : PLANKTON POPULATION DISTRIBUTION

z	Foraminifera (LM)	Radiolaria ^a (LM)	>53 μ m SIZE FRACTION (Whole tests/ m ³)					Dino- flagellates (LM)	Cocco- lithophoridae (SEM)	Diatoms (SEM)
			Diatoms (LM)	Silico- flagellates (LM)	Acantharia (LM)	Dino- flagellates (LM)	Cocco- lithophoridae (SEM)			
32	5780	1605/	140	7775	3815	2000				
50	3760	8690/	35900	6810	6810	940				
113	1350 1970	4690/3500	8840 7250	11950	426	14 137				
188	470 805	3780/2855	2010 3060	3420	73	15 42				
294	800 805	2640/ 2840/2130	2250 2550	3205	180	37 0				
388	232 383	2720/1575	2210	2350	84	5 0				
<53 μ m SIZE FRACTION (Whole tests/ m ³)										
32	1160	1275	9970	8800	0		1.30 x 10 ⁶	0.15 x 10 ⁶		
50	1360	1360	87280	18340	0		0.75 x 10 ⁶	0.40 x 10 ⁶		
113	2015	2370	73770	16960	0		2.03 x 10 ⁶	1.03 x 10 ⁶		
188	1875	2730	29850	10060	0		0.65 x 10 ⁶	0.46 x 10 ⁶		
294	863	1150	15610	6620	0		0.36 x 10 ⁶	0.44 x 10 ⁶		
388	769	1860	12040	5120	0		0.33 x 10 ⁶	0.16 x 10 ⁶		
							0.11 x 10 ⁶	0.03 x 10 ⁶		

a. Radiolarian counts are broken down as: total whole tests (including juveniles)/
adult forms

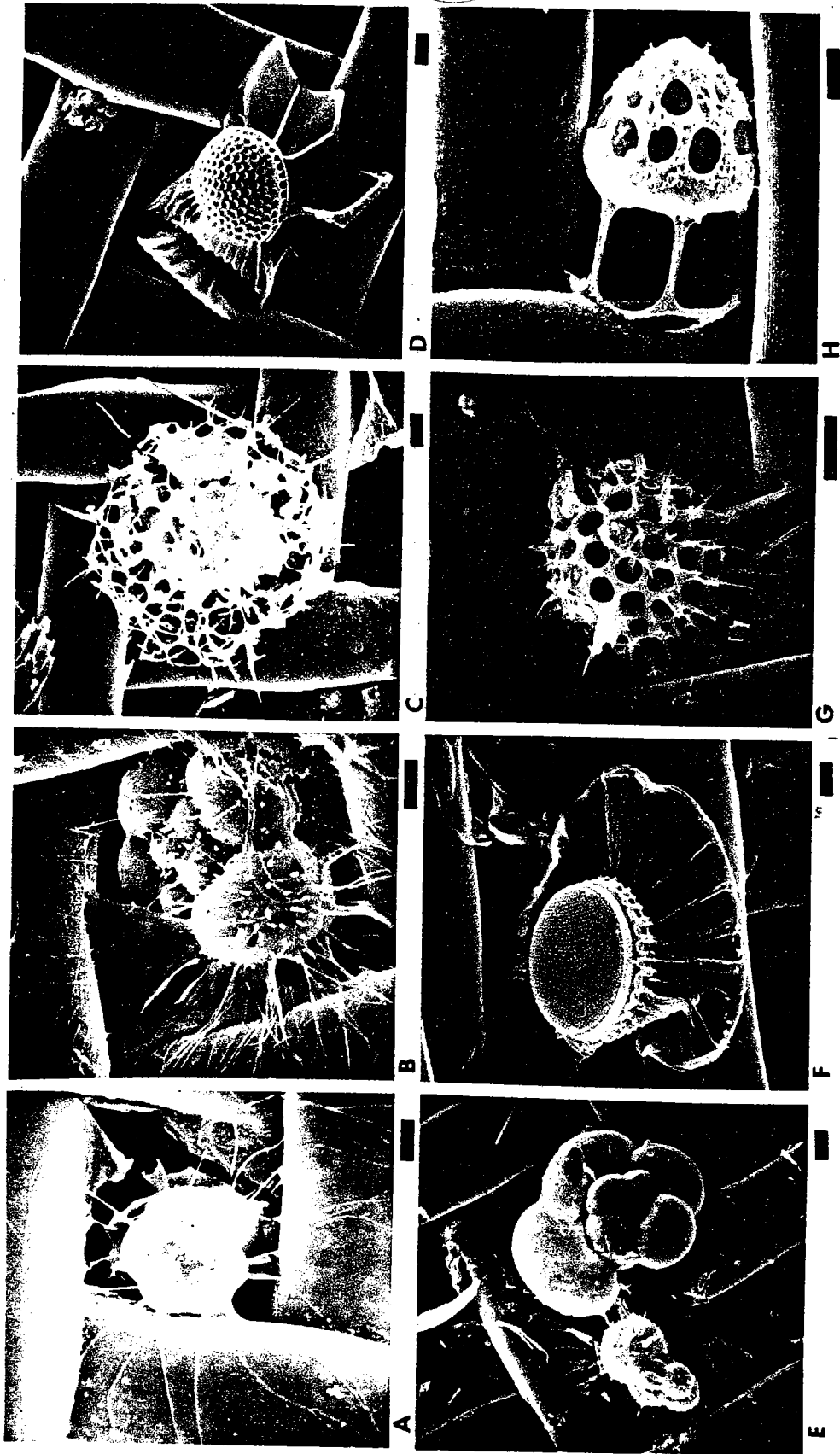
Replicate counts are indicated , LM light microscopy; SEM scanning electron
microscopy

Plate 1

Scanning electron micrographs of plankton sampled by LVFS. Scale is indicated in each photo:

■ 1 μm ; ■ 10 μm ; ■ 100 μm ; Grid visible is 53 μm Nitex.

- A. Foraminifera, fam. Rotaliidae with psuedopodia, 32 m.
- B. Foraminifera, Hastigerina sp. Note reticulopods with associated organic material, 32 m.
- C. Radiolarian with intact inner capsule, 32 m.
- D. Peridinal dinoflagellate, Ornithocercus sp., 32 m.
- E. Foraminifera of the family Globigerinidae, 113 m.
- F. Planktoniella sp., a centrate diatom with a membranous, hyaline extension of extracellular loculi, 50 m.
- G. Radiolarian of the genus, Hexalonche, family Sphaeroidae, 188 m.
- H. Tintinnid, Codonellopsis sp., with fenestrated lorica. Lower margin of lorica is composed of coecoliths, 32 m.



this depth they are largely single prolucula or megalospheric individuals in the early stages of division. Light microscopy of the samples showed that approximately 80% of the Foraminifera tests were occupied at 32 and 50 m and SEM examination of similar forms showed them to be associated with organic material (Plate 1;A,B). These organisms appear to have been live at the time of sampling. Below 50 m only 10 to 20% of the tests were occupied. SEM showed the empty tests to be completely devoid of organic material (Plate 1, E) and essentially "clean". It was also observed that below 100 m the "live" Foraminifera were generally multichambered, microspheric forms seldom seen in the shallower samples and that the larger, megalospheric tests were completely empty. This apparent distribution indicates that alternating sexual (microspheric) and asexual (megalospheric) generations may occur at different depths, but bears further investigation. A detailed study of the Foraminifera is underway and the results will be published when available.

Dinoflagellates (Plate 1, D) also show a maximum population at 32 m and are essentially absent from the >53 μ m fraction below 50 m. This is an indication of the friability of these organisms compared with the Foraminifera.

Radiolaria, diatoms, and Acantharia show maximum population densities at 50 m in the >53 μ m fraction. Apart from the 50 m maximum, the Radiolaria (e.g., Plate 1, C and

G) show little species and developmental variability throughout the water column except for the large number of initial spicules or early developmental stages near 300 m. The diatom population in the $>53\mu\text{m}$ fraction is dominated by coscinodiscoid species (e.g., Plate 1, F) and by Rhizosolenia sp. Below 150 m, the diatom frustules are generally empty and many are fragmented. Their presence and condition is probably a result of predation at shallower depths. Light microscopic examination of the $<53\mu\text{m}$ fraction revealed a diatom maximum also at 50 m; SEM showed a diatom population approximately ten times that determined by light microscopy and revealed many forms, particularly pennate diatoms, that were too small (i.e. $<10\mu\text{m}$) to be seen easily by light microscopy at 400 x. The Acantharia consist primarily of Acanthometridae at the shallower depths; however, it is difficult to classify these organisms below 100 m due to loss of major spines and dissolution of fine structures (see below).

Tintinnids (e.g., Plate 1, D) were relatively rare, having population between $1000/\text{m}^3$ near the surface and $20-30/\text{m}^3$ below 200 m.

Silicoflagellates occur predominately in the $<53\mu\text{m}$ fraction with a maximum at 50 m; the population is essentially uniform, showing no variation in species or developmental stages.

SEM showed the coccosphere distribution to reach a

maximum of 2 individuals per ml at 50 m. Below 50 m, the <53 μ m fraction is dominated by coccoliths and diatom fragments, and at 388 m only the smallest coccospheres (5-10 μ m) survive intact; the larger forms are all fragmented.

The particle maximum coincides with the organisms maxima. Primary producers (and their predators) occupy the upper thermocline in areas where it and the euphotic zone overlap. There, these organisms take advantage of the increased levels of nutrients with some sacrifice of solar energy. The sudden change in condition and numbers of the whole organisms between 50 m and 113 m must be due to primary and secondary level predation.

Organic C, N, P and $\delta^{13}\text{C}$

Analyses were made on the three filters from each depth; these correspond to the <1 μ m (bottom g-f), 1-53 μ m (top g-f), and >53 μ m (Nitex) fractions (Table 6). The total carbon values for the <1 μ m fraction are uncorrected for carbonate (the correction would be <2 %); those for the 1-53 μ m fraction are corrected using the measured carbonate carbon date. The carbonate was removed from the >53 μ m fraction by HCl fumes prior to analysis. While they are low it is assumed that the carbon values measured on the bottom g-f filter are particulate since adsorption of dissolved carbon was ruled out by experiment (Table 2). It is unlikely that washing of the fresh filter with distilled water caused preferential loss of phosphorous or nitrogen relative to carbon. Comparison

TABLE 6: PARTICULATE ORGANIC C, N, P, AND $\delta^{13}\text{C}$
> 53 μm SIZE FRACTION

z (m)	$\delta^{13}\text{C}_{\text{PDB}}$ ($^{\circ}/_{\text{oo}}$)	C_{Org}	$\sigma_{\text{C}_{\text{Org}}}$	$\sigma_{\text{C}_{\text{Org}}}^{\dagger}$	$\text{C}_{\text{Org}}^{* \dagger \dagger}$ (n moles / kg)	N	$\sigma_{\text{N}}^{\dagger}$	N* $\dagger \dagger$	P	$\sigma_{\text{P}}^{\dagger \dagger \dagger}$	$\text{C}_{\text{O}}/\text{N C}_{\text{O}}/\text{P}$ (mole ratio)	$^{\circ}/_{\text{oo}} \dagger \dagger$ organic
32	-23.16	271	168	13.8	> 49	34.4	13.8	> 6.19	1.33	0.33	7.9	99
		280	173	-	> 53	(56.2?)	-	-	-	-	(5?)	(103)
50	-22.72	662	165	-	> 152.3	-	-	-	4.20	0.59	-	(91)
		667	167	20.2	> 120.1	80.7	20.2	> 14.5	-	-	8.3	93
113	-23.32	113	41	4.00	> 52	11.1	4.00	> 5.11	0.408	0.037	10.2	67
		121	44	4.36	> 53	12.1	4.36	> 5.32	-	-	10.0	69
188	-23.62	63.7	28	2.89	> 27	6.56	2.89	> 2.82	0.178	0.005	9.7	61
		65.1	29	2.92	> 27	6.64	2.92	> 2.72	-	-	9.8	66
294	-23.30	47.9	19	2.08	> 20	5.20	2.08	> 2.18	0.111	0.029	9.2	52
		61.0	24	2.59	> 19	6.48	2.59	> 2.01	-	-	9.4	66
388	-23.72	15.9	22	2.25	> 12.2	1.61	2.25	> 1.24	0.073	0.008	9.8	64

< 1 μm SIZE FRACTION

1 - 53 μm SIZE FRACTION

z (m)	δC_{PDB}^{13} (‰)	ΣC^{**} (n moles / kg)	N	P	σ_P	C/N	C/P mole ratio	δC_{PDB}^{13} (‰)	C _{Org} (n moles/kg)	N	P	σ_P	C/N	C/P mole ratio
32	-21.98	161	22.2	1.07	0.08	7.3	151 [±] 7	-19.95	571	73.8	3.29	.18	7.74	174 [±] 4
50	-26.41	234	33.4	1.68	0.49	7.0	139 [±] 24	-24.12 -23.05	670 683	84.3 84.1	4.50	.76	7.96 8.12	149 [±] 20 151 [±] 20
113	-23.10	63.2	9.1	.33	0.06	6.95	190 [±] 22	-22.69 -23.25	268	32.0	1.12	.03	8.38	240 [±] 7
188	-21.06	44.4	4.76	.169	0.006	9.3	263 [±] 5	-22.27 -21.65	222 221	24.2 23.2	.873	.014	9.17 9.51	254 [±] 4 253 [±] 4
294	-21.05	33.6 33.6	2.70 2.67	.247	0.009	12.4 12.6	137 [±] 3	-20.79	208 194	21.8 20.0	.783	.009	9.55 9.69	265 [±] 2 247 [±] 2
388	-21.13	48.9	8.25	.292	0.002	5.9	167 [±] 1	-20.98	164	16.6	.696	.013	9.86	235 [±] 3

53

+ error due to estimate of recovery from dry weight data.

++ analytical value indicates minimum amount of carbon and nitrogen on the prefilter, C_{Org}^*/C_{Org} = recovery of particles.

*** % organic component as $(CH_2O + N)/T$ dry weight of particles removed from the Nitex mesh.

+++ standard deviation of 2 analyses

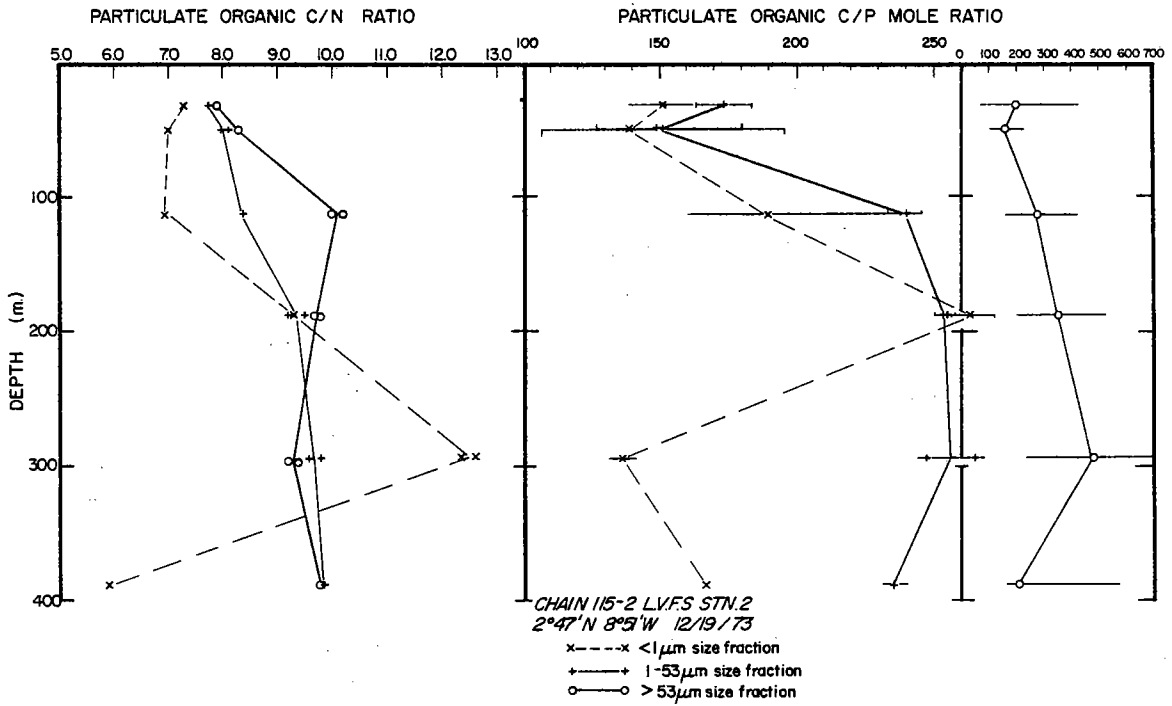
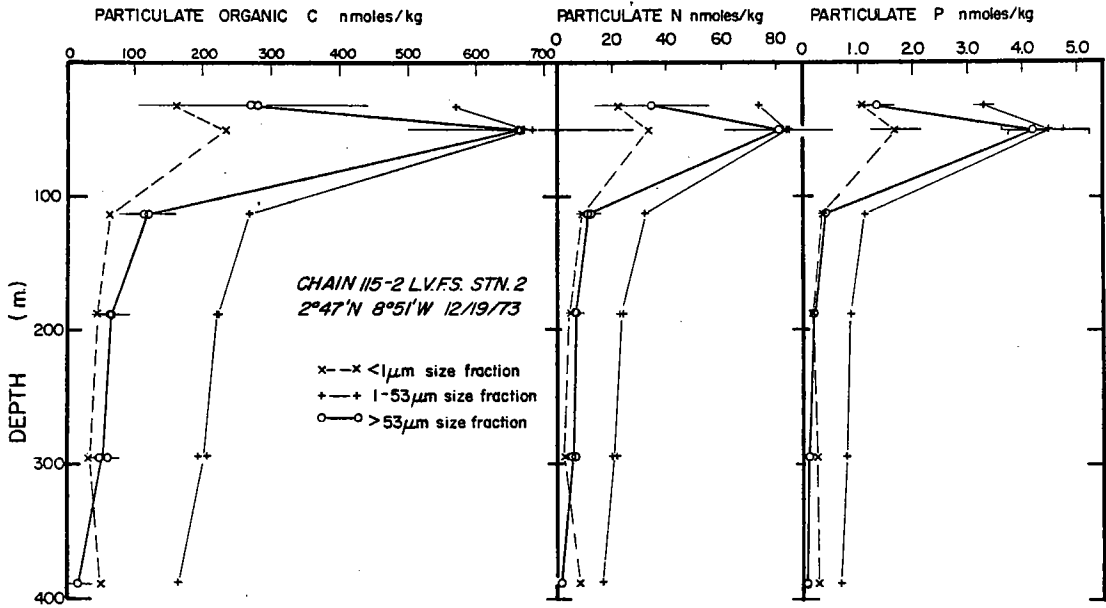
** carbonate contribution to ΣC is less than 2%

of C/P and C/N ratios in the 1-53 μ m fraction with those from Station 1 (12°06'N, 17°43'W) where the filters were not washed indicates no systematic effects attributable to washing (Appendix 0). In the absence of direct experiments, material loss due to washing is indeterminate and is assumed to be small.

All three size fractions display a pronounced maximum in the organic carbon, nitrogen, and phosphorous concentrations at 50 m coincident with the observed maximum population of plankton (Fig. 4). The largest change in concentration of these elements is observed to occur between 50 m and 113 m. The largest gradient is in the >53 μ m fraction and the smallest in the <1 μ m fraction indicating perhaps that filter-feeding organisms utilize the largest particles preferentially. Below 113 m the carbon, nitrogen and phosphorous concentrations decrease slowly with depth. The C/N and C/P ratios of the particles are a function of both size and depth being lowest in the <1 μ m fraction and highest in the >53 μ m fraction.

Bacteria may account for a significant fraction of the material in the <1 μ m fraction. Since elemental composition data are rare for marine bacteria (Vinogradov, 1953) the data for terrestrial species will be taken as typical: C/N = 5; C/P = 50-100 (Porter, 1946; Luria, 1961). Bacteria are found predominantly in association with phytoplankton (Sverdrup, Johnson and Fleming, 1942; Sorokin, 1973) and are frequently associated with maxima

Figure 2-4. Upper C_{org} , N, P profiles for the $<1\mu\text{m}$, $1-53\mu\text{m}$, and $>53\mu\text{m}$ size fractions. The concentration gradients between 50 and 113 m are largest for $>53\mu\text{m}$ and smallest for $<53\mu\text{m}$ particles indicating that grazing organisms strongly influence the particulate distributions over this depth interval. Two points indicate replicate analyses. Lower: Organic C/N and C/P ratios showing size and depth dependent behavior. Large error bars of the $>53\mu\text{m}$ C/P ratio is due to uncertainty in the recovery of material removed from the filter for C and N analysis.



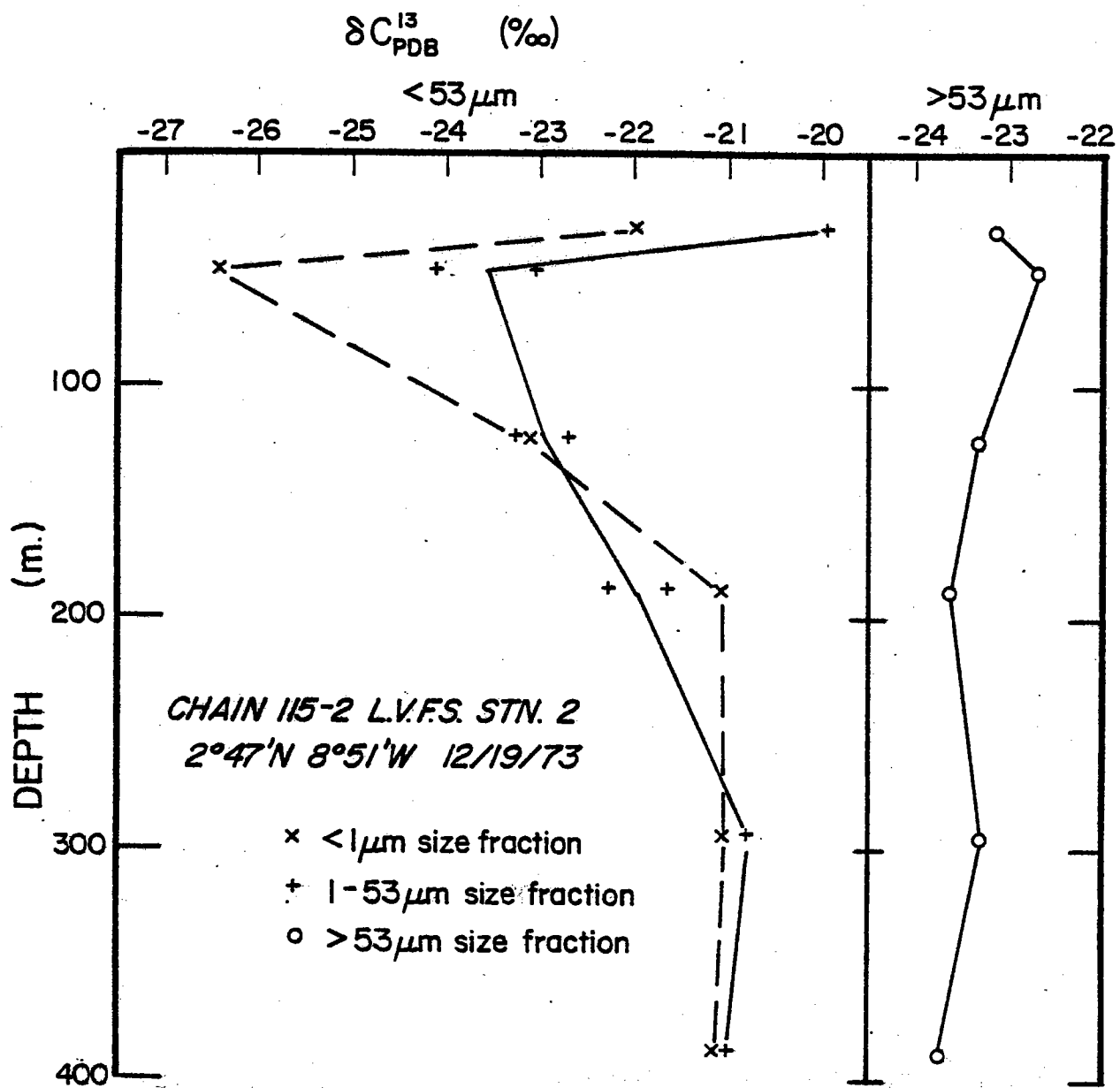
in zooplankton (Youghbluth, 1975), chlorophyll, and particulate matter located at the base of the mixed layer (Sorokin, 1973). Their presence could explain the lower C/N and C/P ratios in the $<1\mu\text{m}$ fraction compared to the larger fractions.

In the $1-53\mu\text{m}$ fraction the C/N ratio increases steadily below 32 m, indicating a 20% preferential loss of N relative to organic C. In contrast, phosphorous is 40% depleted relative to carbon between 50 m and 113 m and shows little further relative loss below this depth. In the $>53\mu\text{m}$ fraction 20% of the N and 50% of the P is lost relative to organic carbon between 50 and 113 m with little further change. It can be concluded from this that phosphorous is more easily lost from the organic fraction than nitrogen.

The $\delta^{13}\text{C}$ analyses were made because it was thought that the values would be a useful indicator of the organic composition of the particulate material. Labile components, such as amino acids have been shown to be C-13 rich relative to refractory organic compounds such as cellulose or "lignin" (Degens, Behrendt, Gotthardt and Reppman, 1968; Williams and Gordon, 1970).

The particulate data (Fig. 5) is complex. The $<53\mu\text{m}$ fractions both show a depletion in C-13 of 4% over the depth interval between 32 m and 50 m. The $>53\mu\text{m}$ fraction shows an increase of .7% over the same interval. This

Figure 2-5. $\delta^{13}\text{C}_{\text{PDB}}$ profiles for the organic carbon in the 3 size fractions. The strong 4‰ fractionation between 32 m and 50 m in the $<1\mu\text{m}$ and $1-53\mu\text{m}$ size fractions is probably due to the presence of bacteria.



behavior is unrelated to the C/N and C/P ratios, which are invariant. The $\delta^{13}\text{C}$ data for the $<53\mu\text{m}$ fractions is not an artifact of filter washing since the $<53\mu\text{m}$ samples analyzed at LVFS Stn. 1 (unwashed) exhibit similar behavior (Appendix 0).

Temperature effects (Sackett, Eckelman, Bender, and Bé, 1965), kinetic effects (Deuser, Degens, and Guillard, 1968), and species differences in plankton (Sackett, Eadie, and Exner, 1973) do not explain the variations observed at this station.

A marine bacteria Nitrosocystis cultured at 20°C was analyzed to have $\delta^{13}\text{C} = -35.7\%$. (Degens, Guillard, Sackett and Hellebust, 1968). If all marine bacteria exhibit the same C-12 enrichment and are an important component of the $<53\mu\text{m}$ fractions at 50 m, then it can be calculated that they comprise approximately 45% and 20% of the organic carbon present in the $<1\mu\text{m}$ and 1-53 μm fractions at 50 m. Sorokin (1973) reports bacterial biomasses in the tropical Pacific (7°N , 135°E ; upper 250 m) in the range between 200 and 950 nmoles $\text{C}_{\text{org}}/\text{kg}$ seawater, consistent with the LVFS data. The presence of marine bacteria in the $<1\mu\text{m}$ and 1-53 μm size fractions accounts for the observed $\delta^{13}\text{C}$ and for the CNP values. The interpretation of the character of the organic compounds present is therefore rather ambiguous. The carbon isotope variations in the particles at this station are quite unlike those reported by Eadie and Jeffrey (1973); the reasons for this difference are unknown.

Major ions: calcium, magnesium, and potassium

The uptake and transport by particles of the major ions of seawater is extremely difficult to study using the dissolved distributions of these elements in the water column. There have been no well documented cases reported for the non-conservative behavior of Na, K and Mg in the water column (Manglesdorf and Wilson, 1972). Ca and Sr show a maximum of 1% variation relative to salinity (Horibe, Endo, and Tsubota, 1974; Brass and Turekian, 1974). The study of these elements in particles is essential to the understanding of the mechanisms affecting their distributions in the water column.

Fig. 6 and Table 7 summarize the particulate distributions of calcium and carbonate in the water column. The $>53\mu\text{m}$ fraction contains 30% and 10% of the total above and below 100 m respectively. Light microscopic and SEM studies show that whole organisms account for most of the carbonate present at 32 m and 50 m, whereas, fragments dominate below 50 m in both 1-53 m and $>53\mu\text{m}$ size fractions. Furthermore, calcium carbonate is the dominant calcium phase in the particles accounting for greater than 80% of the acid leachable calcium; any calcium in excess of carbonate is termed "excess". The $\text{Ca}^{2+}/\text{CO}_3^{=}$ and excess calcium profiles (Fig. 6) show that excess calcium is rapidly lost from the $>53\mu\text{m}$ fraction in the upper 100 m. The 1-53 μm fraction shows excess calcium particularly at

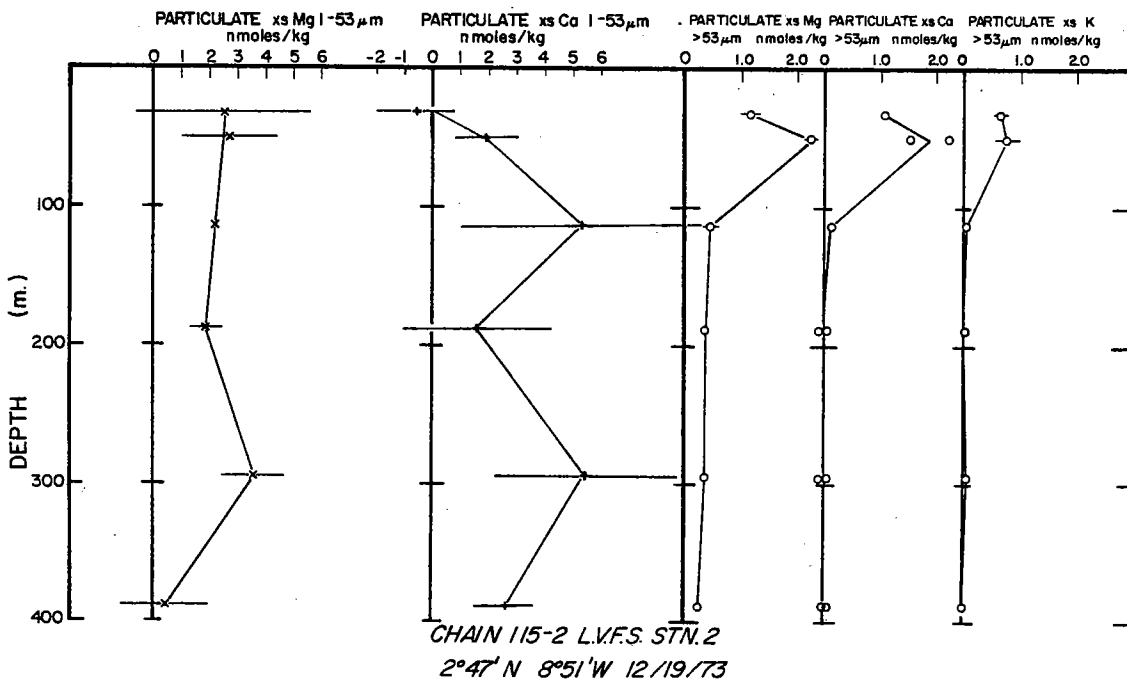
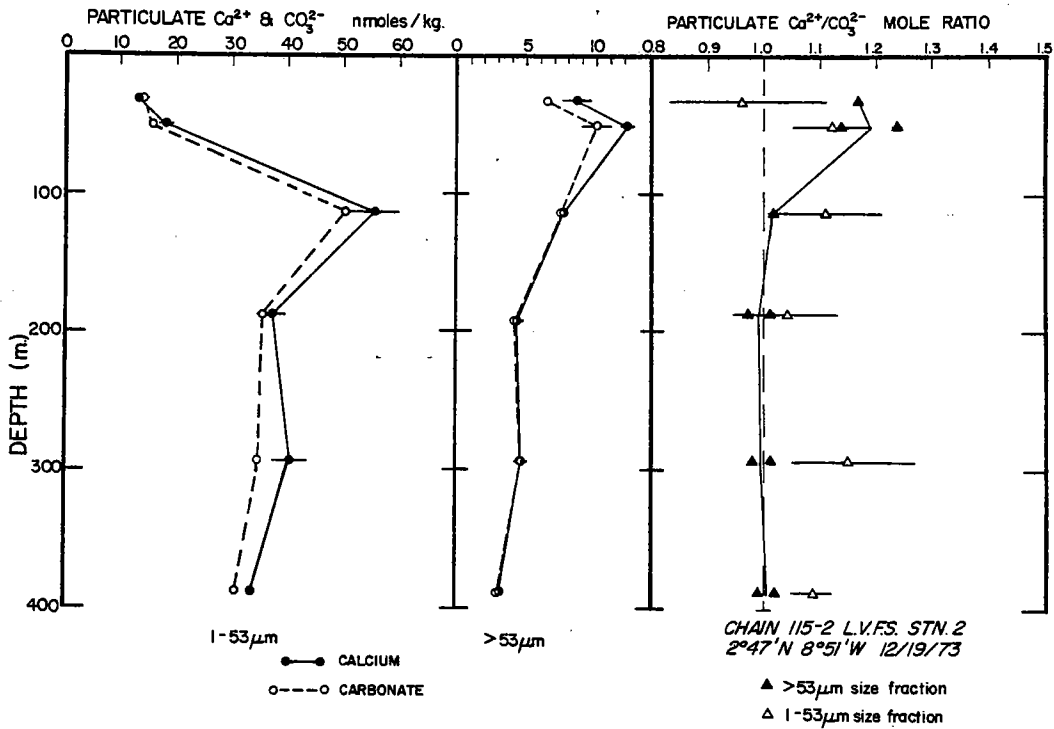
TABLE 7 : PARTICULATE Ca, Carbonate, Mg, K, Sr, and Si
>53 μm SIZE FRACTION (nmoles/kg)

z	C _i	Ca	xS	Ca	C _i /C ₁	Ca/C ₁	Ca _{XS} /C ₁	Ca _{XS} /C _{Ca}	Ca _{XS} /C _{Ca}	Na	xS	Mg	Mg _{XS} /C _{Mg}	K _{XS}	K _{XS} /C _K	Y _{XS} /C _Y	Sr	Sr _{XS} /C _{Sr}	Sr*	Si	Si/C _{Si}
32	a 6.36 b 7.26 c	7.43	1.07	8.5	/1.2	1.7	/1.4	a 33.4 b 40.6 c 26.2	1.14	1.14	1.14	1.17	0.13	0.77	0.63	0.12	0.674	0.674	0.663	d 6.14 e 6.93	6.5/0.6
50	a 9.29 b 10.80 c	11.49	2.20	12.3	/0.7	2.3	/1.3	a 8.55 b 19.1 c 17.8	2.17	2.37	2.25	2.23	0.11	0.50	0.73	0.20	1.045	1.13	1.11	d 25.27 e 25.90	25.6/0.4
113	a 7.49 b 7.18 c	7.62	0.13	7.5	/	7.7	/0.6	a 3.48 b 1.19 c 2.01	0.41	0.38	0.63	0.47	0.14	0.04	0.03	0.01	0.106	0.123	0.110	d 10.75 e 10.27	10.5/0.3
188	a 4.03 b 4.28 c	4.08	0.05	4.2	/0.2	4.4	/0.4	a 2.78 b 3.02 c 3.52	0.32	0.31	0.43	0.37	0.06	0.01	0.014	0.02	0.099	0.078	0.072	d 5.76 e 8.29	7.0/1.8
294	a 4.12 b 5.20 c	4.17	0.05	4.7	/0.8	4.7	/0.4	a 2.06 b 4.31 c 2.00	0.38	0.45	0.27	0.37	0.08	0.01	0.04	0.04	0.053	0.042	0.034	d 5.10 e 5.23	5.2/0.1
388	a 3.11 b 2.85 c	3.18	0.07	3.0	/0.2	3.4	/0.6	a 1.02 b 0.88 c 2.97	0.27	0.27	0.25	0.26	0.01	-0.02	0.00	0.03	0.045	0.043	0.038	d 3.64 e 4.58	4.1/0.7
32	a 13.1 b 14.6	13.9	/1.1	13.3	/0.9	-0.6	/1.4	b 106.6 c 120.0	0.3	4.7	2.5	/3.1	0.35	0.30	/0.07	0.28	f 20.8	0.25			
50	a 15.8 b 17.0	15.8	/	17.7	/1.1	1.9	/1.1	b 136.0 c 134.0	1.5	3.9	2.7	/1.7	0.32	0.30	/0.02	0.28	f 28.4	0.29			
113	a 51.1 b 50.0 c	51.1	58.5	50.3	/0.7	55.6	/4.2	b 21.6 c 21.5	2.2	2.1	2.15	/0.07	0.39	0.40	/0.01	0.31	f 32.2	0.41			
188	a 35.4 b 35.8 c	35.4	39.6	35.6	/0.3	37.2	/2.6	b 39.0 c 34.2	1.7	1.4	1.9	/0.6	0.226	0.218	/0.007	0.156	f 18.0	0.214			
294	a 35.8 b 35.8 c	35.8	42.6	35.0	/0.6	40.4	/3.0	b 21.8 c 14.4	4.4	2.8	3.6	/1.1	0.185	0.190	/0.007	0.131	f 22.8	0.195			
388	a 30.4 b 30.4 c	30.4	32.3	30.4	/0.0	33.0	/1.0	b 135.6 c 156.9	1.2	1.5	0.4	/1.6	0.116	0.109	/0.006	0.053	f 13.8	0.106			

Means/ standard deviations are calculated for multiple analyses
 xs - remaining element after filter blank and seasalt corrections (Mg, K, Sr) e 0.4 M Na₂CO₃ f, 10 M NaOH, 0.4 μm Nucleopore filter
 and carbonate correction (Ca).
 C_i - carbonate carbon Sr* = Sr - 0.0017C_i - non carbonate Sr
 a 20% H₃PO₄ b, 2.2M Acetic acid c, 0.6 N HCl d, 1 M NaOH

Figure 2-6 Upper: Calcium and carbonate in the 1-53 μ m and >53 μ m size fractions showing excess calcium.

Lower: Excess magnesium, calcium, and potassium in the two size fractions. Excess Mg and K are the remaining anomalies in the Mg and K data after correction for filter blank and seasalt (using Na data); xs Ca is the anomaly after filter blank, seasalt, and CaCO₃ is subtracted.



294 m. The excess calcium in the samples above 100 m is probably contained in the cytoplasm of living organisms as the C_{org}/Ca ratios are typical for plankton ($C_{org}/Ca = 160$, Mayzaud and Martin, 1975); the excess calcium at 294 m in the 1-53 μ m fraction is high ($C_{org}/Ca = 30$).

The LVFS samples consistently contain particulate magnesium. Correction of the total magnesium content of the filters for blank and sea salt (using the Na data) always leaves a residual amount of magnesium (defined as "excess" magnesium). In many cases this excess magnesium is several times higher than the blank levels (Table 3). Particulate magnesium has been reported in particles in the deep water of the Gulf of Mexico (Feely, 1975), and in the North Atlantic by Spencer, Brewer, and Bender (in press). The values of "excess" magnesium leachable by acid (Feely, 1975) and total magnesium (Spencer, Brewer and Bender, in press) are similar, suggesting that the bulk of particulate magnesium is acid leachable.

Like excess calcium, excess magnesium in the >53 μ m size fraction shows a maximum at 50 m; unlike excess calcium, excess magnesium is present in the particles below 100 m. In the 1-53 μ m size fraction the profiles of excess magnesium and calcium are similar and, relative to organic carbon, excess magnesium is progressively enriched with depth from a mole ratio of 0.4% to approximately 2% in both size fractions.

Feely (1975) suggested that excess magnesium is present in particles as MgCO_3 . However the $\text{Mg}^{+2}/\text{CO}_3^{-2}$ mole ratio is 20% and 10% above and below 100 m respectively in both size fractions, much greater than the reported values for coccoliths (0.4%, Thompson and Bowen, 1969) and Foraminifera (0.5%, Emiliani, 1955) which are the major carbonate phases in both size fractions. Hence carbonate cannot be the major magnesium phase.

Excess potassium is lost from the $>53\mu\text{m}$ particles in the upper 100 m and behaves like excess calcium, being typically found in the cytoplasm of organisms (M.N. Hughes, 1972). Potassium was not analyzed in the $<53\mu\text{m}$ size fraction because the blank levels were highly variable and exceeded the amounts of potassium expected to be present in the particles.

Ion Exchange and acid leaching experiments

A series of experiments was designed to test whether or not the excess calcium and magnesium observed in the 1-53 μm fraction at 294 m were bound by ion-exchange.

Two 45 mm diameter disks were cut from the top glass fiber filter of this sample (chosen because it had the greatest excess Ca and Mg) and tightly clamped in an acid-leached distilled water-rinsed 47 mm Millipore glass filtration apparatus (effective filtration diameter 35 mm). 100 mls of $10^{-4.5}\text{N}$ NaOH solution was allowed to drip through the filter pair to dissolve the residual sea salt. Further

10 ml aliquots of this solution were allowed to drip through the sample, each for approximately 1 minute before its remaining solution was sucked through the filter using reduced pressure, each aliquot was saved for later analysis. Then fourteen 10 ml aliquots of 0.05 M MgCl_2 (in $10^{-4.5}$ N NaOH) were allowed to drip through the filters in the same fashion. An identical sequence of washes was used to treat two 45 mm disks cut from the bottom glass fiber filter of the 294 m sample. Ten mls of the MgCl_2 solution were added to the $10^{-4.5}$ N NaOH aliquots and similarly ten mls of $10^{-4.5}$ N NaOH were used to the MgCl_2 aliquots. Calcium, strontium, and potassium standards were prepared in the same MgCl_2 -NaOH matrix solution and all aliquots and standards were analyzed for these elements by flame atomic absorption spectroscopy.

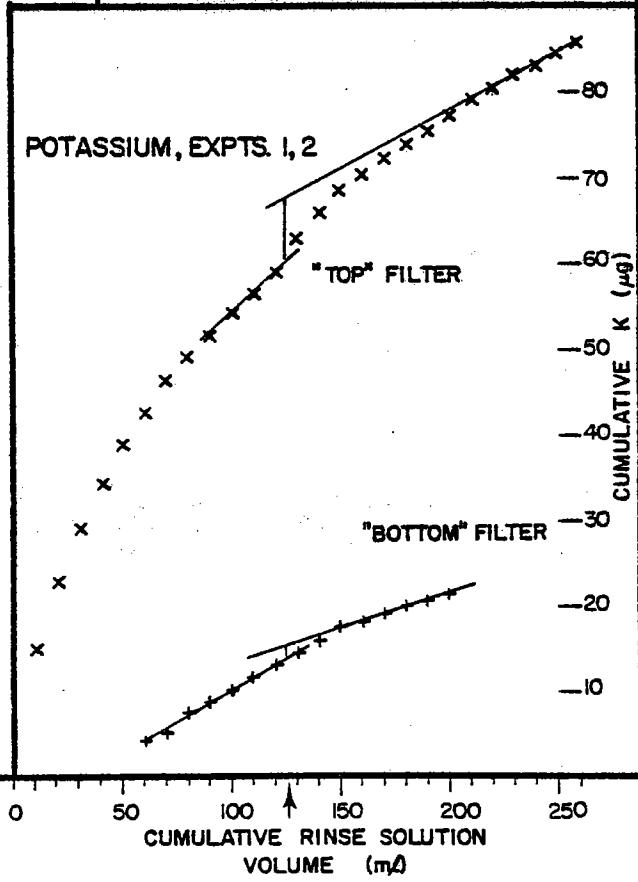
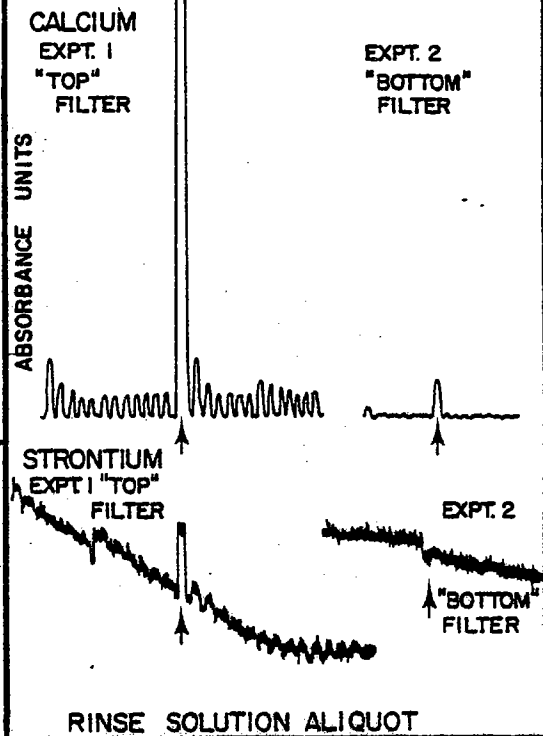
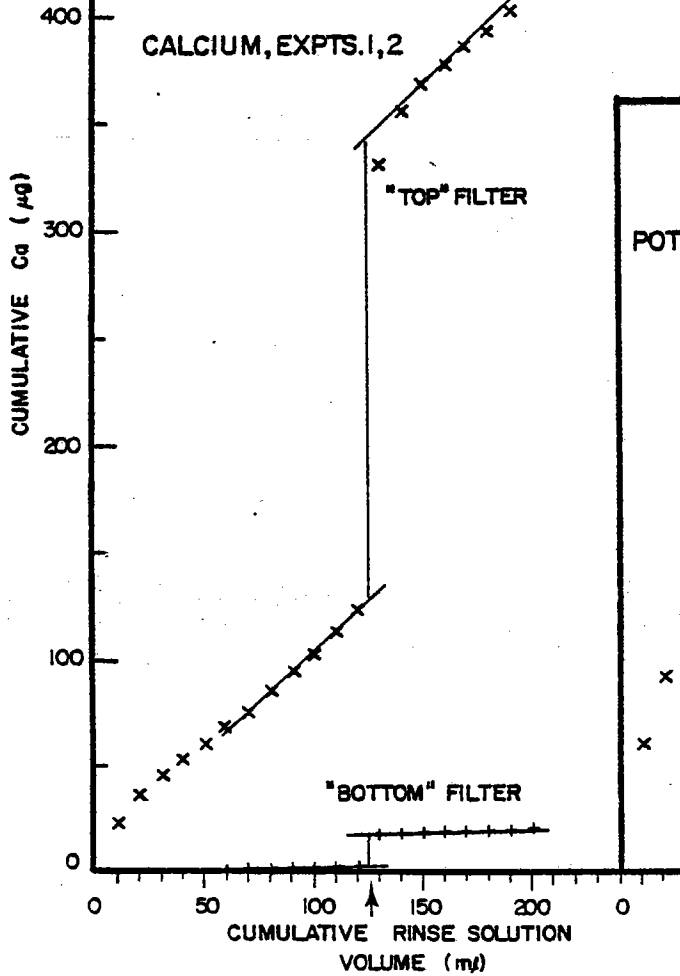
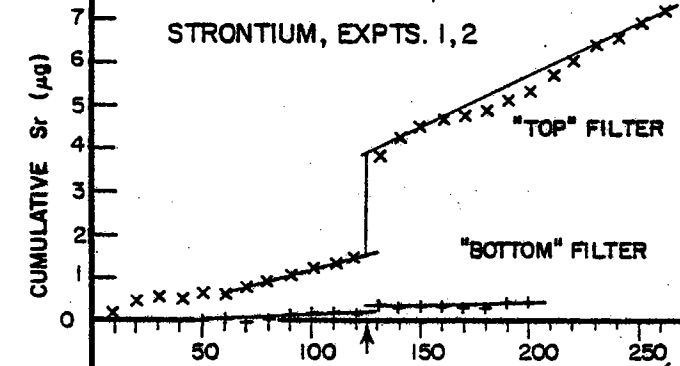
The cumulative analyses for Ca, Sr, and K are plotted against cumulative rinse solution volume (Fig. 7). The first aliquot of the 0.05 M MgCl_2 rinse solution was greatly enriched in calcium and strontium relative to aliquots immediately preceding and following it (see inset, upper right hand part of Fig. 7). The plots of cumulative Ca and Sr exhibit a sharp increase coinciding with the first MgCl_2 aliquot. The cumulative plots then become linear upon completion of ion-exchange. The quantity of ion-exchanged cations was calculated by extrapolating the linear portions of the cumulative plots to the point of the first MgCl_2 aliquot. The vertical separation of the two lines at

Figure 2-7. Ion exchange experiments for calcium, strontium, and potassium. The chart recorder output from the flame AA analysis of the rinse solutions for calcium and strontium is shown in the upper right portion of the figure. The $10^{-4.5}$ N NaOH aliquots are to the left of the big peak which corresponds to the first 0.05 M MgCl_2 in $10^{-4.5}$ N NaOH aliquot. "Top" and "Bottom" correspond to 1-53 μm and $<1\mu\text{m}$ samples from 294 m. The rest of the figure shows the cumulative data plots used to calculate the ion-exchangeable Ca, Sr, and K in the sample. $1/26^{\text{th}}$ of the filter was used for these experiments.

ION EXCHANGE EXPERIMENTS

294m <math> < 53 \mu\text{m}</math> size fraction
 CHAIN 115 L.V.F.S. STN. 2
 2°47'N 8°51'W 12/19/73

First 10mL rinse with 0.05M MgCl_2 (pH.9.5)



this point divided by the area fraction of the filter subsample gives the total quantity of cations bound by ion-exchange for the whole filter. The concentration of cations ion-exchanged on the particles is the difference between the values for the top and bottom glass fiber filter samples. The results of these experiments (1 and 2) are summarized in Table 8.

A similar experiment for Mg was performed on separate filter samples using $10^{-5.7}$ N NaOH aliquots and 0.05M CaCl_2 in $10^{-5.7}$ N NaOH aliquots (Table 8, Expts. 3 and 4). Total exchange capacity of the material was determined by a further experiment in which the calcium was ion-exchanged with 0.1 M NaCl in $10^{-5.7}$ N NaOH solution (Experiments 5 and 6).

The results of experiments 1-4 showed that $\sim 100\%$ of the excess calcium and 17% of the total strontium was bound by ion exchange; little potassium and no magnesium were bound in this fashion. The total ion-exchange capacity of the particles inferred from these results was 96 meq./100 gms. Experiments 5 and 6 have identical results for the exchange capacity of the bottom filter, but gave a lower exchange capacity for the particles on the top filter of 71 meq./100 gms. This result could be low for two reasons: possible degradation of the organic matter which may be the ion-exchanger, and increased rate of dissolution of CaCO_3 due to the lower pH (8.3) used in experiments 3-6.

TABLE 8

ION EXCHANGE EXPERIMENTS pH > 8

(CHAIN 115-2 LVF3 ST# 2, <53µm SAMPLE, z = 294m)

EXPT	SAMPLE	WASH SOL ^N	pH (NaOH)	millimoles of cations exchanged	EXC. meq.	
				Mg ²⁺ Ca ²⁺ Sr ²⁺ K ⁺		
1	"TOP"	0.05 M MgCl ₂	9.5	W 0.142	0.00066 <0.005	0.291
2	"BOTTOM"	0.05 M MgCl ₂	9.5	A 0.0097	0.00002 <0.001	0.0204
1-2	NET EXCHANGE			H 0.132	0.00064 <.004	0.271
3	NEW "TOP"	0.05 M CaCl ₂	8.3	W 0.018	Blank levels	0.036
4	NEW "BOTTOM"	0.05 M CaCl ₂	8.3	A 0.020	too high	0.040
3-4	NET EXCHANGE			H -		-0.004
5	FROM 3	0.1 M NaCl	8.3	>.128	0.0002	>0.261
6	FROM 4	0.1 M NaCl	8.3	0.0013	0.0000	0.062
5-6	NET EXCHANGE			+0.0013	0.0002	>0.199
1,3	SUMMARY TOP			0.0206	0.00066 <.005	0.331
2,4	SUMMARY BOTTOM			0.0213	0.00002 <.001	0.063
	SUMMARY NET EXCHANGE			-0.0007	0.00064 <.004	0.268
	ION-EXCHANGED n moles/kg			-0.08	0.032	0.18
	OBSERVED n moles/kg			3.6 [±] 1.1	5.4 [±] 3.1	0.19
	ION-EXCHANGED/OBSERVED			-0.022	1.13	0.17

Mg is not exchanged under these conditions

at least 70% of xs Ca is ion-exchanged

and 17% of total Sr is ion-exchanged

Aluminosilicate material cannot make an important contribution to the ion exchange capacity of the particles of this sample since over 90% of the total dry weight of the material is biogenic (Table 4). The surface sediments below Station 2 are typically 40% kaolinite, 30% illite, 20% montmorillonite and 10% chlorite in the $<2\mu\text{m}$ carbonate free fraction (Goldberg and Griffin, 1964). The ion exchange capacity of this material is calculated to be 22 meq./100 gms (Bear, 1964). The maximum contribution by aluminosilicates to the total exchange capacity of the particles is therefore less than 3 meq./100 gms.

Bear (1964) has shown that the ratio of monovalent to divalent cations bound on an ion-exchanger in equilibrium with a solution of constant relative ionic composition is a function of the ionic strength of that solution. Ion-exchangers take up divalent in preference to monovalent cations as the ionic strength of the solution is decreased. Washing the particulate matter with distilled water may have changed the relative amounts of bound cations; however, the analyses of the samples from CHAIN 115-2 LVFS Stn. 1 (Appendix 0) revealed excess calcium averaging 3 nmoles kg^{-1} below 50 m indicating that the effect is real and not an artifact of the filter washing procedure.

The samples used in experiments 3-6 were treated with further sets of rinse aliquots: $10^{-5.7} \text{ N NaOH}$ (pH=8.3), laboratory distilled water (pH 5.5), and 10^{-3} N HCl (pH=3.0)

to determine the conditions necessary for the release of the particulate magnesium. The Mg/Ca ratios measured in the wash aliquots from experiment 5 varied between 1.5 and 2 mole percent. The pH 8.3 aliquots from this series of experiments showed an initial value of 14% with subsequent aliquots falling between 3 and 6%; rinse aliquots at pH 5.5 showed little change in the Mg to Ca mole ratio; aliquots of the pH 3 solution showed sharp increase in the magnesium concentration relative to previous aliquots and the Mg/Ca mole ratio rose from 6% to over 30% and fell back to values of near 16%. From the point of the first pH 3 aliquot, a total of 28 μ gs of magnesium was lost from the filter subsample, this was equivalent to 0.8 mgs of magnesium lost from a full sized filter and corresponded to approximately 40% of the excess magnesium observed at 294 m in the 1-53 μ m fraction. The results of this experiment, although not quantitative, clearly demonstrate that Mg is not present as carbonate in particulate matter. The loss of Mg from the particles proceeds extremely slowly at pH 5.5 and it is only at pH 3 that most of the magnesium (in excess of filter blank) is lost from the particles. Phosphate analysis of the pH 3 rinse solutions showed no phosphate accompanying the magnesium. In living organisms magnesium is used in DNA synthesis and some enzymatic reactions; magnesium is bound in the porphyrin ring of chlorophylls and is possibly important in maintaining the structure of cell walls

(M.N. Hughes, 1972). The particulate C_{org}/Mg mole ratio in the surface waters is 250/1 and compares well with the plankton analyses of Mayzaud and Martin (1975), $C_{org}/Mg = 350$. The C_{org}/Mg ratio decreases to values between 100 and 50 below 200m. If Mg is organically bound, then its carrier is progressively enriched in the organic material in both size fractions. It is unlikely that aluminosilicates are a source for the magnesium since their structures should not be degraded by the chemical conditions of this experiment.

Brewer, Wong, Bacon and Spencer (1975) have postulated that the oxidation of one mole of Redfield-Ketchum-Richards (1963) model plankton $((CH_2O)_{106}(NH_3)_{16}(H_3PO_4)_1)$ would yield sixteen moles of nitric acid which would "titrate" the seawater in the deep ocean and lower its alkalinity. Table 9 lists the depth dependence of the cation composition of the organic matter in both size fractions normalized to 106 atoms of carbon (the number used in Redfield model plankton). The table shows that the samples at 32 and 50 m are low in cation content; the ratio of total equivalents of cations to nitrogen is in the range of 0.08 to 0.15 for these samples. Below 50 m, this ratio has the range: 0.11 to 0.36 (0.18, average), for the $>53\mu m$ fraction, 0.30 to 0.86 (0.54 average) for the $1-53\mu m$ fraction. This data shows that cations are an important component of the organic fraction in the deeper samples.

TABLE 9

C, N, P, CATION RELATIONSHIPS IN PARTICLES
 NORMALIZED TO 106 ATOMS OF C

>53 μ m SIZE FRACTION

Z	C _o	N	P	$\overline{xsCa}/\sigma_{xsCa}$	$\overline{xsMg}/\sigma_{xsMg}$	\overline{xsK}
32	106	13.3	0.51	0.41/ -	0.45/.05	0.24
50	106	12.9	0.67	0.30/.08	0.36/.02	0.12
113	106	10.5	0.37	0.12/ -	0.43/.13	0.03
188	106	10.9	0.29	-0.05/.19	0.61/.11	0.02
294	106	11.1	0.21	-0.05/.19	0.70/.15	0.08
388	106	10.7	0.49	0.17/.43	1.75/.06	0.00

1-53 μ m SIZE FRACTION

32	106	13.7	0.61	-0.11/0.15	0.50/0.54	-
50	106	13.2	0.71	0.30/0.17	0.42/0.27	-
113	106	12.7	0.44	2.10/1.70	0.85/0.03	-
188	106	11.3	0.42	0.77/1.24	0.91/0.27	-
294	106	11.0	0.41	2.85/1.64	1.90/0.58	-
388	106	10.7	0.45	1.68/0.64	0.28/1.03	-

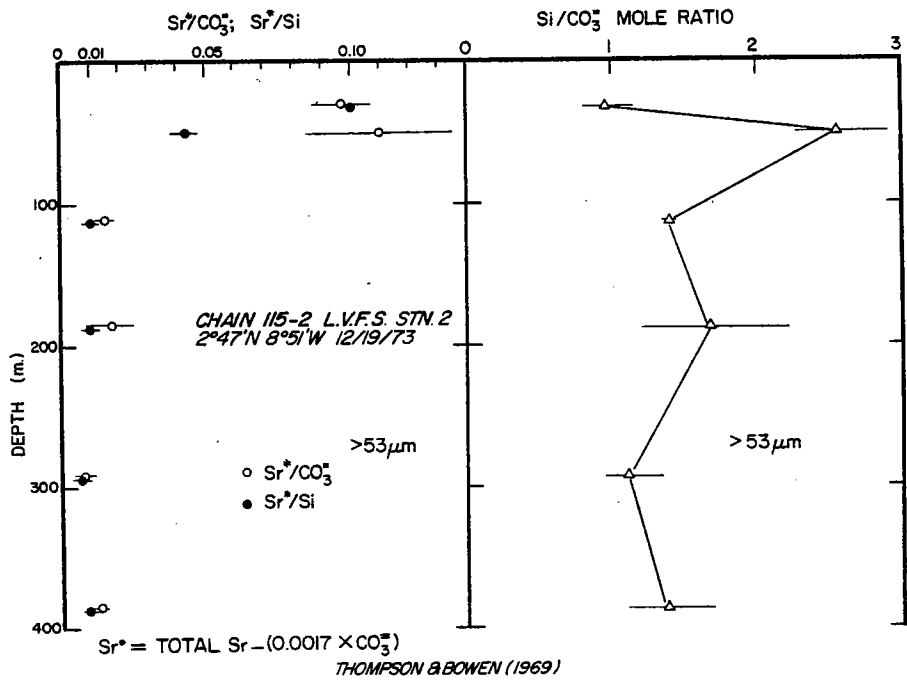
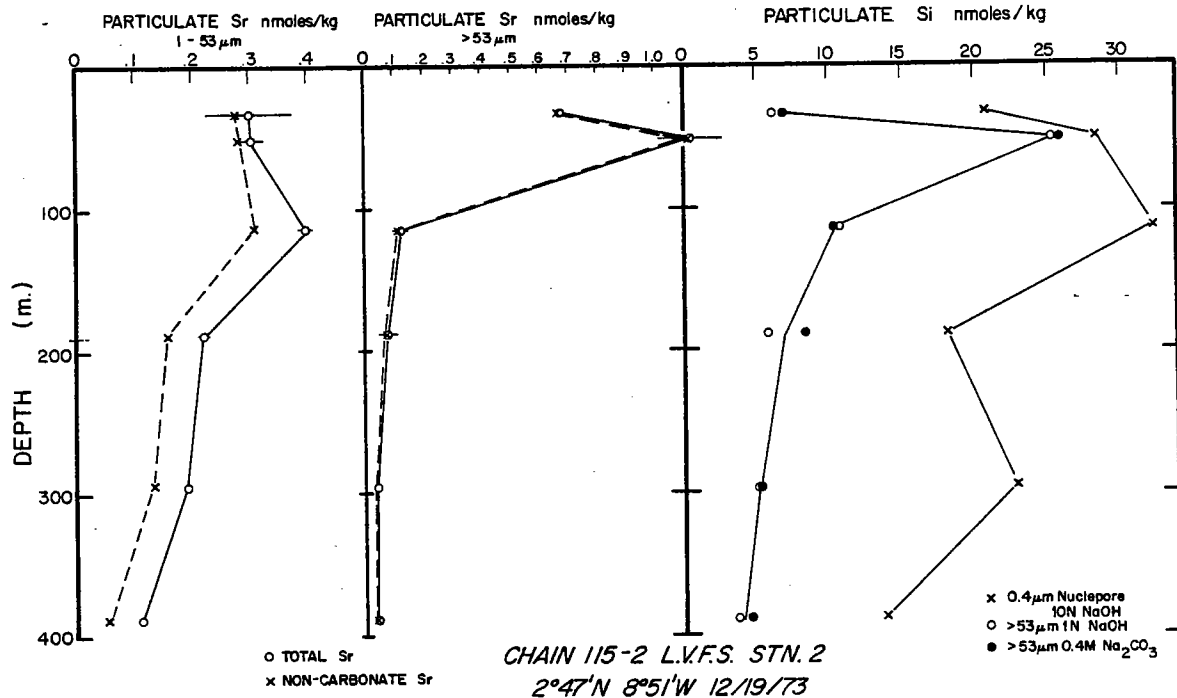
If we assume that the $>53\mu\text{m}$ particles are reactive with the water column, then our data indicates that the reduction of alkalinity due to oxidation of organic matter is 80% that proposed by Brewer, Wong, Bacon, and Spencer (1975). Similarly, for the $1-53\mu\text{m}$ particles, the reduction of alkalinity would be only 50% of that proposed. This compensating effect is due to cations occupying negative sites on organic matter instead of protons. We have demonstrated that there is a change in the C, N, P, and cation content of the particulate matter within the upper 400 m of the water column. It is there that the major anomalies of calcium and alkalinity will probably occur.

Silicon

Fig. 8 shows the particulate Si profiles for the $>53\mu\text{m}$ fraction and for the $0.4\mu\text{m}$ Nuclepore filtered samples. The "bulk" suspended silicate concentration determined by Nuclepore filtration of twenty liter samples is approximately 20-30 nmoles/Kg and compares well with the lowest particulate silicate values (range 19-580 nmoles Si/kg, mean 110 nmoles Si/kg) reported by Copin-Montegut and Copin-Montegut (1972). The difference between the analyses of the $0.4\mu\text{m}$ Nuclepore filters and the $>53\mu\text{m}$ fraction is considered to be representative of the $1-53\mu\text{m}$ fraction, especially in the near surface samples. Therefore it is inferred that the $1-53\mu\text{m}$ Si profile has the same characteristics as the

Figure 2-8. Upper: Silicate in $>53\mu\text{m}$ fraction and from $0.4\mu\text{m}$ Nuclepore filter samples; total strontium and non-carbonate strontium (Sr^*) in $>53\mu\text{m}$ and $<53\mu\text{m}$ fractions.

Lower: Strontium (Sr^*), carbonate and silicate ratios in $>53\mu\text{m}$ size fraction.



1-53 μ m carbonate profile with the exception of the 32 m samples. SEM showed whole diatoms to be the most abundant contributors to opaline silica in the 1-53 μ m fraction at 32 m and 50 m whereas, diatom fragments predominate in the deeper samples. The results of the 1.0 N NaOH and 0.4 M Na₂CO₃ analyses of the >53 μ m fraction were identical.

Strontium

Particulate strontium occurs in three phases: carbonate, celestite and organics.

Thompson and Bowen (1969) and Emiliani (1955) have shown coccolith ooze and Foraminifera to contain 0.17 mole percent Sr. Total strontium analyses were corrected using the carbonate data and the above factor to give non-carbonate strontium, Sr*.

$$\text{Sr}^* = \text{Total Sr} - 0.0017 (\text{carbonate}) \quad (1)$$

From Fig. 8 the 1-53 μ m fraction is progressively depleted in Sr* with increasing depth to less than 50% of the total. However the >53 μ m fraction is composed mainly of non-carbonate strontium. Celestite (SrSO₄) is the major structural component of Acantharia (Bottozzi, Schreiber and Bowen, 1971). SEM and light microscopic studies showed the >53 μ m and <53 μ m fractions to contain whole Acantharia and their fragments respectively.

It was suggested above that 17% of the total strontium in the 1-53 μ m fraction is bound in ion-exchangeable positions on the organic matter at 294 m. This may occur at other depths as well.

Celestite is extremely soluble in seawater; Brass and Turekian (1974) suggest from profile data that Sr is involved in a shallow regenerative cycle similar to phosphate. Thus the order of magnitude decrease of the Sr*/Si and Sr*/CaCO₃ ratios with depth (Fig. 8) may be largely due to dissolution of SrSO₄. However, the Sr*/Si and Sr*/CaCO₃ profiles also reflect the transfer of carbonate, opal, and celestite between the <53 μ m and >53 μ m fractions. Unlike Acantharia (celestite) which occur only in the >53 μ m fraction, coccolithophorids (carbonate) and diatoms (opal) are found in the <53 μ m fraction. The action of filter feeding organisms transfers diatom and radiolarian (opal), foraminiferan (carbonate), and acantharian (celestite) components to the 1-53 μ m fraction by fragmentation; at the same time, the >53 μ m fraction becomes enriched with coccoliths and diatom fragments by aggregation (see below). Thus, loss of strontium from the >53 μ m size fraction by dissolution (and fragmentation) and gain of small carbonate and opal particles from the <53 μ m fraction together determine the Sr*/Si and Sr*/CaCO₃ ratios in the >53 μ m fraction as a function of depth. In contrast, the Si/CaCO₃ mole ratio in the >53 μ m fraction is essentially constant (approximately

Plate 2

Scanning electron micrographs of Acantharia on 53 μ m filters from 32, 50 and 113 m showing effects of dissolution. Scale indication is the same as for Plate 1.

- A. Acantharian of the genus Amphibelone, 32 m.
- B. Enlargement of lower middle spicule of 2 C. Note membranous coating and well-defined edges of the spine, 32 m.
- C. Polar view of Tetralonche Haeckel. Upper portion is thickly coated with mucoid material, 32 m.
- D. Amphibelone sp. similar to 2A and portions of Radiolarian inner capsule, 50 m.
- E. Enlargement of upper left spine, 2F, 50 m.
- F. Equatorial view of Tetralonche, 50 m.
- G. Remains of Tetralonche and portions of two centrate diatoms, Coscinodiscus and Bacteriastrum, 113 m.
- H. Enlargement of 2I. Note: dissolution causes fine structure to appear at edges of spicule in comparison to 2B, 113 m.
- I. Astrolithium heavily coated with debris, 113 m.

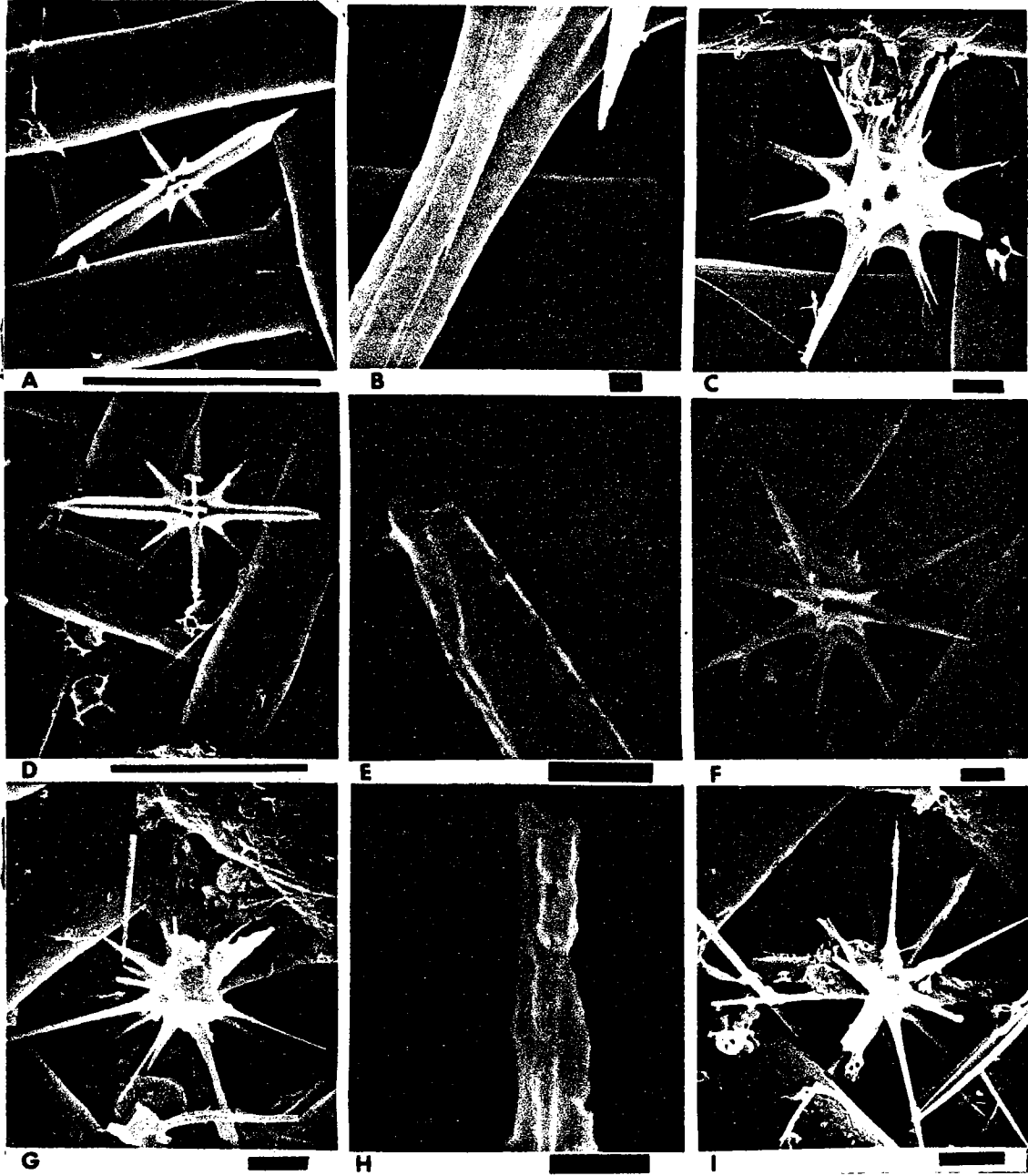
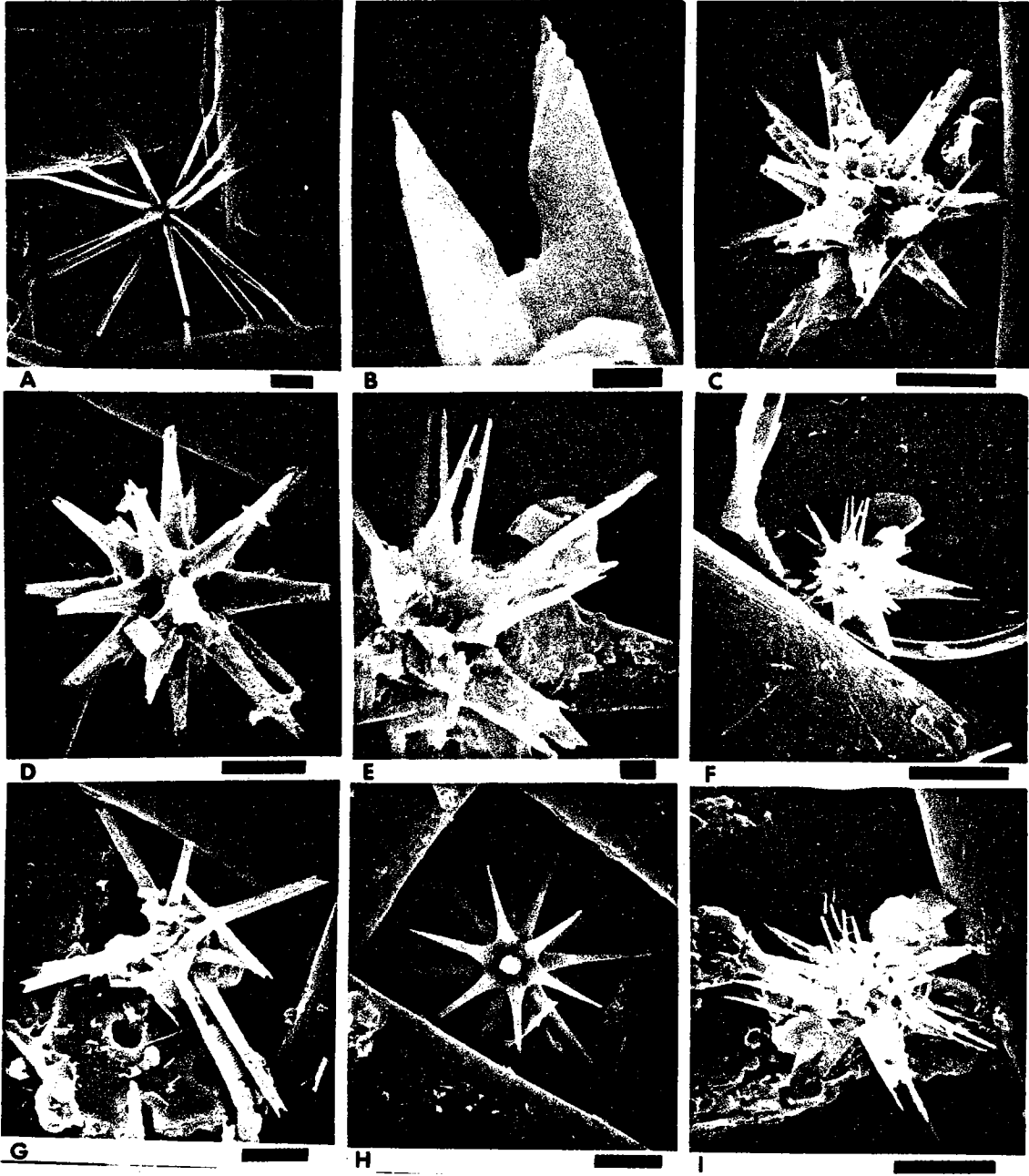


Plate 3

Scanning electron micrographs of Acantharia on 53 μ m filters from 188, 294 and 388 m showing effects of dissolution. Scale indication is the same as for Plate 1.

- A. Acantholithium Sp., with equally, radially arranged spicules, 188 m.
- B. Enlargement of 3C, spicule exhibits double point structure as a result of etching, 188 m.
- C. Acantharian that has lost primary features of spicules due to dissolution and fragmentation. Central area is obscured by tests and debris, 188 m.
- D. Partially dissolved acantharian of the family Stauracanthidae. Note additional opposed spines on major spicules, 294 m.
- E. Enlargement of 3F, showing well developed double point structure due to dissolution, 294 m.
- F. Acantharian with associated organic debris. Remains of a centrate diatom frustule are in the background, 294 m.
- G. Remaining structure of acantharian with non-articulating spicules; probably a member of the family Acanthochiasmidea. Sections of protozoan tests are below the acantharian, 294 m.
- H. Well-preserved Astrolithium bulbiferum, 388 m.
- I. Largely dissolved acantharian with debris in background, 388 m.



1.0) except at 50 m where an increased population of diatoms and Radiolaria exists.

If dissolution of SrSO_4 were the primary process governing the $\text{Sr}^*/\text{CaCO}_3$ and Sr^*/Si ratios then a dramatic change in the preservation of the Acantharia should occur between 50 m and 113 m. The SEM showed the Acantharia at 32 m and 50 m to be well preserved except for mechanical damage (Plate 2, A-F). At 113 m (Plate 2, G-I) most Acantharia structures are virtually undamaged except by breakage but the organic membrane seen to be coating the spines of the Acantharia at 32 m and 50 m is absent in many cases. There is some etching of the spines of a few Acantharia sampled at this depth (Plate 2, H-I), but the extent of dissolution is almost negligible; i.e., ~1%. At 188 m (Plate 3, A-C) there is a larger proportion of mechanically damaged Acantharia and some spines clearly show the effects of dissolution (Plate 3, B-C); a double point structure is observed at the ends of the etched spines. Well preserved Acantharia are common and the extent of dissolution at 188 m is estimated to be only 10%. At 294 m some Acantharia (Plate 3, D-G) are poorly preserved with the "double point" etching pattern having progressed almost the whole length of some spines; an estimated 20-40% dissolution has occurred at this depth. Finally, at 388 m some Acantharia are barely recognizable because of the almost complete dissolution of their spines (Plate 3, I). A few

relatively well preserved Acantharia are also observed at this depth (e.g. Plate 3, H); close examination of their spines also shows the beginnings of the double point etching pattern. Between 50% and 75% of the strontium has been lost from the Acantharia due to dissolution above 400 m with most dissolution occurring at depths below 200 m. Thus the strong gradient in the $\text{Sr}^*/\text{CaCO}_3$ and Sr^*/Si mole ratios between 50 m and 113 m is not due to the dissolution of SrSO_4 but due to the transfer of carbonate, opal, and celestite fragments between the $<53\mu\text{m}$ and $>53\mu\text{m}$ fractions.

Iron

The concentrations of iron in the $1-53\mu\text{m}$ and $>53\mu\text{m}$ fractions are highest at 32 m; only the $<1\mu\text{m}$ fraction exhibits the familiar 50 m maximum. The Fe values (hydroxylamine-hydrochloride, hydrochloric acid leach, Table 10, Fig. 9) average 4.4 ± 1.5 (σ) nmoles Fe/kg and compare well with the values (bulk analysis using INAA of samples from 30% Niskins) of Spencer and Brewer (unpublished data report) of 4 ± 2.6 (σ) nmoles Fe/kg for the upper 400 m at GEOSECS Stn. 40 (4°N , 38°W). In preliminary work determining the best conditions for particulate iron analysis, it was found that the shapes of the particulate iron profiles were the same using much milder conditions (0.6 N HCl, 24 hrs., 25°C) even though the values for particulate iron were an order of magnitude lower. The $<1\mu\text{m}$ fraction exhibits a nearly uniform Fe/P mole ratio of 1.8 ± 0.5 ; in the larger

TABLE 10 : PARTICULATE IRON⁺ (nmoles/kg) and RADIOISOTOPE ACTIVITIES (dpm/100kg)

Z (m)	Fe <1μm	Fe 1-53μm	Fe >53μm	210Pb/σ <1μm	210Pb/σ 1-53μm	210Pb/σ >53μm
32	1.69	3.79	1.32	0.38/.03	0.60/.04	0.181/.013
50	2.09	2.02	1.06	0.24/.03	0.33/.04	0.153/.012
113	0.86, 0.88	1.86, 1.77	0.436	0.012/.006	0.54/.03	0.083/.005
188	0.35	1.96	0.330	0.014/.004	0.46/.03	0.072/.005
294	0.46, 0.46	3.29, 3.58	0.401	0.006/.004	0.54/.03	0.063/.004
388	0.47	3.33	0.360	0.001/.004	0.43/.03	0.041/.004

Z (m)	7Be/σ 1-53μm	214Pb/σ 1-53μm	214Bi/σ >53μm	210Po/σ <1μm	210Po/σ 1-53μm
32	2.3/1.0	<0.03	<0.08	0.4/.10	1.00/.10
50	4.1/1.5	<0.05	<0.10	0.15/.09	0.89/.10
113	<0.05	0.18/.02	0.19/.022	0.06/.03	0.31/.07
188	<0.2	0.22/.03	0.17/.046	0.03/.02	0.43/.08
292	<0.2	0.075/.021	0.086/.032	0.12/.02	0.69/.09
388	<0.2	0.082/.020	0.072/.020	0.06/.02	0.62/.07

+ autoclave 18 hrs. 0.6 N HCl, 0.15 M NH₂OH·HCl replicates are indicated.

Figure 2-9. Upper: Particulate iron showing strong correlation with ^{210}Pb .

Lower: Particulate ^{210}Pb and ^{210}Po , ^{214}Pb and ^{214}Bi , and ^7Be , activities in the 3 size fractions. ^{214}Pb and ^{214}Bi activities are equivalent to the ^{226}Ra activity. ^7Be and ^{226}Ra were undetectable in the $>53\mu\text{m}$ size fraction.

size fractions, the Fe/P ratio varies by an order of magnitude, being lowest (0.25) at 50 m and highest (4-5) below 200 m and indicating the refractory nature of the particulate iron.

Radioisotopes Pb-210 and Po-210, Be-7

The analyses of particulate Pb-210 ($t_{1/2}=22y$), Po-210 ($t_{1/2}=138d$) and Be-7 ($t_{1/2}=53d$) were undertaken with the idea that their activities may be used to assign average settling rates for the particles in each size fraction and hence allow independent calculation of vertical fluxes.

Analytical results for Pb-210 and Po-210 are shown in Fig. 9 and summarized in Table 10. It was not possible to analyze the $>53\mu m$ samples soon enough to determine Po-210; only Pb-210 data is available for this size fraction.

Maximum particulate Pb-210 activities are found at 32 m in all size fractions. The only other element showing a surface maximum is iron and the two elements are seen to covary (Fig. 9). Because the principal source of Pb-210 in the upper part of the water column is delivery from the atmosphere, the similarity between the two distributions (note especially the $>53\mu m$ size fraction) may indicate an atmospheric source for particulate iron.

The particulate Po-210 maximum at 32 m does not reflect the atmospheric source (Po-210/Pb-210 activity ratio in air

and rain water samples is approximately 0.1; Burton and Stewart, 1960; Lambert and Nezami, 1965; Poet, Moore and Martell, 1972), but is due to the rapid uptake of this nuclide from seawater. The greatest enrichment of Po-210 is found at 50 m, the particle maximum, where the Po-210/Pb-210 activity ratio is 2.4. This value of relative enrichment is within the reported range for phytoplankton (Shannon, Cherry and Orren, 1970). It is interesting to note, however, that Po-210 and Pb-210 are more highly concentrated in particulate matter than in plankton (Table 11). In the <1 μ m size fraction Pb-210 is essentially absent below 50 m unlike Po-210 which is readily measurable below this depth. Such behavior is consistent with the known behavior of the Pb and Po isotopes; Po-210 is readily adsorbed onto surfaces and should be enriched in the smallest particle size fraction (Po-210 blank levels were insignificant for glass fiber filters exposed to seawater for several hours).

Particulate Po-210 activity passes through a well developed minimum at 113 and 188 m, where the Pb-210/Po-210 activity ratios are less than 1.0. This behavior is consistent with the conclusion of Bacon (1975) that Po-210 is rapidly recycled within the thermocline, where the Po-210/Pb-210 activity ratios in filtered seawater frequently exceed 1.0. This data also indicates that Po-210 and Pb-210 exist in separate particulate phases in the

TABLE 11 : LEAD - 210 and POLONIUM - 210 CONTENTS OF PARTICULATE MATTER COMPARED WITH THOSE OF PLANKTON. Units: dpm/gm dry weight Total range reported is given along with medians (in parentheses).

	Pb - 210	Po - 210
CHAIN 115-2 LVFS Stn. 2		
particulates : < 1 μ m	60-710 (85)	190-1090 (310)
1-53 μ m	100-430 (320)	170- 560 (350)
> 53 μ m	62-610 (215)	n.d.
Phytoplankton*	0.5-3.1 (0.9)	1.9-7.3 (4.8)
Zooplankton*	0.4-2.8 (1.0)	10.0-30.9 (13.)
Zooplankton [†]	0.2-6.1 (1.4)	2.2-196. (30.)

* Based on Shannon, Cherry, and Orren (1970); assumed wet to dry weight ratio = 20.

† Turekian, Kharkar, and Thomson (1974).

shallow samples.

Be-7 ($t_{1/2} = 53\text{d}$) has a stratospheric origin and is probably introduced at the sea surface by wet deposition (Silker, 1972). Both the 1-53 μm and >53 μm fractions were analyzed but the only measurable activities were found at 32 and 50 m in the 1-53 μm fraction. The correlation with organic carbon (4×10^4 D.P.M./mole C, and 6×10^4 D.P.M./mole C at 32 and 50 m respectively) may be a phenomenon of surface adsorption rather than active uptake since the >53 μm fraction exhibited no measurable Be-7 activity at 50 m.

Ra-226 as determined by Pb-214 and Bi-214

A by-product of the Be-7 analyses was that measurable activities of Pb-214 ($t_{1/2} = 26.8\text{m}$) and Bi-214 ($t_{1/2} = 19.7\text{m}$) were found in the 1-53 μm samples; no measurable activity was found in the >53 μm samples. These isotopes are short lived daughters of Ra-226 ($t_{1/2} = 1622\text{y}$); assuming no loss of Rn-222 ($t_{1/2} = 3.82\text{d}$), the activities of Pb-214 and Bi-214 are equivalent to that of Ra-226. Ra-226 is important in that it is an independent radioactive tracer of oceanic circulation, having different sources than carbon-14. The understanding of the particulate Ra-226 distribution and fluxes in the ocean is necessary to provide sufficient constraints on the rates of regeneration of particulate Ra-226 in the water column, and hence allow its use as a time tracer of oceanic circulation.

The shapes of the Pb-214 and Bi-214 profiles closely resemble that of calcium carbonate and opal. The inferred Ra-226 distribution is unlike that of Sr* or total organic C, N and P suggesting that the bulk of the Ra-226 is fixed in the hard parts of the plankton found growing above 100m. Maximum values of Ra-226/CaCO₃ and Ra-226/Si are calculated to be $6.5 \times 10^{-11} \pm 2.5 \times 10^{-11}$ (σ) and $2.0 \times 10^{-10} \pm 1.3 \times 10^{-10}$ (σ) respectively. Some Ra-226 may be associated with a refractory component of organic matter like xs Mg or xs Ca. The application of vertical advection-diffusion models to the dissolved distribution of Ra-226, alkalinity and silicate in the deep tropical Pacific gives an average in-situ production ratio of Ra-226/CaCO₃ = 6×10^{-11} and Ra-226/Si = 5×10^{-11} (Chung and Craig, 1973; Edmond, 1974). These agreeing estimates are uncertain because the calculated rates of regeneration of carbonate and opal within the water column included zero at the 95% confidence limit (2σ).

LARGE PARTICLES AND VERTICAL FLUXES

Large aggregate particles, particularly fecal pellets, have been suggested as important in the sedimentation of clay minerals, coccoliths, coccospheres, diatoms (Bramlette, 1961; Goldberg and Griffin, 1964; Biscaye, 1965; Calvert, 1966; Schrader, 1971; Manheim, Hathaway, and Uchupi, 1972;

Plate 4

Scanning electron micrographs of biogenic debris on 53 μ m filters from various depths. Scale indication is the same as for Plate 1.

- A. Remains of a crustacean carapace discarded during a molt, 388 m.
- B. Central view of abdominal segments and appendages of a copepod exoskeleton; valvar view of diatom Asteromphalus, 113 m.
- C. Folded, membranous material from a crustacean carapace, 113 m.
- D. Portions of crustacean opal and thoracic appendages, 113 m.
- E. Magnification of 4F, typical fecal pellet incorporating coccoliths, intact coccolithophorids, diatom frustules and organic materials, 113 m.
- F. Typical fecal pellets, 113 m.

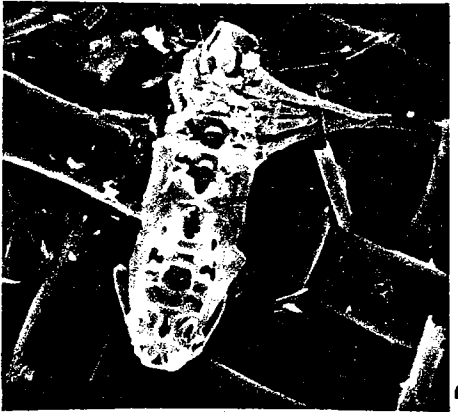
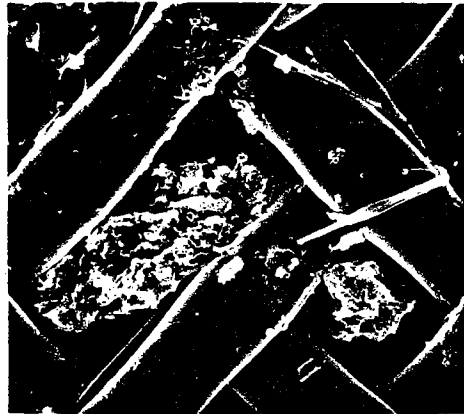
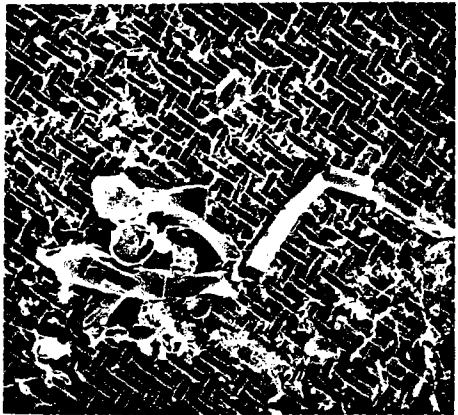
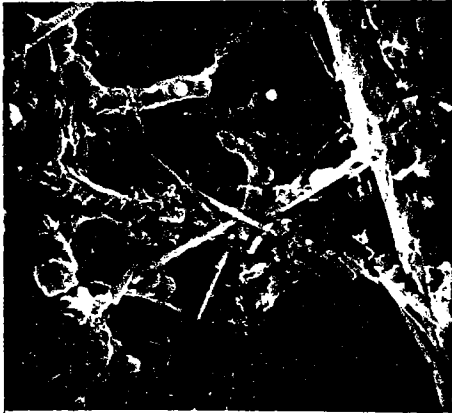


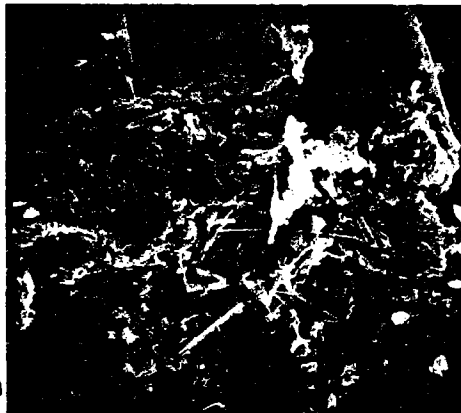
Plate 5

Scanning electron micrographs of biogenic material on 53 μ m filters from various depths. Scale indication is the same as for Plate 1.

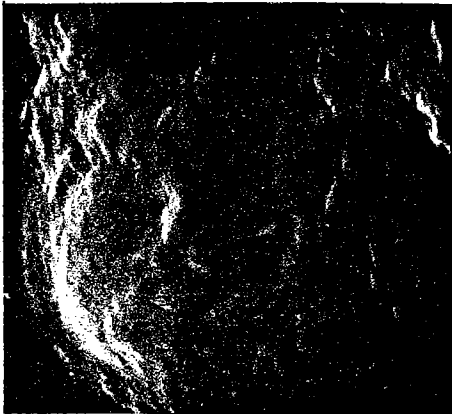
- A. Mucoid web-like organic material held in the 53 μ m grid of the prefilter, 32 m.
- B. Hyaline-sheetlike particle, 50 m.
- C. Magnification of 5B, surface of this material is completely devoid of small particles such as coccoliths, 50 m.
- D. Fecal matter containing fragments of Acantharia, 388 m.
- E. Magnification of 5F showing contents of fecal matter. Contains a diversity of coccoliths, diatom and protozoan fragments, 388 m.
- F. Typical fecal matter, 388 m.
- G. Magnification of 5H, fecal matter containing Acantharian spine, fragmented tests and frustules as well as organic material, 388 m.
- H. Fecal matter, 388 m.



D



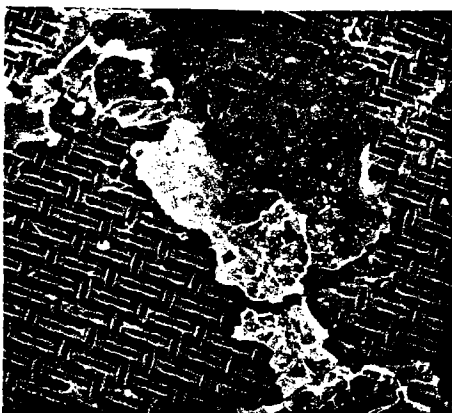
H



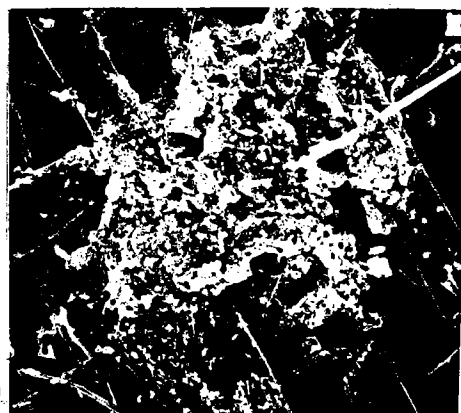
C



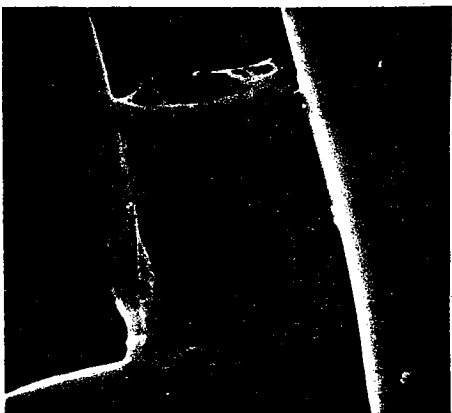
G



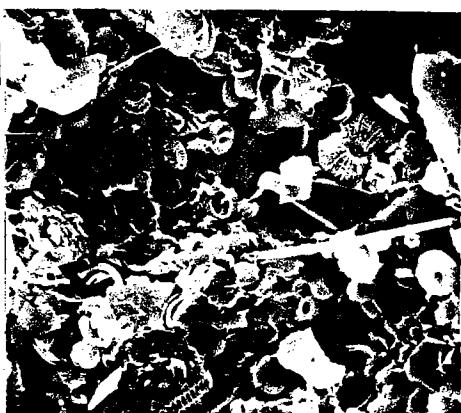
B



F



A



E

Listizin, 1972; Honjo, 1975; Roth, Mullin, and Berger, 1975) and carbon (Menzel, 1974). The state of preservation and distribution of coccoliths, and the distribution of clay minerals in sediments can only be explained in terms of rapid vertical transport of these small particles to the sediments with little or no interaction with the water column. The occurrence of bottom dwelling organisms below zones of high surface biological productivity (Heezen and Hollister, 1971) must also reflect increased transport of organic carbon to the sediments in these areas. Model calculations such as those of McCave (1975) showed that large particles such as fecal pellets would be rare in the water column and hence would be missed by conventional techniques used to sample particulate matter in the water column. Indeed, Bishop and Edmond (1976) have shown this to be true for waters shallower than 400 m. The LVFS sampling was designed to test the hypothesis of "fecal pellet" sedimentation.

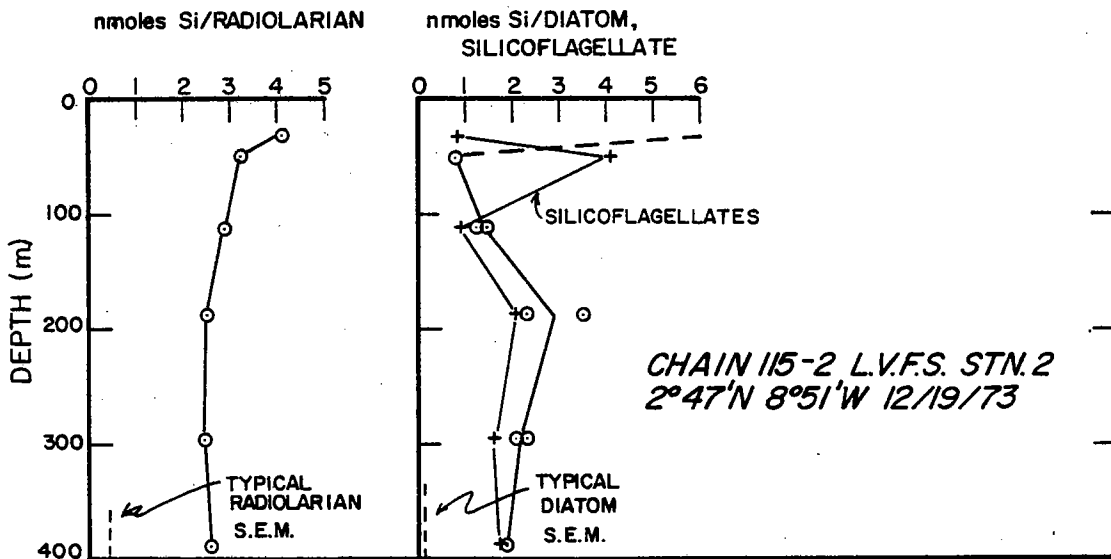
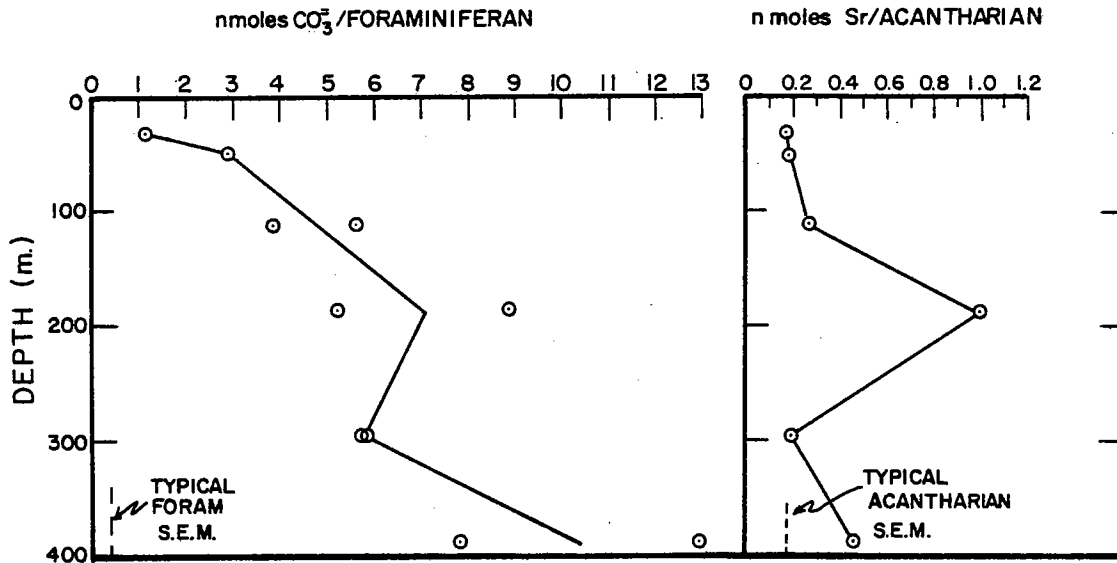
Plates 4 and 5 show the morphology of large single and composite organic particles. These particles fall into the classifications: crustacean appendage and carapace material (Plate 4, A-D); mucoid material (Plate 5, A); hyaline or sheet like material (Plate 5, B, C); fecal pellets (Plate 4, E, F); and, fecal matter (Plate 5, D-H). The distinguishing feature of both the fecal pellets and fecal matter is that they contain coccospheres, coccoliths, whole

and fragmented diatom frustules, small organic particles, as well as fragments of Foraminifera, Radiolaria and Acantharia. The fecal pellets are generally cylindrically shaped and well aggregated; the fecal matter less so. Smaller particles in these classes have probably been recognized by Gordon (1970) and Riley (1970).

Fig. 10 shows the profiles of carbonate/Foraminifera, silicate/Radiolaria, silicate/diatom, and Sr*/Acantharia in the $>53\mu\text{m}$ size fraction (whole tests and frustules only). The carbonate/Foraminifera profile shows an order of magnitude increase with depth indicating the enrichment of the $>53\mu\text{m}$ fraction with coccoliths and other carbonate fragments. Silicate/Radiolaria or diatom profiles are non-variant; the values are much higher than those calculated for Radiolaria and diatoms in the LVFS samples. Sr*/Acantharia increases by a factor of 5 down to 188 m and then suddenly drops back to near surface values deeper. These observations are consistent with SEM studies of the large particles which showed them to become progressively enriched in fragments (coccoliths, broken diatoms, broken Radiolaria and Acantharia spines) with increasing depth and also showed loss of SrSO_4 below 200 m due to dissolution.

A quantitative light microscopic and SEM study of the size distribution and morphology of the large particles sampled at 388 m was made in order to calculate the vertical

Figure 2-10. Carbonate per Foraminifera, silicate per Radiolaria and per diatom, non-carbonate strontium per Acantharia, ratios in the $>53\mu\text{m}$ size fraction indicate that the contribution of whole organisms to total carbonate, opal, and celestite is small at 388 m.



fluxes of mass, organic carbon, silicate, and carbonate through 388 m.

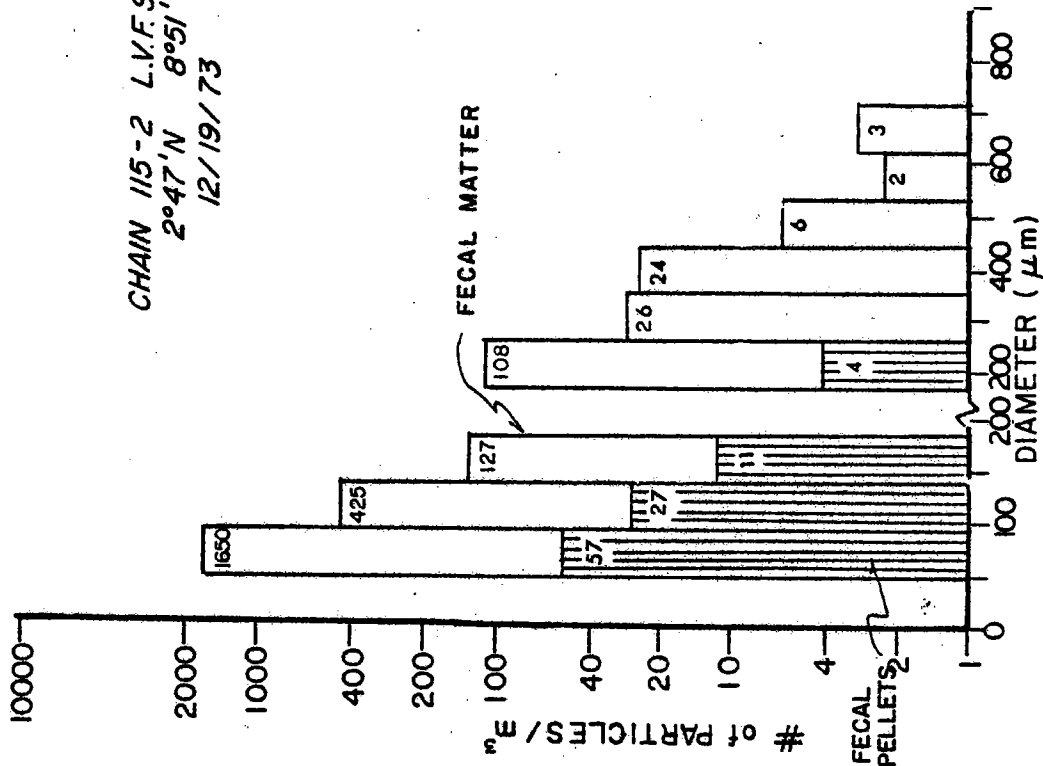
Fig. 11 shows the size distribution of Foraminifera (dark and light grey bars) and Foraminifera fragments (light gray and white bars) determined by scanning approximately 1/50th of the 53 μ m prefilter area of the 388 m sample. SEM measurements of broken Foraminifera were used to calculate a dry weight density of 0.5 gm/cm³ (total volume of calcite walls \times ρ_{calcite} \div spherical test volume, radius d = maximum dimension) based upon their geometry and 1 μ m wall thickness. The size distribution data together with the calculated dry weight density shows that whole Foraminifera contribute 0.15 nmoles/kg of seawater or 5% to the total suspended carbonate concentration in the >53 μ m fraction. The size distribution, typical shapes and thicknesses of the Foraminiferan fragments shows that they account for only 1% of the total carbonate on the 53 μ m filter. Approximately 94% of the >53 μ m carbonate, largely coccoliths, is bound in aggregate particles.

The contribution of whole and fragmented Radiolaria, diatoms, and silicoflagellates to total silica in the >53 μ m fraction is harder to estimate. Moore (1969), showed that the average Radiolaria (estimated size, 100 μ m) in recent sediments from the tropical Atlantic weighed 0.05 μ gm or contained 0.7 nmoles Si (assuming opal contains 15% water,

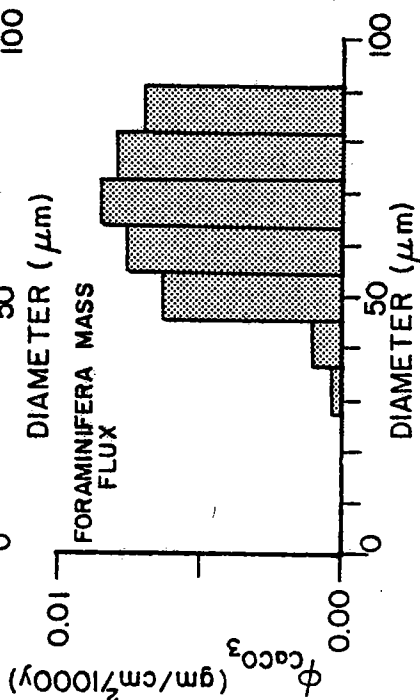
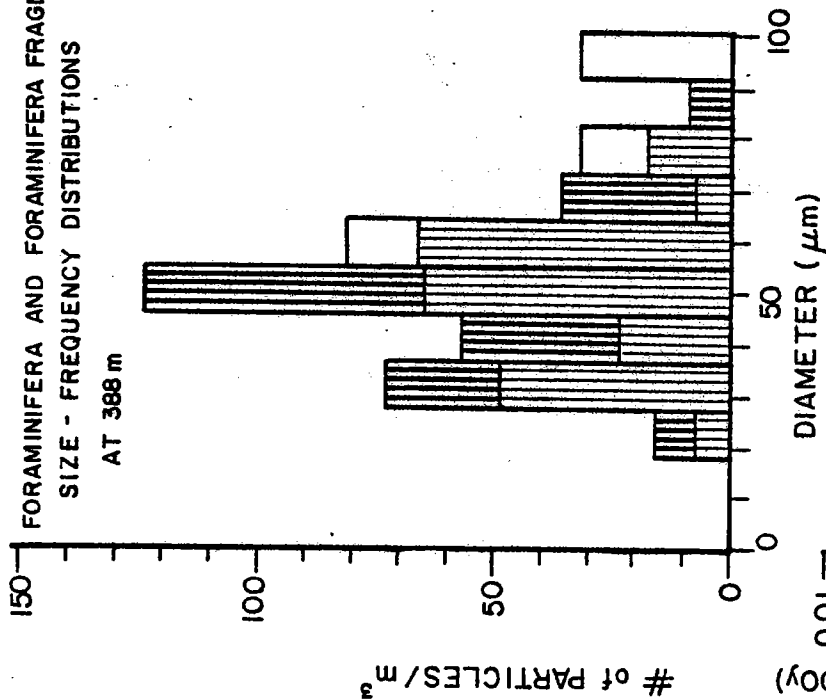
Figure 2-11. Left: Upper, size frequency distribution of Foraminifera (dark and light grey bars) and Foraminifera fragments (white and light grey bars) per cubic meter based on 442 liter subsample; lower, carbonate mass flux through 388 m carried by Foraminifera. Right: size-frequency distribution of fecal matter and fecal pellets contained in a cubic meter based on a 442 liter subsample, the $>300\mu\text{m}$ particles were counted on a filter subsample equivalent to 1045 liters.

CHAIN 115-2 L.V.F.S. STN. 2
 2°47'N 8°51'W
 12/19/73

FECAL MATTER AND FECAL PELLET
 SIZE - FREQUENCY DISTRIBUTIONS
 AT 388 m



FORAMINIFERA AND FORAMINIFERA FRAGMENT
 SIZE - FREQUENCY DISTRIBUTIONS
 AT 388 m



Moore, 1969). A typical (70 μ m) Radiolarian at 388 m at this station is estimated to contain 0.4 nmoles Si. Similarly the average 60 μ m diatom accounts for 0.11 nmoles Si and the largest (40 μ m) silico-flagellate would contain 0.012 nmoles Si. The total silicon in whole organisms may account for 22% of the total present on the 53 μ m filter. Separate fragments are estimated to account for an additional 3% of the total silica. Thus 75% of the total silica is composed of diatom and radiolarian fragments within the fecal material.

The mole ratio of carbonate to silicate in the large aggregate particles is 0.90 at 388 m (from Table 9 and above discussion). These particles are calculated to be 60% organic by weight (CH₂O + N) from a comparison of the dry weights of the particles removed from the 53 μ m filter with the results of C, N analysis of this material (see Table 6). Thus, organic carbon, calcium carbonate, and opal make up 24%, 22.5% and 17.5% respectively of the dry weight of fecal pellets and fecal matter.

Large particle flux through 388 m

Stokes' (1901) law is used to calculate the particulate flux.

$$v_d = \frac{g}{18\eta} \Delta\rho d^2 \quad \text{cm/sec} \quad (2)$$

v_d is the particle settling velocity; η , the water viscosity, is 0.0145 poise at 388 m; d is the diameter of the particle, g is the gravitational acceleration, $\Delta\rho$ is the density contrast of the particle with seawater.

$$v_d = 3.75 \times 10^3 \Delta\rho d^2 \quad \text{cm/sec} \quad (3)$$

The mass flux, ϕ_d is:

$$\phi_d = m_d v_d \quad \text{gm/cm}^2/\text{sec} \quad (4)$$

$$= n_d \frac{\pi}{6} d^3 \rho_p v_d \quad (5)$$

where n_d is the number of particles of size d , per ml of seawater; ρ_p is the dry weight density of the particles, m_d is the suspended mass concentration of particles of size d .

Thus:

$$\phi_d = 1.96 \times 10^3 n_d \Delta\rho \rho_p d^5 \quad (6)$$

Naturally occurring particles are neither spherical, nor do they have smooth surfaces. This is taken into account by actually measuring the settling velocities of particles and calculating the density contrast of the particles with the seawater, $\Delta\rho'$, if they fell according to Stokes' law. This approach is rather circular, but it does allow us to draw on literature describing the settling behavior of these

particles to calculate vertical fluxes. ρ_p is the dry weight of the particle divided by volume of a sphere of diameter d . It is assumed constant for a given particle type.

Thus:

$$\phi_d = 1.96 \times 10^3 n_d \Delta\rho' \rho_p d^5 \quad \text{gm/cm}^2/\text{sec} \quad (7)$$

or

$$\phi_d = 6 \times 10^{13} n_d \Delta\rho' \rho_p d^5 \quad \text{gm/cm}^2/1000\text{y} \quad (8)$$

in sedimentary units.

The vertical fluxes of mass, carbonate, opal and organic carbon may be calculated for this material using measurements of d , n_d and chemical composition which may be precisely determined. ρ_p and $\Delta\rho'$ may be obtained from the literature or estimated by SEM.

Flux of Foraminifera Tests

The lower portion of Fig. 11 illustrates the carbonate flux-size distribution for the Foraminifera at 388 m. For the mass flux calculations, $\rho_p = 0.5 \text{ gm/cm}^3$ and $\Delta\rho' = 0.3 \text{ gm/cm}^3$ (Berger and Piper, 1972); the total flux is 0.22 mmoles (0.022 gm) $\text{CaCO}_3/\text{cm}^2/1000\text{y}$ and is carried by Foraminifera larger than $50\mu\text{m}$ in size (see Fig. 11).

No Foraminifera larger than 100 μ m were encountered on the subsample studied (equivalent to 440 liters of seawater) even though typical Foraminiferan ooze contains tests up to several hundred μ m in diameter. Foraminifera 180 μ m in size were encountered on subsamples of shallower filters. Their absence from the 388 m sample coupled with the presence of large (100 μ m) fragments suggests that the >100 μ m Foraminifera concentration has been lowered to less than $1/m^3$ at 388 m by grazing organisms. The number of large Foraminifera at this depth is consistent with the results of Berger (1968).

The Radiolaria silica flux is calculated to be 0.23 mmoles Si (0.016 gm opal)/cm²/1000y using the values $d = 70\mu\text{m}$, $\rho_p = 0.1 \text{ gm/cm}^3$ (Moore, 1969), $\Delta\rho' = 0.1 \text{ gm/cm}^3$ (assumed), and $n_d = 1.6 \times 10^{-3}$ (Table 5); the diatom and silicoflagellate fluxes are negligible.

Fecal Matter and Pellet Fluxes

The right hand side of Fig. 11 shows the size distributions of both fecal matter and fecal pellets based on a filter subsample equivalent to 440 liters of seawater at 388 m; in the case of the fecal matter distributions, the particles >300 μ m were counted on a filter area equivalent to 1050 liters of seawater. The data (plotted on a vertical log scale) shows the fecal pellets are rare compared to the fecal matter. The dry weight density, ρ_p , of a fecal pellet is estimated to be approximately 0.5 gm/cm^3 (Wiebe, Boyd,

and Winget, 1976 ; Honjo, 1976). The value for $\Delta\rho'$ is assumed to be 0.2 gm/cm^3 (range $0.1-0.5 \text{ gm/cm}^3$) based on Smayda (1971) and Fowler and Small (1972). Both ρ_p and $\Delta\rho'$ are calculated based on d = maximum pellet dimension. The fecal matter is assumed to have a dry weight density of 0.2 gm/cm^3 (these particles are less densely packed than pellets), and $\Delta\rho' = 0.05$ (they are irregularly shaped). The fecal matter dimension, d , is the average of length and width; the ratio of length to width of this material ranged from 1 to 5 with 87% of the particles having a ratio of <2 .

The flux calculations are summarized in Tables 12, 13, and 14 which show that fecal matter and fecal pellets account for 99% of the mass flux through 388 m. The fluxes are: 94 mmoles (1.10 gm) $C_{\text{org}}/\text{cm}^2/1000\text{y}$; 10.9 mmoles (1.09 gm) $\text{CaCO}_3/\text{cm}^2/1000\text{y}$, mainly coccoliths; and 12.1 mmoles Si (0.85 gm opal)/ $\text{cm}^2/1000\text{y}$, mainly diatom fragments. For comparison, Listizin (1972) reported Holocene mass sedimentation rates of between 1.8 and $4.5 \text{ gm/cm}^2/1000\text{y}$; since this material is mainly carbonate and opal then the rate reported is in agreement with the calculated flux. Edmond (1974) has suggested that carbonate and opal are rapidly sedimented and that the transport of these different chemical species by a common carrier (e.g. fecal matter) explains the 1:1 correlation of alkalinity with silicate in seawater over much of the world's oceans.

TABLE 12

MASS FLUX OF FECAL PELLETS THROUGH 388 m^{*}

$d \times 10^4$ (μm) ^{**}	$n_d \times 10^3$ (#/l)	$m_d \times 10^9$ ($\mu\text{g}/\text{l}$)	ϕ_m	$\phi_{C_{\text{org}}}$ ($\text{gm}/\text{cm}^2/1000\text{y}$)	ϕ_{CaCO_3}	ϕ_{opal}
46	0.057	0.001	0.0007	0.0002	0.0002	0.0001
91	0.027	0.005	0.010	0.002	0.002	0.002
137	0.011	0.007	0.032	0.008	0.007	0.006
183	0.004	0.006	0.049	0.012	0.011	0.009
TOTAL FECAL PELLET FLUX			0.091	0.022	0.021	0.016

* based on count of filter area equivalent to 440 liters.

** maximum length of pellet, length to width ratio averages

3.

TABLE 13

MASS FLUX OF FECAL MATTER THROUGH 388m[†]

$d \times 10^4$ (μm) ^{††}	$n_d \times 10^3$ (#/l)	$m_d \times 10^9$ ($\mu\text{g}/\text{l}$)	Φ_{mass}	$\Phi_{\text{C}_{\text{org}}}$ ($\text{gm}/\text{cm}^2/1000\text{y}$)	Φ_{CaCO_3}	Φ_{opal}
47	1.650	0.016	0.002	0.000	0.000	0.000
91	0.425	0.034	0.016	0.004	0.004	0.003
137	0.127	0.034	0.037	0.009	0.008	0.006
183	0.108	0.069	0.132	0.032	0.030	0.023
274	0.026	0.056	0.240	0.058	0.054	0.042
365	0.024	0.122	0.935	0.225	0.210	0.164
457	0.006	0.060	0.714	0.171	0.161	0.125
548	0.002	0.034	0.592	0.142	0.133	0.104
639	0.003	0.082	1.919	0.461	0.432	0.336
TOTAL FECAL MATTER FLUX			4.590	1.102	1.033	0.803

[†] based on count of filter area equivalent to 440 liters;
for >274 μm particles the filter area corresponded to 1045l.

^{††} d is the average dimension = $(\ell+w)/2$; ℓ/w ranges from
1-5, averages 2.

TABLE 14

FLUX SUMMARY FOR $>53\mu\text{m}$ PARTICLES AT 388m

Particle	Φ_{mass}	$\Phi_{\text{C}_{\text{org}}}$ ($\text{gm}/\text{cm}^2/1000\text{y}$)	Φ_{CaCO_3}	Φ_{opal}
FECAL MATTER	4.59	1.102	1.033	0.803
FECAL PELLETS	0.091	0.022	0.021	0.016
FORAMINIFERA	0.022	-	0.022	-
RADIOLARIA	0.02	-	-	0.02
TOTAL MASS FLUX	4.72	1.124	1.076	0.845
TOTAL CHEMICAL* FLUX		93.5	10.8	12.1

* $\text{mmoles}/\text{cm}^2/1000\text{y}$

Comparison of the organic carbon flux through 388 m, 94 mmol C/cm²/1000y, with the carbon productivity of these waters, 750-1500 mmol C/cm²/1000y (U.N.-F.A.O., 1972) suggests that at least 87% of the organic carbon, 91% of the nitrogen and 97% of the phosphorous fixed by photosynthesis in the surface waters has been recycled above 388 m. If the remaining carbon reaches the ocean floor and is consumed by bottom dwelling organisms, the resultant oxygen consumption would be 94 mmol O₂/cm²/1000y (2.4 ml O₂ at S.T.P./m²/hr) and compares with in situ bottom respirometer measurements of oxygen consumption of 20 mmol O₂/cm²/1000y (0.5 ml O₂ S.T.P./m²/hr; Smith and Teal, 1973) at 1850 m, 39°N, 70°W. More recent measurements of Smith were reported by Wiebe, Boyd, and Winget (1976) to be 117 mmol O₂/cm²/1000y (3.0 ml O₂ S.T.P./m²/hr) at 24°50'N, 77°40'W at 2000 m depth. The large particle organic carbon flux through 388 m appears therefore to be sufficient to satisfy the respiratory requirements of bottom dwelling organisms.

It is of interest to calculate the particulate flux of Pb-210 through 388 m which should approximate the delivery rate of atmospheric Pb-210 to the sea surface (Bacon, 1975). At 388 m the Pb-210 activity of particles in the >53μm size fraction is 0.38 dpm/mg. The mass flux of 4.8 mg/cm²y estimated above for this depth yields a Pb-210 flux of 1.8 dpm/cm²y; a result that is in fair

agreement with estimates of atmospheric Pb-210 delivery rates. Bacon (1975) for example, estimated a flux of $0.6 \text{ dpm/cm}^2\text{y}$ for the tropical North Atlantic. This value was an average for a large oceanic region; a station, such as CHAIN 115 LVFS Stn. 2, situated close to the continental source, would be expected to receive higher than average fluxes. In any case the result shows that the Pb-210 flux carried by particles larger than $53\mu\text{m}$ is sufficient to maintain the Pb-210 material balance for the upper layers of the water column.

A further check on the model parameter, ρ_p can be made by calculating the suspended mass and element concentrations due to the various categories of large particles (Table 15). The calculated mass and element concentrations are lower than those observed, consistent with the microscopic observation that many aggregate particles $<53\mu\text{m}$ were present on the prefilter. The flux carried by these particles, is insignificant ($0.07 \text{ gm/cm}^2/1000\text{y}$; $m_d = 0.7 \times 10^{-9} \text{ gm/cm}^3$, $d = 40\mu\text{m}$, $\Delta\rho' = 0.05 \text{ gm/cm}^3$). Thus the assumed fecal matter dry weight density is consistent with the data.

The flux calculations above are based on several assumptions about the sinking behavior of the material collected by the LVFS. We have tried to constrain the values of the model parameters where possible but some,

TABLE 15

SUSPENDED PARTICULATE CONCENTRATION SUMMARY ; >53 μ m AT 388m

Particle	C _{org}	CaCO ₃	SiO ₂	mass
FECAL MATTER	10.1	1.14	1.27	0.507
FECAL PELLETS	0.41	0.046	0.051	0.021
FORAMINIFERA	-	0.15	-	0.015
FORAMINIFERA FRAGMENTS		0.02	-	0.002
RADIOLARIA + FRAGMENTS	-	-	1.03	0.070
TOTAL	10.5	1.36	2.35	0.545
OBSERVED	15.9*	2.98	4.11	1.08*

* result is probably low, >53 μ m C/P ratio is a factor of 2 lower than expected; see Table 6, Figure 4, Estimate C_{org} ~ 25 nmoles/kg; [P.M.] = 1.5 μ g/kg.

particularly, $\Delta\rho'$, of fecal matter, are based largely on SEM evidence. As a result the flux calculations are probably within a factor of 2 or 3 of the true value. It must be stressed that these calculations are based on samples collected over a period of one day from an area of the ocean of a few tens of square kilometers. Whether or not the particle flux changes with time remains to be determined.

One of the most important conclusions from this calculation is that the fecal material is important in sedimentation of small particles such as coccoliths; however, it appears that most of the mass flux is carried by fecal matter rather than fecal pellets as had been previously suggested. Furthermore, this material is capable of satisfying the respiratory requirements of the bottom dwelling organisms found in association with areas of high surface productivity.

Flux of <53 μ m particles

A crude estimate of the sinking velocity of the 1-53 μ m particles may be made using the Be-7 data, assuming that Be-7 remains associated with its particulate carrier (e.g. organic carbon). The Be-7 activity at 50 m divided by that at 113 m (normalized to C_{org}) is >32 corresponding to a Be-7 decay over a time interval of at least 5 half lives (265 d).

The particle settling velocity is $<3 \times 10^{-4}$ cm/sec, corresponding to a Stokes' Law particle diameter of $5\mu\text{m}$ ($\Delta\rho = 0.2 \text{ gm/cm}^3$). The mass flux, $<0.1 \text{ gm/cm}^2/1000\text{y}$, is less than 2% of the total mass flux carried by the $>53\mu\text{m}$ particles. The main assumption that Be-7 and its carrier are not fractionated by degradative processes operating over this depth interval may be violated. Be-7 might be rapidly lost from particles as in the case of Po-210. Diffusive fluxes are likely to be negligible (Riley, 1970; McCave, 1975).

SUMMARY AND CONCLUSIONS

The samples of particulate matter collected at this station have been analyzed for the major biogenic chemical elements, $\delta^{13}\text{C}$, iron, and radioisotopes ^{210}Pb , ^{210}Po , ^7Be , ^{214}Pb , and ^{214}Bi . Microscopic analyses have been made to determine the size and morphologic distributions of the particles in order to understand the mechanisms important in controlling the vertical distributions and fluxes of particles within the upper 400 m.

1) A particle maximum occurs in the upper thermocline at 50 m and is associated with the plankton maximum. Sharp vertical concentration gradients between 50 m and 113 m of particulate mass, whole organisms, and organic carbon, nitrogen and phosphorous are probably maintained by the

action of filter feeding organisms.

2) C/N and C/P ratios of the organic particles are a function of size and depth; the ratios are lowest in the $<1\mu\text{m}$ size fraction and highest in the $>53\mu\text{m}$ size fraction. The occurrence of bacteria and the grazing activities of zooplankton may account for this size dependent behavior.

3) The $\delta^{13}\text{C}$ distributions bear little resemblance to those of particulate C, N, and P. The presence of bacteria (being isotopically light, $\delta^{13}\text{C} = -36\text{‰}$) at 50 m may explain the 4‰ depletion of C-13 between 32 and 50 m observed for the $<1\mu\text{m}$ and 1-53 μm size fractions. The $>53\mu\text{m}$ particles behave in a fashion consistent with the results of other workers; however, the probable presence of bacteria in all size fractions complicates the use of C-13/C-12 ratios of the organic carbon as an indicator of its composition.

4) 80-100% of the particulate calcium is balanced by carbonate. The remaining "excess" calcium is likely a component of organism cytoplasm at 32 m and 50 m and bound by ion-exchange in the 1-53 μm size fraction deeper in the water column. Ion-exchange capacity of the 1-53 μm particles at 294 m was measured to be 96 meq/100 gms (dry weight).

5) Particulate magnesium is not ion-exchangeable, nor is it in carbonate or phosphate phases. It is readily released from the particles on exposure to 10^{-3} N HCl and

is probably strongly bound to a refractory component of the organic matter. Mg/C_{org} increases from 0.4 to 2 mole % down the water column to 400 m.

6) Particulate organic matter is enriched in cations with depth to the extent that bound cation charge nearly equals the nitrogen content of the particles at 294 m. The major anomalies in the calcium and alkalinity distributions postulated recently are probably restricted to the upper thermocline where most of the organic matter is recycled.

7) Acantharia and their fragments comprise the bulk of the particulate Sr in the $>53\mu m$ size fraction. Their dissolution progresses most rapidly below 188 m. 17% of the total Sr is bound by ion exchange (like Ca) in the 1-53 μm particles at 294 m. In the upper 388 m some 50-75% of the $>53\mu m$ Sr has been lost due to dissolution of $SrSO_4$.

8) Si and $CaCO_3$ distributions are controlled primarily by processes of fragmentation and aggregation within the upper 388 m. Small carbonate and opal particles are progressively enriched in the large particles with increasing depth.

9) Particulate Fe and Pb-210 both exhibit a maximum at 32 m, consistent with an atmospheric source for both these elements.

10) The greatest enrichment of Po-210 relative to Pb-210 was observed to be at 50 m, the organisms maximum. Po-210 appears to exist in a separate phase from the Pb-210 and displays nutrient-like behavior as evidenced by its rapid depletion relative to Pb-210 between 50 m and 113 m. Po-210 is most strongly enriched relative to Pb-210 on the $<1\mu\text{m}$ particles below 50 m consistent with its chemical behavior.

11) Be-7 exhibits a correlation with organic carbon at 32 m and 50 m. Decay of the Be-7 between 50 m and 113 m allows an estimate of the sinking velocity of the $<53\mu\text{m}$ organic particles over this depth interval of $<3 \times 10^{-4} \text{ cm/sec}$. The $<53\mu\text{m}$ carbon flux is possibly $0.5-1.0 \text{ mmoles C/cm}^2/1000\text{y}$, less than 1% of the large particle flux through 388 m.

12) $\text{Ra-226}/\text{CaCO}_3$ and $\text{Ra-226}/\text{Si}$ mole ratios are 7×10^{-11} and 2×10^{-10} respectively in the $1-53\mu\text{m}$ size fraction. The Ra-226 flux into the deep ocean is probably between 0.9 and $2.6 \times 10^{-12} \text{ moles Ra-226/cm}^2/1000\text{y}$ at this station; Ra-226 shows no correlation with total organic carbon or SrSO_4 in particles.

13) From the flux calculations it is seen that 87% of the organic carbon, 91% of the nitrogen, and 94% of the particulate phosphorous is recycled in the upper 400 m at this station. The elemental composition of the organic flux through 388 m is: $\text{C}_{106}\text{N}_{11}\text{Mg}_{1.1}\text{Ca}_{0.2}\text{P}_{0.2}$. The carbon flux has a $\delta^{13}\text{C}$ value of -23.7% compared to the suspended carbon value of -21.2% . It is sufficient to meet the respiratory

requirements of bottom dwelling organisms ($94 \text{ mmol C/cm}^2/1000\text{y}$).

14) The Fe, Mg and Sr fluxes are 1.2, 0.9, and 0.15 $\text{mmol/cm}^2/1000\text{y}$. The Mg flux is such that it has no measurable effect on the dissolved Mg concentration.

15) Flux calculations give values for carbonate (mainly coccoliths) and opal (mainly diatom fragments) deposition of 10.9 and 12.1 $\text{mmol/cm}^2/1000\text{y}$ (1.09 and 0.85 $\text{gm/cm}^2/1000\text{y}$) respectively in agreement with observed sediment accumulation rates for carbonate. The flux ratio of carbonate and opal is consistent with the calculations of Edmond (1974).

16) The calculated Pb-210 flux ($1.8 \text{ dpm/cm}^2/\text{y}$) is consistent with the results of Bacon (1975).

17) Transit times for the fecal material through the 4 km deep water column are estimated to be on the order of 10-15 days. The lateral displacement due to deep ocean advection if unidirectional with depth (3 cm/sec) would be between 26 and 39 kms, indicating that the resulting sediment distributions would reflect oceanic variability of this scale.

18) We observe that fecal material accounts for only 4% of the total particulate suspended mass concentration but accounts for over 99% of the vertical flux through 388 m.

All these points indicate that dramatic changes in the character of the particulate matter occur within the shallowmost 400 m (particularly between 50 and 113 m at this station). Most of the particles are biogenic and their distribution and sedimentation is controlled primarily by biological processes within this depth interval. In addition to carbonate and opal carriers, organic matter has been shown to have ion-exchange and binding capacity and hence may be significant in minor and trace element fluxes in the ocean.

The next chapter contains an improved model for the settling behavior of fecal matter based on the settling behavior of disk shaped particles and empirical relations governing the density contrast of the particles with seawater as a function of particle size. The resulting mass flux was determined to be approximately $2 \text{ g cm}^{-1} 1000\text{y}^{-1}$ and fell within the accepted error of the spherical model discussed above. None of the basic conclusions of this chapter are changed significantly.

References

- Bacon, M.P. (1975), "Applications of Pb-210/Ra-226 and Po-210/Pb-210 disequilibria in the study of marine geochemical processes", Ph.D. Thesis, MIT-WHOI, 165 pp.
- Bear, F.E. (1964), Chemistry of the Soil, Reinhold Publishing Corporation, N.Y., 515 pp.
- Berger, W.H. (1968), "Planktonic Foraminifera: Shell Production and Preservation", Ph.D. Thesis, UCSD, 241 pp.
- Berger, W.H., J.W. Piper (1972), "Planktonic Foraminifera: Differential settling, dissolution, and redeposition", Limnology and Oceanography, 17, pp. 275-287.
- Biscaye, P.E. (1965), Mineralogy and sedimentation of recent deep sea clay in the Atlantic Ocean and adjacent seas and oceans, Geol. Soc. Amer. Bull., 76, pp. 803-832.
- Bishop, J.K.B., J.M. Edmond (1976), A new large volume filtration system for the sampling of oceanic particulate matter, J. Mar. Res., 34, pp. 181-198.
- Bottazzi, E.M., B. Schreiber, V.T. Bowen (1971), Acantharia in the Atlantic: their abundance and preservation, Limnology and Oceanography, 16, pp. 677-684.

- Bramlett, M.N. (1961), Pelagic sediments, Oceanography,
M. Sears, ed., A.A.A.S., Washington, D.C., pp. 345-366.
- Brass, G.W., K.K. Turekian (1974), Strontium distribution in
GEOSECS oceanic profiles, Earth Plan. Sci. Letters,
26, 81-87.
- Brewer, P.G., G.T.F. Wong, M.P. Bacon, D.W. Spencer (1975),
oceanic calcium problem?, Earth and Planet. Sci. Letters,
26, pp. 81-87.
- Burton, W.M., N.G. Stewart (1960), Use of long-lived natural
radioactivity as an atmospheric tracer, Nature, 186,
pp. 584-589.
- Calvert, S.E. (1966), Accumulation of diatomaceous silica
in the sediments of the Gulf of California, Geological
Soc. Amer. Bull., 77, pp. 569-596.
- Carpenter, J.H. (1965), The Chesapeake Bay Institute technique
for the Winkler dissolved oxygen method, Limnology
and Oceanography, 10, pp. 141-143.
- Chung, Y., H. Craig (1973), Radium-226 in the eastern
equatorial Pacific, Earth and Planet. Sci. Letters,
17, pp. 306-318.
- Copin-Montegut, C., G. Copin-Montegut (1972), Chemical
analyses of suspended particulate matter collected in
the northeast Atlantic, Deep Sea Research, 19, pp. 445-
452.

- Craig, H. (1953), The geochemistry of the stable carbon isotopes, Geochimica et Cosmochimica Acta, 3, pp. 53-92.
- Culmo, R. (1969), Automatic microdetermination of carbon, hydrogen, and nitrogen: improved combustion train and handling techniques, Mikrochimica Acta, (Wien), pp. 175-180.
- Degens, E.T. (1969), Biogeochemistry of stable carbon isotopes, Organic Geochemistry, eds. G. Eglinton, M.T.J. Murphy, Springer-Verlag, Berlin, New York, pp. 304-328.
- Degens, E.T., R.R.L. Guillard, W.M. Sackett, and J.A. Hellebust (1968), Metabolic fractionation of carbon isotopes in marine plankton - I. Temperature and Respiration experiments", Deep Sea Research, 15, pp. 1-9.
- Degens, E.T., M. Behrendt, B. Gotthardt, and E. Reppman (1968), Metabolic fractionation of carbon isotopes in marine plankton - II. Data on samples collected off the coasts of Peru and Ecuador, Deep Sea Research, 15, pp. 11-20.
- Deuser, W.G., E.T. Degens, and R.R.L. Guillard (1968), Carbon isotope relationships between plankton and seawater, Geochimica et Cosmochimica Acta, 32, pp. 657-660.

- Edmond, J.M. (1974), On the dissolution of carbonate and silicate in the deep ocean, Deep Sea Research, 21, pp. 455-480.
- Eadie, B.J., L.M. Jeffrey (1973), $\delta^{13}\text{C}$ analyses of oceanic particulate organic matter, Marine Chemistry, 1, pp. 199-209.
- Emiliani, C. (1955), Mineralogical and chemical composition of the tests of certain pelagic Foraminifera, Micropaleontology, 1, pp. 377-380.
- Feely, R.A. (1975), Major element composition of the particulate matter in the near-bottom nepheloid layer of the Gulf of Mexico, Marine Chemistry, 3, pp. 121-156.
- Fowler, S.W., L.F. Small (1972), Sinking rates of euphausiid fecal pellets, Limnology and Oceanography, 17, pp. 293-296.
- Goldberg, E.D., J.J. Griffin (1964), Sedimentation rates and mineralogy in the South Atlantic, J. Geophys. Res., 69, pp. 4293-4309.
- Gordon, D.C., Jr. (1970) A microscopic study of organic particles in the North Atlantic Ocean, Deep Sea Research, 17, pp. 175-186.
- Grassé, P.P., ed. (1953), Traite de Zoologie, 1, pt. 2, Masson et Cie, Paris, France.
- Heezen, B.C., C.D. Hollister, (1971), The Face of the Deep, Oxford University Press, New York, 658 pp.

- Hendey, N.I. (1964), An Introductory Account of the Smaller Algae of British Coastal Waters, Part V: Bacillariophyceae (diatoms), Fishery Investigations, Series IV, 317 pp.
- Honjo, S. (1975), Dissolution of suspended coccoliths in the deep-sea water column and sedimentation of coccolith ooze, in Sliter, W.V., Be, A.W.H., and Berger, W.H., eds., Dissolution of deep-sea carbonates: Cushman Foundation for Foraminiferal Research Spec. Pub. 13, pp. 114-128.
- Honjo, S. (1976), Coccoliths: Production, transportation and sedimentation, Marine Micropaleontology, 1, 65 - 79.
- Horibe, Y., K. Endo, H. Tsubota (1974), Calcium in the South Pacific and its correlation with carbonate alkalinity, Earth Planet. Sci. Letters, 23, pp. 136-140.
- Hughes, M.N. (1972), The Inorganic Chemistry of Biological Processes, Wiley, New York. 304 pp.
- Hurd, D.C. (1972), Interactions of biogenic opal, sediment, and seawater in the central equatorial Pacific, Ph.D. Thesis, Hawaii Institute of Geophysics, University of Hawaii. 81 pp.
- Kudo, R.R. (1966) Protozoology, Charles C. Thomas, Springfield, Illinois.
- Lambert, G., M. Nezami (1965), Importance des retombees seches dans le bilan du plomb 210, Ann. Geophysique, 21, pp. 245-251.

- Lisitzin, A.P. (1972), Sedimentation in the World Ocean, Society of Economic Paleontologists and Mineralogists Special Publication 17, 218 pp.
- Luria, S.E. (1961), The Bacteria, 1, Academic Press, N.Y., pp. 1-33.
- Mangelsdorf, P.C., Jr., T.R.S. Wilson (1972), Constancy of ionic properties in the Pacific Ocean, Trans. Am. Geophys. Union, EOS, 53 (4), p. 402.
- Manheim, F.T., J.C. Hathaway, E. Uchupi (1972), Suspended matter in the surface waters of the northern Gulf of Mexico, Limnology and Oceanography, 17, pp. 17-27.
- Mayzaud, P., J.-L. Martin (1975), Some aspects of the biochemical and mineral composition of marine plankton, J. Experimental Mar. Biol. and Ecol., 17, pp. 297-310.
- McCave, I.N. (1975), Vertical flux of particles in the ocean, Deep Sea Research, 22, pp. 491-502.
- Menzel, D.W. (1974), Primary productivity, dissolved and particulate organic matter, and the sites of oxidation of organic matter, in: The Sea, 5 E.D. Goldberg, ed., John Wiley & Sons, N.Y., pp. 659-678.
- Menzel, D.W., R.F. Vaccaro (1964) The measurement of dissolved organic and particulate carbon in seawater, Limnology and Oceanography, 9, pp. 138-142.
- Moore, T.C., Jr. (1969), Radiolaria: change in skeletal weight and resistance to solution, Geol. Soc. Amer. Bull., 80, pp. 2103-2108.

- Mullin, J.B., J.P. Riley (1955), The colorimetric determination of silicate with special reference to sea and natural waters, Anal. Chim. Acta, 12, pp. 162-176.
- Murphy, J., J.P. Riley (1962) A modified single solution method for the determination of phosphate in natural waters, Anal. Chim. Acta, 27, pp. 31-36.
- Poet, S.E., H.E. Moore, E.A. Martell (1972), Lead 210, bismuth 210 and polonium 210 in the atmosphere: accurate ratio measurement and application to aerosol residence time determination, J. Geophys. Res., 77, pp. 5255-5265.
- Porter, J.R. (1946), Bacterial Chemistry and Physiology, Wiley, 1073 pp.
- Redfield, A.C., B.H. Ketchum, F.A. Richards (1963), The influence of organisms on the composition of seawater, in: The Sea, 2, M.N. Hill, ed. J. Wiley and Sons, N.Y., pp. 26-77.
- Riley, G.A. (1970), Particulate and organic matter in seawater, Advances in Mar. Biol., 8, pp. 1-118.
- Roth, P.H., M.M. Mullin, and W.H. Berger (1975), Coccolith sedimentation by fecal pellets: laboratory experiments and field observations, Geol. Soc. Amer. Bull., 86, pp. 1079-1084.

- Sackett, W.M., W.R. Ecklemann, M.L. Bender, and A.W.H. Be,
Temperature dependence of carbon isotopes composition
in marine plankton and sediments, Science, 148, pp.
235-237.
- Sackett, W.M., B.J. Eadie, M.E. Exner (1973), Stable
isotope composition of organic carbon in recent
Antarctic sediments, Advances in Organic Chemistry,
proc. 6th International Meeting on Organic Geochemistry,
pp. 661-671.
- Saunders, R.P., D.A. Glenn (1969) Diatoms, Memoirs of the
Hourglass Cruises, 1, part 3, pp. 1-119.
- Schrader, H.J. (1971), Fecal pellets: role in sedimentation
of pelagic diatoms, Science, 174, pp. 55-57.
- Shannon, L.V., R.D. Cherry, M.J. Orren (1970), Polonium-210
and Lead-210 in the marine environment, Geochimica et
Cosmochimica Acta, 34, pp. 701-711.
- Silker, W.B. (1972), Beryllium-7 and fission products in
the GEOSECS II water column and applications of their
oceanic distributions, Earth and Planet. Sci. Letters,
16, pp. 131-137.
- Smayda, T.J. (1971) Normal and accelerated sinking of
phyto-plankton in the sea, Marine Geol., 11, pp. 105-122.
- Smith, K.L., Jr., J.M. Teal (1973) Deep sea benthic
community respiration: an in situ study at 1850 meters,
Science, 179, p. 282.

- Sorokin, Y.I. (1973) Data on biological productivity of the western Tropical Pacific Ocean, Marine Biol., 20, pp. 177-196.
- Spencer, D.W., P.G. Brewer, M.L. Bender (in press), The distribution of particulate Al, Ca, Sr, Ba, and Mg in the Northwestern Atlantic Ocean, Earth and Planet. Sci. Letters.
- Stokes, G.G. (1901) Mathematical and Physical Papers, Vol. III, Cambridge University Press, 413 pp.
- Stookey, L.L. (1970) Ferrozine - a new spectrophotometric reagent for iron, Analytical Chem., 42, pp. 779-781.
- Sverdrup, H.U., M.W. Johnson, R.H. Fleming (1942), The Oceans: Their Physics, Chemistry and General Biology, Prentice Hall, 1087 pp.
- Thompson, G., V.T. Bowen (1969) Analyses of coccolith ooze from the deep tropical Atlantic, J. Mar. Res., 27, pp. 32-37.
- Turekian, K.K., D.P. Kharkar, J. Thompson (1974), The fate of ^{210}Pb and ^{210}Po in the ocean surface, J. Rech. Atmos., 8, pp. 639-646.
- U.N.-F.A.O. (1972) Atlas of the Living Resources of the Seas, Dept. of Fisheries, U.N.-F.A.O., Rome.
- Vinogradov, A.P. (1953), The Elementary Chemical Composition of Marine Organisms, Memoir II, Sears Foundation of Marine Research, New Haven, 647 pp.

- Wiebe, P.H., S.H. Boyd, C. Winget (1976) Particulate matter sinking to the deep-sea floor at 2000m in the Tongue of the Ocean, Bahamas with a description of a new sedimentation trap, J. Mar. Res., 34, 341-354.
- Williams, P.M., L.I. Gordon (1970), Carbon-13: Carbon-12 ratios in dissolved and particulate organic matter in the sea, Deep-Sea Research, 17, pp. 19-27.
- Youngbluth, M.J. (1975), The vertical distribution and diel migration of euphausiids in the central waters of the eastern South Pacific, Deep Sea Research, 22 (8), pp. 519-536.

CHAPTER 3

THE CHEMISTRY, BIOLOGY, AND VERTICAL
FLUX OF PARTICULATE MATTER
FROM THE UPPER 400 M
OF THE CAPE BASIN IN THE
S.E. ATLANTIC OCEAN

Introduction

The chemistry and vertical flux of particulate matter is of prime importance in determining the removal and regeneration sites of the many elements involved in biogeochemical cycles. Elements such as organic carbon, nitrogen and phosphorus are fixed by plankton within the surface ocean and are regenerated predominantly in the shallow thermocline. Other biogenic components such as carbonate and opal have deep regenerative cycles governed by both the chemistry and physical circulation of the deep ocean. Many other stable and radioactive non-conservative elements are involved in these cycles either actively, as micro-nutrients or skeletal materials, or passively, by adsorption onto particle surfaces or by coprecipitation in carbonate, opal, or celestite phases. Their regeneration is therefore determined by the chemistry and settling behavior of their carrier phases. Particle distributions within the upper 400 m of the open ocean are almost entirely determined by biological processes of production, respiration, predation, fragmentation and aggregation (Chap. 2).

One important feature of deep sea sediments is the abundance of fine material such as coccoliths, diatom frustules, and terriginously derived clay minerals. A growing literature has suggested that these particles are rapidly sedimented within fecal material (Bramlette, 1961; Goldberg and Griffin, 1964; Biscaye, 1965; Calvert, 1966; Schrader, 1971; Manheim,

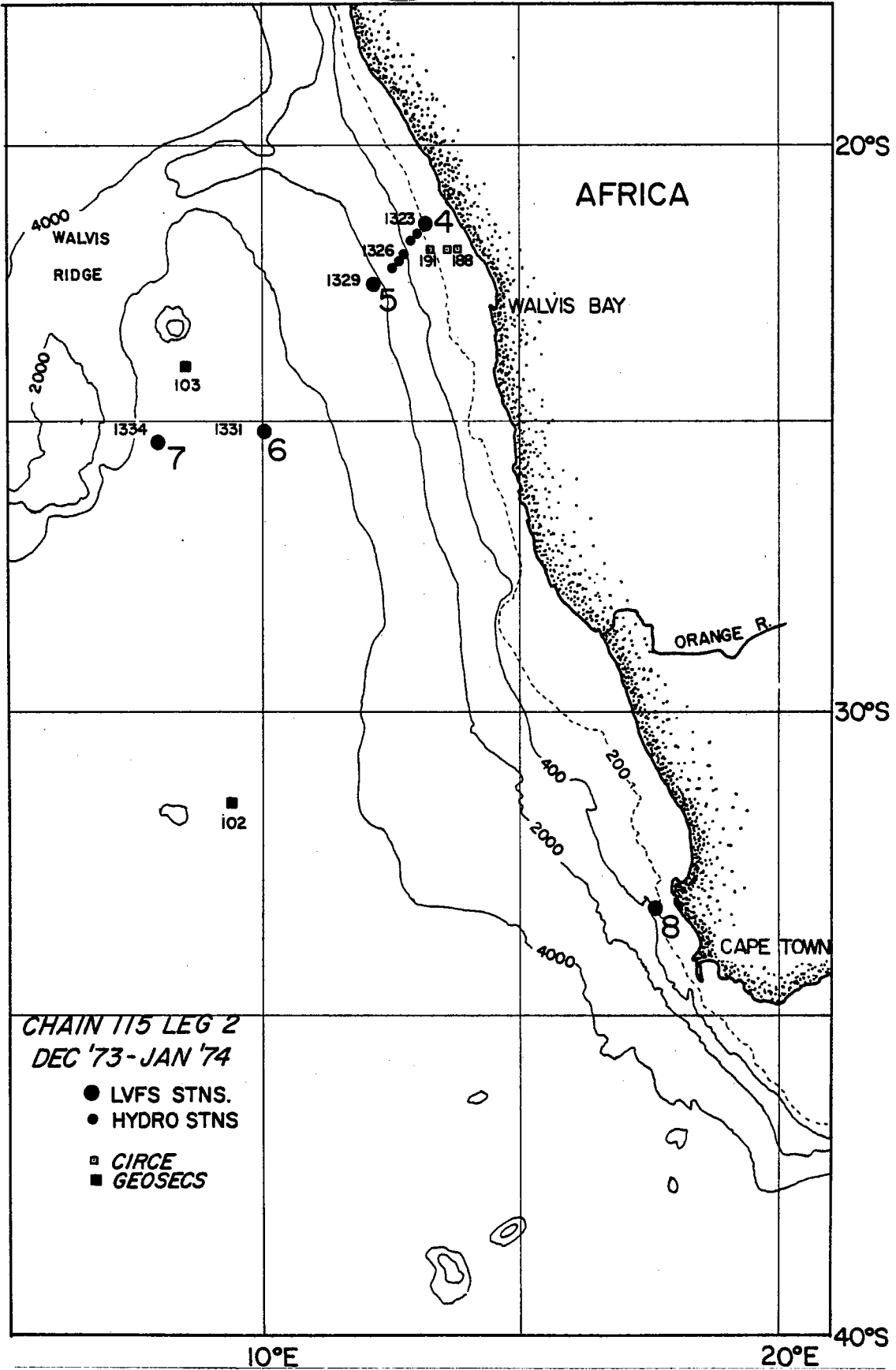


Fig. 3-1 , Station locations for LVFS and hydrographic profiles taken within the Cape Basin.

Hathaway and Uchupi, 1972; Roth, Mullin, and Berger, 1975; Honjo, 1975 and 1976; Krishnaswami and Sarin, 1976; and Chap. 2). The importance of the rapid transport of fine material to the sea floor within fecal material lies in the fact that its residence time and hence opportunity for interaction with the water column is greatly reduced. It is important to determine if fecal material dominates the sedimentation of fine material, especially in areas of low biological productivity.

Five LVFS stations were occupied in the Cape basin of the S.E. Atlantic ocean during the Southlant expedition (R/V CHAIN 115, leg 2, Dakar-Capetown, Dec. 1973 - Jan. 1974). Stations 4, 5, and 8 (Fig. 1) fall in areas of high biological productivity associated with upwelling along the S.W. African coast (Hart and Currie, 1960); Station 7 lies within the central gyre of the S. Atlantic, an area of generally low productivity. The aeolian contribution to the particulate matter in the surface waters of the Cape basin is probably negligible (Chester, Elderfield, Griffin, Johnson, and Padgham, 1972; and Krishnaswami and Sarin, 1976).

The hydrographic, biological and particulate mass and elemental distributions (Na, Mg, Ca, K, Sr, Si, carbonate, total C, and N) at these stations are used to elaborate upon the conclusions of Chap. 2. The systematic differences between the LVFS and Niskin particulate data are discussed. The size distributions of Foraminifera, fecal pellets, and fecal matter

from the 400 m samples at stations 5, 6, and 7, together with the chemical data and two mass flux models are used to calculate the composition and magnitude of the particle flux as a function of biological productivity.

Methods

Bishop and Edmond (1976) have treated in detail the description of the LVFS, filtration sequence, and filter handling technique at sea and in the laboratory prior to chemical analysis. The analytical methods are outlined in Chap. 2. Precision of these analyses was established by replicates. Following the practice of Chap. 2 all particulate analyses are expressed in mole units except where explicitly stated (Appendix 1).

Ancillary hydrographic data (Appendix 2) was obtained using the methods of Carpenter (1965) O_2 , Mullin and Riley (1955) Si, and Murphy and Riley (1962) PO_4 . Salinity was measured at W.H.O.I. on stored samples (6 months).

Temperature and depth were determined by standard thermometric technique.

Hydrography

The hydrography of the S.W. African continental margin, including the locations of LVFS stations 4, 5, and 8 has been studied by numerous workers (Hart and Currie, 1960; DeDecker, 1970; Calvert and Price, 1971; Jones, 1971; Bang, 1971;

BATHYTHERMOGRAPH RECORDS NEAR LVFS STNS 4 & 8

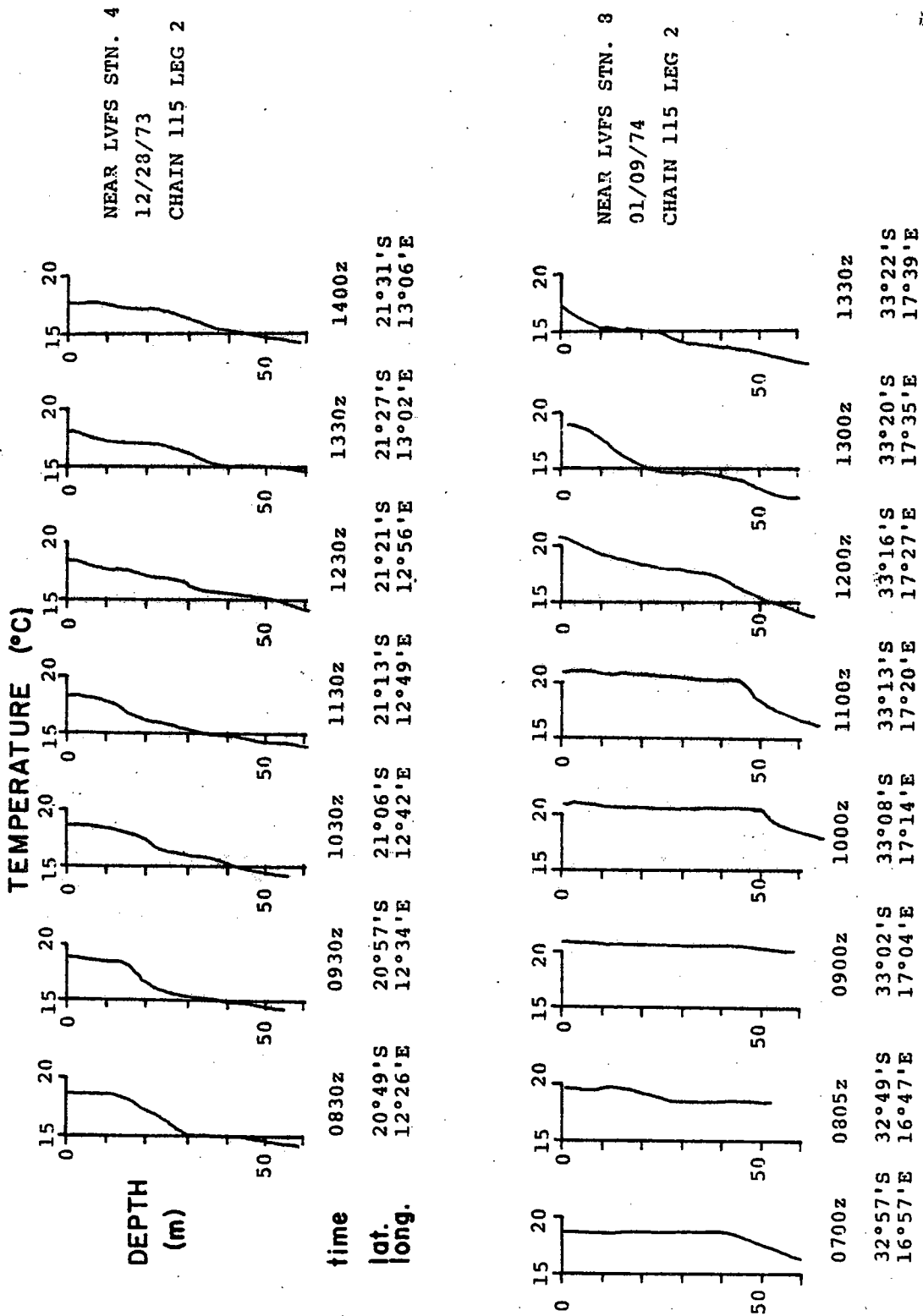


Fig. 3-2 , Bathythermograph records obtained near LVFS stations 4 and 8.

Bang, 1973; and Bang and Andrews, 1974). Time and spatial variability is a characteristic feature of the area (Bang, 1971; Bang and Andrews, 1974), therefore a hydrographic survey was necessary to characterize the LVFS stations.

The winds during the survey were less than 10 knots from the south at Stns. 4 and 5, 15 knots from the SSE at Stn. 6, and increased from 20 to 40 knots from the SSE at Stn. 7 forcing the station work to be sharply curtailed. The wind was 15 knots from the south at Stn. 8.

Closely spaced Bathythermograph profiles near Stations 4 and 8 (Fig. 2) show the presence of a weakly developed mixed layer to 15 or 20 m at 4; those near station 8 show horizontal temperature gradients as large as 8°C over 30 km and no mixed layer. The mixed layer was developed to 30, 50, and 65 m at LVFS Stns. 5, 6, and 7. All stations exhibit a weak salinity maximum in the upper thermocline and those between LVFS Stns. 4 and 5 showed considerable structure in all hydrographic properties (Figs. 3, 4 and 5).

The physical circulation has been described by Hart and Currie (1960) as a northward flowing surface current near the coast (Benguela Current), a poleward flowing compensation current located at the shelf edge at a depth of several hundred meters, a general onshore transport of water from depths of several hundred meters, and upwelling near the coast or at the shelf edge with offshore transport of the surface water. This

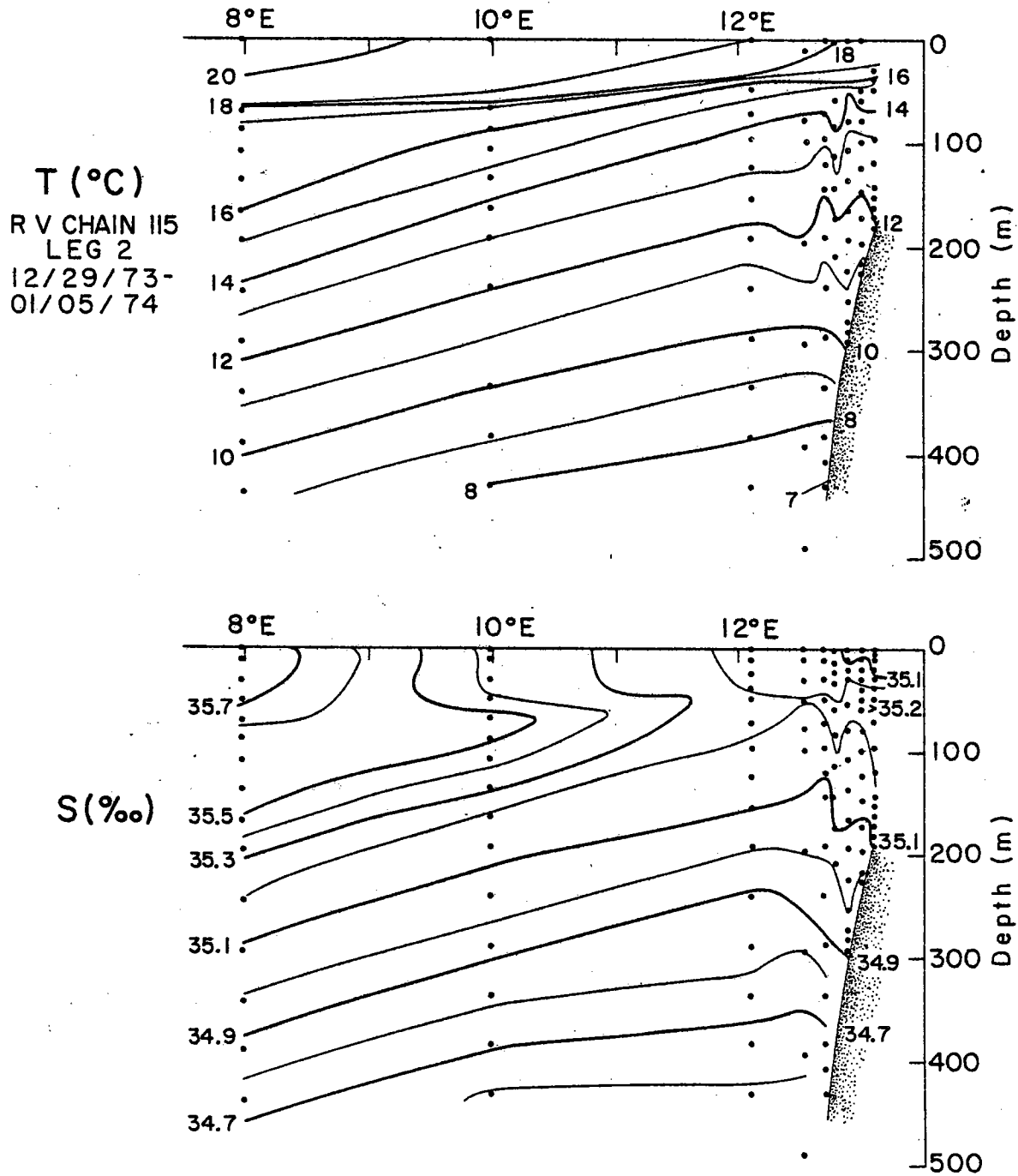


Fig. 3-3 , Temperature and Salinity sections for stations near Walvis Bay.

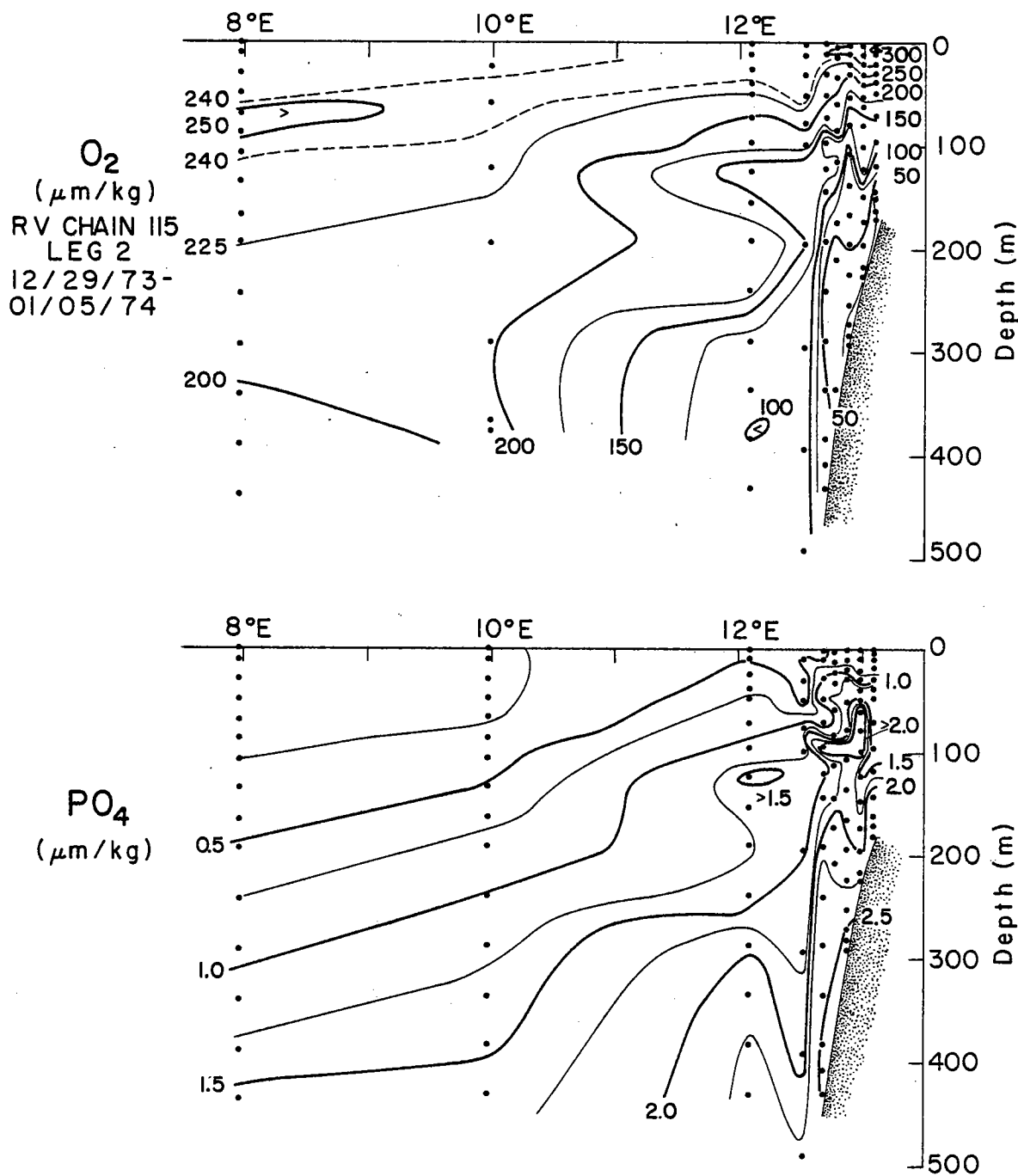


Fig. 3-4 , Dissolved oxygen and phosphate sections for stations near Walvis Bay.

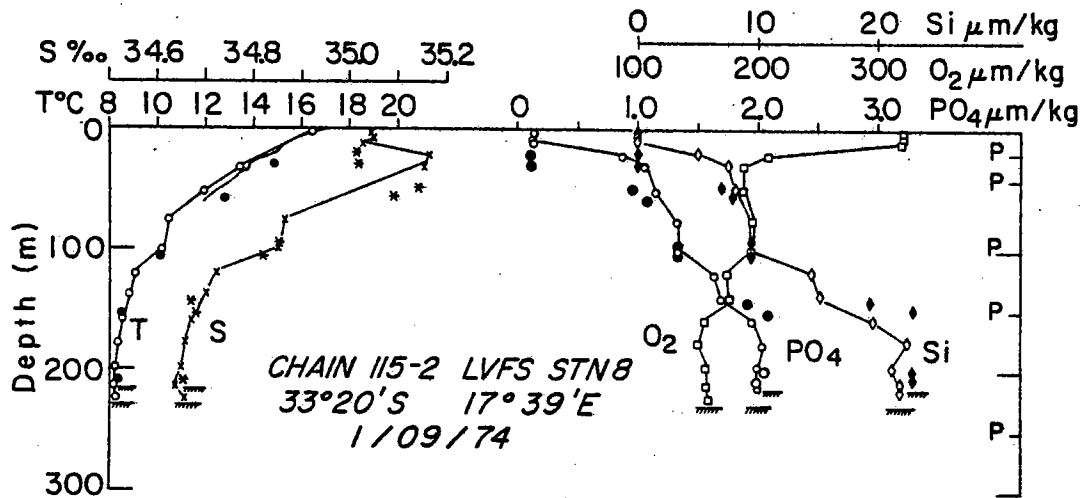
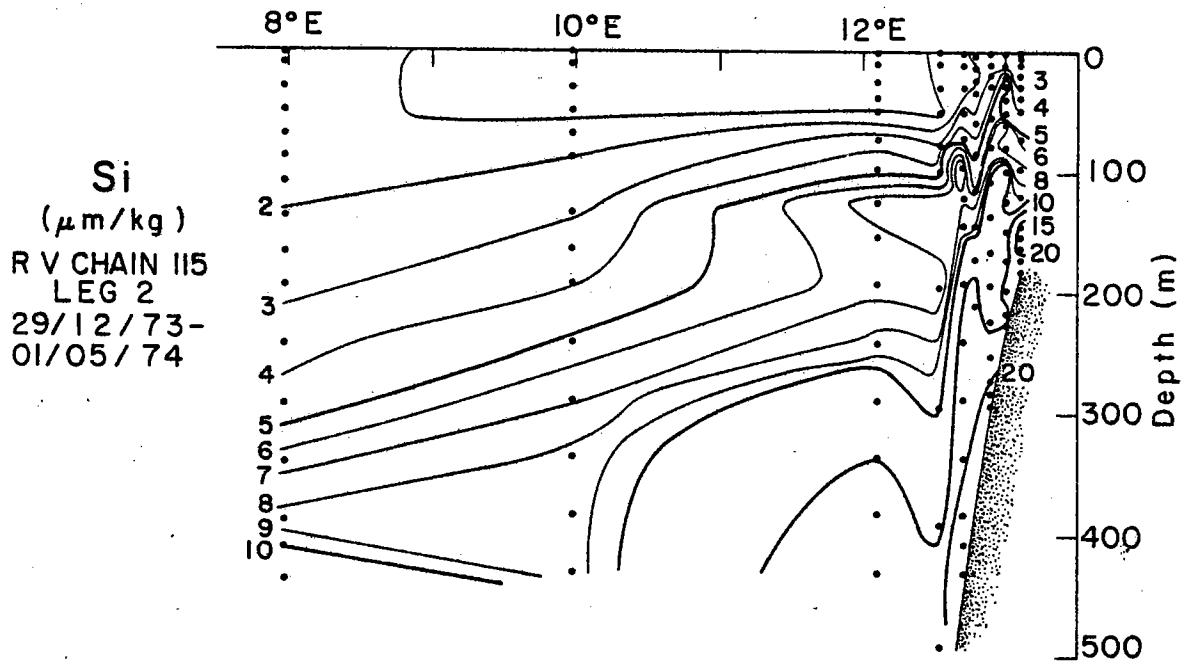


Fig. 3-5 , Silicate section for the stations near Walvis Bay; Hydrographic data for stations near LVFS station 8.

circulation scheme causes nutrient enrichment of the coastal waters by a mechanism similar to that found operating in estuaries (Hart and Currie, 1960; Calvert and Price, 1971) and is responsible for the departure of the distributions of Si, PO_4 , and O_2 from their offshore relationships with salinity (Figs. 6 and 7); Calvert and Price (1971) regard salinity to be unchanged by precipitation and evaporation processes at the surface making this parameter a useful tracer of upwelled water. During active upwelling, which is believed to be driven by the local winds, the onshore-offshore circulation is accelerated. During quiescence, the circulation is sluggish and the intense regeneration of the organic matter rapidly consumes dissolved oxygen in the shelf water causing the marine mortalities which are commonly associated with such conditions (DeDecker, 1970).

The poleward flowing compensation current (Hart and Currie, 1960) is identified by being nearly isothermal (Bang, 1973), intensely depleted in oxygen (DeDecker, 1970), and by having anomalous temperature and salinity properties. The data obtained during this survey show an oxygen depleted layer at 300 m on the shelf with T, S properties that are cooler or more saline than the immediate offshore waters (Figs. 3, 4, and 6). The data obtained during the Circe expedition (Oct. 1968) exhibit the same features and it appears that this water has an offshore origin approximately 100 km to the north. The strongest nutrient anomalies were found in this layer and decreased going offshore. The 120 m

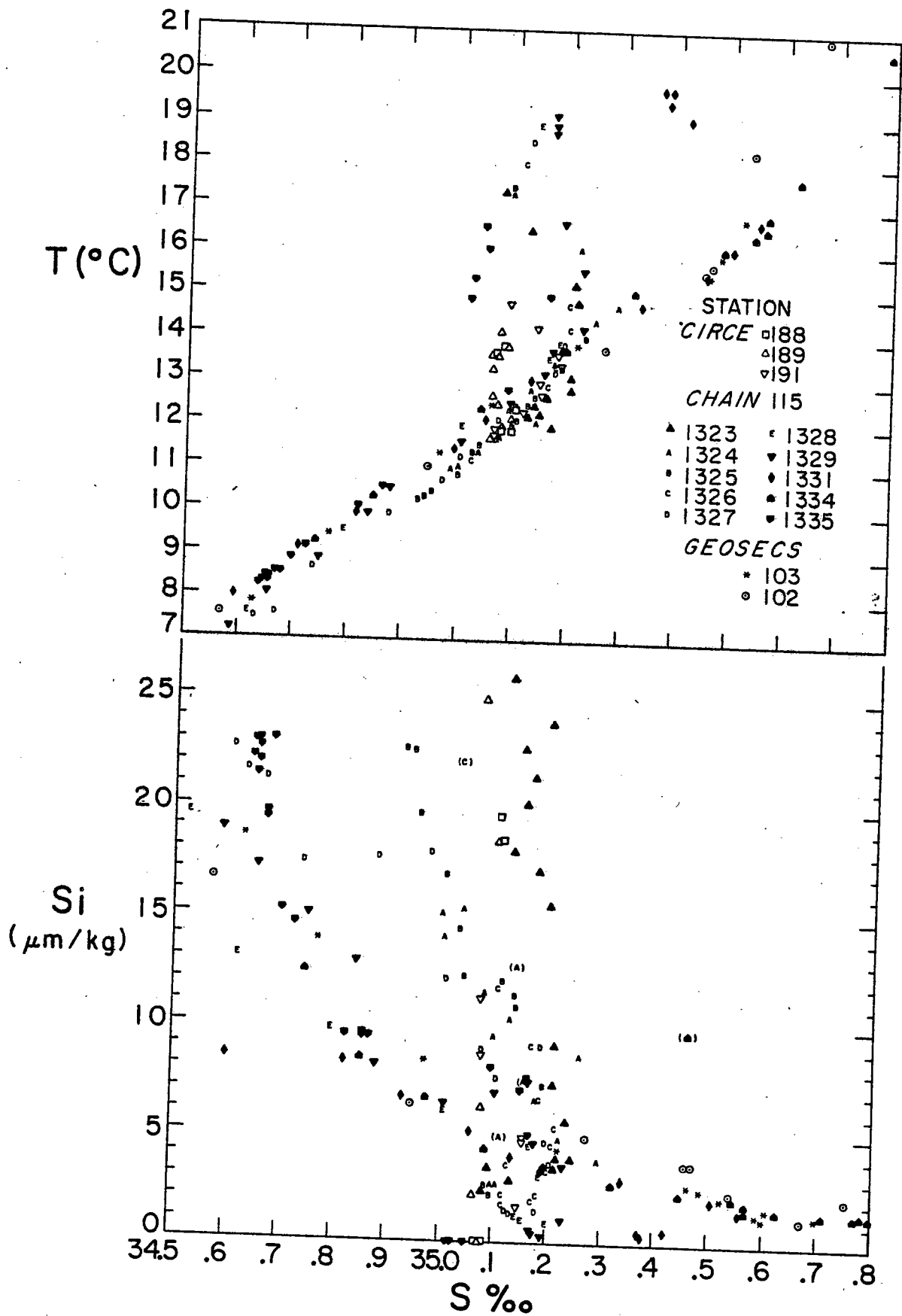


Fig. 3-6 , T-S and Si-S plots for all stations in the Cape Basin.

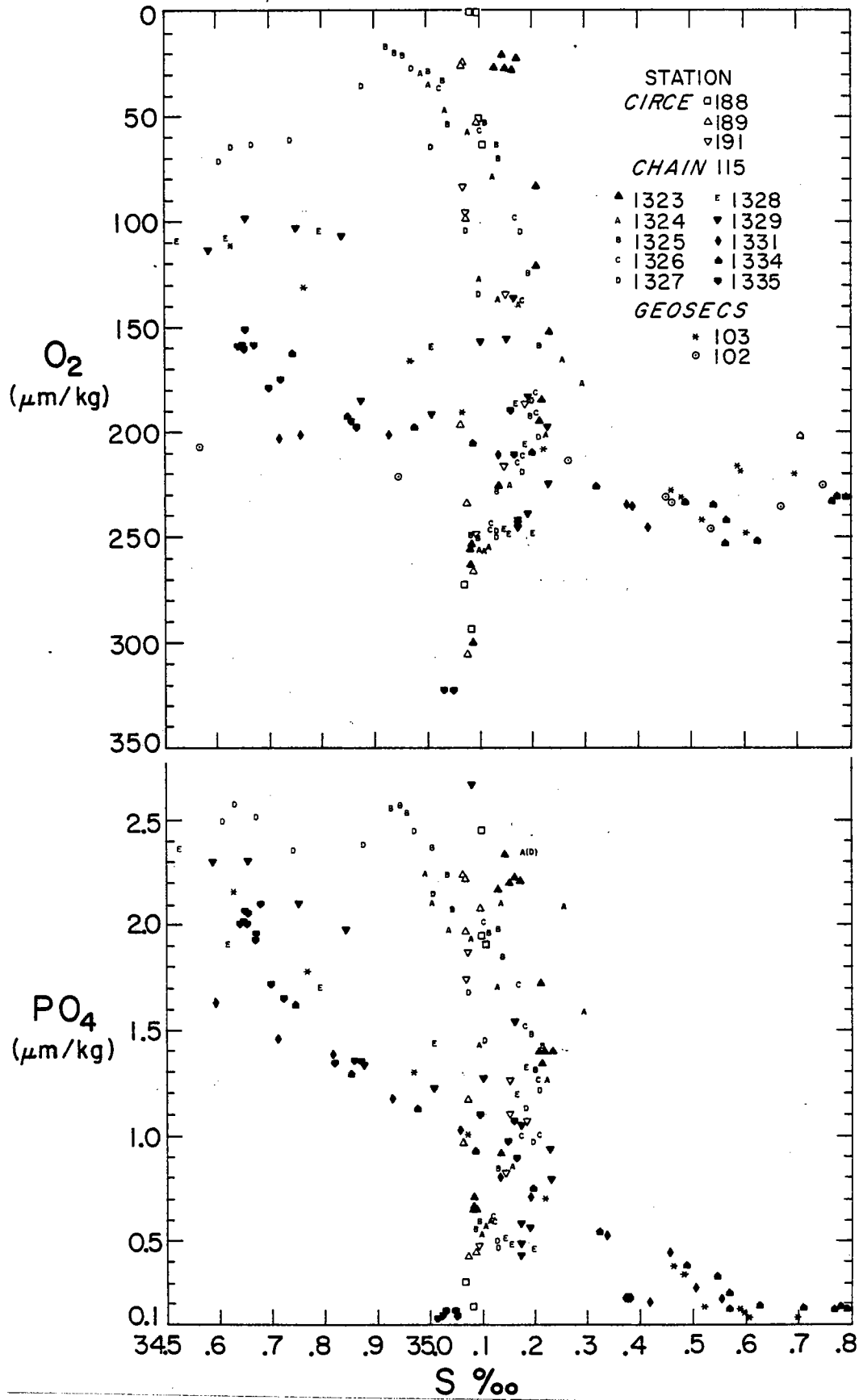


Fig. 3-7 , O_2 -S and PO_4 -S plots for all stations in the Cape Basin.

sample at LVFS Station 5 appears to be a remnant of this deep coastal water (Figs. 4 and 5).

Upwelling at LVFS Station 4 was certainly weaker than at the time of the Circe expedition where 15°C water outcropped at the surface. Hart and Currie (1960) report 18 and 14°C during their surveys of March and September-October 1950 indicating that active upwelling occurs during the spring when the trade winds are well established near Walvis Bay. The 18°C surface water at Station 4 had 0.7 and 2.5 $\mu\text{mol kg}^{-1}$ phosphate and silicate concentrations, was intensely green (visibility 1 or 2 m) and supported abundant sea life and birds indicating high biological productivity. Offshore, at LVFS Station 5, the water was still slightly green and the instruments were visible to depths of approximately 10 m. LVFS Stations 6 and 7 were more typical of open ocean conditions.

The upwelling activity at LVFS Station 8 was similar to that determined by Jones (1971), and Bang (1971) in Feb. 1966, and by Bang and Andrews (1974) in January 1973. These authors found an intense front in this region and showed that upwelling was restricted to within 60 km of the coast. Twenty meter excursions in hydrographic properties were measured by hydrocasts spaced a few hours apart (Fig. 5). The surface waters at Station 8 were soupy green and sea life was extremely abundant. Station 8, therefore, exhibited the features associated with active upwelling whereas Station 4 was typical of relatively quiescent conditions. The other

stations were in areas of moderate (5 and 6) to low biological productivity (7).

Biological distributions

Hart and Currie (1960) studied the systematic variations of plankton in relation to hydrography along the S.W. African coast. Their data represented the fall (March 1950) and spring (Sept.-Oct. 1950) plankton population values but were only semi-quantitative in that they listed the total quantities of organisms caught by vertically hauled plankton nets. The LVFS samples are particularly suited for determining the quantitative, vertical distributions of non-motile organisms as shown in the previous chapter. The $>53 \mu\text{m}$ samples have been analysed by light microscopy as outlined in Chap. 2 and the data (Table 1) is particularly valuable in understanding the chemical distributions in the samples.

A common feature of all stations is the strong vertical gradient in organism abundances within the upper 100 m. This feature necessitated the use of a logarithmic interval when contouring the data (Figs. 8, 9, 10, and 11). The largest number of intact, live organisms were found in the near surface samples and decreased rapidly with depth due to predation and dissolution (Acantharia).

Station 5 had the largest populations of Foraminifera, Acantharia, diatoms, silicoflagellates, tintinnids, and dinoflagellates of the Walvis Bay section stations (4-7).

TABLE 3 - 1 > 53 μ m ORGANISM DISTRIBUTIONS (#/l)

Z FORAMS PT?	A. RAD	J. RAD	C. DIA	S. DIA	P. DIA	G. DIA	SIFLAG	ACANT	TINT	DINOFL	
STATION 4											
20	30.78	1.52	3.04	22.04	12.54	3.42	4.18	11.02	3.80	1.52	4.18
42	8.96	12.67	3.54	5.49	8.02	1.30	.61	3.97	1.23	1.52	.25
100	4.42	4.87	2.58	3.66	1.13	.31	.40	.60	.48	.88	
183	3.60	1.53	.38	8.24	3.16	.48	.82	.48	.10	.14	.10
STATION 5											
20	44.71	2.65	0.09	179.04	37.14	.27	.37	4.84	33.49	.46	3.28
40	34.59	.70	2.16	463.75	24.38	.88	.23	4.84	21.12	1.28	12.60
50	20.60	.06	9.64	45.58	15.72	.28	1.23	44.68	2.13	2.32	.56
88	7.02	.02	2.73	25.14	21.06	.23	.48	4.91	.80	.73	.87
124	5.60	.02	6.98	10.41	3.06	.02	.80	2.19	.83	1.59	.06
199	2.90	.10	4.10	3.13	1.36	.60	.14	1.05	.26	.76	.01
294	2.70		4.20	1.67	.49		.14	.80	.20	.74	
379	1.54		4.64	2.34	1.71		.01	.98	.13	.45	

TABLE 3-1 (cont.)

Z FORAMS PT?	A.RAD	J.RAD	C.DIA	S.DIA	P.DIA	G.DIA	SIFLAG	ACANT	TINT	DINOFL		
STATION 6												
26	13.21	.09	1.75	0.00	1.56	1.79	.05	.05	2.03	30.67	.09	2.12
52	29.20	.53	2.33	0.05	35.56	113.42	1.06	.53	12.19	7.10	.15	.53
113	6.21	.09	2.54	0.36	16.67	.50	9.94	.46	5.67	.96	.81	.13
187	1.80	.02	2.18	0.41	2.00	.04	.26	.03	3.26	.66	.08	.03
289	1.75	.01	1.95	0.14	.77	.21	.34	.05	.61	.23	.03	
386	1.16	.04	1.79	0.18	.97	.10	.30	.04	.72	.23	.04	
STATION 7												
20	2.31		0.78	0.00	.37	.23	.60	.41	14.52	3.91	.18	1.38
75	2.75		2.69	0.03	.40	2.32	.43	.16	17.38	1.14	.03	.19
124	2.21		1.47	0.03	1.22	2.12	.35	.13	7.28	.06	1.25	.16
377	.29		0.93	0.05	.17	.45	.02	.01	.41	.03	.04	

TABLE 3-1 (cont.)

Z FORAMS PT?	A.RAD	J.RAD	C,DIA	S.DIA	P.DIA	G.DIA	SIFLAG	ACANT	TINT	DINOFL
STATION 8										
20	23.61	11.81	1.07	11414.90	870.47	4.29	1.07	640.78	10.73	148.12
42	6.80	4.67	1.01	4431.80	185.50	7789.10	36.33	6.29	0.61	16.84
100	3.96	37.52	5.05	137.70	32.16	18.10	4.20	13.13	.47	2.87
150	.93	5.56	2.78	6.81	5.99	1.09	1.14	.65	.22	.11
251	.82	3.59	0.65	6.69	1.88	.82	.41	.41	.41	.16
Z	-	depth (m)		C.DIA	-	centrate diatoms		SIFLAG	-	silicofla- gellates
FORAMS	-	Foraminifera		S.DIA	-	solenoid diatoms		ACANT	-	Acantharia
PT?	-	Pteropods (?)		P.DIA	-	pennate diatoms		TINT	-	Tintinnids
A.RAD	-	Adult Radiolaria		G.DIA	-	gonoid diatoms		DINOFL	-	dinoflagel- lates
J.RAD	-	Juvenile "								
WHOLE ORGANISMS ONLY										
BLANKS IN THE DATA INDICATE ORGANISMS NOT PRESENT										

Stn. 4 had maximum populations of Radiolaria while Stn. 6 had the same Acantharia population as at 5 and had a strong maximum in solenoid diatoms, dominated by Rhizosoleniaceae. Coccolithophorids were dominant in the $>53 \mu\text{m}$ size fraction at 4 where the population was $750 \ell^{-1}$. These organisms also were the most important contributors to the $<53 \mu\text{m}$ biomass at 4 where replicate samples from 20 m spaced by 8 hours gave population densities of 4400 and $6200 \ell^{-1}$.

Acantharia, Foraminifera, and Radiolaria exhibit contrasting distributions (Fig. 8). Acantharia show a surface maximum at all stations and are most abundant at Stns. 5 and 6 where over $30 \ell^{-1}$ were found. Foraminifera show a surface maximum at Stns. 4 and 5 of 30 and $44 \ell^{-1}$ but have a subsurface maximum at 6 and 7 of 30 and $3 \ell^{-1}$ near the base of the mixed layer. Other organisms that had conical or planar spiral carbonate shells larger than $100 \mu\text{m}$ have been tentatively identified as Pteropods; they may be also juvenile stages of Foraminifera, Spiralina or Silicinidae. They were encountered mainly at Stations 5 and 6 and showed maxima at the base of the mixed layer of 0.7 and $0.5 \ell^{-1}$.

Adult and juvenile Radiolaria are found primarily in the upper thermocline and exhibit deeper maxima than most organisms encountered; populations of approximately $10 \ell^{-1}$ were present at 40 and 50 m at Stations 4 and 5. Fewer than $3 \ell^{-1}$ were found at the maxima located at 110 and 75 m at Stations 6 and 7. Similar vertical distribution trends for both Foraminifera

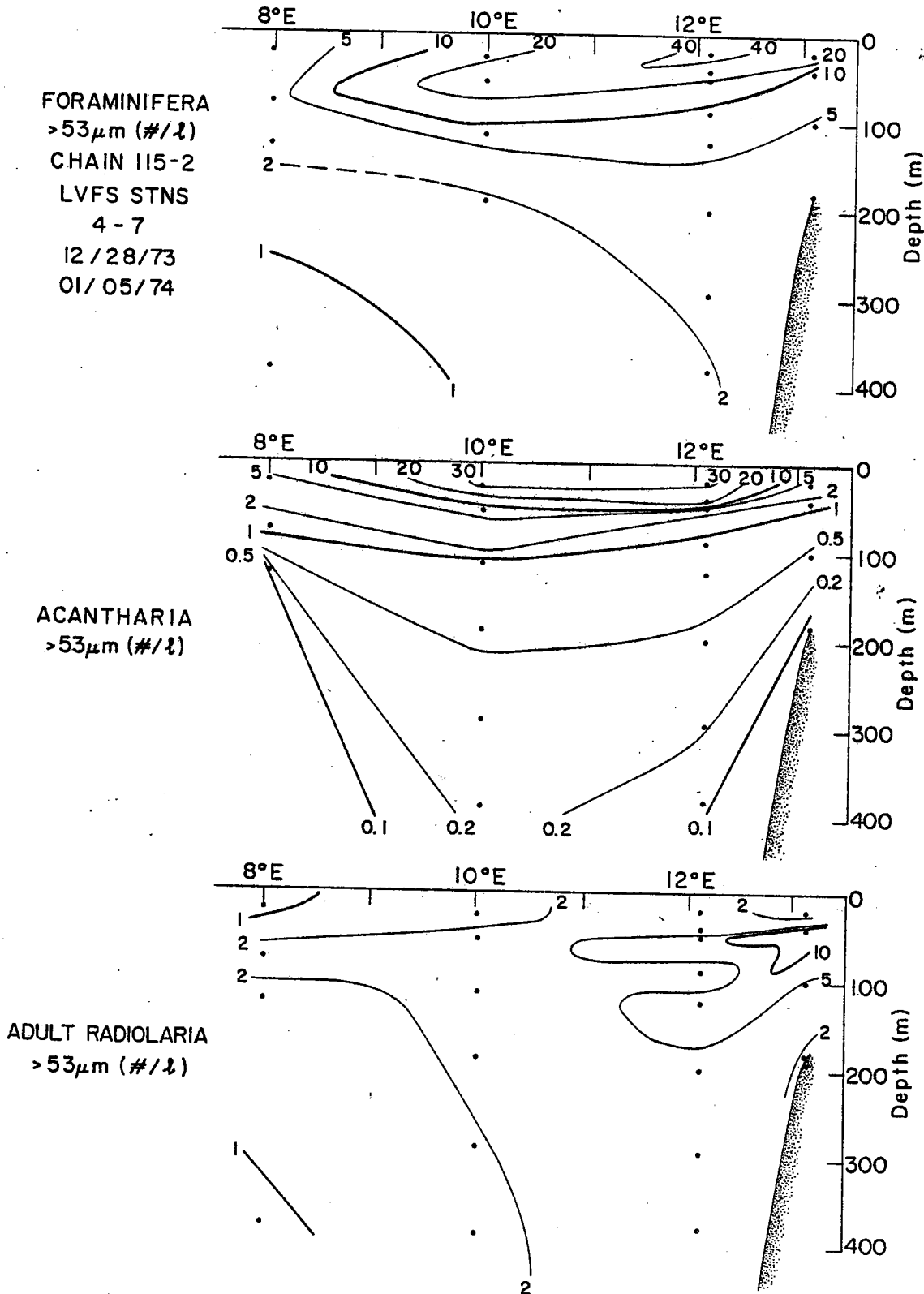


Fig. 3,8 , Distributions of Foraminifera, Acantharia, and Radiolaria for LVFS stations 4 - 7; >53 μ m fraction

and Radiolaria have been observed by Berger (1968) and Petrushevskaya (1971) who used towed 125 μm plankton nets and filtration of 2.5 to 40 ℓ volumes of water to obtain their samples respectively. In spite of the rather contrasting methods, the agreement of the data with that obtained by the LVFS suggests that the occurrence of Radiolaria deeper than Foraminifera is a general phenomenon.

Diatoms (Fig. 9) are concentrated at the surface only at Stn. 4 ($40\ell^{-1}$) and coincide with the base of the mixed layer at Stns. 5 ($500\ell^{-1}$), 6 ($110\ell^{-1}$) and 7 ($4\ell^{-1}$). Of the four categories of diatoms, the centrate and solenoid are the most numerically significant contributions to the $>53 \mu\text{m}$ fraction. Centrate diatoms dominate at Stns. 4 and 5 whereas solenoids dominate at 6 and 7. Pennate and gonioid diatoms are relatively minor contributors to the biomass, being most significant at Stns. 4 and 7. Pennates are most important in the $<53 \mu\text{m}$ fraction as they are typically smaller than $50 \mu\text{m}$ in valvar length (Chap.2)

Silicoflagellates (Fig. 10) were shown to be most numerous in the $<53 \mu\text{m}$ size fraction at LVFS Stn. 2 (Equatorial Atlantic, Chap. 2). Their occurrence in the $>53 \mu\text{m}$ samples is indicative of their vertical distributions. They show a surface maximum at Stn. 4 ($10 \ell^{-1}$); subsurface maxima are observed in the upper thermocline at Stn. 5 ($44\ell^{-1}$) or at the base of the mixed layer at Stns. 6 and 7 (12 and $18 \ell^{-1}$).

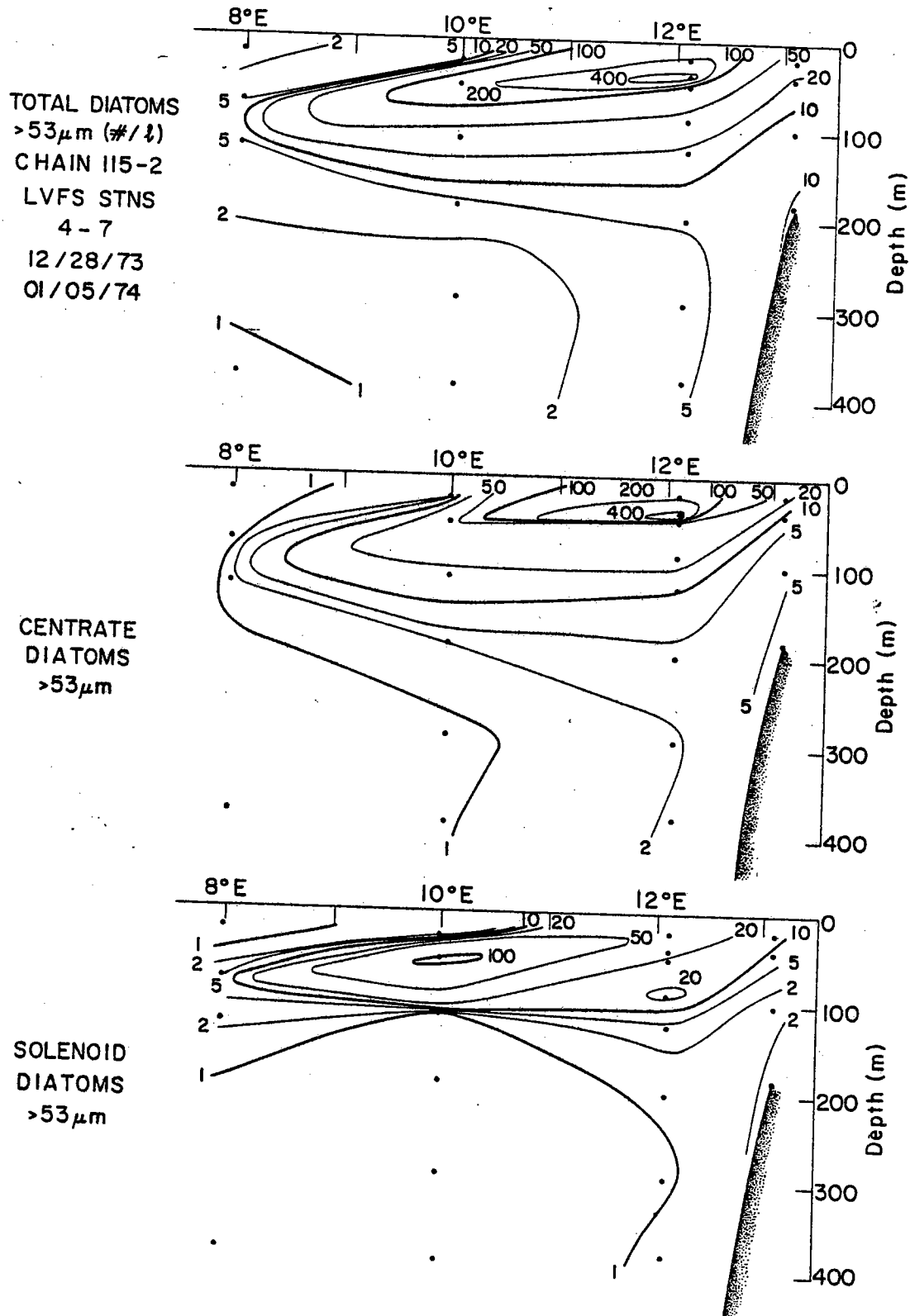


Fig. 3-9 , Distributions of centrate and solenoid diatoms at LVFS stations 4 - 7; >53 μm fraction.

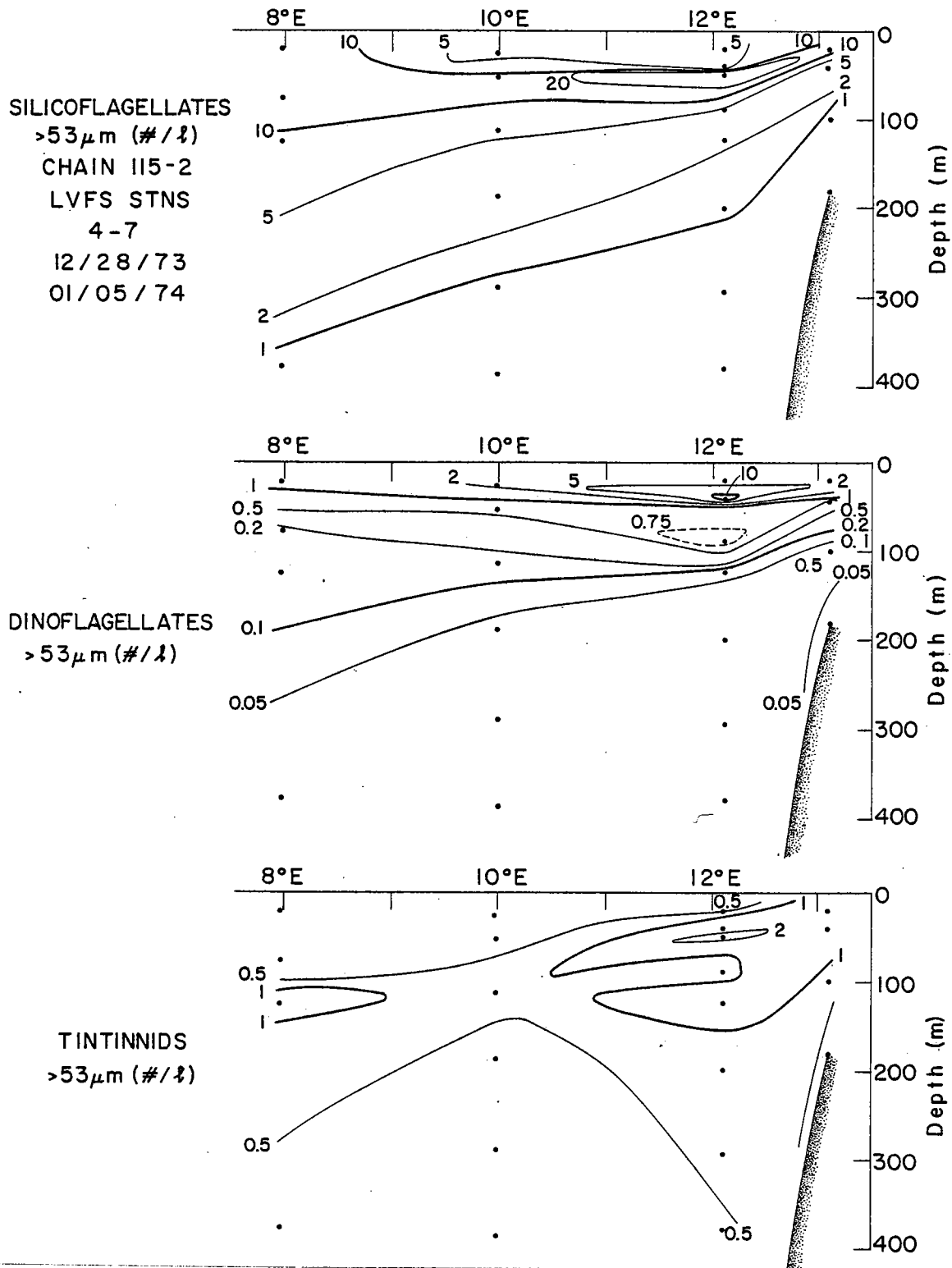


Fig. 3-10, Distributions of silicoflagellates, dinoflagellates, and tintinnids at LVFS stations 4 - 7; >53 μm .

Dinoflagellates are found nearest the surface at Stns. 4 ($4\ell^{-1}$), 6 ($2\ell^{-1}$) and 7 ($1\ell^{-1}$); only 5 ($12\ell^{-1}$) showed a subsurface maximum. This reflects the light requirements of dinoflagellates as they are largely photosynthetic.

Tintinnids are distributed in a similar fashion to Radiolaria with maximum concentrations of $2\ell^{-1}$ at Stns. 4 and 5 and $1\ell^{-1}$ at 6 and 7.

Station 8, near Capetown, had different relative abundances of organisms compared to the Walvis Bay stations. Diatoms were by far the most important contributors to the biomass (Fig. 11). Centrate diatoms have a surface maximum of $12,000\ell^{-1}$ contrasting with pennate diatoms which showed a maximum of $8000\ell^{-1}$ at 42 m. Silicoflagellates and dinoflagellates have strong maxima near the surface of 640 and $150\ell^{-1}$. Acantharia are no more abundant than at other stations and like diatoms, silicoflagellates and dinoflagellates decrease in concentration by three orders-of-magnitude from the surface to 150 m. Foraminifera show a surface maximum of $24\ell^{-1}$; Radiolaria and Tintinnids have maximum populations of 40 and $3\ell^{-1}$ near 100 m. Station 8 exhibits the same vertical distribution patterns for the organisms as found at the other stations, in spite of differences in relative abundances.

The fall (March 1950) hydrographic and biological data of Hart and Currie (1960) is most comparable to that obtained at the LVFS stations near Walvis Bay. These authors

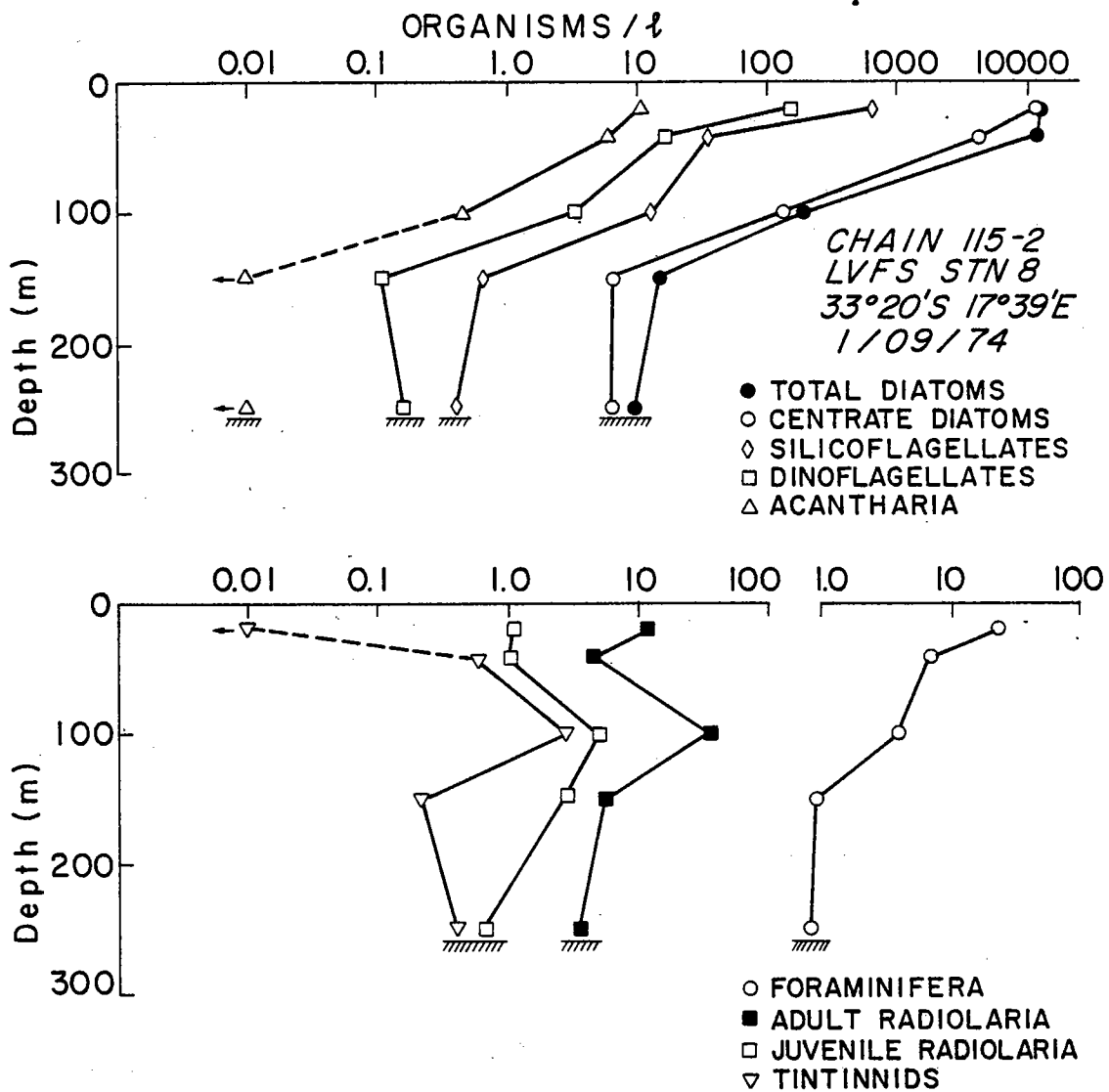


Fig. 3-11, Distributions of organisms at LVFS Stn. 8 near Cape Town

+ indicates organism not encountered in the subsample studied.

found between 10 and 100 million diatoms per vertical haul of a 44 μm mesh 0.5 m plankton net at Stations WS 979-981. A minimum diatom concentration may be calculated from their data assuming that 10 m^3 is a representative volume of water filtered by the net hauled vertically from 50 m. LVFS Station 4 is approximately 35 km offshore and so would be in a similar regime as WS 980 where 50 million diatoms were collected using this technique. The concentration of diatoms would therefore be 5000 diatoms ℓ^{-1} , two orders of magnitude larger than found at LVFS station 4. As noted earlier, coccolithophorids $\sim 50\text{ }\mu\text{m}$ in size had concentrations of approximately 5000 ℓ^{-1} showing a marked contrast to the conditions encountered by Hart and Currie (1960). On the other hand, the diatom distributions at LVFS Station 8 are comparable with those found by these workers.

The deep scattering layer (as observed by 12 kHz PGR) migrated at sunset from the bottom and near bottom at Stations 4 and 8, from 400 m at 5, 450 m at 6, and from 400 m at 7. Sonic backscattering from this layer was most intense at Stations 4, 5, 6, and 8 and rather weak at 7 indicating that deep scattering layer organisms were most rare at Station 7.

The important features of the biological distributions are that the high productivity at Station 4 was almost entirely due to coccolithophorids. Only at Stations 5 and 6 were diatoms important in the $>53\text{ }\mu\text{m}$ size fraction. Station 7

is remarkable in that it was very sparsely populated with plankton. Station 8 was the only station where active upwelling was identified and possessed populations of diatoms consistent with the observations of Hart and Currie (1960).

Dry weight

The dry weight data of Bishop and Edmond (1976) have been slightly adjusted because lower carbon blank values were used than in the original calculation. This stems from the experiment discussed in Chap. 2 where glass fiber filters exposed to seawater were found to have lower blanks than unused filters. The data has also been calculated as $\mu\text{g kg}^{-1}$ to be consistent with Chap. 2. These authors found systematic differences between the dry weight profiles from the LVFS samples and those obtained using the more conventional 30ℓ Niskin samplers and vacuum filtration of 10-20ℓ of seawater through 0.4 μm Nuclepore filters. The comparison of the two filtration techniques should be reiterated because recent work by Gardiner (1976) and the microscopic observations discussed above provide an improved explanation for the discrepancy between the two techniques. Furthermore these filters have been analysed for silica and it is necessary to understand the sample bias due to the Niskin method in order to relate the silica data to the LVFS data.

The $>53 \mu\text{m}$ dry weight distribution reflects the organism distributions discussed above (Fig. 12). Surface maxima

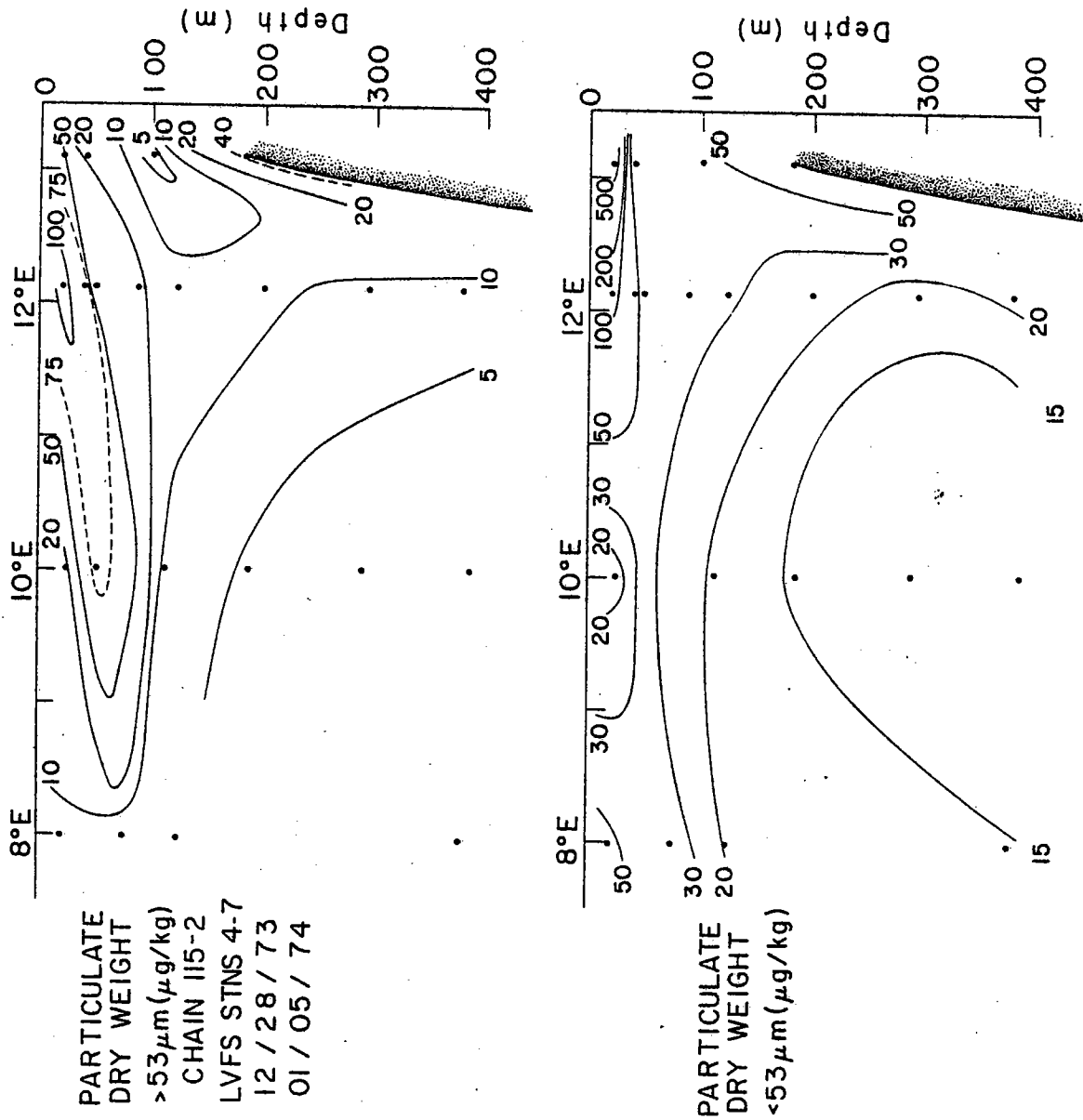


Fig. 3-12, >53 and <53 μm particulate dry weight section for LVFS stations 4 - 7.

(66 and 104 $\mu\text{g kg}^{-1}$) were observed at Stations 4 and 5. A strong subsurface maximum of 95 $\mu\text{g kg}^{-1}$ was found at 52 m at Station 6 and concentrations were everywhere lower than 10 $\mu\text{g kg}^{-1}$ at Station 7. The 800 $\mu\text{g kg}^{-1}$ concentration found near the surface at Station 8 reflected the intense biological production at this station compared with the others. All stations except 7 had higher concentrations than observed at Station 2 in the equatorial Atlantic. The minimum of <5 $\mu\text{g kg}^{-1}$ at 100 m at 4 is lower than found at Station 5 indicating a relatively small concentration of sinking material.

At Station 4, the <53 μm fraction shows a strong surface maximum of 660 and 630 $\mu\text{g kg}^{-1}$ for replicate samples spaced by eight hours. A surface maximum of 110 $\mu\text{g kg}^{-1}$ was also observed at 5. Concentrations were below 30 $\mu\text{g kg}^{-1}$ in the surface waters at 6, and Station 7 showed a weak surface maximum of 50 $\mu\text{g kg}^{-1}$. Of all stations, Station 8 showed the highest concentration with a surface maximum of 1130 $\mu\text{g kg}^{-1}$.

The particulate distributions determined by the Niskin method show discrepancy with the LVFS data (Fig. 13) mostly at stations where the >53 μm fraction is a substantial contributor to the total mass. Where this occurs, the organisms are very large and numerous and thus might be particularly prone to being lost from the filtration apparatus by settling below the level of the valves of the Niskin sampler. The investigations of Gardiner (1976) verify this possibility. He found that as much as 50% of

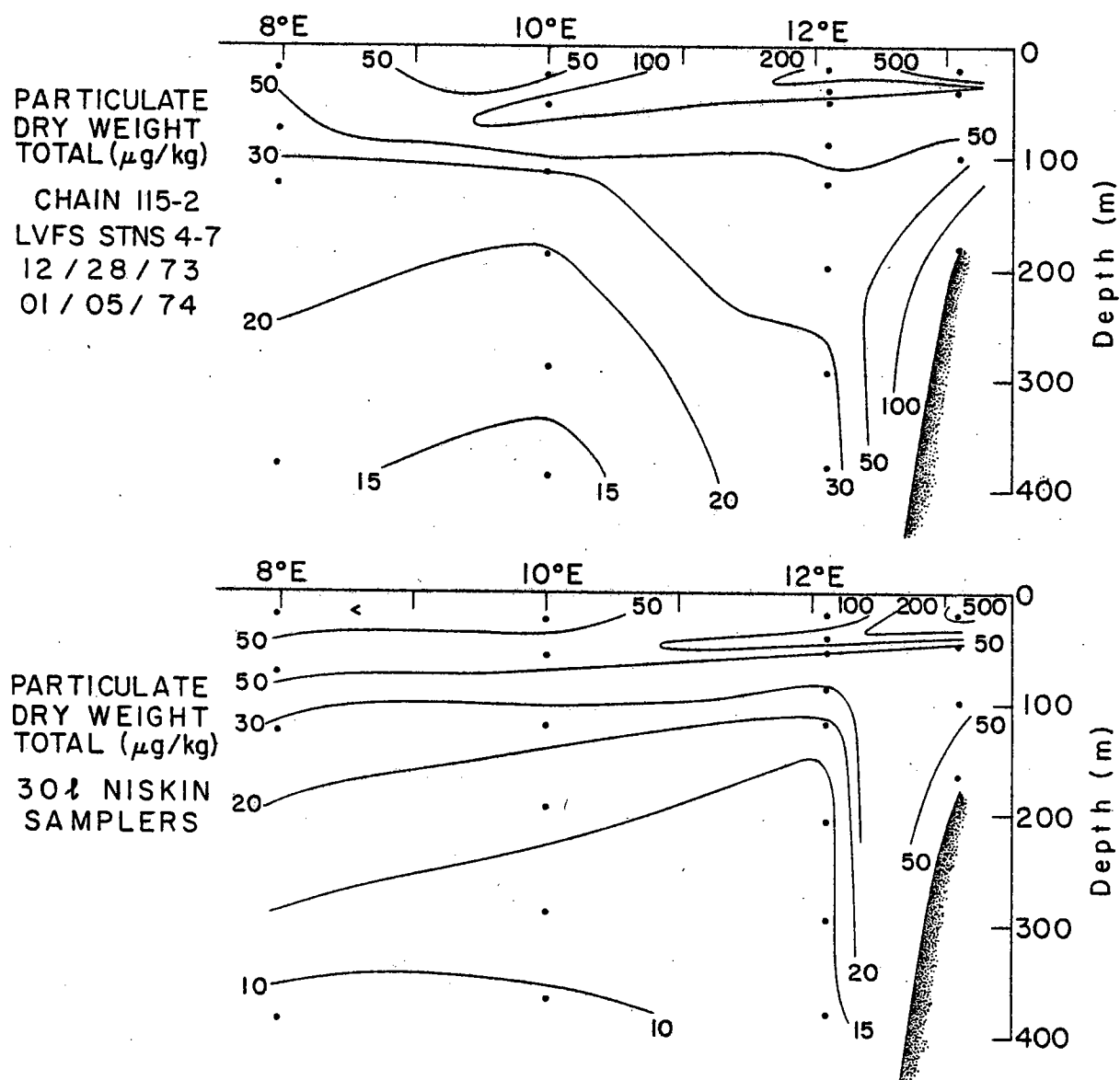


Fig. 3-13, Total dry weight distributions determined by LVFS and NISKIN methods.

the particulate mass within the water sampled had settled below the valves of the sampler. The agreement between the two methods should be good at stations where most particles are smaller than 50 μm or are slowly sinking (Station 4 is a good example); the agreement of the two methods for particulate mass below 100 m is best where the $>53 \mu\text{m}$ component is small. It is unlikely that water column dynamics (Bishop and Edmond, 1976) play an important role in determining the differences between the two methods. Bishop and Edmond (1976) observed good agreement in the particulate distributions measured by the two methods at many stations and thus it may be concluded that major discrepancies will be limited mainly to the near surface waters in moderately productive areas. The recently published (Brewer et al. 1976) GEOSECS particulate data shows agreement within 30% of the LVFS data for the depth interval between 100 and 400 m.

Organic Carbon and Nitrogen

Menzel (1974) has recently reviewed the literature describing the distributions of particulate organic carbon in the ocean. He argues that the presently available data for particulate carbon cannot demonstrate variability in space or time for samples below 100 to 200 m in the ocean. Recent values for this deeper water seldom exceed 800 nmol (10 μg) C kg^{-1} .

Gordon (1971) found scattered values between 170 and 580 nmol (2 and 5 μg) C kg^{-1} for the depths between 200 and

500 m in the tropical north Pacific. His error, using 1.2 μm silver filters and filtration of 10 liters of seawater, was 125 nmol (1.5 μg) C kg^{-1} , the same order of magnitude as the carbon concentrations in the deep water. Similarly, Hobson and Menzel (1969) found values between 170 and 1000 nmol (2 to 12 μg) C kg^{-1} within this depth interval in the southwestern tropical Atlantic. Wangersky (1976) reported higher values (0.8 μm Silver filters) ranging from 250 to 3330 nmol (3 to 40 μg) C kg^{-1} , averaging 1420 nmol (17 μg) C kg^{-1} from the 100 to 500 m depth interval sampled during the Hudson 70 expedition along 30°W between 0 and 30°S. For comparison, Brewer et al. (1976) found an average total particulate mass concentration (0.4 and 0.6 μm Nuclepore filters) of 11.9 μg kg^{-1} for samples collected during the GEOSECS expedition from the same depth interval and region of the south Atlantic. These two sets of data are not reconcilable, although arguments have been made that glass and silver filters are more efficient than membrane filters at retaining particles smaller than their stated pore size (Sheldon 1972, and Feely, 1975).

The LVFS samples are ideal for studying the spatial homogeneity of particulate matter in the waters below the euphotic zone as well as for resolving the discrepancies between total particulate carbon and dry weight measurements. Analyses for C and N were carried out as described in Chap. 2 and the data for the particles retained by the top (1-53 μm fraction) and bottom (<1 μm fraction) glass fiber filters are

shown in contoured sections and profiles for LVFS Stns. 4 to 7, and 8 (Figs. 14, 15, and 16). Data for total carbon is corrected for carbonate to give values for organic carbon.

Sharp concentration gradients observed for the $<53 \mu\text{m}$ particles in the upper 100 m necessitated logarithmic contour intervals. Stns. 4 and 5 exhibited surface maxima (22.1 and $18.4 \mu\text{mol C kg}^{-1}$ for replicate samples at 4, and $3.9 \mu\text{mol C kg}^{-1}$ at 5). Stations 6 and 7 showed maxima near the base of the mixed layer (0.75 and $1.08 \mu\text{mol C kg}^{-1}$). Deeper than 100 m, the values at Stations 5, 6, and 7 fell lower than $0.50 \mu\text{mol C kg}^{-1}$ and below 200 m all were lower than $0.30 \mu\text{mol C kg}^{-1}$. This behavior is comparable to that from Stn. 2 (Chap. 2) where values decreased regularly from 0.33 to $0.22 \mu\text{mol C kg}^{-1}$ between 100 and 400 m. The lowest value encountered at Station 4 was $0.8 \mu\text{mol C kg}^{-1}$ at 100 m and is probably the result of the high surface productivity at this station. The highest concentration levels were observed at Stn. 8 where the concentrations varied between 30 and $1.2 \mu\text{mol C kg}^{-1}$ between the surface and 150 m. As found in Chap. 2, the $<1 \mu\text{m}$ carbon accounted for a substantial fraction of the total sampled; this component was 25 and 50% of the $<53 \mu\text{m}$ carbon of the near surface samples at Stns. 4 and 8.

The particulate nitrogen distribution follows that of organic carbon with levels being lower by a factor of approximately 7. Differences are best illustrated by profiles

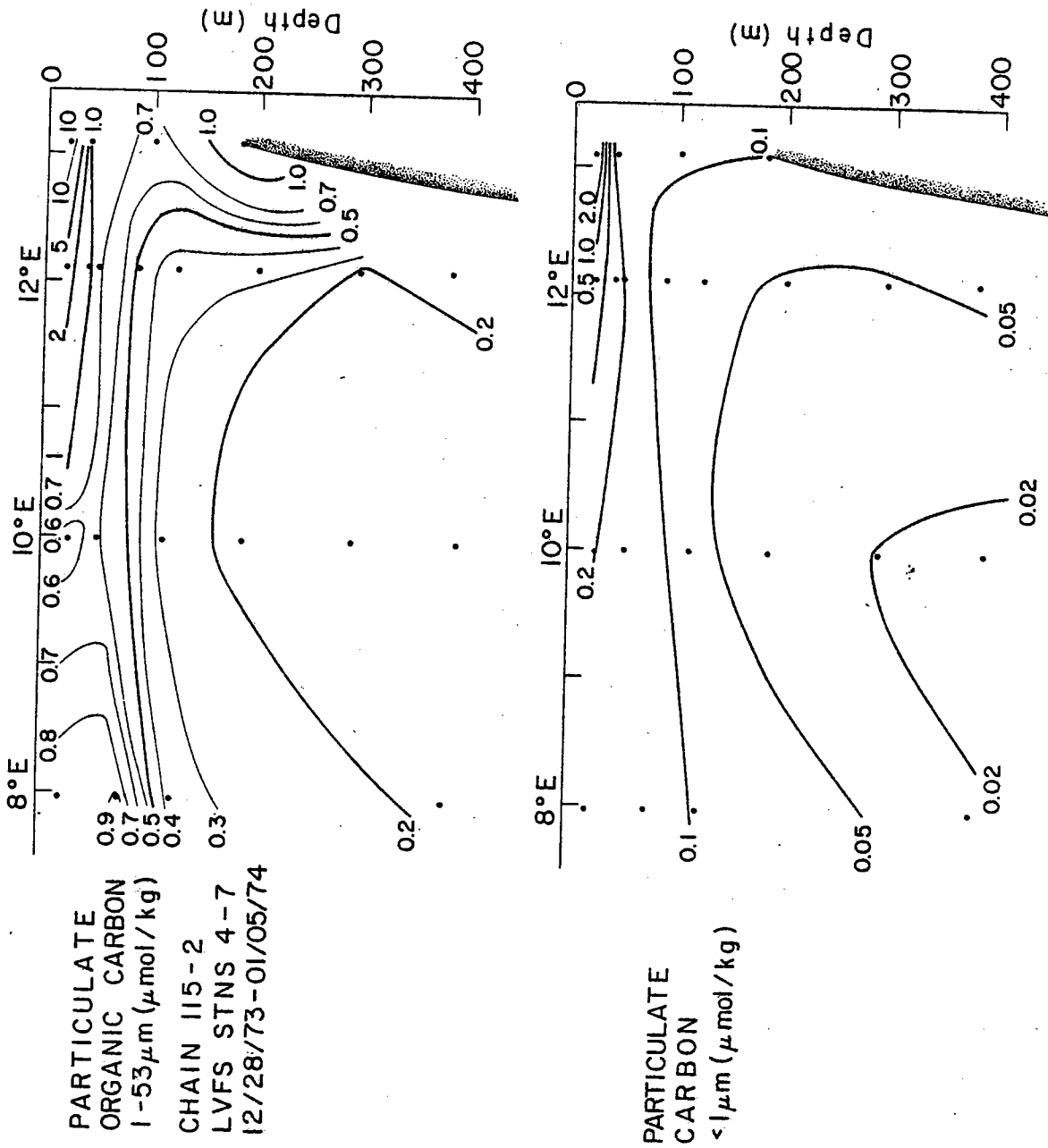
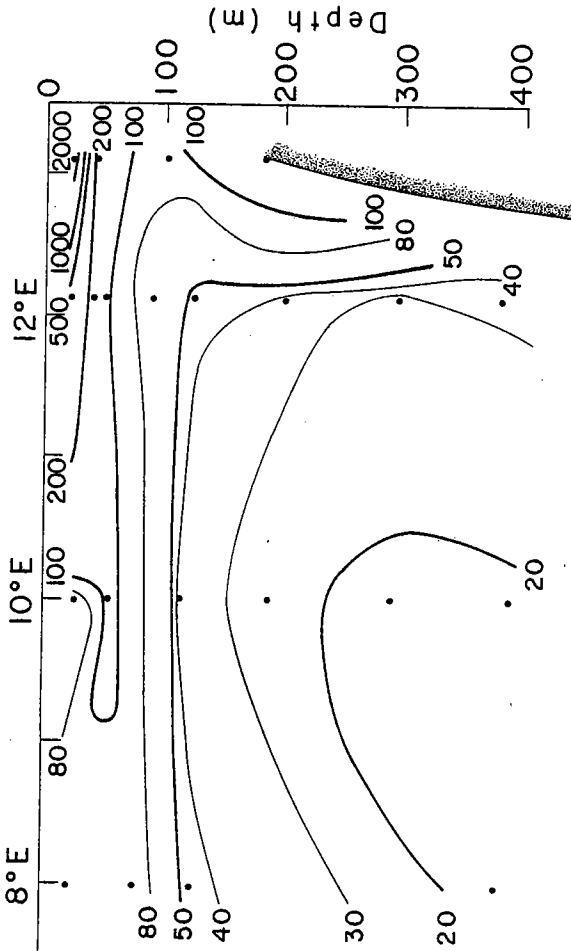
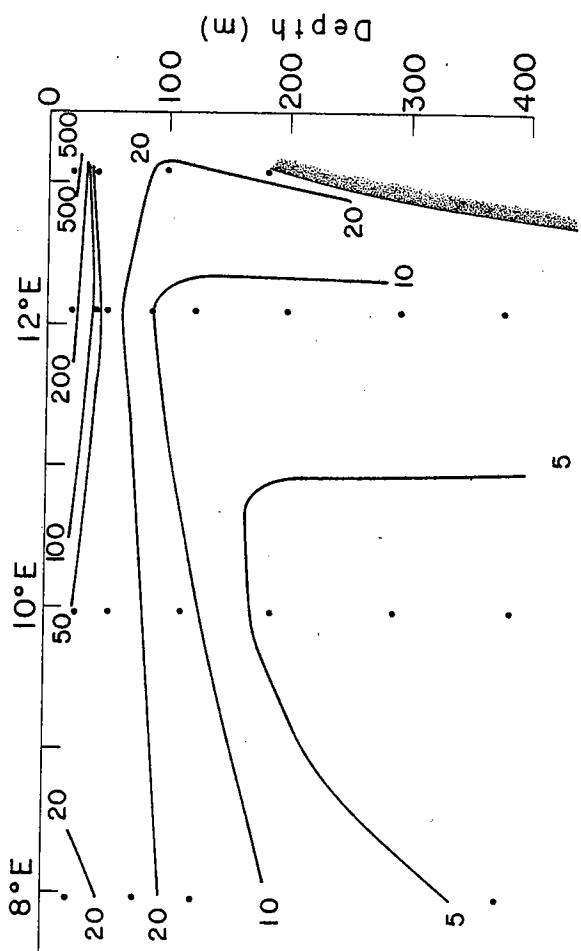


Fig. 3-14, Particulate organic carbon distributions at LVFS stations 4 - 7.



PARTICULATE
NITROGEN
1-53 μm (nmol / kg)
CHAIN 115-2
LVFS STNS 4-7
12/28/73-01/05/74



PARTICULATE
NITROGEN
< 1 μm (nmol / kg)

Fig. 3-15, Particulate nitrogen distributions for LVFS stations 4 - 7.

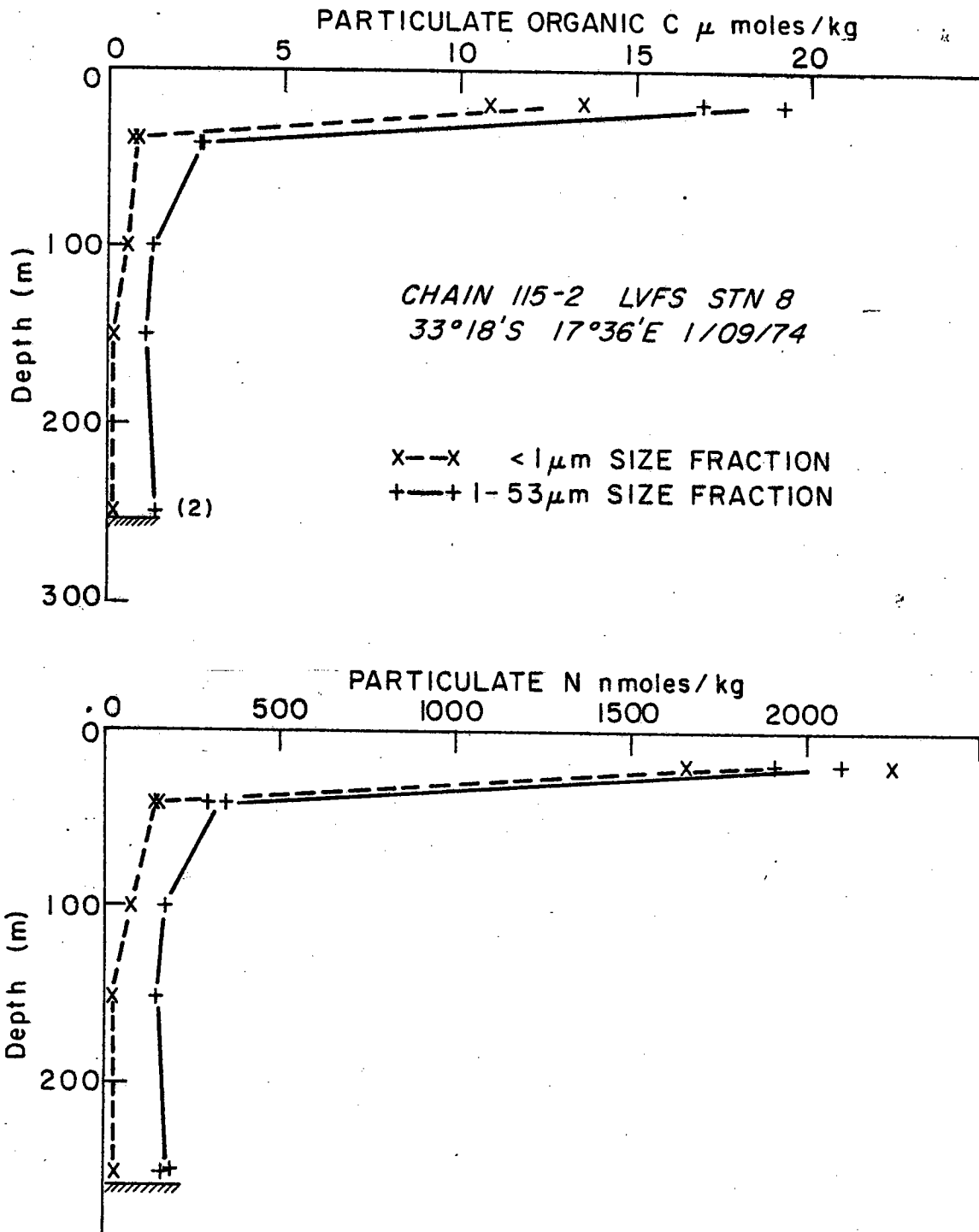


Fig. 3-16, Particulate organic carbon and nitrogen at LVFS station 8.

of organic carbon to nitrogen ratios' (Fig. 17). The 1-53 μm C/N ratios at Stations 4 to 6 are remarkably uniform being 7.3 ± 0.5 (σ) throughout the entire depth interval sampled; these values are in good agreement with those found by Hobson (1971) for the organic material from the surface waters near Walvis Bay (April-May, 1968). Station 7 was the only one that exhibited an increase with depth similar to that found at Station 2. Station 8 showed a C/N ratio maximum of 9 near the surface but otherwise had values comparable to Stations 4 to 6.

In Chap. 2 it was shown that nitrogen rich marine bacteria could account for most of the $<1 \mu\text{m}$ organic material, especially in the near surface waters. This is consistent with the behavior of the C/N ratios with depth at Stations 4 to 8 as well (Fig. 17). At every station the $<1 \mu\text{m}$ fraction ratios were lower than for the 1-53 μm fraction. The near bottom samples at Stations 4 and 8 had ratios between 4 and 5 indicating significant populations of bacteria. These observations are consistent with those of Calvert and Price (1971) who found high concentrations of nitrite in the near bottom water on the shelf and attributed this phenomenon to the presence of denitrifying bacteria. There are probably other kinds of bacteria that contribute to the observed C/N ratios.

The concentrations of particulate organic matter below the euphotic zone depend on the surface productivity but the

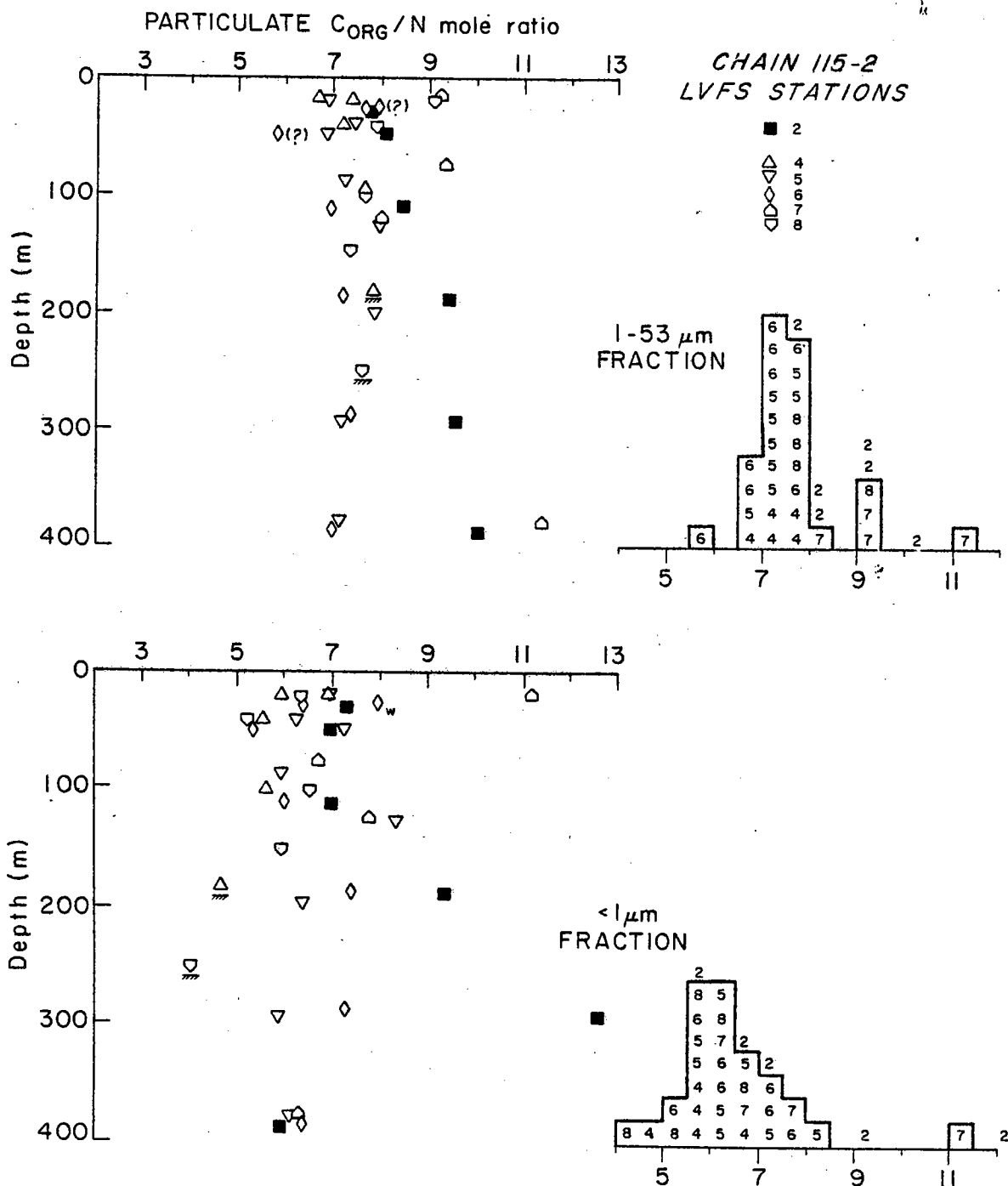


Fig. 3-17, Particulate organic carbon to nitrogen ratios for the < 1 and 1-53 μm fractions at LVFS Stns. 2 and 4-8.

variations are such as to escape detection by the more conventional sampling methods. The variability found in the LVFS samples is contrary to the hypothesis of Menzel (1974) that the particulate organic matter is distributed uniformly in space below a depth of 100 to 200 m.

The strong similarity of the sections for $<53 \mu\text{m}$ dry weight and C and N immediately suggests the important contribution of organic matter to the total dry weight. The vertical distribution of organic matter expressed as a percentage of total dry weight (calculated as " $\text{CH}_2\text{O} + \text{N}$ " for the $<53 \mu\text{m}$ fraction and as "total dry weight - carbonate - opal - celestite" for the $>53 \mu\text{m}$ fraction). Fig. 18 shows that organic matter accounts for nearly 100% of the total dry weight of material at the surface. The organic component falls to 50 and 60% within the upper 400 m for the <53 and $>53 \mu\text{m}$ fractions indicating preferential regeneration of organics. Near bottom $<53 \mu\text{m}$ samples at stations 4 and 8 show stronger depletion in organic material indicative of resuspended relatively organic poor biogenic sediments.

The striking feature of the organism, dry weight, and organic carbon and nitrogen distributions observed at all stations is the strong vertical concentration gradient within the upper 100 m. This feature can only be maintained by grazing organisms feeding on the phytoplankton and microzooplankton populations found in the euphotic zone.

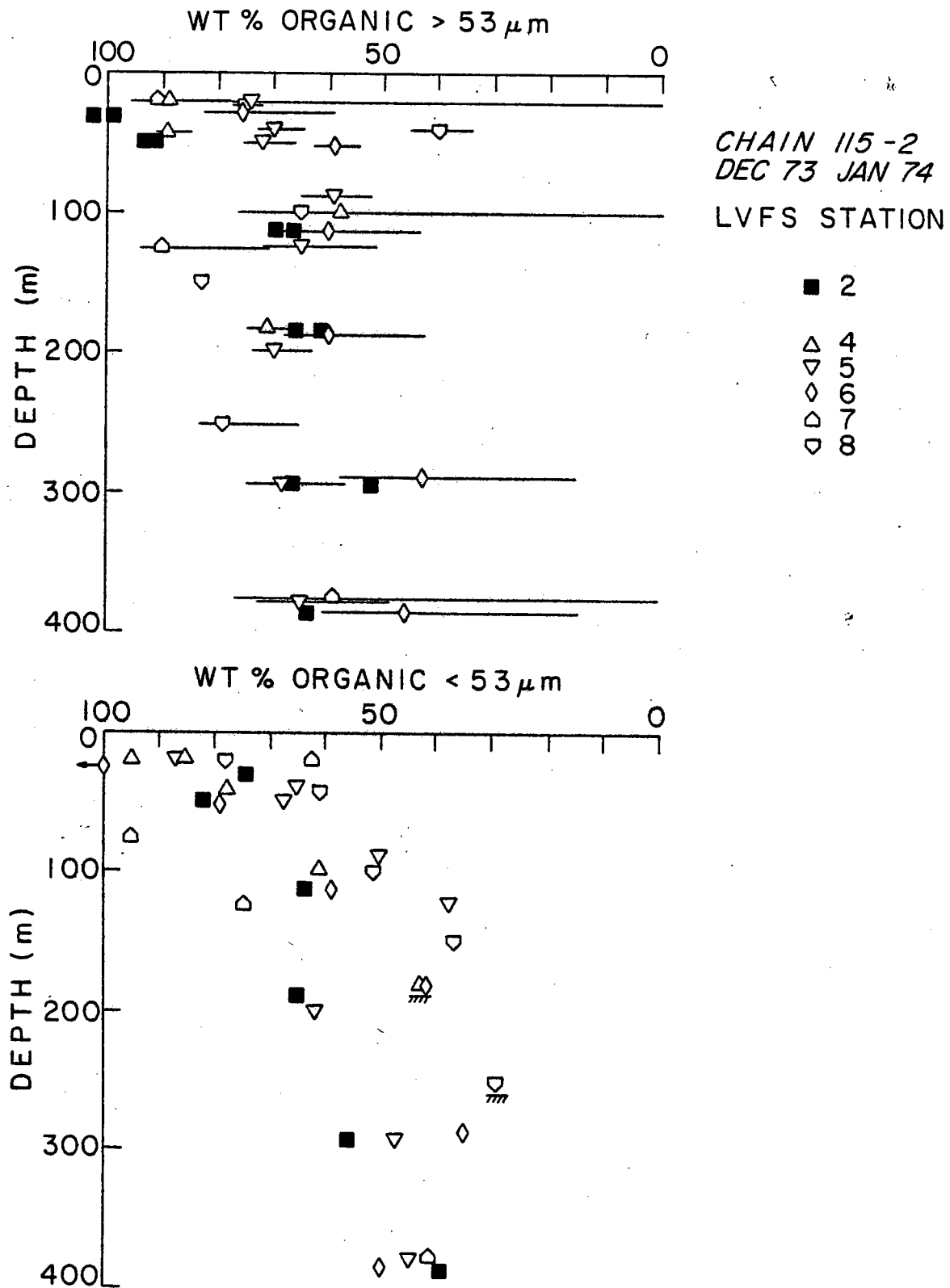


Fig. 3-18, Percentage of dry weight attributable to organic matter in the >53 and <53 μm fractions.

Excess major ions Ca, K, and Mg

Ca, K, and Mg have been shown to be associated with organic matter (Chap. 2). These elements are present in the cell material of plankton (Mayzaud and Martin, 1975) and perform important biochemical functions (Hughes, 1972). The particulate matter below the euphotic zone at Station 2 contained both ion exchange and complexing sites for these elements. The importance of the organic fraction as a carrier of minor and trace elements to the deep ocean is indicated by the occurrence of strontium at ion-exchangeable positions on the organic matter (Chap. 2) and by the correlations of dissolved Cd and Ni with phosphate (Boyle, Sclater, and Edmond, 1976; Bender, and Gagner 1976; and Sclater, Boyle, and Edmond, 1976).

The $>53 \mu\text{m}$ particulate excess Ca, K, Mg, and dry weight distributions are very similar (Figs. 19, 20, and 12). The estimated ratios for particulate organic carbon to excess Ca and Mg fall within the range of 100 - 200 to 1 for the near surface samples and are comparable to those found at Station 2. Excess Ca and K show similar detail in distribution (for instance the double maxima at 40 and 88 m at Station 5) which is not found in the Mg data. This together with the generally higher C_{org}/Ca and C_{org}/Mg ratios for the deeper samples indicates that Mg occurs in a more refractory phase, consistent with Chap. 2. Below 100 m xs Ca and K occurred

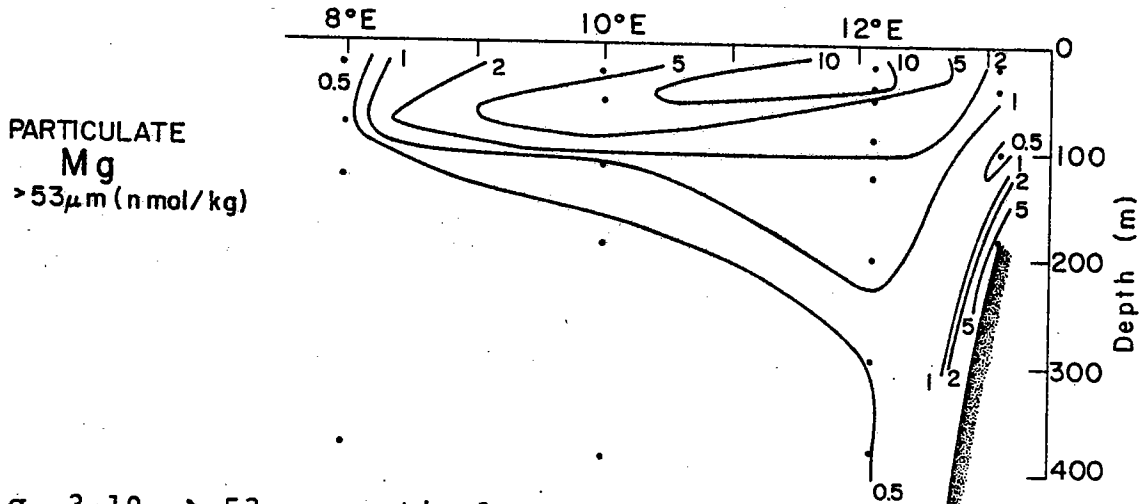
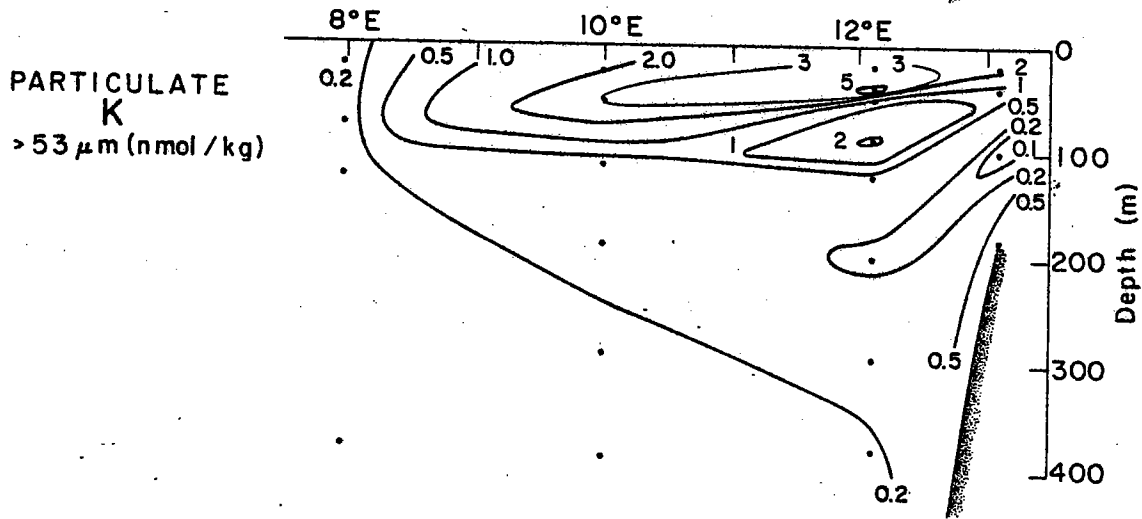
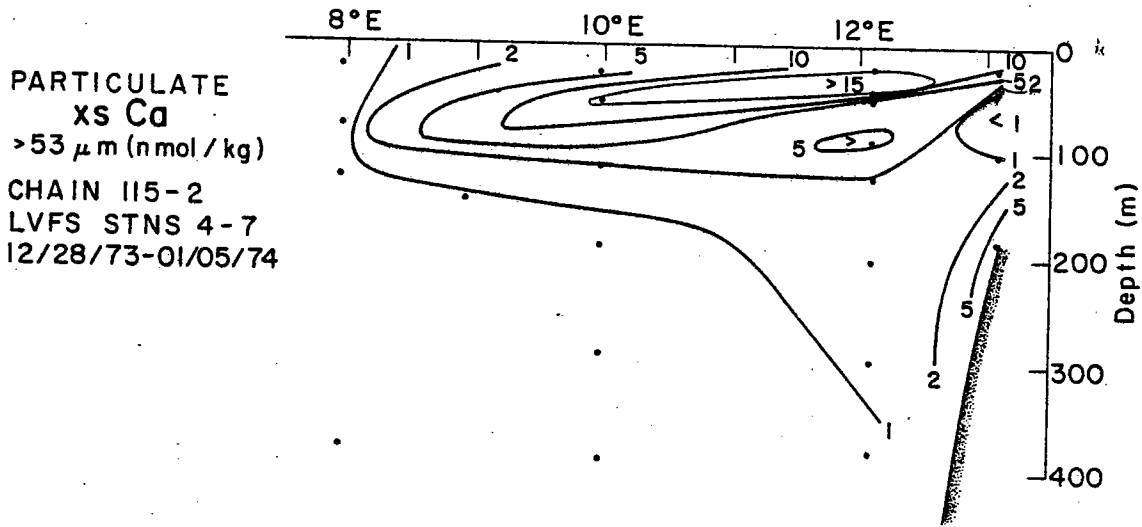
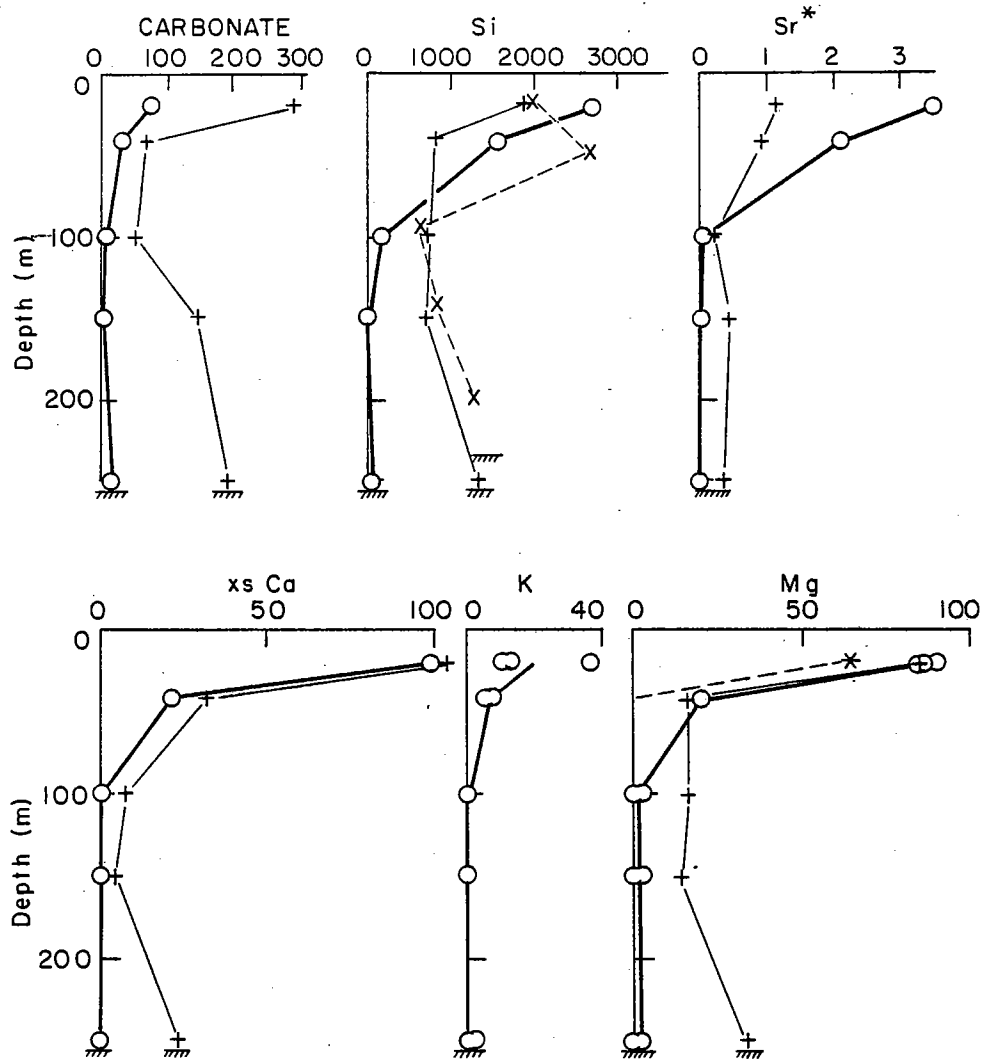


Fig. 3-19, > 53 μm particulate excess Ca, K, and Mg distributions at LVFS stations 4 - 7.



CHAIN 115-2 LVFS STN 8
33°18'S 17°36'E 1/09/74

○—○ $>53\mu\text{m}$ P.M. n mol/kg
+—+ $<53\mu\text{m}$ P.M. n mol/kg
x---x $0.4\mu\text{m}$ NUCLEPORE, 30 l NISKIN

Fig. 3-20, >53 and $<53\mu\text{m}$ particulate carbonate, Si, Sr*, excess Ca, K, and Mg at LVFS station 8. The $<53\mu\text{m}$ Si is calculated from the difference between the dry weight concentration and the sum of the chemical analyses for each sample.

in significant quantities relative to Mg at stations 4, 5, and 8 contrasting with relative depletions at stations 6 and 7 which were similar to Station 2. Excess Ca and K are involved in a shallow regenerative cycle and are present in the deeper samples only in areas of high productivity.

The 1 to 53 μm excess Ca and Mg data is presented in profiles (Figs. 20 and 21) because the two surface-most samples at Station 6 gave negative concentrations of Mg using the calculation scheme outlined in Chap. 2. This apparently resulted from the preferential dissolution of seasalt Mg relative to Na after these two samples were rewashed with distilled water in the lab. The only other significant exception to the scheme for the calculation of the Mg data was observed for the surface sample at Station 8; compared to the average blank for all samples (0.62 ± 0.20 (σ) mg Mg per filter, 33 samples), replicate analyses of the bottom filter for this sample gave values of 1.12 and 1.23 mg Mg which fell outside the 2σ limits of error established from the other samples. The 1-53 and <1 μm values for this sample were recomputed using the average blank value. This change lowered the 1-53 μm C_{org}/Mg ratio from 1350 to 210 and gave a value of 165 for the <1 μm fraction; these ratios fall in the range 100-200 found for the other near surface samples.

The ratio of total equivalents of cations to nitrogen (Fig. 22) is a measure of the reduction of the proposed effect

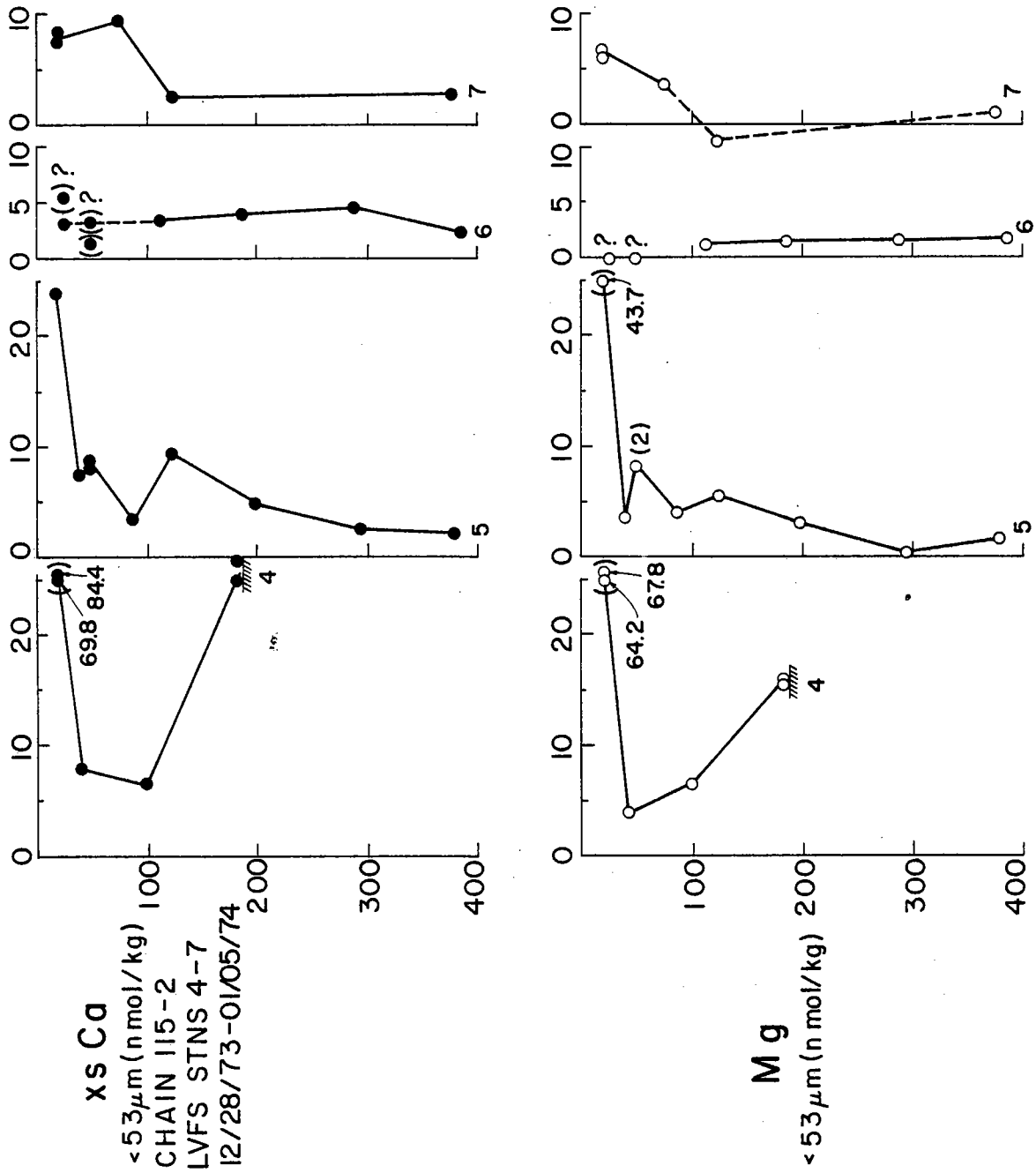


Fig. 3-21, < 53 μm particulate xs Ca and Mg for stations 4 - 7.

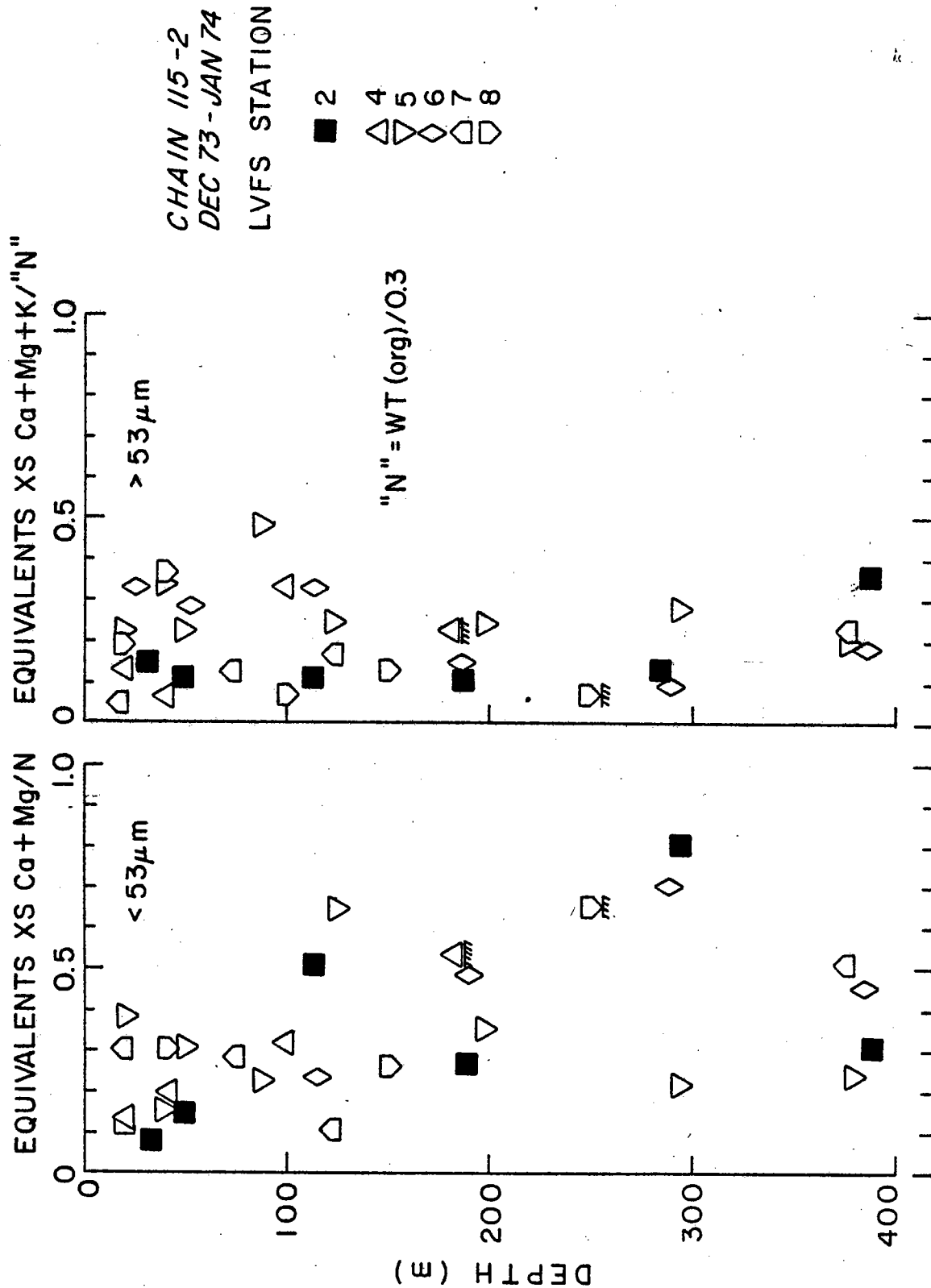


Fig. 3-22, > 53 and <53 μm ratios of particulate excess cation charge to nitrogen at LVFS stations 2 and 4 - 8.

upon seawater alkalinity produced by the oxidation of organic nitrogen (Brewer, Wong, Bacon, and Spencer, 1975). In the case of the $>53 \mu\text{m}$ size fraction, nitrogen has not yet been determined but may be calculated according to:

$${}^{\text{N}} = \text{Wt.}_{\text{org}} / 0.3 \text{ nmol kg}^{-1} \quad (1)$$

where the organic dry weight is calculated as outlined above and the C/N ratio is assumed to be 10 (Chap. 2). The cation charge to nitrogen ratio for the >53 and $<53 \mu\text{m}$ fractions is 0.22 for the samples shallower than 100 m; deeper samples show no change for the $>53 \mu\text{m}$ fraction but increase to values averaging 0.4 for the $<53 \mu\text{m}$ fraction. The result is essentially the same as found at Station 2. The proposed decrease in alkalinity resulting from the oxidation of organic matter is compensated at least 20% by the cations associated with the material.

Calcium and carbonate

Brewer et al. (1975) base their argument on the comparison of the oceanic calcium and alkalinity distributions assuming that calcium is a better tracer than alkalinity for carbonate dissolution. The profiles of Ca/carbonate ratio (Fig. 23) for both size fractions further demonstrate the involvement of calcium in other cycles besides that of precipitation and dissolution of calcium carbonate.

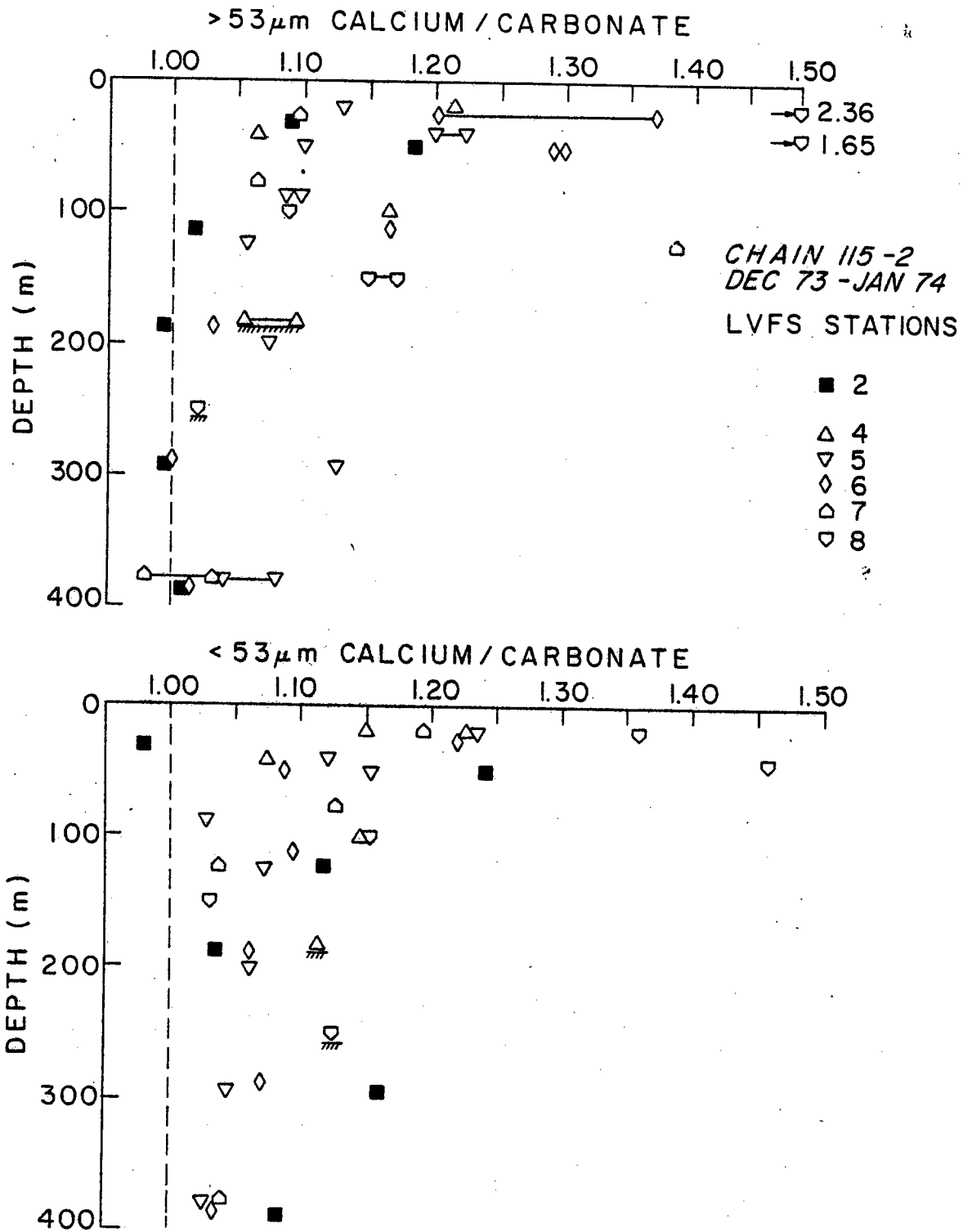


Fig. 3-23, > 53 and < 53 μm particulate Ca to carbonate ratios at LVFS stations 2 and 4 - 8.

The $>53 \mu\text{m}$ fraction shallower than 100 m had calcium to carbonate ratios of approximately 1.25 for Stations 4, 5, and 6 (and 2); 1.10 for Station 7, and 2.4 for Station 8. Values below 100 m were approximately 1.07 at Stations 4 and 5 and 1.00 at 6 and 7. Station 8 had values 1.15 and 1.02 for the 150 m and near bottom samples. The calcium to carbonate ratio in the $<53 \mu\text{m}$ fraction falls between 1.10 and 1.20 for most samples shallower than 100 m. The exception to this is at Station 8 where values above 1.4 were encountered. Below 100 m the ratio typically fell around 1.07.

The interpretation of particulate calcium as calcium carbonate must be treated with great care as calcium is decoupled from carbonate, especially in areas of high productivity such as in upwelling areas and polar regions where diatoms predominate. Let us assume that the calcium to organic carbon ratio in primary producers is 1:200 (a minimum estimate) and that the yearly productivity of the oceans is 23×10^9 tons C per year (Koblentz-Mishke, Volkovinsky, and Kabanova, 1970); this means that 1×10^{13} moles of calcium are fixed in the organic tissue of plankton each year. The total calcium carbonate precipitation by organisms has been estimated by Li, Takahashi, and Broecker (1969) to be $7 \pm 2 \times 10^{13}$ moles y^{-1} . The average calcium to carbonate removal ratio is therefore between 1.13 and 1.2 and could be as high as 1.4 if a value of $C_{\text{org}}/x_s \text{ Ca} = 100$ is used.

This coupled with the fact that xs Ca and carbonate are involved in shallow and deep regenerative cycles respectively, invalidated the use of surface seawater as a reference as was done in the analysis of Brewer et al. (1975). Even if there is a 25% underestimate in the amount of carbonate dissolved each year (as stated by Brewer, et al., 1975), the ratio of calcium to carbonate removal is changed only slightly. As yet there is no convincing evidence that any in situ process other than the dissolution of calcium carbonate alters the alkalinity distribution in the deep ocean.

Carbonate

Most particulate carbonate is produced by coccolithophorids and Foraminifera. These organisms occupy the >53 and <53 μm fractions respectively, with the exception of the near surface sample at Station 4. The >53 μm carbonate distribution resembles that of the Foraminifera in the surface waters (Figs. 24 and 8; 20 and 11). These distributions become separated in the deeper samples because of the enrichment of the large particles with coccoliths with depth (Chap. 2). The vertical distributions of the ratio of total carbonate to Foraminifera for these samples (Fig. 25) demonstrates that this is a general feature of the particulate matter in the S.E. Atlantic. The anomalously high ratio at 88 m (*) at Station 5 is the only instance where sizable Foraminifera made an appreciable contribution to the total carbonate. Two thirds of the measured carbonate was attributable to 430 μm diameter (range 350 to 520 μm) Orbulina Universa (Hecht, Be, and Lott, 1976) which had a concentration of $0.14 \ell^{-1}$. The near

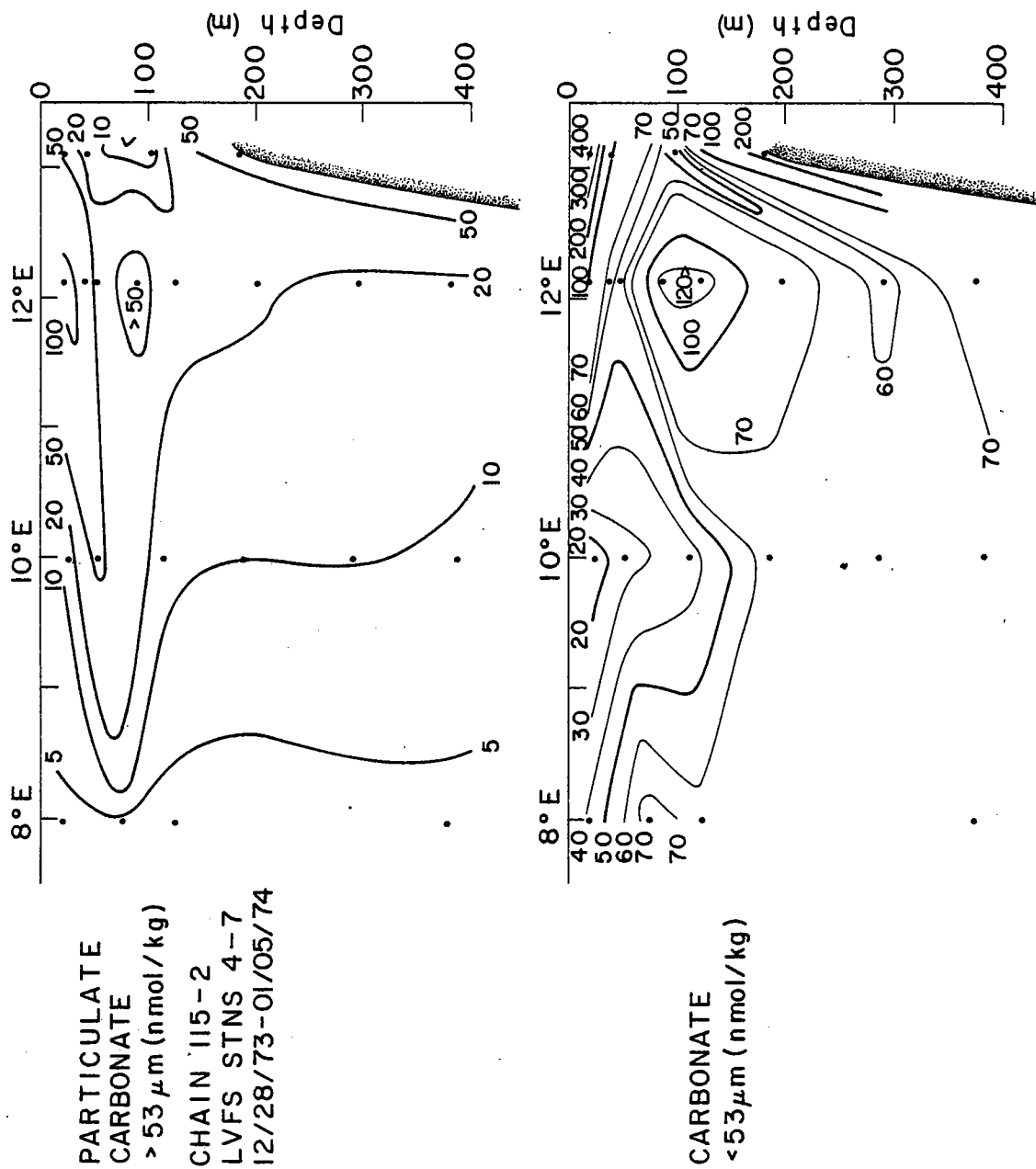


Fig. 3-24, > 53 and < 53 μm particulate carbonate distributions at LVFS stations 4 - 7.

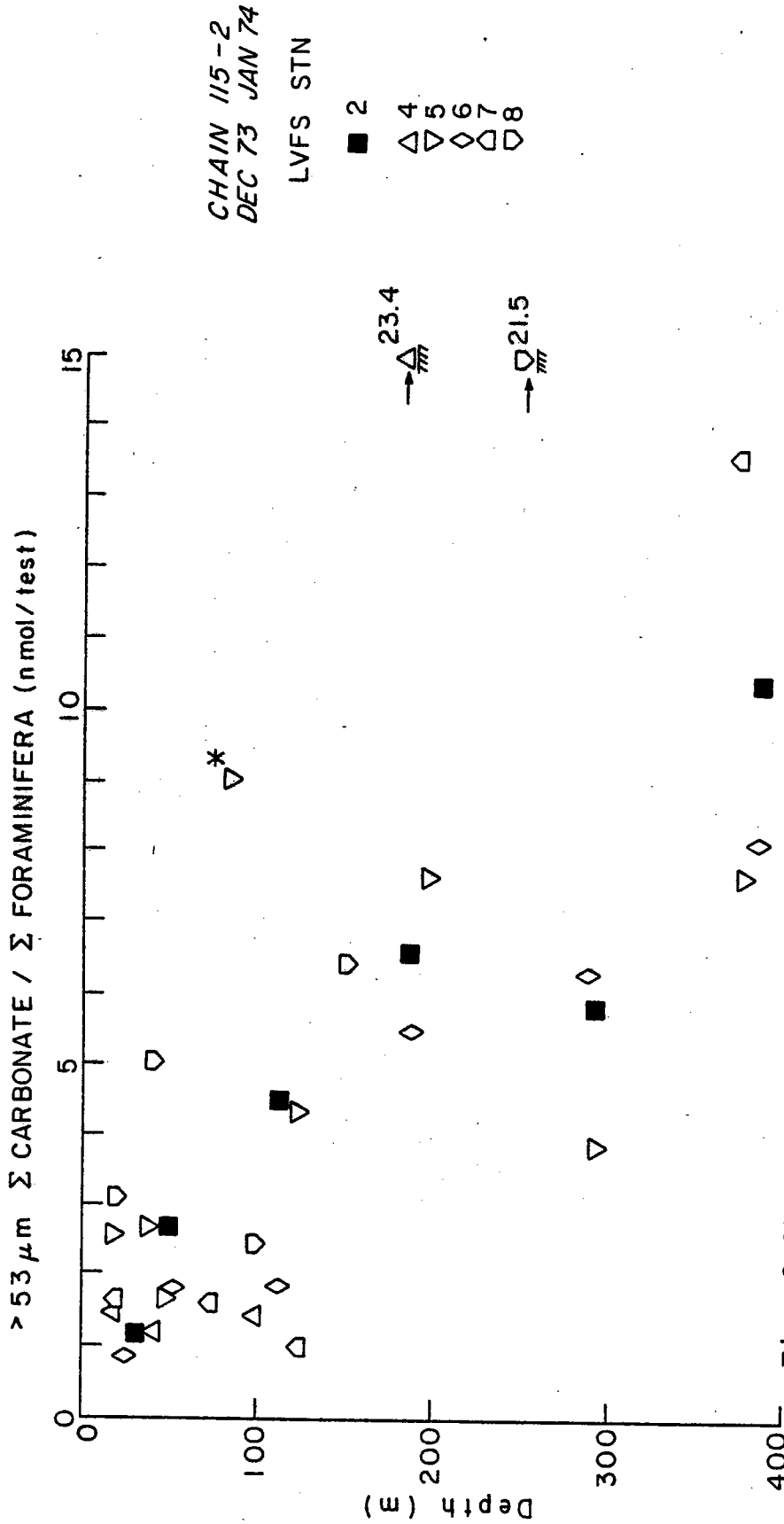


Fig. 3-25, > 53 μm total carbonate to total Foraminifera ratio indicating the enrichment of the large particles with coccoliths. (*) indicates the significant contribution of Orbulina Universa to the >53 μm carbonate at LVFS station 5.

bottom samples at Stations 4 and 8 show very high ratios and are most strongly enriched in coccoliths. The increase of total carbonate to total Foraminifera ratio with depth can only be the result of continual regrazing of the large particles by detritus feeding organisms living within the upper 400 m.

Surface maxima were observed for the $<53 \mu\text{m}$ carbonate at Stations 4, 5, and 8 (Figs. 24 and 20). Replicate samples from 20 m at Station 4 gave concentrations of 470 and 370 nmol kg^{-1} and had coccolithophorid populations of 6.2 and 4.4 per ml; since these organisms dominate the carbonate of this sample the amount of carbonate per organism may be estimated to be 7.6 and 7.0 $\times 10^{-2}$ nmol, approximately 45 times the amount estimated by Honjo (1976) for typical open ocean coccolithophorids. These organisms were approximately 50 μm in size at Station 4 compared to 10-20 μm observed at the other stations.

The $<53 \mu\text{m}$ surface maxima at the other stations are also almost entirely due to coccolithophorids. Station 5 exhibited a peculiar distribution where whole coccospheres at 20 and 40 m, coccoliths at 50 m, and a mixture of coccoliths and coccospheres at 88 m were the significant contributors to the $<53 \mu\text{m}$ carbonate. The secondary coccosphere maximum at 88 m could indicate that this water had been recently near the surface. Station 6 showed a carbonate minimum nearest the surface reflecting a rather sparse population of coccolithophorids.

Station 7 showed a weak surface minimum with maximum values at 75 m. Coccoliths dominated the $<53 \mu\text{m}$ carbonate for all samples below 100 m.

One remarkable feature is the spatial variability of the $<53 \mu\text{m}$ carbonate in the deeper samples. For instance, the low (44 nmol kg^{-1}) at 100 m and high (120 nmol kg^{-1}) at 88 and 124 m at Stns. 4 and 5 are most likely due to advective motion of the water into or out of the section (Fig. 24). The uniformity of the carbonate concentrations in the deep water at Stns. 6 and 7 is noteworthy; concentrations 66 ± 1.4 (σ) nmol kg^{-1} were found for five samples. These values are almost twice those found at Station 2 indicating significant spatial variability in the carbonate distribution. The near bottom maxima observed at Stations 4 and 8 (250 and 190 nmol kg^{-1}) are most likely resuspended bottom material as indicated above.

The importance of coccospheres as a source for the carbonate in both size fractions cannot be overstressed. They determine the carbonate distribution almost exclusively in the $<53 \mu\text{m}$ fraction. Below 100 m the $>53 \mu\text{m}$ fraction carbonate is also largely coccoliths.

Silicate

The $>53 \mu\text{m}$ silicate is determined largely by diatoms as indicated by the close correspondence between Figs. 26 and 9. The maximum Si concentration observed for Stations

PARTICULATE SILICATE CONCENTRATIONS FROM NUCLEPORE0.4 μ m FILTERS : TABLE 3-2

STATION	Z (m)	P.M. (μ g/kg)	Si (nmol/kg)	Opal (wt %/o)
CH 115-2-4 21°28'S 13°07'E 12/28/73	19	598.	81.9	0.9
	48	47.5	92.2	13.6
	97	41.4	96.0	16.2
	165	76.6	342.	31.3
CH 115-2-5 22°36'S 12°07'E 12/30-31/73	20	84.3	203.3	16.9
	40	162.3	311.2	13.4
	57	37.9	90.7	16.8
	86	29.4	55.9	13.3
	119	16.1	35.5	15.4
	209	10.4	24.4	23.2
	285	14.8	27.9	17.9
	380	11.3	21.3	13.2
CH 115-2-6 25°10'S 10°01'E 1/03/74	24	39.1	102.7	18.4
	58	60.9	223.9	25.7
	121	21.0	73.2	24.4
	193	17.4	49.0	19.7
	289	14.0	52.3	26.2
	366	9.4	42.8	31.9

TABLE 3 - 2 (cont.)

STATION	Z (m)	P.M. ($\mu\text{g}/\text{kg}$)	Si (nmol/kg)	opal (wt %)
CH 115-2-7 25°22'S 7°58'E 1/05/74	19	45.6	8.5	1.3
	72	66.0	16.3	1.7
	125	24.6	21.9	6.2
	182	-	11.7	(6.)
	288	73.0(?)	13.5	(6.)
	365	7.6	23.3	21.5
CH 115-2-8 33°18'S 17°36'E 1/09/74	19	692.	1992.	20.2
	47	410.	2682.	45.8
	94	84.9	639.	52.7
	141	137.6	855.	43.5
	198	210.	1281.	42.7

Opal wt % calculation assumes 70 gm/mol Si

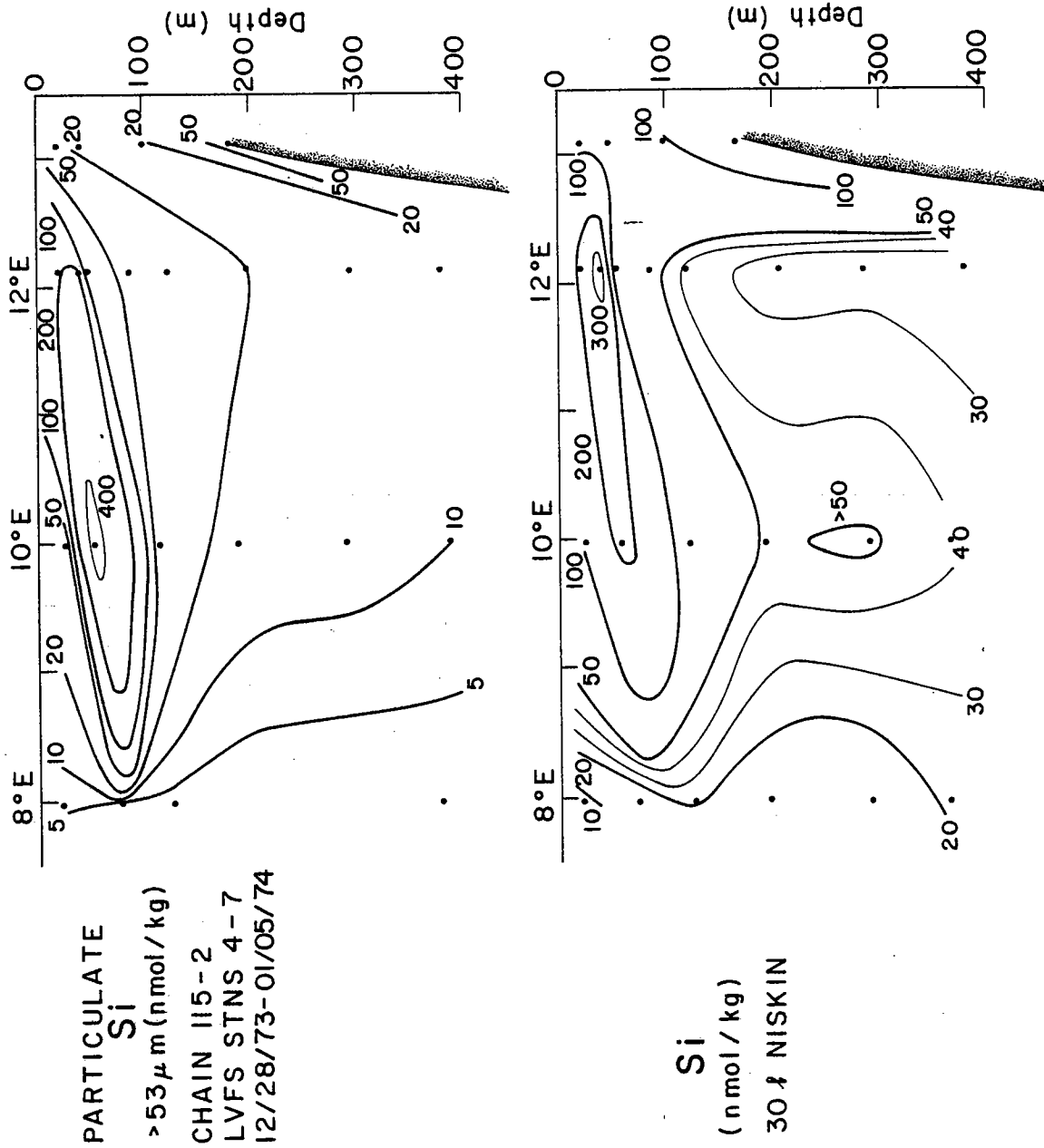


Fig. 3-26, Particulate silicate: >53 μ m and NISKIN-0.4 μ m Nuclepore fractions at LVFS stations 4 - 7. The NISKIN method has missed the maximum at 52 m at station 6.

4 to 7 was 450 nmol kg^{-1} coincident with the maximum in solenoid diatoms at 52 m at Station 6. Centrate diatoms appear to determine the other features of the silicate distribution in the near surface waters.

Station 8 had the highest particulate silicate concentration of $2700 \text{ nmol kg}^{-1}$ at 20 m, attributable mainly to centrate diatoms. This predominance allows the calculation of $0.24 \text{ nmol silica per diatom frustule}$, approximately twice that estimated for centrate diatoms at Station 2 (Chap. 2). As indicated earlier, diatoms are minor contributors to the plankton at Station 4; however, the near bottom Si maximum indicates that this is either not usually the case or that particles enriched in Si are being transported by the deep circulation onto the shelf from offshore areas of higher opal productivity.

The $<53 \mu\text{m}$ silica could not be measured directly because glass fiber filters were used. Niskin casts were made both to intercalibrate the dry weight measurements (obtained using similar methods as described by Brewer et al. 1976) with the LVFS and to provide samples for the estimation of the $<53 \mu\text{m}$ silicate (Table 2).

Fig. 26 demonstrates the similarity between the silicate concentrations determined by the Niskin method and the distributions of centrate diatoms and also gives an impression of the distribution of the $<53 \mu\text{m}$ silica in the waters below 100 m. The contribution to total dry weight by

opal was less than 1% for the 20 m sample at Station 4, consistent with the observation that coccolithophorids dominate the biomass. This contrasts with the 30% contribution to dry weight for the near bottom sample at this station. Station 6 had the highest percentage of silica of all stations on the Walvis Bay section, averaging 25% compared to 16 and 6% at Stations 5 and 7. This reflects the $>53 \mu\text{m}$ silicate maximum at 52 m at this station. Silica averaged 40% of the dry weight of the particulate matter sampled at Station 8. The horizontal gradients in the Niskin silicate values contrast with those for the $<53 \mu\text{m}$ carbonate. It is possible that the fine particles have very short residence times within the upper 400 m, their distributions being controlled by the local population of grazing organisms, especially in areas of high biological productivity.

There are several methods for estimating the $<53 \mu\text{m}$ silicate concentration. The first is based on the assumption that the Niskin method represents the total suspended silicate concentration:

$$<53 \mu\text{m Si} = \text{Si}_{\text{nis}} - >53 \mu\text{m Si} \quad (2)$$

This approach uses the assumption of Chap. 2 but produces negative results, particularly for the samples shallower than 100 m. A second assumption is that the Niskin silicate concentration is equivalent to that of the $<53 \mu\text{m}$ size

fraction:

$$<53 \mu\text{m Si} = \text{Si}_{\text{nis}} \quad (3)$$

this assumption is based upon the conclusions of Bishop and Edmond (1976). The third method uses the difference between the <53 μm dry weight and that determined by summing the chemical analyses of the samples (chem. wt.):

$$<53 \mu\text{m Si} = \frac{(<53 \mu\text{m dry wt.} - <53 \mu\text{m chem. wt.})}{0.07} \quad (4)$$

where 0.07 is the conversion between μg and nmoles Si. Results for this calculation are listed in Appendix 1 and the major assumption for this method is that opal is the only major particulate phase not measured in the chemical analyses. An example of this calculation is given for Station 8 where the values are plotted with (+) symbols. The fourth method is based on the assumption that the fraction of opal in the Niskin and <53 μm fraction is similar. Therefore the <53 μm Si is calculated from the Niskin weight percentage and the <53 μm dry weight.

$$<53 \mu\text{m Si} = \frac{(\text{Si}_{\text{nis}})}{\text{Wt}_{\text{nis}}} \times (<53 \mu\text{m dry wt.}) \quad (5)$$

All these methods worked well for the samples below 100 m; however, it is difficult to determine which is the most

representative of the natural situation.

Silicate and Carbonate

The distributions of dissolved silicate and specific alkalinity covary over much of the world's oceans indicating the dissolution of opal and carbonate in a ratio of approximately 2 to 1; departure from this behavior is observed only in the upwelling areas of the extreme north Pacific and Antarctic (Edmond, 1974) where siliceous organisms dominate the plankton (Lisitzin, 1972). The ratio of silicate and carbonate in the $>53 \mu\text{m}$ fraction should reflect this variation.

Fig. 27 shows the vertical variation of Si to carbonate ratio in the $>53 \mu\text{m}$ fraction and estimated for the $<53 \mu\text{m}$ fraction. Error bars in the lower figure represent the range of values calculated using the schemes outlined above. Values that were obviously invalid were omitted from the averages and indicated range. For samples below 100 m Method 1 represented the lower limit of silica to carbonate ratio.

The $>53 \mu\text{m}$ fraction shallower than 60 m had Si/carbonate ratios between 0.8 and 46.0 between Stations 4 and 8; intermediate values of 8.5, 2.4, and 1.4 were found at Stations 5, 6, and 7. These values are consistent with the biological data where diatoms were minor and major contributors to the biomass at Stations 4 and 8. The vertical profiles show

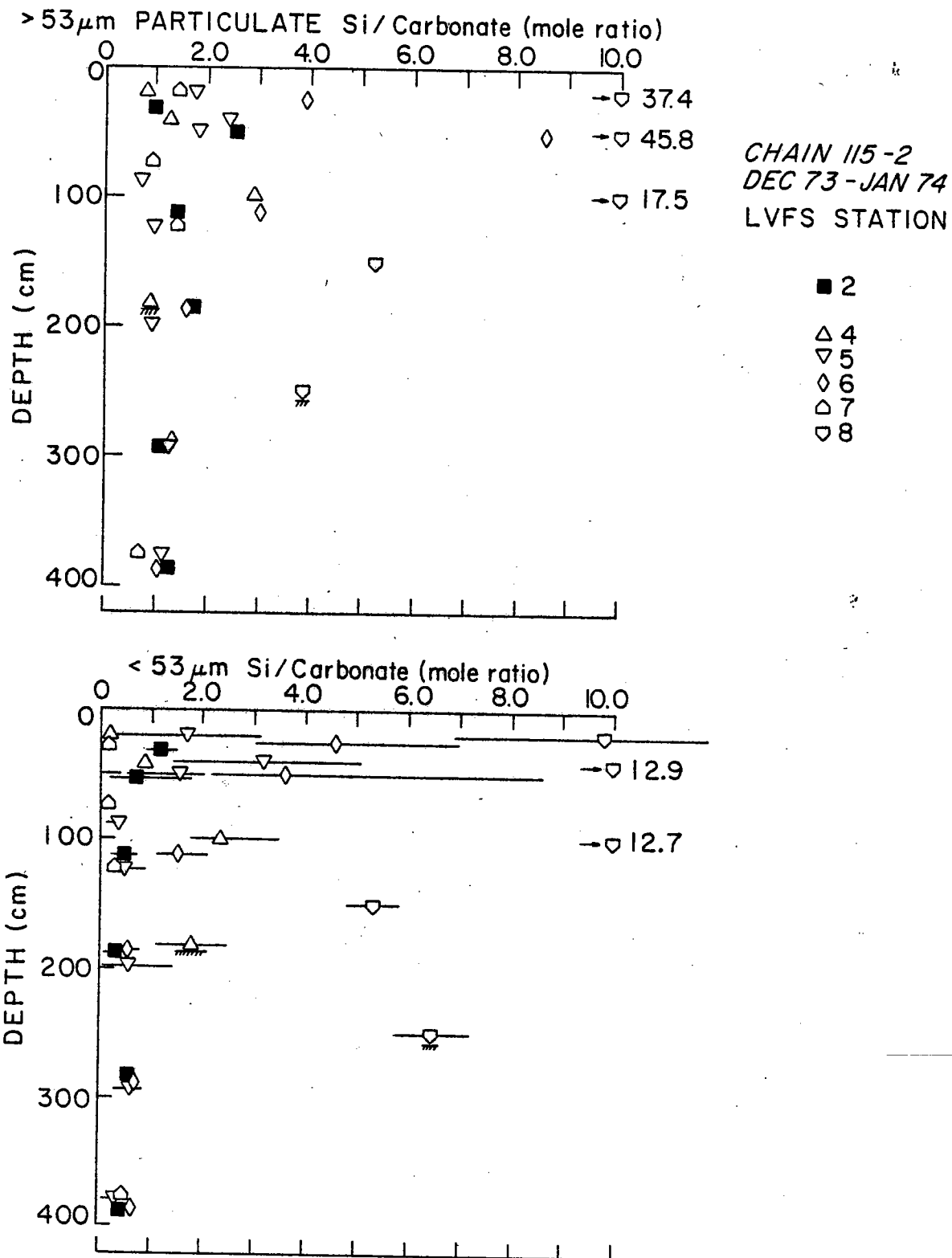


Fig. 3-27. >53 and <53 μm particulate silicate/carbonate ratios at LVFS stations 2 and 4 - 8.

that the Si/carbonate ratios decrease regularly with depth to values near one at 400 m at stations 5, 6, and 7. The 400 m values are indicative but not precisely those of the particle flux and are 1.15, 1.05, and 0.70 at Stations 5, 6, and 7 compared with 1.25 found at Station 2. Assuming no appreciable dissolution of opal, the decrease of Si/carbonate ratio with depth can only occur if the particles are continuously reworked by grazing organisms, incorporating silica poor <53 μm particles into the >53 μm particles as they sink through the upper 400 m. Since the <53 μm particles represent a rather sizeable reservoir of material, there will be little change in the <53 μm silica to carbonate ratio although a gentle increase with depth should be observed.

Strontium

Most particulate strontium is produced by Acantharia in the surface layer. These organisms are found exclusively within the >53 μm size fraction and are of interest because they are potential carriers of ^{90}Sr and perhaps trace elements into the deep ocean. Besides being present as SrSO_4 , strontium is a minor component of carbonate, and is also present at ion exchangeable sites on organic matter. Sr^* , non-carbonate strontium, is calculated from the relation used in Chap. 2:

$$\text{Sr}^* = \text{Sr} - 0.0017^* \text{ carbonate} \quad (6)$$

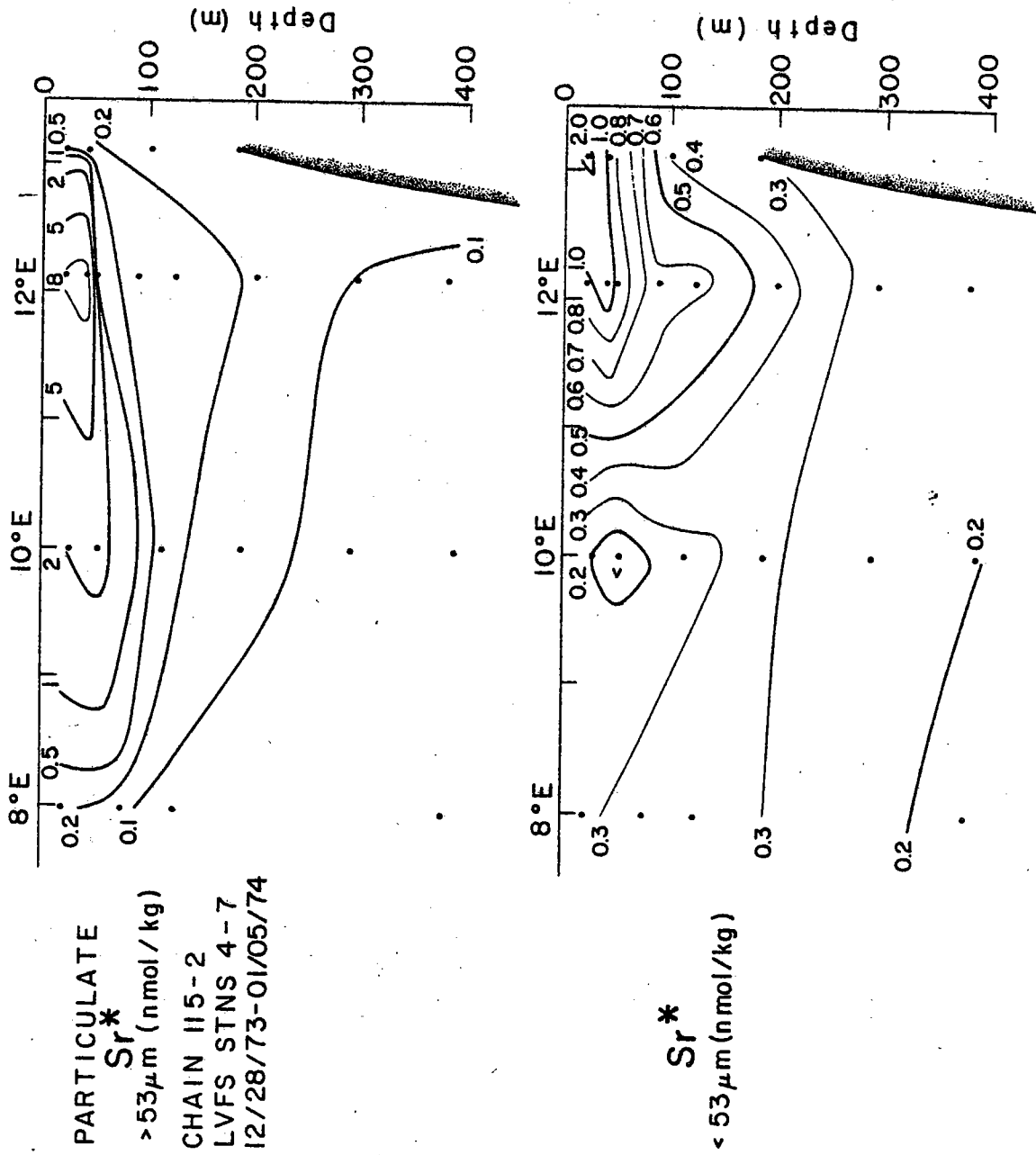


Fig. 3-28, >53 and <53 μm particulate non-carbonate strontium distributions (Sr*).

The $>53 \mu\text{m}$ Sr^* distribution (Fig. 28 and 20) shows an intense maximum (8 nmol kg^{-1}) at 20 and 40 m at Station 5. High concentrations of 3 and 2 nmol kg^{-1} were observed in the near surface waters at 8 and 6 reflecting the relative importance of *Acantharia* at these stations; however, a higher biomass of *Acantharia* is indicated at Station 5. Lower Sr^* concentrations were observed in the samples from Stations 4 and 7 (0.4 and 0.2 nmol kg^{-1}) and fall below those found at Station 2 (1.1 nmol kg^{-1}) in the equatorial Atlantic. Vertical gradients are most pronounced for Sr^* as found for the *Acantharia* population and indicate dissolution of SrSO_4 with depth (Chap. 2).

The $>53 \mu\text{m}$ fraction Sr^*/Sr ratios decreased from near surface values of approximately 1.0 to 0.8 at 400 m at Stations 5, 6, and 7, comparable to the behavior observed at Station 2. The lowest ratios were found for the near bottom samples from Stations 4 and 8 where values of 0.56 and 0.0 indicated that the SrSO_4 dissolution was most pronounced.

The $<53 \mu\text{m}$ Sr^* distribution shows maxima of approximately 2 and 1.2 nmol kg^{-1} nearest the surface at Stations 4 and 8; 1.1 nmol kg^{-1} at 40 m at 5; and approximately 0.3 nmol kg^{-1} below 100 m at Stations 6 and 7. These latter values are similar to those found at Station 2. The maximum observed for the $<53 \mu\text{m}$ carbonate at 88 and 124 m at Station 5 is shown only as a weak feature in the $<53 \mu\text{m}$ Sr^* data. The decrease of Sr^*

concentrations with depth to values below 0.2 nmol kg^{-1} is most likely due to dissolution. Sr^*/Sr ratios in this size fraction were typically 0.8 near the surface and fell to values between 0.65 and 0.5 by 400 m at Stations 5, 6, and 7; the near bottom samples from Stations 4 and 8 had values near 0.5 again indicating relatively advanced dissolution of SrSO_4 .

The overall trend to this data suggests that Sr^* is more rapidly supplied to the deeper waters at stations of high productivity allowing higher concentration levels to persist. In cases where the supply is low (Station 7) or the particles exposed to seawater longer (the near bottom samples at 4 and 8) the concentration levels relative to other inorganic components are generally the lowest.

Vertical flux of large particles through 400 m

Chap. 2 demonstrated that most of the vertical flux of particulate matter at Station 2 was carried by fecal matter. Fecal pellets and Foraminifera were apparently minor contributors to the sediments of this area. It is important to know if sinking fecal material is generally the dominant means by which small particles, such as coccoliths, enter the deep ocean. Fine particles may contribute substantially to the vertical flux in areas of low biological productivity.

Approximately $1/20$ th of each $>53 \mu\text{m}$ sample from 400 m (equivalent to 0.56, 0.95, and 0.96 m^3 seawater) at Stations 5, 6, and 7 was scanned at 100x to determine the size

distributions of Foraminifera, fecal pellets, and fecal matter. The fecal matter size distributions were extended by placing the whole samples on a light table and counting the particles larger than 1 mm in size.

The particle distributions (Figs. 29, 30 and 31) are plotted as frequency histograms (Foraminifera and fecal pellets) and also as log cumulative-number (greater than diameter, d) versus $\log d$ following the practice of McCave (1975) (Foraminifera, fecal pellets, and fecal matter); This latter representation was the only convenient way of showing the distribution of fecal matter. The use of the cumulative distribution derives from that introduced by Junge (1963) who found that the size distribution of atmospheric aerosols followed:

$$\frac{dn}{d(\log r)} = cr^{-\beta} \quad (7)$$

where n is the number of particles smaller than radius r and β and c are constants. McCave (1975) reviewed the application of this distribution to Coulter Counter measurements and showed that oceanic particulate matter present below 200-400 m had cumulative number-size distributions which followed:

$$N = ad^{-m} \quad (8)$$

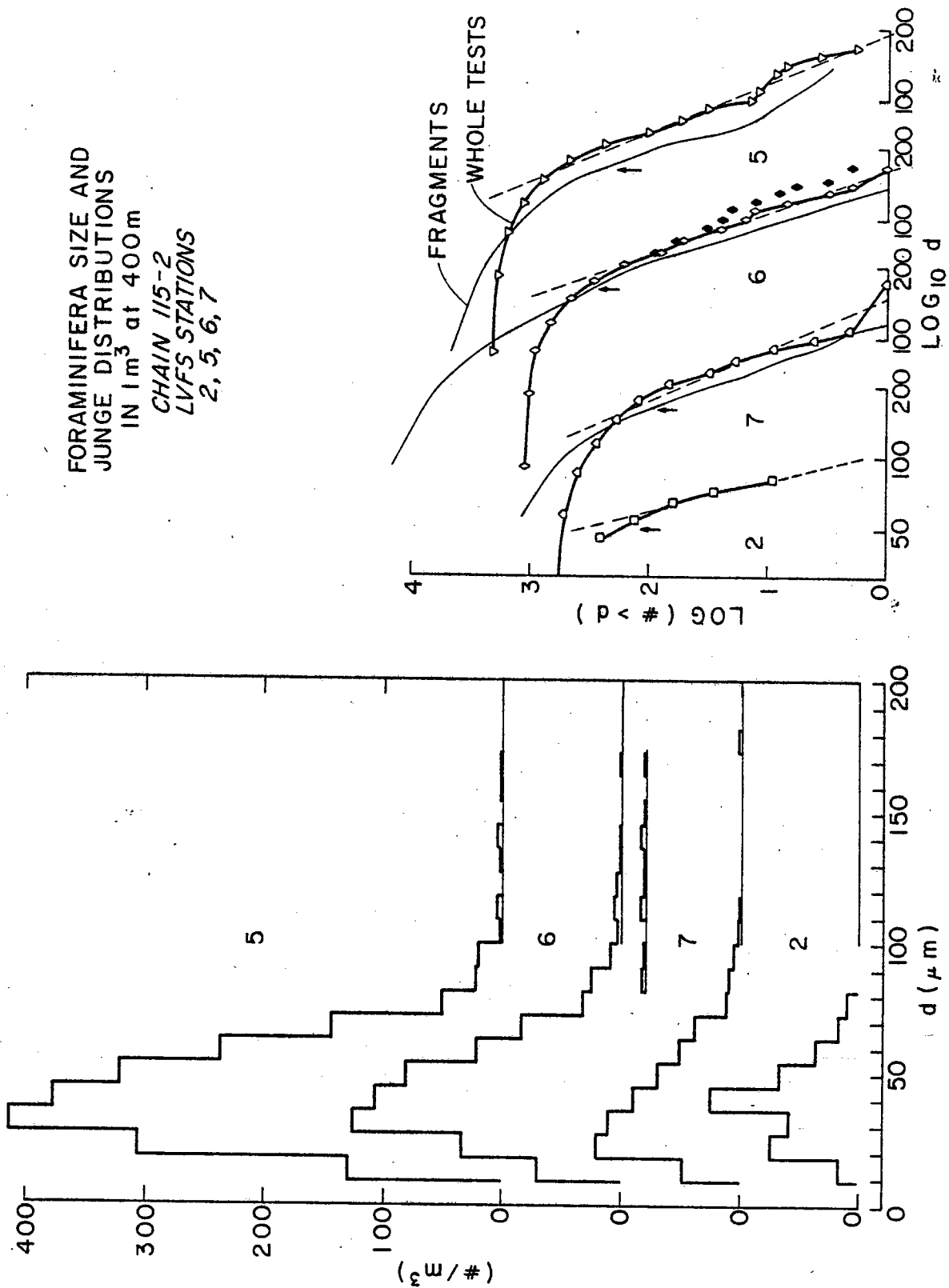


Fig. 3-29, Foraminifera size and Junge distributions in 1 m³ samples from 400 m at LVFS stns. 2, 5, 6, and 7. Solid symbols indicate Pteropod shells at stn. 6.

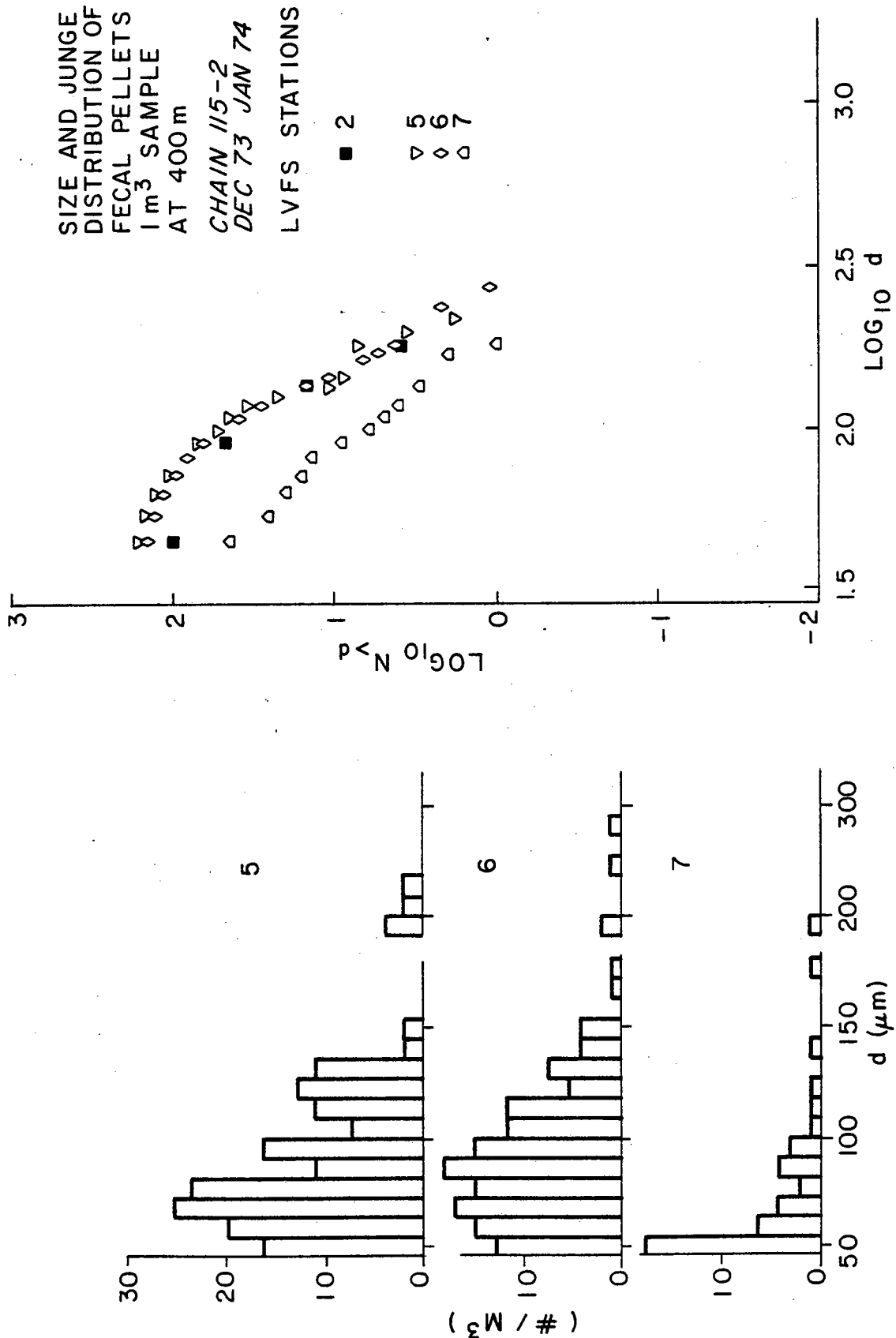


Fig. 3-30, Size and Junge distributions for fecal pellets in the >53 μm fraction samples from 400 m at LVFS stns. 2, 5, 6, and 7.

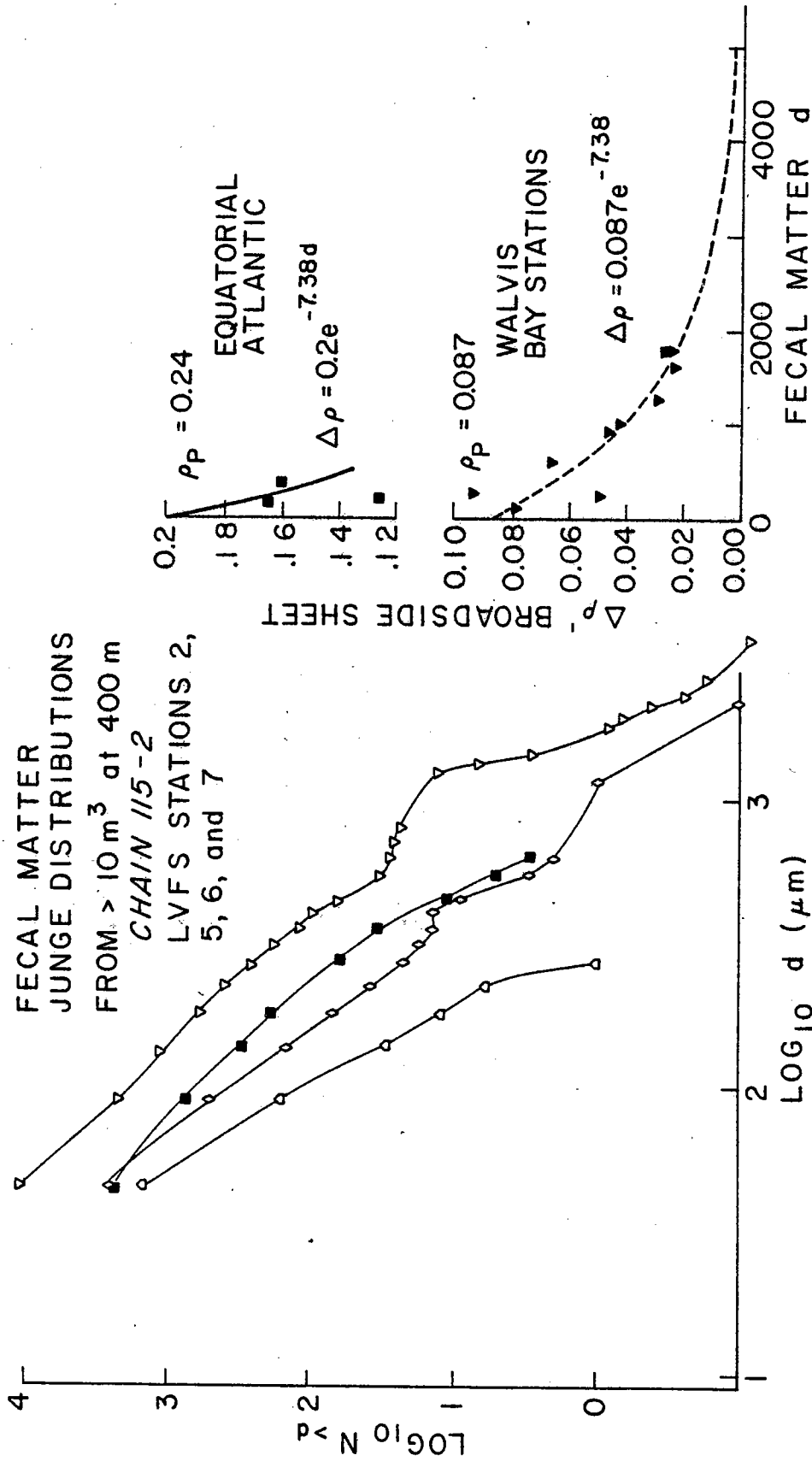


Fig. 3-31, Junge distributions of fecal matter at LVFS stns. 2, 5, 6, and 7; density parameters for fecal matter from LVFS stations 2 and 5.

where N is the number of particles larger than diameter d , and \underline{m} and \underline{a} are constants; this equation may be derived directly from Eq. 7. McCave (1975) found that particles in the size range 1 to 100 μm were described by Junge distributions having \underline{m} values between 2.4 and 3.6, and \underline{a} values between 10^3 and 10^4 .

Table 3 summarizes the values of these parameters determined from the distributions of Foraminifera, Foraminifera fragments, fecal pellets, and fecal matter. The Junge distribution slopes (\underline{m}) were 5.7 (range 4.6 - 7.7) for Foraminifera; 5.3 (range 4.1 - 6.3) for Foraminifera fragments; 3.8 (range 2.8 - 4.6) for fecal pellets; and 4.3 (range 3.8 - 4.9) for fecal matter. Both the \underline{m} and \underline{a} values for these distributions are higher than those found by McCave indicating that large and small particles have independent distributions.

The trend to higher \underline{m} values with particle size indicates that the distributions can be extrapolated using Eq. 8 to give estimates of the maximum concentration of particles present in volumes of seawater larger than 1 m^3 . Such extrapolations depend on the particles being uniform in nature and origin but may be incorrect if the sample fails to include any particles of a given type or if there is no distinction made between them. For instance, the extrapolation of the Junge distribution for Foraminifera at Station 5 would predict that there would be only 1 Foraminifera per 10 m^3 larger than 310 μm in diameter, similarly 1 per 100 m^3 larger than 500 μm . A

TABLE 3 - 3

JUNGE DISTRIBUTION PARAMETERS OF $>53 \mu\text{m}$ PARTICLES AT
LVFS STATIONS 2, 5, 6, and 7

FORAMINIFERA		$\rho_p = 0.5 \text{ g cm}^{-3}$	$\Delta\rho' = 0.3 \text{ g cm}^{-3}$		
Station	Diameter interval μm	(# pts.)	a	m	
5	55 - 173	(11)	1.010×10^5	4.813	
6	64 - 173	(10)	2.499×10^6	5.606	
6*	82 - 173	(8)	1.980×10^5	4.946	
7	55 - 183	(8)	8.772×10^3	4.563	
2	64 - 91	(3)	5.674×10^9	7.712	
FORAMINIFERA FRAGMENTS					
5	64 - 146	(4)	1.198×10^3	4.050	
6	64 - 146	(8)	3.321×10^7	6.317	
7	64 - 128	(6)	1.728×10^5	5.397	

* Includes Pteropod shells (?)

TABLE 3 - 3 cont.

FECAL PELLETS		$\rho_p = 0.5 \text{ g cm}^{-3}$	$\Delta\rho' = 0.2 \text{ g cm}^{-3}$	
Station	Diameter interval		a	m
5	119 - 237 (7)		6.850×10^3	4.050
6	128 - 292 (8)		1.254×10^3	3.717
7	82 - 201 (8)		2.744×10^0	2.803
2	137 - 228 (2)		9.83×10^4	4.595
FECAL MATTER		$\rho_p = 0.087 \text{ g cm}^{-3}$	$\Delta\rho' = 0.087 \text{ g cm}^{-3}$	
5	913 - 3652 (9)		8.194×10^9	4.852
6	913 - 2374 (5)		1.521×10^7	4.275
7	91 - 320 (5)		3.213×10^4	4.215
		$\rho_p = 0.24 \text{ g cm}^{-3}$	$\Delta\rho' = 0.2 \text{ g cm}^{-3}$	
2	234 - 730 (5)		1.040×10^5	3.752

survey of the sample indicated that there were approximately 6 tests of Orbulina Universa present ranging from 430 to 480 μm and averaging 470 μm in diameter yielding a concentration of 0.5 m^{-3} , approximately 50 times that predicted using the Junge distribution. At this station, these organisms had a distinct distribution compared with the other globigerinoid Foraminifera. Accepting this note of caution, the Junge distributions will be used later to extrapolate the fecal pellet and Foraminifera fluxes.

Foraminifera at 400 m were most abundant at Station 5 where there were 2090 m^{-3} ranging in size between 10 and 180 μm (Figs. 8 and 29) reflecting the population maximum in the surface waters. There were 1110 and 560 m^{-3} at Stations 6 and 7 up to 180 μm in size; this is compared with 406 m^{-3} up to 100 μm in size found at Station 2. The 400 m sample from Station 6 also had significant concentrations (10 m^{-3}) of Pteropod (tentatively identified) shells ranging in size from 100 to 200 μm in size. These shells are shown separately in the size distributions but are included in the Junge distributions shown in Fig. 29. The Foraminifera and Pteropod (?) fragments were most abundant at Station 6 and an interesting feature at all stations is the close correspondence between the \underline{m} values of the Junge distributions of Foraminifera and fragments indicating that a common process (grazing) may control their distributions.

Fecal pellets were most abundant at Station 5 where there were 164 m^{-3} . Their concentrations were 143 m^{-3} and 44 m^{-3} at stations 6 and 7, compared with 110 m^{-3} at Station 2.. Pellets up to $300 \mu\text{m}$ in length were encountered on the filter subsample at Station 6.

Fecal matter shows the most dynamic range in concentration being most abundant at Station 5 and rarest at 7 where the largest particles were 4 mm and $350 \mu\text{m}$ respectively. The morphology of fecal matter is varied; besides containing an abundance of coccoliths, coccospheres, diatom frustules and fragments, and other small particles, the larger particles have been observed to contain sizable Foraminifera, Acantharia, Radiolaria, copepod and other crustacean carapaces and appendages, and fecal pellets. Virtually every kind of particle observed individually on the prefilters can be found within fecal matter.

Vertical flux models

Two models will be used to describe the sinking behavior of Foraminifera and fecal pellets and of fecal matter. The derivation of the first model is contained in Chap. 2:

$$\phi_d = \frac{n_d g \pi \Delta \rho \rho_p d^5}{108 \eta} \quad \text{gm cm}^{-2} \text{sec}^{-1} \quad (9)$$

$$\text{or} \quad \phi_d = 6 \times 10^{13} n_d \Delta \rho \rho_p d^5 \quad \text{gm cm}^{-2} 1000\text{y}^{-1} \quad (10)$$

where all parameters are as defined in Chap. 2. Seawater

viscosity, η , differs by less than 4% at all stations considered and given the other errors in the model is assumed constant at 0.0144 poise. The density parameters $\Delta\rho'$ and ρ_p are included in Table 3. Total mass flux is therefore:

$$\phi_{\text{meas}} = \sum_d \phi_d \quad (11)$$

Model 2: Fecal matter

The settling behavior of fecal matter is poorly determined (Chap. 2). Its important contribution to the vertical flux at Station 2 necessitated laboratory sinking experiments. Fecal matter from Stations 2 and 5 was carefully removed from the 400 m filters. After measurements of cross-sectional area and thickness, individual particles were weighed on a microbalance to permit an estimation of their dry weight densities, ρ_p . They were subsequently transferred to small beakers filled with distilled water and degassed for 2 hours within a vacuum chamber to remove the air from the pore spaces within the particles. Each particle was sucked into a wide mouth transfer pipette and allowed to settle until it became trapped on the meniscus at the pipette tip. The pipette was slowly introduced into the center of the settling column (1 l graduated cylinder) filled with 28°C distilled water at rest (30 min.). The particle was immediately released upon immersion of the pipette and

its travel times were recorded as it passed the 100 ml graduations on the cylinder (spaced at 3.4 cm intervals). Travel times were rejected if the particle came within 1 cm of the cylinder wall.

The fecal matter was approximately disk shaped and sank broadside on to the direction of travel and so the equation for the sinking velocity of a broadside disk (Lerman, Lal, and Dacey, 1975) was considered more appropriate than Stokes' Law (spherical particles) for comparison with the measured fall velocities.

$$v_d = \frac{g \Delta\rho h d}{10.2\eta} \quad \text{cm sec}^{-1} \quad (12)$$

where h has been determined empirically to be

$$h = 0.052d + 0.0045 \quad \text{cm} \quad (13)$$

and d is the disk diameter with equivalent surface area.

$\Delta\rho$ was calculated using the measured fall velocities (Fig. 31).

This parameter appears to decrease exponentially with d:

$$\Delta\rho = f \times \Delta\rho^0 \quad \text{gm cm}^{-3} \quad (14)$$

where $\Delta\rho^0$ is the density contrast of the particles of smallest diameter and

$$f = e^{-7.38d} \quad (15)$$

Therefore the empirically determined settling velocity for fecal matter is:

$$v_d = \frac{g}{10.2\eta} \Delta\rho^{\circ} fhd \quad \text{cm sec}^{-1} \quad (16)$$

The mass concentration of particles of size d is given by:

$$m_d = \frac{n_d \rho_p \pi d^2 h}{4} \quad \text{gm cm}^{-3} \quad (17)$$

The values for ρ_p were determined to be 0.24 gm cm^{-3} , and 0.087 gm cm^{-3} for the fecal matter at Stations 2 and 5.

The vertical flux of fecal matter is therefore:

$$\Phi_d = v_d \times m_d \quad \text{gm cm}^{-2} \text{ sec} \quad (18)$$

$$= 1.67 \times 10^{14} n_d \rho_p \Delta\rho^{\circ} fh^2 d^3 \text{ gm cm}^{-2} 1000y^{-1} \quad (19)$$

and the total flux for measured size distributions is

$$\Phi_{\text{meas}} = \sum_d \Phi_d \quad \text{gm cm}^{-2} 1000y^{-1} \quad (20)$$

Extrapolation of the vertical flux using the Junge distributions is accomplished by calculating n_d :

$$n_d = a \left((d - \Delta d/2)^{-m} - (d + \Delta d/2)^{-m} \right) \quad \text{ml}^{-1} \quad (21)$$

where Δd is the size interval used for the size distributions of Foraminifera and fecal pellets (10^{-3} cm) and fecal matter (5×10^{-3} cm). The limit is established by observations of maximum typical size of Foraminifera in sediments (500 μ m) (Berger and Piper, 1972) and of fecal pellets (500 μ m; from Wiebe, Boyd, and Winget, 1976) collected by sediment trap. The size limit for fecal matter is unknown but very large.

The extrapolated mass flux is added to that determined over some size interval from the measured distributions

$$\phi_{\text{extrap.}} = \phi_{\text{meas.}} + \phi_{\text{Junge}} \quad (22)$$

$$d = 0 \text{ to } D \quad d = D \text{ to limit}$$

where D is approximately 100 μ m for fecal pellets and Foraminifera and is generally near the largest size measured for the fecal matter.

Vertical fluxes through 400 m

The measured and extrapolated cumulative mass fluxes for Foraminifera, fecal pellets, and fecal matter are plotted in Fig. 32 and listed in Table 4. The vertical mass flux of Foraminifera was highest ($1.2 \text{ gm cm}^{-2} 1000\text{y}^{-1}$) at Station 5 where Orbulina Universa determined approximately 75% of the total flux. The flux was least at Station 2 where $0.02 \text{ gm cm}^{-2} 1000\text{y}^{-1}$ was calculated. About 50% of the "Foraminifera" flux at Station 6 may be due to Pteropods (?).

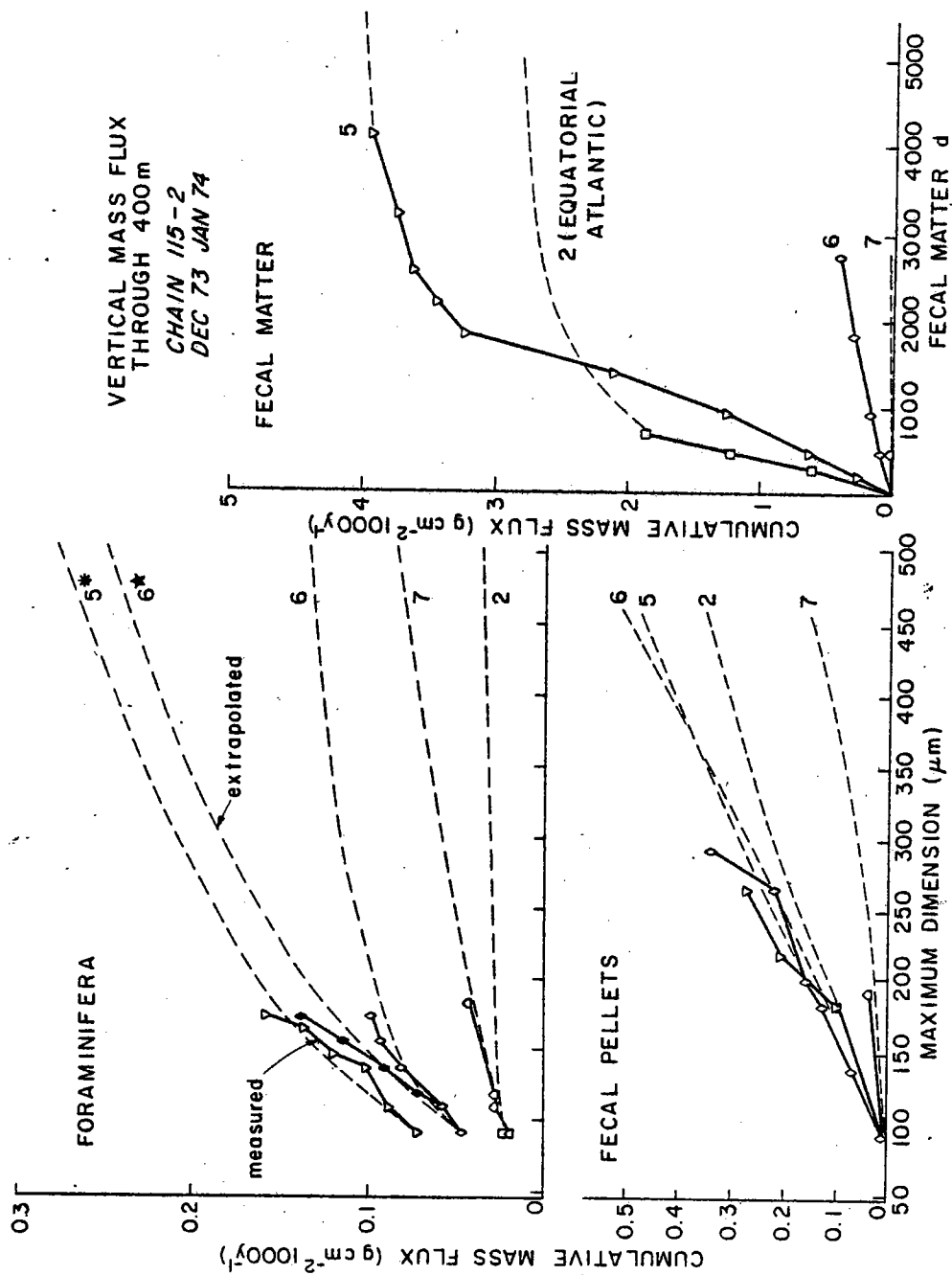


Fig. 3-32, Cumulative mass fluxes through 400m at LVFS stns. 2, 5, 6, and 7 for Foraminifera, fecal pellets, and fecal matter. (*): measured Foraminifera flux = $1.3 \text{ g cm}^{-2} 1000\text{y}^{-1}$ including Orbulina Universa at stn. 5. (Star): solid symbols indicate carbonate flux including Pteropod tests (?) at stn. 6.

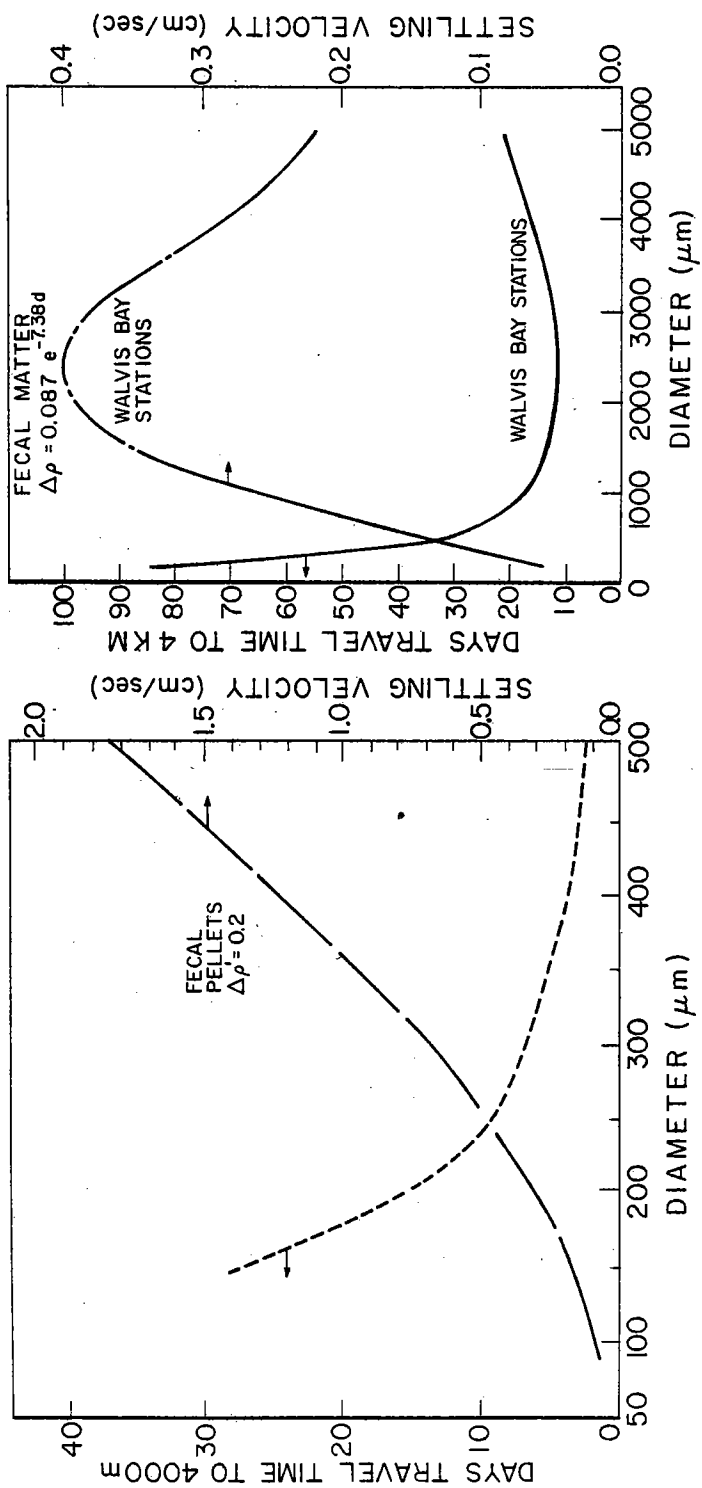


Fig.3-33, Model derived settling behavior as a function of size for fecal pellets (left hand side: spherical model) and for fecal matter (right hand side: empirical model).

TABLE 3 - 4 PARTICLE FLUX THROUGH 400 μ ($\text{g cm}^{-2} 1000\text{y}^{-1}$)

STATION	FORAMINIFERA		FECAL PELLETS		FECAL MATTER		TOTAL	
	meas.	extr.	meas.	extr.	meas.	extr.	meas.	extr.
5	0.159	0.277	0.266	0.529	3.939	4.032	4.364	4.838
5 [†]	1.173	1.291					5.378	5.852
6	0.099	0.134	0.334	0.576	0.401	0.477	0.834	1.187
6*	0.139	0.248					0.874	1.301
7	0.043	0.085	0.037	0.181	0.025	0.029	0.105	0.295
2	0.022	0.029	0.091	0.372	1.847	2.783	1.960	3.184

meas. Mass flux calculated from the observed particles size distributions

extr. Mass flux extrapolated through the use of Junge distributions to

size $d = 500 \mu\text{m}$ for Foraminifera and fecal pellets and to

size $d = 5000 \mu\text{m}$ for fecal matter.

* includes Pteropod (?) flux † includes flux contributed by

Orbulina Universa

A scan of the whole sample failed to turn up any Pteropod shells larger than 300 μm or any Foraminifera larger than 350 μm ; their distributions were consistent with the Junge extrapolation.

Fecal pellets had the highest mass flux at Station 6 and lowest at Station 7 where the measured fluxes were 0.33 and 0.04 $\text{gm cm}^{-2}1000\text{y}^{-1}$ (extrapolated values were 0.58 and 0.18 $\text{gm cm}^{-2}1000\text{y}^{-1}$). The extrapolated flux at Station 2 was four times that measured. Comparison of the cumulative flux and vertical settling velocities as a function of size indicates that most material contributing to the flux sinks faster than 0.1 cm sec^{-1} or would settle to 4000 m in less than 30 days (Fig. 33).

Fecal matter was observed to be extremely abundant at Stations 2 and 5. Values for the mass flux of this material were determined to be 2 and 4 $\text{gm cm}^{-2}1000\text{y}^{-1}$ using the measured size distributions. These particles carried equivalent mass (0.5 $\text{gm cm}^{-2}1000\text{y}^{-1}$) as fecal pellets at Station 6 but made negligible contribution to the flux at 7. Most fecal matter contributing to the mass flux settles faster than 0.1 cm sec^{-1} .

An estimate of the elemental ratios of the vertical flux was made following the procedure outlined in Chap. 2. The material on the prefilters at 400 m was assumed to be approximately 60% by weight organic (from Fig. 18) and therefore 24% by weight elemental carbon. The analyses of carbonate and opal were corrected by subtracting the

contributions of Foraminifera and of Radiolaria and diatoms to give the proportions of these elements in the fecal material (Table 5). Applying these percentages to the total mass fluxes of fecal material it is possible to arrive at an estimate of the chemical fluxes.

The total chemical fluxes (Table 6) are highest for organic carbon, carbonate, and opal at Station 5, and lowest at Station 7, showing variation by over an order of magnitude. The organic to carbonate carbon ratios were greater than 4 at Stations 5 and 6 and less than 3 at Station 7. These values are compared with that of Station 2 where the ratio was 8.5. Similarly, the Si/carbonate ratios in the particle flux showed a decrease from values between 0.9 and 0.45 at Station 5 to between 0.16 and 0.23 at Station 7; again the highest ratio (1.06) was calculated for Station 2. These ratios are all lower than the 2:1 dissolution flux for silicate to carbonate inferred from the distributions of dissolved silicate and alkalinity in the tropical oceans (Edmond, 1974).

If the dependence of the vertical particle flux upon surface productivity can be established, then it will be possible to estimate the global particulate flux from the maps of surface productivity. The U.N.-F.A.O. (1972) atlas shows that the annual primary productivity of the surface waters in the Cape Basin varies from >1500 to $<300 \mu\text{moles C cm}^{-2}\text{y}^{-1}$ from the coast of S.W. Africa near Station 4 to the interior

TABLE 3 - 5 MAJOR COMPONENT ANALYSIS OF > 53 μm FECAL MATERIAL
 FROM 400m AT STATIONS 2, 5, 6, AND 7 (nmol kg^{-1})

Station	[CaCO_3 Forams Net F.M.]	[Si Rads Diatoms Net F.M.]	Si/ CaCO_3 F.M.					
5	11.86	0.71	11.15	13.53	1.84	0.44	11.25	1.01
6	9.51	0.50	9.01	9.97	0.72	0.12	9.13	1.01
7	3.85	0.18	3.67	2.53	0.37	0.07	2.09	0.57
2	3.0	0.15	2.85	4.1	0.63	0.24	3.23	1.13

FECAL MATERIAL	WEIGHT % C_{Org}	WEIGHT % CaCO_3	WEIGHT % OPAL
5	24.0	23.4	16.6
6	24.0	23.4	16.6
7	24.0	28.6	11.4
2	24.0	22.5	17.5

THE CHEMICAL COMPOSITION OF FECAL PELLETS AND FECAL MATTER IS ASSUMED SIMILAR

TABLE 3 - 6 TOTAL CHEMICAL FLUX > 53 μm PARTICLES ($\text{mmol cm}^{-2} 1000\text{y}^{-1}$)

Station	$\sum \text{CaCO}_3$		$\sum \text{Si}$		$\sum \text{C}_{\text{org}}$		Si/CaCO_3		$\text{C}_{\text{org}}/\text{CaCO}_3$	
	meas.	extr.	meas.	extr.	meas.	extr.	meas.	extr.	meas.	extr.
5	11.43	13.44	9.97	10.87	84.10	91.22	0.87	0.81	7.36	6.79
5 [†]	21.59	23.59					0.46	0.46	3.90	3.87
6	2.71	3.80	1.74	2.50	14.70	21.06	0.64	0.66	5.42	5.54
6*	3.11	4.95					0.56	0.51	4.72	4.26
7	0.61	1.45	0.10	0.34	1.24	4.20	0.16	0.23	2.05	2.89
2	4.58	7.39	4.85	7.89	38.76	63.10	1.06	1.07	8.46	8.53

of the S. Atlantic gyre which includes Station 7. From the discussion of the biological distributions at Stations 4-7 it is apparent that the productivity pattern was different than implied by this map. Since the large particles are derived from biological production in the surface waters and have residence times of the order of several days in the upper 400 m, the $>53 \mu\text{m}$ integrated mass within the upper 400 m might be a useful measure of biological productivity.

The mass fluxes for fecal matter and for Foraminifera at Stations 5, 6, and 7 show an exponential decrease with "productivity"; whereas the flux for fecal pellets shows a gentle decrease (Fig. 34). The particles contributing most to the vertical flux of fine material are therefore fecal matter and fecal pellets in areas of high and low productivity respectively.

The organic carbon flux also shows an exponential decrease with integrated $>53 \mu\text{m}$ mass for the same stations. If the integrated mass is linearly related with productivity, then it appears that the recycling efficiency for organic matter in the upper 400 m is highest in areas of low productivity. If the productivity of the surface waters at Station 7 was $200 \text{ nmol C cm}^{-2} 1000\text{y}^{-1}$, then between 99.5 and 98% of the organic matter had been recycled within the upper thermocline at this station. Similarly, if the productivity at Station 5 was $1500 \text{ nmol C cm}^{-2} 1000\text{y}^{-1}$, then the recycling efficiency was approximately 94%. The sinking material at

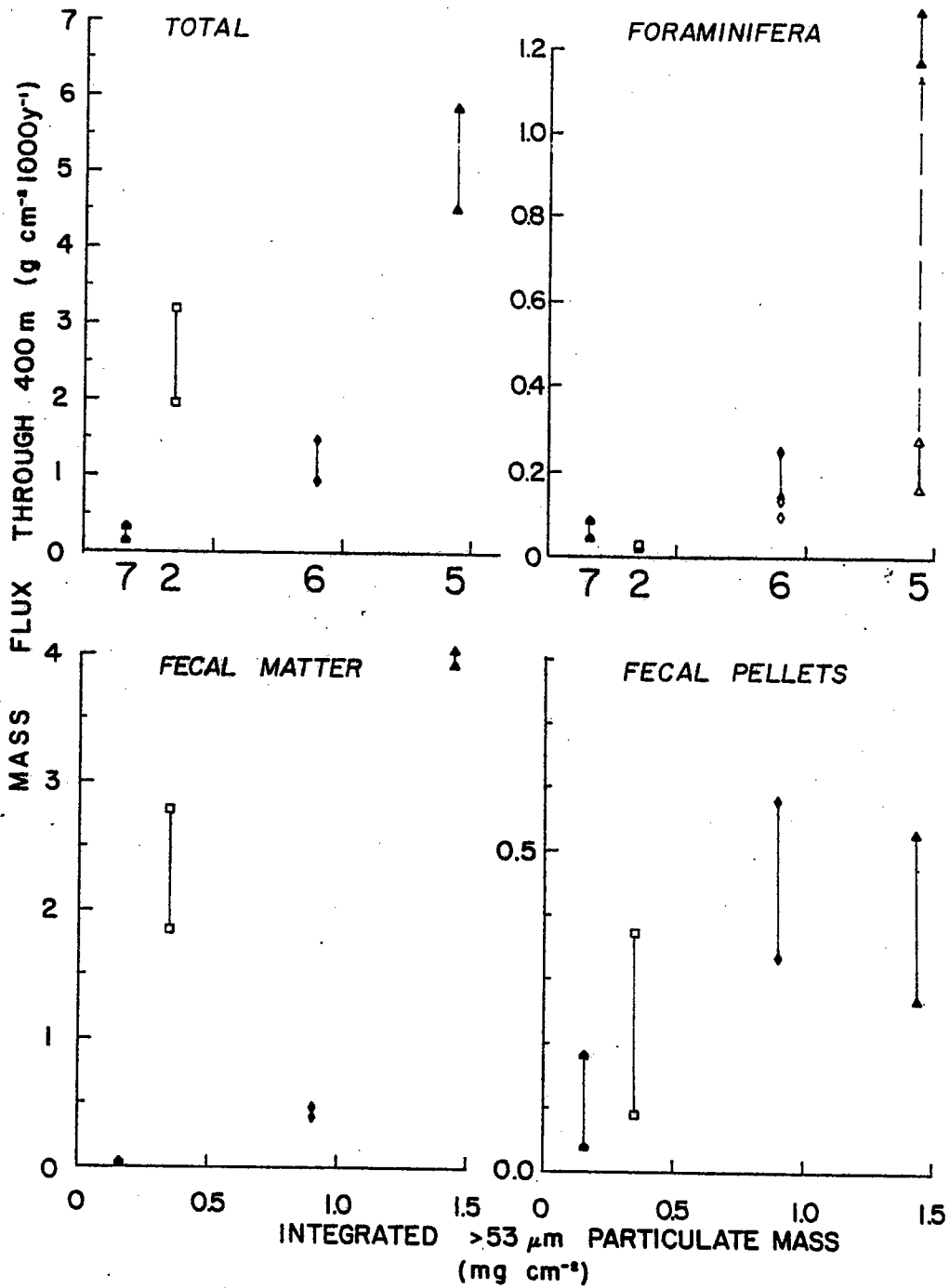


Fig. 3-34, mass flux through 400m as a function of integrated $>53 \mu\text{m}$ mass ("productivity") at LVFS stns. 2, 5, 6, and 7.

TABLE 3 - 7 SUSPENDED MASS CONCENTRATION SUMMARY ($\mu\text{g kg}^{-1}$)

Particle	Stn. 5	Stn. 6	Stn. 7	Stn. 2
Foraminifera	0.071	0.044	0.018	0.015
fecal pellets	0.051	0.051	0.008	0.021
fecal matter	0.734	0.105	0.030	0.346
Radiolaria	0.160	0.059	0.031	0.070
Total	1.016	0.265	0.087	0.452
measured	6.1	3.1	1.4	1.1
% >53 μm ...				
dry weight	16.6	8.6	6.2	41.1
% total				
dry weight	4.0	1.9	0.5	3.2

all stations contributed less than 4% to the total suspended mass concentration at 400 m (Table 7), consistent with the conclusions of Chap. 2.

Station 2 in the equatorial Atlantic had an anomalously high fecal matter mass flux relative to the other carriers. This material differed from that found at the Walvis Bay stations in that it was opaque and brownish rather than white in reflected light. Furthermore it was determined to have approximately three times the density of the material typical of Stations 5, 6, and 7. Therefore there are apparent regional differences in the composition of fecal matter. On the other hand, there are relatively subtle differences in the morphology of fecal pellets and Foraminifera between stations.

An estimate of the $<53 \mu\text{m}$ particle flux can be made using the $<3 \times 10^{-4} \text{cm sec}^{-1}$ settling velocity derived for this size fraction from ^7Be measurements at Station 2. The fluxes are <0.19 , <0.12 , and $<0.14 \text{ gm cm}^{-2} 1000\text{y}^{-1}$ at Stations 5, 6, and 7 respectively. They are relatively minor compared to the $>53 \mu\text{m}$ fluxes at Stations 5 and 6 but may account for between 30 and 50% of the total mass flux at Station 7.

Summary and Conclusions

The particulate biological, morphological, and chemical distributions have been determined within the upper 400 m at five LVFS stations in the Cape Basin of the S.E. Atlantic Ocean. The results from these stations have established the

oceanic significance of many of the features of the particulate distributions found at Station 2 (Chap. 2).

1) The particle maximum coincided with the maxima in the phyto- and microzooplankton. Its depth at a given station was determined by the stratification of the surface waters. In areas where the mixed layer was poorly developed or absent (Stations 4, 5, and 8) the particle maximum occurred nearest the surface. At other stations, the particle maximum was found within several meters of the base of the mixed layer.

2) Acantharia, dinoflagellates, Foraminifera, diatoms, coccolithophorids, Radiolaria, and tintinnids showed consistent distributional patterns. Acantharia always showed a surface maximum (like dinoflagellates) although they appeared to have a larger biomass at 40 and 52 m at Stations 5 and 6. Centrate diatoms were the most important members of the $>53 \mu\text{m}$ diatom population, particularly at Station 8 where they dominated the biomass. The single exception was found at 52 m at Station 6 where solenoid diatoms were most abundant. Both diatoms and Foraminifera exhibited similar distributions and were most concentrated in the surface water at Stations 4 and 8, and at the base of the mixed layer at Stations 6 and 7. At Station 5, diatoms were most abundant at 40 m, whereas Foraminifera were most numerous nearest the surface. Radiolaria and tintinnids exhibited similar distributions and had maximum populations in the upper thermocline, deeper than those of the other organisms.

3) The organic C/N ratios of the 1-53 μm particulate matter at Stations 4, 5, 6, and 8 were remarkably constant, being 7.3 ± 0.5 (σ). This contrasts with Station 7 where the C/N ratio increased from a surface value of 9.0 to 11.3 at 400 m, similar to the behavior found at Station 2. The agreement of the near-shore C/N ratios with the theoretical value of 7 derived from the Redfield-Ketchum-Richards (1963) model implies that the oceanic nutrient distributions may be significantly controlled by processes of production and consumption in areas of high biological productivity.

The <1 μm organic C/N ratios were consistently lower than those for the 1-53 μm material, probably indicative of the presence of marine bacteria in this fraction. The <1 and 1-53 μm fractions of the near surface sample at Station 8 had comparable quantities of both carbon and nitrogen indicating an extremely high bacterial population. These organisms may also be an important fraction of the <1 μm particles near the bottom at the shelf Stations 4 and 8.

4) Excess Ca and K were distributed similarly in the >53 μm fraction and showed shallow regenerative cycles; these elements were measureable in the 400 m samples only in areas of high biological productivity. Mg was distributed in a similar fashion as found at Station 2 and was probably bound in a refractory organic phase.

5) The presence of cations in association with organic matter, either as components of organism cytoplasm or at ion-exchangeable and complexing sites underscores the potential of this phase as a carrier of other minor and trace elements present in seawater. Furthermore, the particulate data indicates that the proposed reduction of seawater alkalinity due to the oxidation of organic matter (Brewer et al., 1975) is at least 20% compensated by the substitution of some protons (assumed in the Redfield-Ketchum-Richards (1963) model) by cations. The alkalinity problem posed by Brewer et al. (1975) will be best resolved by direct measurements of the major cations and anions in plankton sampled in the open ocean.

6) The particulate calcium and carbonate distributions are decoupled especially in areas of high diatom productivity. Calcium to carbonate ratios as high as 2.5 were observed for the surface sample at Station 8. On the other hand, the excess Ca to organic carbon ratio falls in the range of 1:100-200 at all stations. The cycling of excess calcium is estimated to be between 1 and 2×10^{13} moles y^{-1} in the world's ocean compared with $7 \pm 2 \times 10^{13}$ moles y^{-1} estimated for carbonate production by Li, Takahashi, and Broecker (1969). The removal of calcium and carbonate from the surface mixed layer is in the ratio of between 1.13 and 1.4 making this water a poor reference for the comparison of the calcium and alkalinity

distributions as was done in the treatment of Brewer et al. (1975). As yet there is no convincing evidence that any in situ process other than the dissolution of calcium carbonate alters the alkalinity distribution in the deep ocean.

7) The distribution of $>53 \mu\text{m}$ carbonate resembles that of Foraminifera in the upper 100 m with a divergence in distributions being observed in the deeper water due to fragmentation of Foraminifera and aggregation of coccoliths into the large particles by detritus feeding organisms. This process explains the order-of-magnitude increase with depth of the total carbonate to total Foraminifera ratio found at all stations.

8) Coccolithophorids were the dominant source of particulate carbonate at most stations. They entirely dominated the $<53 \mu\text{m}$ distributions in the euphotic zone (at Station 4 they were most of the biomass) and their coccoliths comprised the bulk of the suspended carbonate below 100 m. Some features of the deep carbonate distribution are probably determined by lateral advective processes.

9) Centrate diatoms dominated the $>53 \mu\text{m}$ silicate distributions in the upper 100 m at all stations except Station 6 where solenoid diatoms were most important at 52 m.

10) The $<53 \mu\text{m}$ particulate Si was distributed differently from carbonate contributing as much as 50% to the total suspended mass at Station 8 and as little as 1%

to the surface sample at Station 4. Contributions varied with averages of 15, 25, and 6% being found for the samples at Stations 5, 6, and 7. The relative high at Station 6 may be derived from the intense $>53 \mu\text{m}$ Si maximum at 52 m.

11) The $>53 \mu\text{m}$ Si/carbonate ratios decreased from surface values between 0.8 and 45 to values near 1.0 at 400 m. This decrease is the result of exchange of material between the sizeable reservoir of $<53 \mu\text{m}$ material (having Si/carbonate ratios of approximately 0.5 below 100 m) and the $>53 \mu\text{m}$ fraction. This process is governed by detritus feeding organisms.

12) The $>53 \mu\text{m}$ non-carbonate Sr distribution reflected that of Acantharia in the near surface samples. Deeper concentrations were highest relative to the other inorganic components in areas of high biological productivity, apparently being determined by the rates of supply of fresh material from the surface layer, and dissolution.

13) The size distributions of Foraminifera, Foraminifera fragments, fecal pellets, and fecal matter were measured on filter subsamples equivalent to 0.56, 0.95, and 0.96 m^3 of seawater at Stations 5, 6, and 7. Foraminifera ranged in size from 20 to $180 \mu\text{m}$ on these subsamples but shells as large as 480 and $350 \mu\text{m}$ were found during preliminary scans of the whole samples at Stations 5 and 6. Pteropod (?) shells up to $180 \mu\text{m}$ and fecal pellets up to $300 \mu\text{m}$ in size were also encountered in the subsample from Station 6.

Fecal matter as large as 4 mm was found at Station 5.

14) The observed particle distributions differed from those predicted by McCave (1975), large particles being somewhat rarer than guessed by his extrapolation of Junge distributions fitted to Coulter Counter measurements of 1-100 μm particles.

15) Two flux models for spherical and disk shaped particles were used to calculate the vertical fluxes of Foraminifera and fecal pellets and of fecal matter. The particles contributing most to the vertical flux sank faster than 0.1 cm sec^{-1} and would reach 4000 m in less than 30 days. Fecal matter and Foraminifera (Orbulina Universa) were the major contributors to the vertical flux at Station 5; fecal matter, fecal pellets, and Foraminifera at 6; and fecal pellets and Foraminifera at 7. The mass fluxes were calculated for these stations to range between 5.4 and $5.9 \text{ gm}^{-2}\text{cm}^{-1}$; 0.87 and 1.30; and between 0.10 and $0.30 \text{ gm cm}^{-2}1000\text{y}^{-1}$. The flux of fine material was almost the same as the large particle flux at Station 7; whether or not the fine material reaches the bottom depends upon the rates of degradation of the organic matter and of dissolution of carbonate and opal.

16) The $>53 \mu\text{m}$ organic carbon fluxes were estimated to be between 84 and 91; 15 and 21; and between 1 and $4 \text{ mmol C cm}^{-2}1000\text{y}^{-1}$ at Stations 5, 6, and 7 indicating an exponential decrease relative to surface productivity (assumed linearly

related to integrated $>53 \mu\text{m}$ mass in the upper 400 m). It is estimated that approximately 94% and 99% of the total carbon production is consumed by organisms within the upper 400 m at Stations 5 and 7. This is consistent with the observed decrease in organic to carbonate carbon ratio in the flux from values exceeding 3.5 to approximately 2.0 between Stations 5 and 7.

17) The Si/carbonate ratio calculated for the flux was in the range of 0.9 to 0.5 at Station 5; 0.7 to 0.5 at Station 6; and 0.1 to 0.2 at Station 7. These values all are lower than the average dissolution ratio of 2 determined from the dissolved silicate and alkalinity distributions in the tropical oceans (Edmond, 1974). This difference demonstrates that the particle flux may be quite distinct in composition in a given area; however, advective processes serve to effectively mask the local regeneration anomaly.

18) The large particles responsible for the vertical flux contribute less than 4% to the total suspended mass concentration of particulate matter at 400 m. Their flux may largely control the deep ocean distributions of the many non-conservative chemical tracers involved in the bio-geochemical cycle. Besides carrying organic, carbonate, and opal phases, these particles may also transport significant quantities of celestite, and terriginously derived material to the deep ocean.

References

- Bang, N.D. (1971) The Southern Benguela Current region in February, 1966: Part II. Bathythermography and air-sea interactions, Deep-Sea Research, 18, 209-224.
- Bang, N.D. (1973) Characteristics of an intense ocean frontal system in the upwell regime west of Capetown, Tellus, 25, 256-265.
- Bang, N.D., W.R.H. Andrews (1974) Direct current measurements of a shelf-edge frontal jet in the Southern Benguela System, J. Mar. Res., 32, 405-417.
- Bender, M. and C. Gagner (1976) Dissolved copper, nickel, and cadmium in the Sargasso Sea, J. Mar. Res., 31, 119-128.
- Berger, W.H. (1968) Planktonic Foraminifera: Shell production and preservation, Ph.D. Thesis, Univ. of California, San Diego, 241 pp.
- Berger, W.H., J.W. Piper (1972) Planktonic Foraminifera: Differential settling, dissolution, and redeposition, Limnology and Oceanography, 17, 275-287.
- Biscaye, P.E. (1965) Mineralogy and sedimentation of recent deep sea clay in the Atlantic Ocean and adjacent seas and oceans, Geol. Soc. Amer. Bull., 76, 803-832.
- Bishop, J.K.B., J.M. Edmond (1976) A new large volume filtration system for the sampling of oceanic particulate matter, J. Mar. Res., 34, 181-198.
- Boyle, E.A., F. Sclater and J.M. Edmond (1976) On the marine geochemistry of cadmium, Nature, 263, 42-44.

- Bramlette, M.N. (1961) Pelagic sediments, Oceanography, M. Sears, ed., A.A.A.S., Washington, D.C., 345-366.
- Brewer, P.G., G.T.F. Wong, M.P. Bacon, D.W. Spencer (1975) An oceanic calcium problem?, Earth and Planet. Sci. Lett., 26, 81-87.
- Brewer, P.G., D.W. Spencer, P.E. Biscaye, A. Hanley, P.L. Sachs, C.L. Smith, S. Kadar, and J. Fredericks (1976) The distribution of particulate matter in the Atlantic Ocean, Earth and Planet. Sci. Lett., 32, 393-402.
- Calvert, S.E. (1966) Accumulation of diatomaceous silica in the sediments of the Gulf of California, Geol. Soc. Amer. Bull., 77, 569-596.
- Calvert, S.E. and N.B. Price (1971) Upwelling and nutrient regeneration in the Benguela Current, October 1968, Deep-Sea Res., 18, 503-523.
- Carpenter, J.H. (1965), The Chesapeake Bay Institute technique for the Winkler dissolved oxygen method, Limnology and Oceanography, 10, 141-143.
- Chester, R., H. Elderfield, J.J. Griffin, R.L. Johnson, and R.C. Padgham (1972) Eolian dust along the eastern margins of the Atlantic Ocean, Mar. Geol., 13, 91-105.
- De Decker, A.H.B. (1970) An oxygen-depleted subsurface current off the west coast of South Africa, Division Sea Fisheries Investigational Report, 84, 24 pp.
- Edmond, J.M. (1974) On the dissolution of carbonate and silicate in the deep ocean, Deep-Sea Res., 21, 455-480.
- Feely, R.A. (1975) Major-element composition of the particulate matter in the near-bottom nepheloid layer of the

- Gulf of Mexico, Mar. Chem., 3, 121-156.
- Gardiner, W.D. (1976) Incomplete extraction of rapidly settling particles from water samplers, Limnology and Oceanography (in press).
- Goldberg, E.D., J.J. Griffin (1964) Sedimentation rates and mineralogy in the South Atlantic, J. Geophys. Res., 69, 4293-4309.
- Gordon, D.C., Jr. (1971) Distribution of particulate organic carbon and nitrogen at an oceanic station in the central Pacific, Deep-Sea Res., 18, 1127-1134.
- Hart, T.J. and Currie, R.I. (1960) The Benguela Current, Discovery Reports, 31, 123-298.
- Hecht, A.D., A.W.H. Bé and L. Lott (1976) Ecologic and paleoclimatic implications of morphologic variation of Orbulina universa in the Indian Ocean, Science, 194, 422-423.
- Hobson, L.A., D.W. Menzel (1969) The distribution and chemical composition of organic particulate matter in the sea and sediments off the east coast of South America, Limnology and Oceanography, 14, 159-163.
- Hobson, L.A. (1971) Relationships between particulate organic carbon and micro-organisms in upwelling areas off southwest Africa, Investigacion Pesquera, 35, 195-208.
- Honjo, S. (1975) Dissolution of suspended coccoliths in the deep-sea water column and sedimentation of coccolith ooze, in Sliter, W.V., Bé, A.W.H., and Berger, W.H., eds.,

- Dissolution of Deep-Sea Carbonates: Cushman Foundation for Foraminiferal Research Spec. Pub. 13, 114-128.
- Honjo, S. (1976) Coccoliths: production, transportation and sedimentation, Marine Micropaleontology, 1, 65-79.
- Hughes, M.N. (1972) The inorganic chemistry of biological processes, New York, Wiley, 304 pp.
- Jones, P.G.W. (1971) The southern Benguela Current region in February, 1966: Part I., Chemical observations with particular reference to upwelling, Deep-Sea Res., 18, 193-208.
- Junge, C.F. (1963) Air Chemistry and Radioactivity, Academic Press, New York, 113-123.
- Koblentz-Mishke, O.J., V.V. Volkovinsky, J.G. Kabanova, (1970) Plankton primary production of the world ocean in: Scientific Exploration of the South Pacific, ed. W.S. Wooster, National Academy of Sciences, Washington, D.C., 183-193.
- Krishnaswami, S., and M.M. Sarin (1976) Atlantic surface particulates: composition, settling rates and dissolution in the deep sea, Earth and Planet. Sci. Lett., 32, 430-440.
- Lerman, A., D. Lal, and M.F. Dacey, (1975) Stoke's settling and chemical reactivity of suspended particles in natural waters, in: Suspended Solids in Water, Gibbs, R.J. (ed.), Plenum Press, 17 - 47.

- Li, Y.H., T. Takahashi, W.S. Broecker (1969) Degree of saturation of CaCO_3 in the oceans, J. Geophys. Res., 74, 5507-5525.
- Lisitzin, A.P. (1972) Sedimentation in the World Ocean, S.E.P.M. Spec. Publ. 17, 218 pp.
- Manheim, F.T., J.C. Hathaway, E. Uchupi (1972) Suspended matter in the surface waters of the northern Gulf of Mexico, Limnology and Oceanography, 17, 17-27.
- Mayzaud, P., J.-L. Martin (1975) Some aspects of the biochemical and mineral composition of marine plankton, J. Experimental Mar. Biol. and Ecol., 17, 297-310.
- McCave, I.N. (1975) Vertical flux of particles in the ocean, Deep-Sea Res., 22, 491-502.
- Menzel, D.W. (1974) Primary productivity, dissolved and particulate organic matter, and the sites of oxidation of organic matter, in: The Sea, Vol. 5, E.D. Goldberg, ed., John Wiley & Sons, N.Y., 659-678.
- Mullin, J.B., J.P. Riley (1955) The colorimetric determination of silicate with special reference to sea and natural waters, Anal. Chim. Acta, 12, 162-176.
- Murphy, J., J.P. Riley (1962) A modified single solution method for the determination of phosphate in natural waters, Anal. Chim. Acta, 27, 31-36.
- Petrushevskaya, M.G. (1971) Spumellarian and Nassellarian Radiolaria in the plankton and bottom sediments of the central Pacific, The Micropaleontology of Oceans,

- B.M. Funnell and W.R. Riedel, eds., Cambridge at the University Press, 309-319.
- Redfield, A.C., B.H. Ketchum, F.A. Richards (1963) The influence of organisms on the composition of seawater, in: The Sea, 2, M.N. Hill, ed., J. Wiley & Sons, N.Y., 26-77.
- Roth, P.H., M.M. Mullin, and W.H. Berger (1975) Coccolith sedimentation by fecal pellets: laboratory experiments and field observations, Geol. Soc. Amer. Bull., 86, 1079-1084.
- Schrader, H.J. (1971) Fecal pellets: role in sedimentation of pelagic diatoms, Science, 174, 55-57.
- Sclater, F., E.A. Boyle, J.M. Edmond (1976) On the marine geochemistry of nickel, Earth and Planet. Sci. Lett., 31, 119-128
- Sheldon, R.W. (1972) Size separation of marine seston by membrane and glass fiber filters, Limnol. Oceanog., 17, 494-498
- U.N.-F.A.O. (1972) Atlas of the Living Resources of the Seas, Dept. of Fisheries, U.N.-F.A.O., Rome.
- Wangersky, P.J. (1976) Particulate organic carbon in the Atlantic and Pacific Oceans, Deep-Sea Res., 23, 457-466.
- Wiebe, P.H., S.H. Boyd, C. Winget (1976) Particulate matter sinking to the deep-sea floor at 2000 m in the Tongue of the Ocean, Bahamas with a description of a new sedimentation trap, J. Mar. Res., 34, 341-354.

CHAPTER 4

THE DISTRIBUTION OF PARTICULATE MATTER
COLLECTED BY LARGE VOLUME IN SITU FILTRATION
TO 1500 M IN THE EQUATORIAL
PACIFIC OCEAN

Introduction

A ship-powered Large Volume in situ Filtration System (LVFS) has been used routinely over the past several years to sample particulate matter from the upper 400 m of the Atlantic Ocean (Bishop and Edmond, 1976). The modifications to the LVFS described in this note have enabled the system to be operated successfully to 1500 m in the Equatorial Pacific Ocean (R/V MELVILLE, Pleiades Leg 2, June-July 1976, Balboa to Balboa). This modified system is capable of taking 4 discrete samples per lowering, splitting the particulate matter in situ into >53 and <53 μm size fractions using 53 μm Nitex mesh and a pair of 1 μm glass fiber filters in series. Flow rate information is telemetered to the surface via the electro-mechanical cable used to support and power the filtration system. These two modifications permit the system to be operated at high efficiency to depths exceeding those of the nutrient extrema (excluding Si) in the oceans.

The Four Filter Large Volume in situ Filtration System (LVFS-4)

The basic features of the filtration system (Fig. 4-1) are the same as described by Bishop and Edmond (1976). Differences are: the substitution of a bronze centrifugal pump (Aurora Pump, No. Aurora, Ill.) in place of the original cast iron one; the addition of submersible valve actuator (Pre-Con Inc. Bellevue, Washington) mated to a 2-inch Mod.

**FOUR FILTER LARGE
VOLUME FILTRATION
SYSTEM**

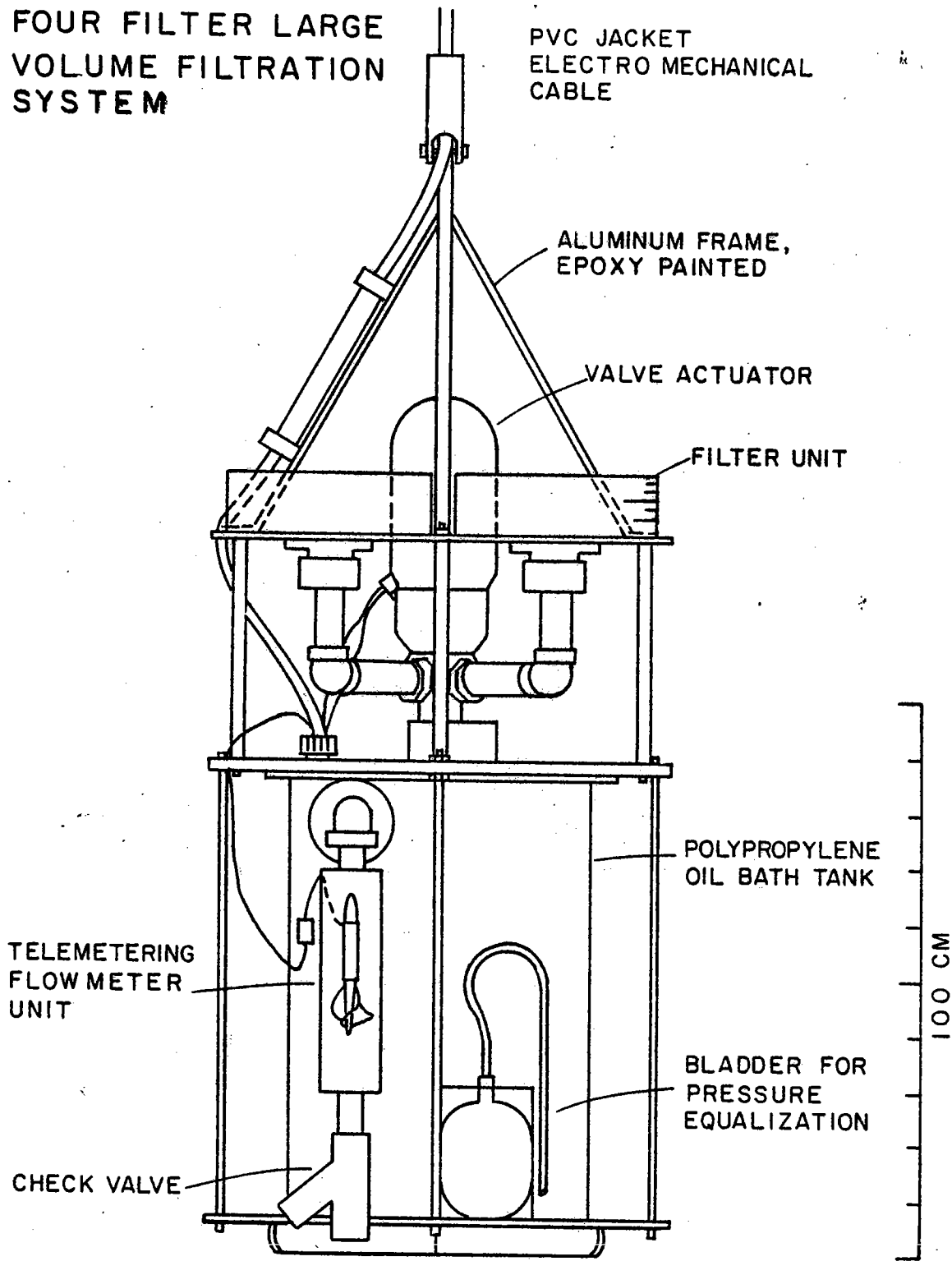


Fig. 4-1 , Four filter Large Volume in situ Filtration System (LVFS-4).

2557L stainless steel and teflon rotor valve (Q.C.I. Inc., Malden, Mass.) mounted over the pump intake in place of the single filter unit shown in Bishop and Edmond (1976); the use of PVC pipe and pipe fittings to connect four horizontally mounted filter holders to the valve; and the use of a more complex electro-mechanical cable (Boston Insulated Wire and Cable Co., Boston, Mass.) to power and support the instrument. Power for the pump (480 VAC, 3 phase, 2.3 kW) and valve actuator motor, control and position indication (120 VAC, 3 phase, 1 kW) as well as flow meter information is transmitted via the 1500 m cable between the LVFS-4 and the ship. All control is direct from the surface.

Shipboard handling of the LVFS-4 was identical to that for the LVFS described by Bishop and Edmond (1976); however, operation at depth was somewhat different. Each cast of four filters was made in order of increasing depth at horizons preselected using the shipboard-generated hydrographic data. Sampling was terminated when the flow rate dropped below 0.7 l sec^{-1} , the LVFS-4 lowered to the next depth, and the valve actuated to select a new filter. After indication that the valve had been turned to the proper position, the pump was restarted and the flow meter data recorded for the new sample. The depth of the LVFS-4 was determined by 12 kHz echo-sounder.

The filter holder configuration and filtration sequence

for the LVFS-4 is identical to that used in the LVFS, save for the use of an additional baffle plate to further protect the samples from being disturbed while the other filters are being used.

The 53 μm Nitex prefilters and the Mead 935-BJ glass fiber filters were cut from bulk rolls of the material using a 30.5 cm diameter polycarbonate template. They were later leached in a 1 N 1:1 mixture of hot nitric and hydrochloric acids, twice, before rinsing with distilled-deionized-distilled water until the rinse effluent showed neutral pH. The Nitex prefilters were dried at 60°C to constant weight before they were placed in acid leached polyethylene bags, whereas the glass fiber filters were partially dried before being combusted at 500°C for several hours. They were cooled and weighed before being placed in acid leached polyethylene bags.

The handling of the filters before and after use aboard ship was carried out in a laminar flow clean air bench. The used filters were washed with two 250 ml portions of distilled water to reduce their seasalt content before being placed in a 60°C drying oven for several days. When dry, the samples were transferred to their original acid leached poly bags for storage until analysis in the laboratory. This method of preservation was considered superior to freezing as was done for the filters from the previous expeditions. The filters were redried in the laboratory before weighing as described in Bishop and Edmond (1976).

Flow meter calibration

A General Oceanics Mod. 2031 reed switch flowmeter was substituted for the Mod. 2030 flowmeter used in the original LVFS. It's calibration was carried out at the same time as the other flowmeter and gave the following relation between flow rate, F , and count rate, CPS.

$$F = 0.0716 (\text{CPS})^{1.2155} + 0.54 \text{ } \mu \text{ sec}^{-1} \quad (1)$$

The standard deviation assumed typical for this type of flowmeter is $0.04 \text{ } \mu \text{ sec}^{-1}$ taken from the more extensive calibration of the other flowmeter. Bishop and Edmond (1976) assumed that the flow rate decreased exponentially with time:

$$F = F_0 e^{-kt} \text{ } \mu \text{ sec}^{-1} \quad (2)$$

where F_0 is assumed to be $2.95 \text{ } \mu \text{ sec}^{-1}$, and k is the decay constant. This constant was then determined by comparing total flowmeter counts (ΣCPS) registered for each sample with tabulated values computed as a function of k and t :

$$\Sigma \text{CPS} = (1/A)^b \int_0^t (F_0 e^{-kt} - C)^b dt \quad \text{counts} \quad (3)$$

where $A = 0.0716$, $b = 1/1.2155$, and $C = 0.54 \text{ } \mu \text{ sec}^{-1}$.

Therefore total flow is:

$$F = F_0/k (1 - e^{-kt}) \ell \quad (4)$$

Table 4-1 summarizes the flow volumes calculated according to this scheme, m^3 (MOD.), and from the integrated real time flowmeter data, m^3 (MEAS.). The error listed is calculated from the product of the flow rate error ($0.04 \ell \text{ sec}^{-1}$) and the time for the filtration of each sample. In all cases the model and measured flow volumes agreed to within the one sigma error limits determined by the flowmeter calibration; the model values fall several percent higher than those from the real time flow meter data. Given this good agreement, recalculation of the data obtained during the earlier cruises is unnecessary. The weight of seawater filtered is calculated using the measured flow volume and in situ density of the seawater.

Dry weight measurements

The procedure for the calculation of the particulate dry weight concentration is outlined in Bishop and Edmond (1976). One major improvement in technique was the use of 25.4 cm diameter polycarbonate templates to cut the effective filter areas from the used glass fiber filters. Also the Nitex prefilters were preweighed. The preliminary profiles of dry weight for the $>53 \mu\text{m}$ and $<53 \mu\text{m}$ size fractions do not include sea salt corrections which are relatively minor.

TABLE 4 - 1 FLOW METER DATA

CAST	SAMPLE	Z	t	Σ CPS	m ³ (MOD.)	m ³ (MEAS.)	ERROR	TONS
1	G 102	15	1680	8645	1.84	1.85	0.07	1.89
	G 103	40	1500	5470	1.23	1.32	0.06	1.35
	G 104	60	3000	11705	2.62	2.81	0.12	2.88
	G 105	100	7200	39465	8.26	8.12	0.30	8.33
	G 114	200	9510	60560	12.11	11.98	0.39	12.30
2	G 111	350	10800	68885	13.81	13.49	0.44	13.87
	G 112	500	12000	71515	14.64	14.23	0.49	14.64
	G 113	724	14600	89825	18.21	17.68	0.60	18.22
3	G 118	900	15600	100945	20.15	19.70	0.64	20.32
	G 115	1100	14100	93805	18.56	18.08	0.58	18.67
	G 116	1300	14400	99145	19.39	18.93	0.59	19.56
	G 117	1500	14410	97045	19.12	18.60	0.61	19.24

MOD. - CALCULATED FLOW VOLUME USING ASSUMPTIONS OF BISHOP AND EDMOND (1976)

MEAS. - CALCULATED FLOW VOLUME USING TELEMETERED FLOW INFORMATION

TONS - METRIC TONS, Z - METERS, t - SECS, ERROR = (0.041*t)/1000 m³

Results

Sampling was carried out in three casts of four filters each (Table 4-2) with samples taken in order of increasing depth. The flow rate-time relationship (Fig. 4-2) was shown to decrease exponentially to a flow rate of approximately 0.5 l sec^{-1} rather than to zero as assumed by Bishop and Edmond (1976). This observation explains the slight discrepancy in the flow volumes calculated using the two methods outlined above. The higher initial flow rates for the first samples of casts 2 and 3 are probably due to the fact that the LVFS-4 had not cooled to ambient temperature.

The total particulate mass profile (Fig. 4-3) shows a sharp particle maximum of $110 \text{ } \mu\text{g kg}^{-1}$ at 40 m (approximately 10 m below the base of the mixed layer) relative to concentrations of 60 and $50 \text{ } \mu\text{g kg}^{-1}$ at 15 and 60 m. The final sample in cast 1, at 100 m, showed a concentration of approximately $35 \text{ } \mu\text{g kg}^{-1}$. The concentrations from the second cast show a steady decrease with depth from 22 to $12 \text{ } \mu\text{g kg}^{-1}$ over the depth interval of 200 to 725 m; deeper concentrations were all rather uniform at approximately $11 \text{ } \mu\text{g kg}^{-1}$.

An interesting feature of the mass profile is the continual decrease in the $>53 \text{ } \mu\text{m}$ particle concentration from values of approximately $10 \text{ } \mu\text{g kg}^{-1}$ for the 15 and 60 m samples to near $1 \text{ } \mu\text{g kg}^{-1}$ for the samples deeper than 1000 m. This suggests that active processes operate to alter the

TABLE 4 - 2 LVFS CAST POSITIONS

CAST	DATE	LATITUDE	LONGITUDE
1	6/29/76	0° 49.1' N	86° 10.1' W
2	7/02-03/76	0° 41.5' N	86° 2.2' W
3	7/07-08/76	0° 39.4' N	86° 6.3' W

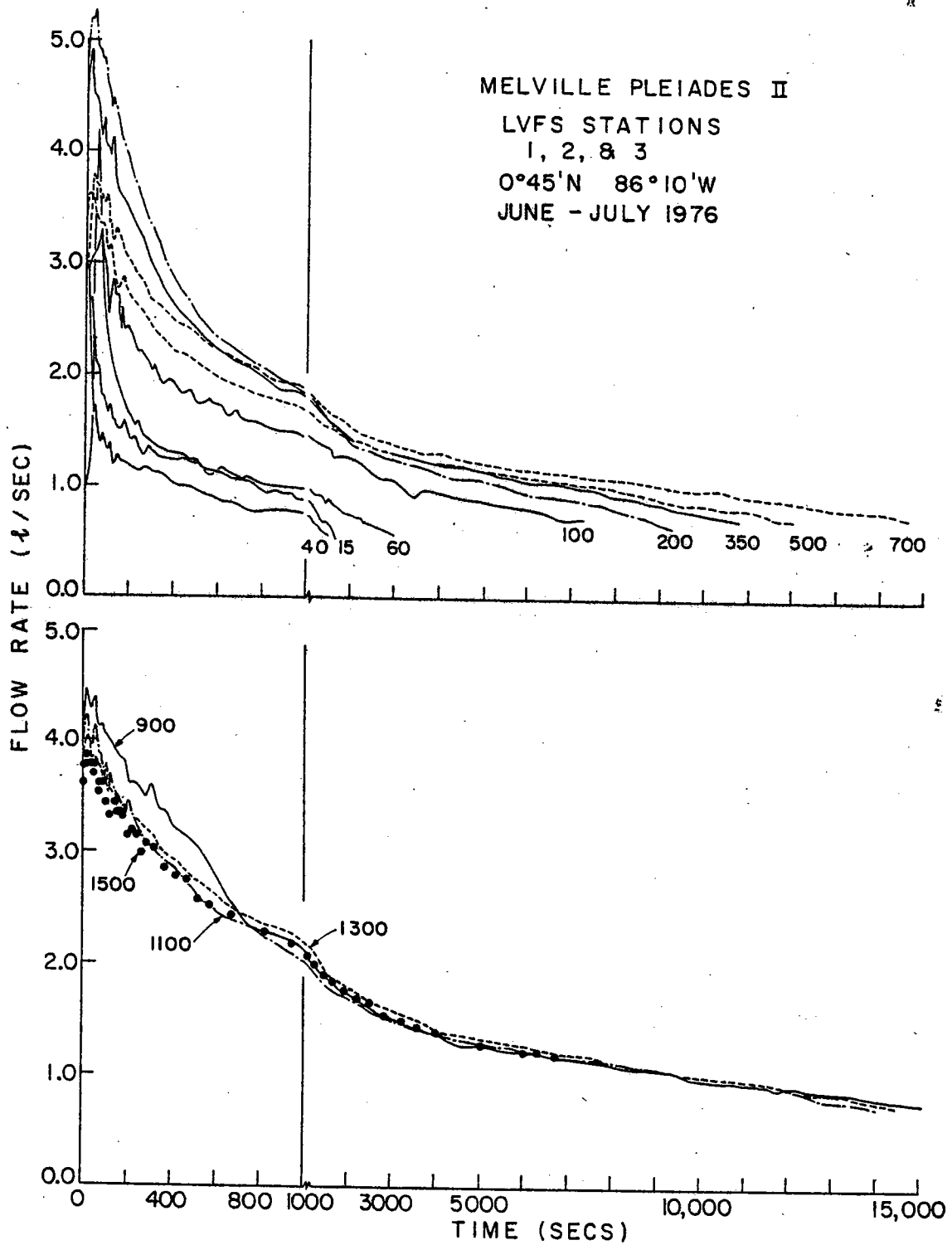


Fig. 4-2 , Flow rate versus time for samples to 1500 m.

particle distributions to depths of at least 1000 m in this region of the equatorial Pacific.

Referring back to the flow meter data it is apparent that the first order effect on the flow rate-time relationship for any sample is that of particle concentration. Second order effects are due to changes in particle size distribution and chemical composition. This means that it will be possible to use the flow meter data while at sea to deduce the major features of the particle distribution at a given station.

Summary

A modified Large Volume in situ Filtration System has been successfully operated to 1500 m in the equatorial Pacific to collect 12 particulate matter samples in three casts. Comparison of the flow volume data calculated according to the model of Bishop and Edmond (1976) to that determined by integration of the real time flow data shows excellent agreement to within the stated precision of the flow measurement. The model results are several percent high on average.

The flow rate-time relationship reflects the distribution of particulate mass in the water column making the flow meter data a useful measure of the particulate distributions while at sea. Furthermore it is apparent that active processes, such as the grazing activities of coprophagous organisms, operate at least to 1000 m to alter the particle size distributions in the Galapagos region of the Pacific Ocean.

This profile will be used to calculate the in situ regeneration of nutrient elements, carbonate and opal phases between 200 and 1500 m using the procedures established in the preceding chapters.

Reference

Bishop, J.K.B., and J.M. Edmond (1976), A new large volume in situ filtration system for the sampling of oceanic particulate matter, J. Mar. Res., 34, 181-198.

APPENDIX 0PARTICULATE DATA FROM LVFS STATION 1.

The data for LVFS station 1 are included in this thesis because they are referenced in Chapter 2 (and in Bishop, Ketten, Edmond, Bacon, and Silker, 1977). The analyses for the $>53 \mu\text{m}$ Size fraction are not included as the data are not yet complete. Replicate analyses for carbon, nitrogen, and phosphorus were somewhat poorer than found for the other LVFS stations, probably due to analysis error. No Mg data are reported because the sea salt levels in the filters were an order-of-magnitude higher than encountered on the distilled water rinsed filters. As a result the detection of the Mg anomaly was impossible; the calcium data are less influenced and so are reported. All symbols are defined in Appendix 1.

LVFS Station 1 Mystery Data Appendix 0.

	<1 μm SIZE FRACTION		1-53 μm SIZE FRACTION			
Z	\bar{P}	\bar{C}_o/\bar{P}	$\delta^{13}\text{C}$	\bar{P}	\bar{C}_o/\bar{P}	$\delta^{13}\text{C}$
20	1.62	157	-20.8	5.07	170	-19.60
50	5.95	146	-23.9	17.65	135	-22.78
113	0.33	148	-24.7	1.96	176	-21.90
221	0.26	154	-23.3	1.48	195	-21.17
291	0.21	138	-22.5	1.08	194	-20.88
378	0.29	107	-23.3	1.18	171	-20.72

\bar{P} : average P concentration nmoles kg^{-1}

\bar{C}_o/\bar{P} : organic carbon to phosphorus mole ratio

LVPS STATION C115 1 1-93 MICRON SIZE FRACTION NANOMOLES/KG							LVPS STATION C115 1 ORGANIC C AND N NANCMOLES/KG						
Z	CA	CI	SR	SR*	XS CA	MG	Z	<1 MICRON FRACTION			1-93 MICRON FRACTION		
								C	N	C/N	C	N	CRGC/N
20	2.1	9.8	0.227	0.209	-8.3		20	234.	35.0	6.70	737.	145.4	5.07
20	-2.7	10.4	0.189	0.171	-13.0		20	276.	45.8	6.04	988.	157.2	6.28
50	37.9	39.3	0.803	0.736	18.9		50	876.	177.2	4.91	2388.	312.3	7.64
50		38.4											
113	27.4	26.8	0.374	0.328	0.2		113	49.	8.7	5.62	344.	50.5	6.81
113		27.7											
221	34.0	29.9	0.267	0.214	3.4		221	35.	10.3	3.43	294.	33.0	8.97
221	33.2	31.0	0.283	0.231	2.6		221	45.	6.0	7.61	288.	33.7	8.49
221		30.9											
291	25.6	23.3	0.143	0.104	2.5		291	29.	-	-	210.	24.3	8.62
291		23.0					291				183.	20.7	8.82
378	25.6	20.4	0.179	0.144	4.9		378	31.	9.0	6.20	202.	28.2	7.17
378		21.0											

LVPS STATION C115 1 < 93 MICRON SIZE FRACTIONS AVERAGES NANOMOLES/KG

Z	CA	CI	SR	SR*	XS CA	MG	COBG	N	CI<1	NI<1	CHEM WT	DRY WT	TCNS
20	-0.3	10.3	0.21	0.19	-10.4		842	151.3	255	40.3	36.84	55.2	3.02
50	37.9	39.1	0.80	0.74	18.9		2388.	312.3	870.	177.2	109.47	90.8	1.99
113	27.4	27.2	0.37	0.33	0.2		344.	50.5	49.	8.7	15.41	16.2	11.28
221	33.6	30.6	0.27	0.22	3.0		291.	33.4	38.	6.2	13.37	13.1	14.13
291	25.6	23.1	0.24	0.18	2.5		196.	22.5	29.	-	9.33	12.8	21.49
378	25.6	20.7	0.18	0.14	4.9		202.	28.2	31.	5.0	9.76	7.3	22.26

LVPS STATION C115 1 < 93 MICRON SIZE FRACTIONS MGS

Z	TONS	SAMP	NA(8)	NA(8)	NA(8)	MG(8)	SR(8)	CELK	NBLK	CA(8)	CI(8)
20	3.02	14	199.9	183.7	7.2		0.00	2.2	0.24	91.1	5.4
20	3.02	14	206.6	166.8	7.2		0.00	2.2	0.24	96.8	11.4
20	3.02	14			7.2		0.00	2.2	0.24		
50	1.99	16	129.5	100.9	7.2		0.00	2.2	0.24	70.6	21.9
50	1.99	16			7.2		0.00	2.2	0.24		22.3
113	11.28	19	109.0	94.1	7.2		0.00	2.2	0.24	75.6	16.1
113	11.28	19			7.2		0.00	2.2	0.24		10.1
221	14.13	18	95.6	78.3	7.2		0.00	2.2	0.24	75.3	11.0
221	14.13	18	96.0	73.2	7.2		0.00	2.2	0.24	70.4	11.0
221	14.13	18			7.2		0.00	2.2	0.24		30.3
291	21.49	17	140.8	135.1	7.2		0.00	2.2	0.24	80.8	8.5
291	21.49	17			7.2		0.00	2.2	0.24		21.2
378	22.26	15	184.7	298.1	7.2		0.00	2.2	0.24	29.2	6.7
378	22.26	15			7.2		0.00	2.2	0.24		9.9

APPENDIX 1PARTICULATE DATA OBTAINED BY LARGE VOLUME IN SITU FILTRATION

ALL ELEMENTAL CONCENTRATIONS ARE REPORTED IN NANOMOLES KG^{-1}
SEASALT CORRECTED

Z	- meters
CA	- calcium
CI	- carbonate
SI	- silicate (opal)
SR	- strontium
SR*	- non-carbonate strontium
XS CA	- non-carbonate calcium
MG	- magnesium excess relative to seasalt ratio with sodium
K	- potassium excess relative to seasalt ratio with sodium
NA	- seasalt sodium concentration of the samples
WT(I)	- sum of dry weights calculated for carbonate, opal, and celestite ($\mu\text{g kg}^{-1}$)
WT	- dry weight measured ($\mu\text{g kg}^{-1}$)
A	- leach by 20 % H_3PO_4 + 0.6 N HCl
C	- leach by 0.6 N HCl.

LVFS STATION C115 4 GREATER THAN 53 MICRON SIZE FRACTION
(NANOMOLES/KG)

Z	CA	CI	SI	SR	SR*	XS	CA	MG	K	NA	WT(I)	WT
20	45.25			0.1950				1.12		100.85	C	
20	55.96	46.10	37.61			9.86		4.59		85.80	A	7.31
	57.80			0.596	0.518			1.84	2.29	51.88	C	66.5
42	11.75	11.04	14.15			0.71		1.51	0.45	2.44	A	2.14
	12.66			0.261	0.243			0.63	0.73	12.96	C	19.4
100	7.40	6.36	18.48			1.04		0.61	0.12	9.44	A	1.95
	8.31			0.128	0.117			0.24	0.03	18.87	C	4.6
183	91.89	83.95	70.89			7.95		6.26	0.60	51.85	A	13.41
	88.68	83.95	"			4.74		5.71	1.16	35.03	A	46.3
	96.79			0.332	0.189			5.63	0.79	23.92	C	

LVFS STATION C115 5 GREATER THAN 53 MICRON SIZE FRACTION
(NANOMOLES/KG)

Z	CA	CI	SI	SR	SR*	XS	CA	MG	K	NA	WT(I)	WT
20	129.69 140.63	114.72	198.78	8.541	8.346	14.97	13.77	2.77	3.46	30.37 25.17	A C	26.91 103.8
40	111.54 114.87 147.14	91.20 95.68	209.66 237.86	9.252	9.093	20.34 19.19	12.05 13.85	5.04 5.09	5.30	39.59 52.05 34.39	A A C	25.49 27.91 88.3
50	39.58 38.02	35.99	64.81	0.659	0.598	3.59	4.05 4.21	0.82 0.62		15.02 9.20	A C	8.25 29.2
88	63.85 74.07 65.68	58.33 68.08	45.05	0.514	0.407	5.53 5.99	3.17 3.21 4.12	3.83 1.51 1.01		16.05 15.87 8.83	A A C	9.08 10.05 22.3
124	25.82 29.22	24.44	23.16	0.353	0.312	1.38	1.48 1.81	0.53 0.39		6.15 2.62	A C	4.13 11.8
199	23.99 23.75	22.34	20.49	0.206	0.168	1.65	1.73 1.76	0.09 0.22		5.34 3.19	A C	3.70 12.3
294	11.84 11.10	10.51	13.44	0.103	0.085	1.33	0.49 0.50	0.45 0.37		7.48 5.30	A C	2.01 6.3
379	13.83 11.37 19.49 11.37	12.81 10.91	14.80 12.26	0.139 0.079	0.119 0.058	1.03 0.45	0.29 0.63 0.75 0.47	-0.02 0.26 0.17 0.08		13.03 16.41 8.60 3.45	A A C C	2.34 1.97 6.1 6.1

LVFS STATION C115 6 GREATER THAN 53 MICRON SIZE FRACTION
(NANOMOLES/KG)

Z	CA	CI	SI	SR	SR*	XS	CA	MG	K	NA	WT(I)	WT
26	14.02	10.23	43.27			3.79	4.07	1.33	32.69	A	4.43	18.5
	14.28	11.88				2.40	-0.29	1.01	64.11	A	4.60	18.5
	18.47			2.064	2.045		3.21	3.21	69.27	C		
52	71.18	54.80	466.67			16.38	9.80	2.40	29.71	A	38.60	93.1
	68.66	53.17	451.22			15.49	8.78	2.40	38.90	A	37.36	93.1
	70.28			2.516	2.425		10.04	4.39	52.16	C		
113	13.60	11.67	35.10			1.93	0.89	0.23	12.17	A	3.67	9.1
	15.52			0.250	0.230		0.98	0.36	7.03	C		
187	10.23	9.91	15.78			0.32	0.26	0.04	9.42	A	2.12	5.3
	11.73			0.139	0.121		0.31	0.65	5.53	C		
289	10.99	10.98	14.57			0.01	0.13	0.04	10.56	A	2.13	3.8
	11.73			0.094	0.076		0.26	0.15	8.76	C		
386	9.65	9.51	9.97			0.13	0.33	0.04	1.48	A	1.66	3.1
	9.22			0.067	0.051		0.22	0.10	6.50	C		
	9.29			0.079	0.063		0.23	0.10	4.33	C		

LVFS STATION C115 7 GREATER THAN 53 MICRON SIZE FRACTION
(NANOMOLEES/KG)

Z	CA	CI	SI	SR	SR*	XS CA	MG	K	NA	WT(I)	WT
20	4.21 3.72	3.85	5.51	0.243	0.236	0.36	0.04 0.32	0.08 0.00	62.87 39.09	0.81	9.1
75	4.78 5.62	4.49	4.13	0.149	0.141	0.29	0.11 0.15	-0.29 0.18	26.63 37.82	0.77	-4.7
124	3.11 2.29 2.72	2.24	3.15	0.029 0.020	0.026 0.016	0.87	0.29	-0.02 0.01 0.13	6.99 6.43 4.08	0.45	4.6
377	3.93 3.80 3.91	3.81 3.88	2.53	0.034	0.028	0.13 -0.08	0.26 0.16 0.05	0.10 -0.07 0.01	3.98 2.86 2.87	0.56	1.4

LVFS STATION C115 8 GREATER THAN 53 MICRON SIZE FRACTION
(NANOMOLEES/KG)

Z	CA	CI	SI	SR	SR*	XS	CA	MG	K	NA	WT (I)	WT
20	172.73	73.05	2721.10	3.377	3.252	99.68	85.71	13.31	439.21	A	198.45	798.7
	176.62			3.896	3.772			11.69	416.62	C		
	183.12							37.01	600.21	C		
42	56.24	34.18	1565.30	2.340	2.282	22.06	20.50	8.16	94.40	A	113.38	190.4
	62.48			1.986	1.928		20.43	6.95	22.83	C		
	54.82						20.71	6.60	22.83	C		
100	10.64	9.77	170.60	0.109	0.093	0.86	0.36	0.27	47.85	A	12.94	37.5
	13.14						3.18	0.36	76.71	C		
150	6.67	5.80	32.46	0.038	0.028	0.87	1.02	0.08	71.67	A	2.86	16.6
	7.27	6.21				1.06	3.37	0.61	67.55	A		
	17.39						0.95	0.00	56.84	C		
251	17.84	17.49	68.14	0.026	-0.004	0.35	1.17	0.43	46.70	A	6.52	30.6
	17.71						3.03	1.78	29.56	C		

APPENDIX 1 (cont.)

RATIOS FOR THE $>53 \mu\text{M}$ SIZE FRACTION AT LVFS STATIONS 4 - 8

- Z - meters
- CA/CI - calcium to carbonate ratio (mole units)
- SI/CI - opal to carbonate ratio (mole units)
- SR*/CI - non carbonate strontium to carbonate ratio
(mole units)
- SR*/SR - non-carbonate to total strontium ratio
- XS CA/MG - excess calcium to magnesium ratio (mole units)
- WT(I)/WT - inorganic to total dry weight ratio (mass units)

LVFS STATION C115 4 GREATER THAN 53 MICRON SIZE FRACTION
MOLE RATIOS

Z	CA/CI	SI/CI	SR*/CI	SR*/SR	XS CA/MG	WT(I)/WT
20						
20	1.214	0.816	0.0065	0.869	2.15	0.110
42	1.065	1.282	0.0220	0.928	0.47	0.110
100	1.164	2.907	0.0184	0.915	1.71	0.424
183	1.095 1.056	0.845	0.0022	0.570	1.27 0.83	0.290

LVFS STATION C115 5

20	1.130	1.728	0.0728	0.977	1.09	0.259
40	1.223 1.201	2.299 2.486	0.0998 0.0950	0.983	1.69 1.39	0.289 0.316
50	1.100	1.801	0.0166	0.907	0.88	0.282
88	1.095 1.088	0.772 0.662	0.0071 0.0059	0.791	1.74 1.87	0.407 0.450
124	1.056	0.948	0.0128	0.882	0.93	0.351
199	1.074	0.917	0.0075	0.816	0.96	0.302
294	1.126	1.279	0.0081	0.827	2.70	0.318
379	1.080 1.041	1.156 1.123	0.0069 0.0081	0.855 0.743	3.58 0.71	0.384 0.324

LVFS STATION C115 6 GREATER THAN 53 MICRON SIZE FRACTION
 MOLE RATIOS

Z	CA/CI	SI/CI	SR*/CI	SR*/SR	XS CA/MG	WT(I)/WT
26	1.370	4.229	0.2000	0.991	0.93	0.240
	1.202	3.642	0.1720		-8.30	0.248
52	1.299	8.516	0.0442	0.964	1.67	0.415
	1.291	8.486	0.0456		1.76	0.401
113	1.166	3.009	0.0197	0.921	2.19	0.403
187	1.032	1.593	0.0122	0.878	1.24	0.402
289	1.001	1.326	0.0069	0.802	0.07	0.565
386	1.014	1.048	0.0059	0.758	0.40	0.537
				0.794		

LVFS STATION C115 7

20	1.095	1.432	0.0615	0.973	9.00	0.089
75	1.065	0.919	0.0314	0.949	2.67	*****
124	1.387	1.403	0.0093	0.870	2.96	0.098
				0.809		
377	1.033	0.664	0.0073	0.809	0.48	0.414
	0.980	0.652	0.0071		-0.50	0.419

LVFS STATION C115 8

20	2.364	37.249	0.0481	0.963	1.16	0.248
				0.968		
42	1.645	45.788	0.0616	0.975	1.08	0.595
				0.971		
100	1.088	17.460	0.0095	0.848	2.37	0.345
150	1.150	5.601	0.0048	0.731	0.85	0.173
	1.171	5.226	0.0044		0.31	0.175
251	1.020	3.896	-0.0002	-0.145	0.30	0.213

APPENDIX 1 (cont.)

PARTICULATE MATTER DATA : <53 μ M SIZE FRACTION LVFS STNS

4 - 8

Z - meters

CA - calcium

CI - carbonate

SR - strontium

SR* - non-carbonate strontium

XS CA - non-carbonate calcium

MG - magnesium in excess of seasalt ratio relative to sodium

LVFS STATION C115 4		1-53 MICRON SIZE FRACTION NANOPOLES/KG				
Z	CA	CI	SR	SR*	XS CA	MG
20	536.3	466.5	1.913	1.120	69.8	67.8
20	457.3	372.9	4.188	3.554	84.4	64.2
42	113.0	105.3	1.035	0.856	7.8	4.0
100	51.0	44.5	0.458	0.382	6.5	6.5
183	253.7	228.5	0.751	0.362	25.2	15.9
183	255.4	0.0	0.661	0.272	26.9	15.5

LVFS STATION C115 5		1-53 MICRON SIZE FRACTION NANOPOLES/KG				
Z	CA	CI	SR	SR*	XS CA	MG
20	125.7	101.9	1.077	0.903	23.8	43.7
40	68.4	61.0	1.268	1.164	7.4	3.7
50	63.2	55.1	0.966	0.872	8.1	8.3
50	64.0	0.0	1.017	0.923	8.9	8.2
88	132.2	130.0	0.845	0.627	3.5	4.1
88		127.3				
124	139.4	129.9	0.860	0.639	9.4	5.5
199	84.2	79.3	0.583	0.449	4.9	3.1
294	59.1	56.5	0.333	0.237	2.6	0.4
379	79.7	77.5	0.353	0.221	2.2	1.7

LVFS STATION C115 6		1-53 MICRON SIZE FRACTION NANOPOLES/KG				
Z	CA	CI	SR	SR*	XS CA	MG
26	17.2	14.1	-0.000	-0.024	3.1	-8.8
26		14.2				
26	22.3	16.9	0.231	0.202	5.4	-1.0
52	27.3	26.0	0.186	0.141	1.3	-9.7
52	29.2	0.0	0.139	0.095	3.3	-9.4
113	38.5	35.1	0.352	0.293	3.4	1.2
187	67.4	63.4	0.422	0.314	4.0	1.5
289	67.3	62.8	0.346	0.240	4.6	1.6
386	65.8	63.5	0.318	0.210	2.3	1.8

LVFS STATION C115 7		1-53 MICRON SIZE FRACTION NANOMOL/KG				
Z	CA	CI	SR	SR*	XS CA	MG
20	49.5	41.1	0.277	0.207	8.3	6.8
20	48.7	0.0	0.416	0.346	7.6	6.2
75	85.1	75.5	0.496	0.368	9.6	3.7
124	66.4	64.0	0.455	0.347	2.5	-1.4
377	68.6	65.8	0.255	0.143	2.8	1.1
377		65.8				

LVFS STATION C115 8		1-53 MICRON SIZE FRACTION NANOMOL/KG				
Z	CA	CI	SR	SR*	XS CA	MG
20	389.9	290.9	1.482	0.988	99.0	20.0
20	400.0	0.0	1.853	1.358	109.1	6.7
42	103.5	71.1	1.052	0.931	32.4	16.6
100	63.4	55.0	0.311	0.218	8.4	16.6
150	151.9	147.2	0.692	0.442	4.7	14.3
251	215.5	192.4	0.642	0.315	23.0	33.1
251	217.8	0.0	0.692	0.365	25.4	35.3

APPENDIX 1 (cont.)ORGANIC CARBON AND NITROGEN IN 1 and 1-53 M SIZE FRACTIONS
LVFS STATIONS 4 - 8

- <1 μM - BOTTOM GLASS FIBER FILTER PORE SIZE 1.25 μM
- 1-53 μM - TOP GLASS FIBER FILTER PORE SIZE 1.25 μM AT
98 % EFFICIENCY
- Z - depth meters
- C(<1) - total carbon - blank nanomoles kg^{-1}
- N(<1) - total nitrogen - blank nanomoles kg^{-1}
- C(1-53) - total carbon - carbonate carbon - blank
- N(1-53) - total nitrogen - blank
- C/N - organic carbon to nitrogen ratios (mole units)
- ORGC/N - same thing but for the 1-53 μm fraction

LVFS STATION C115 4 ORGANIC C AND N NANCMOLES/KG

Z	<1 MICRON FRACTION			1-53 MICRON FRACTION		
	C	N	C/N	C	N	ORGC/N
20	5314.	799.7	6.65	17336.	2305.3	7.52
20	5221.	717.9	7.27	16313.	2253.5	7.24
20	2683.	425.7	6.30	15944.	2362.8	6.75
20	2721.	429.0	6.34	15371.	2325.2	6.61
20	2702.	501.1	5.39	15601.	2315.4	6.74
42	139.	25.1	5.54	868.	120.6	7.20
100	108.	19.2	5.64	690.	89.4	7.71
183	111.	21.8	5.08	1208.	145.2	8.32
183	89.	20.9	4.25	1203.	162.3	7.41

LVFS STATION C115 5 ORGANIC C AND N NANCMOLES/KG

Z	<1 MICRON FRACTION			1-53 MICRON FRACTION		
	C	N	C/N	C	N	ORGC/N
20	759.	108.7	6.99	2605.	364.1	7.15
20	555.	231.2	2.40	2511.	361.9	6.94
40	477.	75.7	6.30	1085.	145.5	7.45
50	176.	24.3	7.24	744.	108.3	6.87
88	61.	9.4	6.44	465.	64.0	7.26
88	54.	9.8	5.48	468.	64.3	7.27
124	103.	10.3	10.06	321.	42.8	7.50
124	41.	5.6	7.20	368.	41.8	8.81
124	47.	7.0	6.72	374.	49.1	7.62
199	43.	6.9	6.30	323.	41.2	7.84
199	48.	7.4	6.46	295.	37.8	7.82
294	43.	6.9	6.22	204.	27.8	7.34
294	49.	7.8	6.32	197.	28.9	6.83
294	47.	9.0	5.23	197.	26.3	7.50
379	68.	9.3	7.39	212.	29.0	7.30
379	43.	8.5	5.02	224.	32.7	6.86
379	50.	8.5	5.87	240.	32.0	7.50

LVFS STATION C115 6 ORGANIC C AND N NANCMOLES/KG

Z	<1 MICRON FRACTION			1-53 MICRON FRACTION		
	C	N	C/N	C	N	ORGC/N
26	207.	35.3	5.87	441.	57.4	7.68
26	214.	33.4	6.41	585.	83.2	7.04
26	289.	41.9	6.89	530.	61.9	8.56
26	130.	15.1	8.63	414.	52.4	7.90
26	123.	16.7	7.34	407.	50.8	8.01
52	152.	28.4	5.35	604.	104.2	5.79
113	63.	10.7	5.91	256.	36.7	6.97
187	26.	3.4	7.42	157.	21.8	7.20
239	18.	2.7	6.88	130.	17.4	7.47
289	19.	2.5	7.77	125.	17.1	7.35
386	13.	2.0	6.40	130.	18.7	6.99

LVFS STATION C115 7			ORGANIC C AND N		NANCMOLES/KG	
Z	<1 MICRON FRACTION			1-53 MICRON FRACTION		
	C	N	C/N	C	N	CRGC/N
20	162.	14.5	11.20	845.	93.1	9.08
20	182.	16.2	11.25	869.	92.5	9.39
75	181.	26.9	6.73	902.	96.2	9.37
124	95.	12.2	7.80	344.	42.9	8.01
377	24.	3.7	6.37	176.	15.4	11.39

LVFS STATION C115 8			ORGANIC C AND N		NANCMOLES/KG	
Z	<1 MICRON FRACTION			1-53 MICRON FRACTION		
	C	N	C/N	C	N	CRGC/N
20	13543.	2199.7	6.16	19307.	2095.4	9.21
20	10975.	1675.9	6.55	16793.	1845.1	9.10
42	732.	147.8	4.95	2568.	342.3	7.50
42	803.	141.3	5.68	2533.	297.7	8.51
100	503.	76.6	6.57	1323.	172.0	7.69
150	123.	20.6	5.98	1089.	148.2	7.35
251	112.	27.8	4.02	1368.	190.1	7.20
251	-123.	-3.1	39.65	1357.	169.1	8.03

APPENDIX 1 (cont.)

AVERAGE CONCENTRATIONS FOR <53 μM PARTICULATE FRACTIONS

ALL SYMBOLS AS DEFINED BEFORE EXCEPT:

- CHEM WT - sum of dry weights of organic, carbonate, and celestite phases as well as of the other major ions. ($\mu\text{g kg}^{-1}$)
- DRY WT - gravimetrically determined dry weight concentration ($\mu\text{g/kg}^{-1}$)
- TONS - weight of seawater filtered in metric tons calculated from the in situ density of seawater at the various levels at the LVFS stations.

LVFS STATION C115 4 < 53 MICRON SIZE FRACTIONS AVERAGES NANOMOLES/KG

Z	CA	CI	SR	SR*	XS	CA	MG	CORG	N	C(<1)	N(<1)	CHEM WT	DRY WT	TCNS
20	536.3	466.5	1.91	1.12	69.8	67.8	16824.	2279.4	5268.	758.8	757.17	657.0	-0.36	
20	457.3	372.9	4.19	3.55	84.4	64.2	15639.	2334.5	2702.	451.9	632.60	630.2	0.44	
42	113.0	105.3	1.04	0.86	7.8	4.0	868.	120.6	139.	25.1	43.41	36.1	4.63	
100	51.0	44.5	0.46	0.38	6.5	6.5	690.	89.4	108.	19.2	30.42	34.3	6.73	
183	254.5	228.5	0.71	0.32	26.1	15.7	1206.	153.8	100.	21.3	66.02	90.3	3.80	

LVFS STATION C115 5 < 53 MICRON SIZE FRACTIONS AVERAGES NANOMOLES/KG

Z	CA	CI	SR	SR*	XS	CA	MG	CORG	N	C(<1)	N(<1)	CHEM WT	DRY WT	TCNS
20	125.7	101.9	1.08	0.90	23.8	43.7	2558.	363.0	657.	170.0	116.39	132.5	1.59	
40	68.4	61.0	1.27	1.16	7.4	3.7	1085.	145.5	477.	75.7	56.69	77.8	2.34	
50	63.6	55.1	0.99	0.90	8.5	8.3	744.	108.3	176.	24.3	35.71	44.1	4.49	
88	132.2	128.7	0.85	0.63	3.5	4.1	466.	64.2	57.	9.6	30.00	33.7	7.29	
124	139.4	129.9	0.86	0.64	9.4	5.5	354.	44.5	64.	7.6	26.92	32.7	8.63	
199	84.2	79.3	0.58	0.45	4.9	3.1	309.	39.5	45.	7.1	19.59	24.3	11.74	
294	59.1	56.5	0.33	0.24	2.6	0.4	200.	27.7	46.	7.9	13.71	14.8	15.42	
379	79.7	77.5	0.35	0.22	2.2	1.7	225.	31.2	54.	8.7	16.88	20.4	13.25	

LVFS STATION C115 6 < 53 MICRON SIZE FRACTIONS AVERAGES NANOMOLES/KG

Z	CA	CI	SR	SR*	XS	CA	MG	CORG	N	C(<1)	N(<1)	CHEM WT	DRY WT	TCNS
26	17.2	14.1	-0.00	-0.02	3.1	-8.8	518.	67.5	237.	36.9	25.45	22.9	3.46	
26	22.3	16.9	0.23	0.20	5.4	-1.0	410.	51.6	126.	15.9	18.98	22.9	3.46	
52	28.3	26.0	0.16	0.12	2.3	-9.5	604.	104.2	152.	28.4	27.03	14.5	2.46	
113	38.5	35.1	0.35	0.29	3.4	1.2	256.	36.7	63.	10.7	13.99	17.1	9.72	
187	67.4	63.4	0.42	0.31	4.0	1.5	157.	21.8	26.	3.4	12.44	13.9	15.97	
289	67.3	62.8	0.35	0.24	4.6	1.6	128.	17.2	19.	2.6	11.23	13.5	20.76	
386	65.8	63.5	0.32	0.21	2.3	1.8	130.	18.7	13.	2.0	11.12	12.6	22.62	

LVFS STATION C115 7 < 53 MICRON SIZE FRACTIONS AVERAGES NANOMOLES/KG

Z	CA	CI	SR	SR*	XS	CA	MG	CORG	N	C(<1)	N(<1)	CHEM WT	DRY WT	TONS
20	49.1	41.1	0.35	0.28	8.0	6.5	857.	92.8	172.	15.3	37.06	51.7	2.47	
75	85.1	75.5	0.50	0.37	9.6	3.7	902.	96.2	181.	26.9	42.34	35.6	2.76	
124	66.4	64.0	0.46	0.35	2.5	-1.4	344.	42.9	95.	12.2	20.47	18.6	8.52	
377	68.6	65.8	0.25	0.14	2.8	1.1	176.	15.4	24.	3.7	13.02	15.3	22.85	

LVFS STATION C115 8 < 53 MICRON SIZE FRACTIONS AVERAGES NANOMOLES/KG

Z	CA	CI	SR	SR*	XS	CA	MG	CORG	N	C(<1)	N(<1)	CHEM WT	DRY WT	TONS
20	395.0	290.9	1.67	1.17	104.1	13.4 ⁺	18050.	1970.3	12259.	1937.8	998.49	1131.5	0.31	
42	103.5	71.1	1.05	0.93	32.4	16.6	2551.	320.0	768.	144.6	115.12	170.7	1.41	
100	63.4	55.0	0.31	0.22	8.4	16.6	1323.	172.0	503.	76.6	64.59	112.9	2.20	
150	151.9	147.2	0.69	0.44	4.7	14.3	1089.	148.2	123.	20.6	54.12	105.0	2.64	
251	216.6	192.4	0.67	0.34	24.2	34.2	1363.	179.6	-5.	12.4	64.59	161.2	2.31	

+ 1-53 μm Mg = 87.0 nmol kg⁻¹

<1 μm Mg = 73.6 nmol kg⁻¹

APPENDIX 1 (cont.)RATIOS FROM THE ANALYSES OF THE <53 μM SIZE FRACTIONS:AVERAGES

- CA/CI - calcium to carbonate mole ratio
- SR*/CI - non-carbonate strontium to carbonate mole ratio
- SR*/SR - non-carbonate to total strontium ratio
- XSCA/MG - excess calcium to magnesium mole ratio
- EQUIV/N - total equivalents of excess Ca and Mg charge divided by particulate nitrogen (1-53 μm fraction)
- C/N (>1) - organic carbon to nitrogen ratio (1-53 μm fraction)
- C/N (<1) - carbon to nitrogen ratio of the material retained on the bottom glass fiber filter.
- WTPER - CHEM WT/DRY WT sum of measured biogenic components divided by total dry weight times 100.
- SI(NMOL) = (DRY WT - CHEM WT)/0.07 molecular wt. of opal is assumed to be 70 gm mol⁻¹
- SI/CI = SI(NMOL)/CI

LVFS STATION C115 4			<53 MICRON SIZE FRACTIONS					RATIOS		
CA/CI	SR*/CI	SR*/SR	XSCA/MG	EQUIV/N	C/N(>1)	C/N(<1)	WTPER	SI(NMOL)	SI/CI	
20	1.150	0.0024	0.585	1.03	0.121	7.38	6.94	115.2	*****	-3.07
20	1.226	0.0095	0.849	1.32	0.127	6.70	5.98	100.4	-34.3	-0.09
42	1.074	0.0081	0.827	1.94	0.195	7.20	5.54	120.3	-104.5	-0.99
100	1.146	0.0086	0.835	0.99	0.291	7.71	5.64	88.7	55.4	1.24
183	1.114	0.0014	0.483	1.66	0.543	7.84	4.67	73.1	346.9	1.52

LVFS STATION C115 5			<53 MICRON SIZE FRACTIONS					RATIOS		
CA/CI	SR*/CI	SR*/SR	XSCA/MG	EQUIV/N	C/N(>1)	C/N(<1)	WTPER	SI(NMOL)	SI/CI	
20	1.234	0.0089	0.839	0.55	0.372	7.05	3.87	87.8	230.2	2.26
40	1.121	0.0191	0.918	2.00	0.152	7.45	6.30	72.9	301.6	4.95
50	1.154	0.0163	0.903	1.02	0.310	6.87	7.24	81.0	119.8	2.17
88	1.028	0.0049	0.741	0.86	0.239	7.26	5.95	89.0	52.9	0.41
124	1.073	0.0049	0.743	1.72	0.670	7.95	8.34	82.3	82.5	0.64
199	1.062	0.0057	0.769	1.58	0.407	7.83	6.38	80.6	67.3	0.85
294	1.046	0.0042	0.712	6.08	0.218	7.21	5.88	92.6	15.6	0.28
379	1.028	0.0029	0.627	1.25	0.251	7.22	6.13	82.7	50.4	0.65

LVFS STATION C115 6			<53 MICRON SIZE FRACTIONS					RATIOS		
CA/CI	SR*/CI	SR*/SR	XSCA/MG	EQUIV/N	C/N(>1)	C/N(<1)	WTPER	SI(NMOL)	SI/CI	
26	1.219	*****	*****	-0.35	-0.169	7.68	6.42	111.1	-36.4	-2.58
26	1.319	0.0119	0.875	-5.68	0.173	7.95	7.95	82.9	56.0	3.31
52	1.088	0.0046	0.762	-0.24	-0.139	5.79	5.35	186.4	-179.1	-6.89
113	1.096	0.0083	0.830	2.84	0.248	6.97	5.91	81.8	44.4	1.26
187	1.063	0.0050	0.744	2.71	0.500	7.20	7.42	89.5	20.8	0.33
289	1.073	0.0038	0.692	2.91	0.711	7.41	7.31	83.2	32.5	0.52
386	1.036	0.0033	0.660	1.26	0.437	6.99	6.40	88.2	21.2	0.33

LVFS STATION C115 7			<53 MICRON SIZE FRACTIONS				RATIOS			
CA/CI	SR*/CI	SR*/SR	XSCA/MG	EQUIV/N	C/N(>1)	C/N(<1)	WTPER	SI(NMOL)	SI/CI	
20	1.194	0.0067	0.748	1.23	0.312	9.24	11.22	71.7	209.2	5.09
75	1.127	0.0049	0.741	2.58	0.277	9.37	6.73	118.9	-96.3	-1.28
124	1.038	0.0054	0.761	-1.75	0.049	8.01	7.80	110.0	-26.7	-0.42
377	1.042	0.0022	0.561	2.53	0.502	11.39	6.37	85.1	32.6	0.50

LVFS STATION C115 8			<53 MICRON SIZE FRACTIONS				RATIOS			
CA/CI	SR*/CI	SR*/SR	XSCA/MG	EQUIV/N	C/N(>1)	C/N(<1)	WTPER	SI(NMOL)	SI/CI	
20	1.358	0.0040	0.666	7.79	0.119	9.16	6.33	88.2	1900.2	6.53
42	1.456	0.0131	0.885	1.95	0.307	7.97	5.31	67.4	793.9	11.16
100	1.153	0.0040	0.700	0.51	0.291	7.69	6.57	57.2	690.2	12.55
150	1.032	0.0030	0.638	0.33	0.257	7.35	5.98	51.5	726.9	4.94
251	1.126	0.0018	0.491	0.71	0.651	7.59	-0.44	40.1	1380.2	7.17

APPENDIX 1 (cont.)

BOTTOM FILTER ANALYSES AND BLANKS FOR LVFS STATIONS 4 - 8

- Z - meters
- TONS - metric tons of seawater filtered
- SAMP - sample identification code: chronological order
- NA(T) - blank corrected sodium content (mgs) on top filter
- NA(B) - " " " " " " bottom "
- NABLK - sodium blank for filters from the same batch
will be assumed constant for that batch. (values based on Rockport experiment
- MG(B) - magnesium leached from the filters in excess of seasalt, values are typical of Rockport Blanks and so are assumed to be filter blank. (mgs)
- SR(B) - strontium blank for the Chain data is reported as zero mainly because the values were low and the filter analyses of the top samples had already been corrected for the bottom filter blanks. (mgs)
- CBLK - carbon blank assumed (on the basis of the Rockport experiment) for the samples from a given batch of glass fiber filters. (mgs)
- NBLK - similar story (mgs)
- CA(B) - total calcium corrected for seasalt on bottom filter. (micromoles)
- CI(B) - total carbonate on bottom filter (micromoles) the (B) analysis is subtracted from that of the top glass fiber filter (T).
- 0.0 - zeros imply no data.

LVFS STATION C115 4			<53 MICRON SIZE FRACTION						MICROMOLES		
			MGS								
Z	TONS	SAMP	NA(T)	NA(B)	NABLK	MG(B)	SR(B)	CBLK	NBLK	CA(B)	CI(B)
20	0.36	32	8.9	10.4	6.1	0.59	0.00	3.4	0.05	67.9	1.8
20	0.36	32	0.0	0.0	0.0	0.00	0.00	3.4	0.05	0.0	0.0
20	0.44	35	4.8	1.7	6.1	0.87	0.00	3.4	0.05	75.2	2.6
20	0.44	35	0.0	0.0	0.0	0.00	0.00	3.4	0.05	0.0	0.0
20	0.44	35	0.0	0.0	0.0	0.00	0.00	3.4	0.05	0.0	0.0
42	4.63	33	4.7	11.6	6.1	0.75	0.00	3.4	0.05	75.4	9.3
100	6.73	36	3.2	8.0	6.1	0.60	0.00	3.4	0.05	69.4	6.4
183	3.80	34	8.7	18.3	6.1	0.84	0.00	3.4	0.05	67.9	26.5
183	3.80	34	10.2	19.8	6.1	0.84	0.00	3.4	0.05	69.4	0.0

LVFS STATION C115 5			<53 MICRON SIZE FRACTION						MICROMOLES		
			MGS								
Z	TONS	SAMP	NA(T)	NA(B)	NABLK	MG(B)	SR(B)	CBLK	NBLK	CA(B)	CI(B)
20	1.59	37	43.8	27.3	6.1	0.41	0.00	3.5	0.05	63.1	11.4
20	1.59	37	0.0	0.0	0.0	0.00	0.00	3.5	0.05	0.0	0.0
40	2.34	39	16.2	23.6	5.7	0.76	0.00	3.1	0.13	63.4	13.2
50	4.49	42	28.3	18.5	5.7	0.54	0.00	3.1	0.13	62.8	10.7
50	4.49	42	27.2	15.8	5.7	0.47	0.00	0.0	0.00	62.4	0.0
88	7.29	44	7.0	3.3	5.7	0.61	0.00	3.1	0.13	69.5	7.6
88	7.29	44	0.0	0.0	0.0	0.00	0.00	3.1	0.13	0.0	6.1
124	8.63	41	5.9	8.6	5.7	0.27	0.00	3.1	0.13	72.1	17.6
124	8.63	41	0.0	0.0	0.0	0.00	0.00	3.1	0.13	0.0	0.0
124	8.63	41	0.0	0.0	0.0	0.00	0.00	3.1	0.13	0.0	0.0
199	11.74	43	8.8	11.6	5.7	0.60	0.00	3.1	0.13	69.5	17.8
199	11.74	43	0.0	0.0	0.0	0.00	0.00	3.1	0.13	0.0	0.0
294	15.42	40	16.3	23.3	5.7	0.96	0.00	3.1	0.13	78.4	23.5
294	15.42	40	0.0	0.0	0.0	0.00	0.00	3.1	0.13	0.0	0.0
294	15.42	40	0.0	0.0	0.0	0.00	0.00	3.1	0.13	0.0	0.0
379	13.25	38	8.0	23.2	5.7	0.49	0.00	3.1	0.13	61.5	26.1
379	13.25	38	0.0	0.0	0.0	0.00	0.00	3.1	0.13	0.0	0.0
379	13.25	38	0.0	0.0	0.0	0.00	0.00	3.1	0.13	0.0	0.0

LVFS STATION C115 6			<53 MICRON SIZE FRACTION						MGS		MICROMOLES	
Z	TONS	SAMP	NA(T)	NA(B)	NABLK	MG(B)	SR(B)	CBLK	NBLK	CA(B)	CI(B)	
26	3.46	45	25.6	55.6	5.7	0.67	0.00	3.1	0.13	70.8	34.5	
26	3.46	45	0.0	0.0	0.0	0.00	0.00	3.1	0.13	0.0	34.2	
26	3.46	45	0.0	0.0	0.0	0.00	0.00	3.1	0.13	0.0	0.0	
26	3.46	450	1.4	-0.1	5.7	0.94	0.00	3.1	0.13	62.3	4.3	
26	3.46	450	0.0	0.0	0.0	0.00	0.00	3.1	0.13	0.0	0.0	
52	2.46	47	-0.1	0.7	5.3	1.64	0.00	3.1	0.13	71.0	3.3	
52	2.46	47	-0.4	0.5	5.3	1.64	0.00	0.0	0.00	70.3	0.0	
113	9.72	50	5.2	11.0	5.3	0.81	0.00	3.1	0.14	70.5	11.2	
187	15.97	49	5.2	5.6	5.3	0.74	0.00	3.1	0.14	74.2	12.5	
289	20.76	48	17.6	5.9	5.3	0.66	0.00	3.1	0.14	82.6	21.9	
289	20.76	48	0.0	0.0	0.0	0.00	0.00	3.1	0.14	0.0	0.0	
386	22.62	46	25.9	9.5	5.3	0.17	0.00	3.1	0.14	73.7	23.6	

LVFS STATION C115 7			<53 MICRON SIZE FRACTION						MGS		MICROMOLES	
Z	TONS	SAMP	NA(T)	NA(B)	NABLK	MG(B)	SR(B)	CBLK	NBLK	CA(B)	CI(B)	
20	2.47	51	11.5	3.7	5.3	0.74	0.00	3.1	0.14	66.8	0.8	
20	2.47	51	11.4	3.5	5.3	0.77	0.00	3.1	0.14	67.5	0.0	
75	2.76	53	5.2	2.8	6.6	0.93	0.00	3.4	0.10	67.9	2.2	
124	8.52	54	3.3	2.9	6.6	1.73	0.00	3.4	0.10	80.1	5.4	
377	22.85	52	7.8	17.9	5.3	0.77	0.00	3.1	0.14	87.6	30.6	
377	22.85	52	0.0	0.0	0.0	0.00	0.00	0.0	0.00	0.0	33.9	

LVFS STATION C115 8			<53 MICRON SIZE FRACTION						MGS		MICROMOLES	
Z	TONS	SAMP	NA(T)	NA(B)	NABLK	MG(B)	SR(B)	CBLK	NBLK	CA(B)	CI(B)	
20	0.31	55	12.4	32.6	6.6	1.12	0.00	3.4	0.10	77.5	1.1	
20	0.31	55	11.6	32.8	6.6	1.23	0.00	3.4	0.10	75.8	0.0	
42	1.41	56	6.4	12.2	5.3	0.47	0.00	3.4	0.10	48.4	1.8	
42	1.41	56	0.0	0.0	0.0	0.00	0.00	3.4	0.10	0.0	0.0	
100	2.20	57	3.9	7.6	5.3	0.35	0.00	3.4	0.10	57.1	3.2	
150	2.64	59	20.0	4.7	5.3	0.60	0.00	3.4	0.10	68.9	5.4	
251	2.31	58	7.0	2.5	5.3	0.64	0.00	3.4	0.10	65.9	7.8	
251	2.31	58	6.0	2.5	5.3	0.58	0.00	3.4	0.10	65.4	0.0	

APPENDIX 2

HYDROGRAPHIC DATA OBTAINED DURING LEG 2 OF THE SOUTHLANT
EXPEDITION : R.V. CHAIN CRUISE 115
DAKAR - CAPETOWN (Dec.14 1973-Jan.10 1974)

- DEPTH - meters corrected
- TEMP P. - in situ temperature calculated using protected reversing thermometers.
- TEMP U. - in situ temperature calculated from unprotected thermometer readings corrected for pressure anomaly due to depth.
- SALINITY - measured at the end of the cruise at W.H.O.I.
- SI - dissolved silicate measured using the method of Mullin and Riley (1955) unfiltered samples.
- O2 - oxygen calculated using the winkler method as modified by Carpenter (1965).
- PO4 - phosphate measured using the method of Murphy and Riley (1962)

stations marked NIS were taken with 30 liter niskin bottles with nansen bottles for depth control
other stations also are assigned a W.H.O.I. hydrostation number.

CHAIN 115 LEG 2 HSI320 AT LVFS STN 1
0700Z 12 04.5N 17 41.4W 12/15/73

DEPTH	BOTTOM DEPTH = M			
	TEMPERATURE P.	SALINITY (O/CO)	SI (MICROMOLES/KG)	PC4
0	26.94	35.096	1.2	175. 0.15
10	26.96	35.099	1.2	173. 0.02
19	26.96	35.093		173. 0.01
29	24.18	35.637	1.7	179. 0.12
48	18.45	35.800	4.6	123. 0.72
72	15.68	35.543		60. 1.40
96		35.520	7.6	61. 1.57
120	14.46	35.469	8.1	67. 1.50
144	14.04	35.399	8.3	68. 1.47
168	13.57	35.363	9.1	69. 1.54
192	12.75	35.321	8.8	68. 1.47
221		35.268	9.4	122. 1.44
250	12.28	35.219	9.7	76. 1.57
278	12.23	35.305	9.6	70. 1.57
307	11.93	35.301	10.2	65. 1.73
336	11.60	35.247	11.5	61. 1.70
384	11.04	35.213	12.6	45. 1.87
432	10.47	35.192	13.6	43. 1.87
480	9.69	35.123	16.0	45. 2.11
528	8.69	34.985	19.0	49. 2.11

CHAIN 115 LEG 2 NIS 1 AT LVFS STN 1
0800Z 12 04.5N 17 41.4W 12/16/73

DEPTH	BOTTOM DEPTH = M			
	TEMPERATURE P.	SALINITY (O/CO)	SI (MICROMOLES/KG)	PC4
49		35.747		
107		35.513		
214		35.274		
282		35.224		
369		35.227		
378	10.90	35.204		

CHAIN 115 LEG 2 H51321 AT LVFS STN 2
080CZ 02 40.8N 08 54.3W 12/19/73

CHAIN 115 LEG 2 N15 2 AT LVFS STN 2
040CZ 02 40.8N 08 54.3W 12/20/73

DEPTH	BOTTOM DEPTH = M			BOTTOM DEPTH = P			
	TEMPERATURE P.	SALINITY (G/CO)	SI O2 (MICROMOLES/KG)	TEMPERATURE P.	SALINITY (G/CO)	SI O2 (MICROMOLES/KG)	
1	28.05	34.685	1.0	198.	0.07	24	34.789
7		34.684	1.0	203.	0.00	49	35.683
17		34.907		203.	0.01	110	35.576
27		35.369	0.9	202.	0.04	185	35.391
46	17.97	35.785	3.7	149.	0.83	286	35.176
71		35.675		135.	1.05	377	34.879
96	15.66	35.600	5.3	131.	1.15	387	34.851
120	14.94	35.522	6.4	124.	1.18		
145	14.35	35.464	6.8	118.	1.23		
169	14.02	35.412	6.7	136.	1.17		
194	13.73	35.373	7.2	124.	1.22		
224		35.338	7.7	115.	1.33		
253	12.92	35.275	8.7	104.	1.46		
283	11.69	35.129	10.9	104.	1.56		
312	11.12	35.052	11.0	106.	1.70		
341	10.32	34.961	13.3	108.	1.70		
391	8.77	34.803	15.5	98.	1.93		
441	7.77	34.710	17.3	112.	2.00		
490	7.06	34.656	18.9	122.	2.16		
539	6.32	34.575	22.1	125.	2.14		

CHAIN 115 LEG 2 NIS 3 AT LVFS STN 3
2244Z 07 57.35 00 23.6E 12/23/73

CHAIN 115 LEG 2 HS1322 AT LVFS STN 3
0730Z 07 57.35 00 23.6E 12/23/73

DEPTH	BOTTOM DEPTH = M		BOTTOM DEPTH = M		SI O2 PC4 (MICROMOL/KG)	SI O2 PC4 (MICROMOL/KG)	DEPTH	TEMPERATURE P.	SALINITY (O/CO)	TEMPERATURE P.	SALINITY (O/CO)	SI O2 PC4 (MICROMOL/KG)
	TEMPERATURE U.	SALINITY (O/CO)	TEMPERATURE U.	SALINITY (O/CO)								
1	24.65	36.205	1.1	218.	0.29		24					
9		36.182	1.1	219.	0.19		49					
18		36.190	1.2	219.	0.18		97					
27		36.186	1.0	222.	0.22		194					
45	19.29	36.008	3.0	169.	0.70		282					
67		35.675	5.1	99.	1.21		379					
89		35.516	6.1	100.	1.42		388					
111		35.388	7.0	99.	1.44							
134	13.06	35.314	7.7	98.	1.49							
152		35.263	8.0	101.	1.58							
171		35.194	8.6	113.	1.55							
193		35.142	9.0	99.	1.64							
215	11.13	35.092	10.1	93.	1.72							
239		35.053	10.7	83.	1.78							
263		35.003	11.2	85.	1.89							
287		34.977	11.6	85.	1.84							
327	9.71	34.921	12.9	72.	2.02							
366		34.869	14.1	67.	2.16							
405		34.819	15.7	48.	2.37							
444	7.98	34.782	17.4	50.	2.39							

CHAIN 115 LEG 2 HS1323 AT LVFS STN 4
1405Z 21 30.45 13 05.7E 12/28/73

BOTTOM DEPTH = 190 M

DEPTH	TEMPERATURE P.	SALINITY (O/CO) U.	SI (MICROMOLES/KG)	O2 (MICROMOLES/KG)	PC4
0	17.28	35.083	2.3	256.	0.71
5		35.088	2.3	301.	0.65
10		35.084	2.3	263.	0.66
20		35.085	2.4	254.	0.65
29	16.40	35.135	2.8	226.	0.91
38	15.15	35.214	3.4	195.	1.34
48	14.75	35.219	3.9	185.	1.40
71		35.235	5.6	153.	1.40
95	13.04	35.210	7.3	121.	1.40
119	12.74	35.211	9.1	84.	1.72
143	12.59	35.165	21.4	28.	2.23
152	12.35	35.144	22.7	21.	2.34
162	12.21	35.152	20.2	27.	2.20
171	12.16	35.130	18.0	27.	2.17
181	11.91	35.175	17.1	23.	2.21

CHAIN 115 LEG 2 NIS6 AT LVFS STN 4
2140Z 21 25.9S 13 04.4E 12/28/73

BOTTOM DEPTH = 177 M

DEPTH	TEMPERATURE P.	SALINITY (O/CO) U.	SI (MICROMOLES/KG)	O2 (MICROMOLES/KG)	PC4
19		35.093		3.5	
48		35.247		4.9	
97		35.197		15.5	
165		35.197		23.9	
170	12.13	35.121		26.2	

CHAIN 115 LEG 2 HS1324 SECTION STN A
0410Z 21 37.8S 12 59.5E 12/29/73

BOTTOM DEPTH = 230 M

DEPTH	TEMPERATURE P.	SALINITY (0/CO)	SI (MICROMOLE/KG)	O2	PC4 (MICROMOLE/KG)	
0	17.27	35.099	2.7	256.	0.53	
10		35.108	2.7	257.	0.57	
20		35.115	4.9	256.	0.59	
29		35.158	7.5	225.	0.85	
39	15.97	16.03	35.223	4.8	202.	1.27
49		14.67	35.294	3.9	177.	1.59
59		14.34	35.256	8.6	166.	2.09
78		13.31	35.179	6.5	139.	2.35
98	12.75	12.75	35.136	12.7	138.	2.11
123		12.30	35.097	9.5	128.	1.43
147		12.02	35.127	10.3	79.	1.71
172	11.65	11.67	35.078	11.4	57.	1.93
196		11.32	35.036	15.3	47.	1.98
216		10.94	35.004	14.1	35.	2.11
225	10.88	10.89	34.991	15.2	30.	2.25

CHAIN 115 LEG 2 HS1325 SECTION STN B
0615Z 21 47.8S 12 52.9E 12/29/73

BOTTOM DEPTH = 300 M

DEPTH	TEMPERATURE P.	SALINITY (0/CO)	SI (MICROMOLE/KG)	O2	PC4 (MICROMOLE/KG)	
0	17.41	35.097	2.1	250.	0.59	
10		35.088	2.6	250.	0.55	
19		35.131	3.6	228.	0.84	
29		35.199	3.5	193.	1.31	
53	13.95	13.97	35.215	5.3	159.	1.42
78		13.30	35.193	7.2	125.	1.48
107	12.56	12.56	35.138	10.9	70.	1.85
136		12.37	35.132	11.3	64.	1.98
165	12.00	12.02	35.109	12.0	53.	1.97
194		11.48	35.040	12.3	54.	2.08
224		11.29	35.031	14.4	33.	2.22
253	10.75	10.80	35.003	16.9	29.	2.37
272		10.42	34.955	19.7	21.	2.53
282		10.29	34.941	22.6	20.	2.57
292	10.24	10.23	34.927	22.7	17.	2.56

CHAIN 115 LEG 2 HSI326 SECTION STN C
0811Z 21 55.4S 12 46.7E 12/29/73

BOTTOM DEPTH = 335 M

DEPTH	TEMPERATURE P.	SALINITY (0/00)	SI (MICROMGLES/KG)	O2	PO4
3	17.96	35.120	2.2	247.	0.61
13		35.123	1.7	245.	0.59
23		35.175	1.9	215.	1.00
33		35.184	2.2	212.	1.06
58	14.68	35.209	3.4	192.	1.00
83	14.17	35.208	4.5	182.	1.27
113	13.27	35.184	6.6	138.	1.52
143	12.85	35.170	9.0	99.	1.72
173	11.94	35.103	11.7	56.	2.01
208	11.15	35.027	22.1	37.	2.22

CHAIN 115 LEG 2 HSI327 SECTION STN D
1032Z 22 03.7S 12 41.8E 12/29/73

BOTTOM DEPTH = 440 M

DEPTH	TEMPERATURE P.	SALINITY (0/00)	SI (MICROMGLES/KG)	O2	PO4
0	18.48	35.131	1.5	247.	0.47
10		35.129	1.6	251.	0.50
29		35.181	1.5	219.	1.13
48		35.209	3.6	202.	1.21
72	13.74	35.196	4.6	185.	0.97
96	13.17	35.182	9.1	104.	2.35
120	12.50	35.103	7.7	134.	1.45
143	12.08	35.075	8.9	114.	1.68
191	11.21	35.007	12.2	64.	2.15
239	10.70	34.973	18.0	26.	2.45
287	9.89	34.877	17.7	35.	2.39
335	8.61	34.740	17.5	61.	2.35
382	7.59	34.668	21.3	63.	2.52
406	7.50	34.631	21.7	64.	2.58
430	6.93	34.607	22.8	72.	2.50

CHAIN 115 LEG 2 HSI328 SECTION SYN E
 1440Z 22 15.25 12 31.9E 12/29/73

DEPTH	BOTTOM DEPTH =		TEMPERATURE P.	SALINITY (O/CO)	SI (MICROMLES/KG)	O2 PC4
	U.	F				
0				35.143		
10	18.87			35.144	1.3	247. 0.51
30				35.155	1.1	249. 0.48
50				35.201	0.9	249. 0.46
76	13.79	13.82		35.186	3.1	207. 1.32
98		13.49		35.168	4.5	187. 1.19
196		11.89		35.008	6.1	160. 1.44
294		9.50		34.794	9.7	184. 1.70
392	7.61	7.58		34.618	13.0	108. 1.91
490		6.30		34.524	19.6	109. 2.35
508	5.32	5.33		34.461	23.2	108. 2.54
672	4.70	4.75		34.436	26.0	130. 2.41
765	4.25	4.28		34.486	34.1	158. 2.35
860		4.11		34.481	36.3	159. 2.39
956				34.488	38.6	159. 2.41

CHAIN 115 LEG 2 HS1329 AT LVFS STN 5
065CZ 22 36.65 12 05.9E 12/30/73

BOTTOM DEPTH = 2430 M

DEPTH	TEMPERATURE P.	SALINITY U.	SI (MICROMOLES/KG)	O2 (MICROMOLES/KG)	PC4
0	19.03	35.173	0.5	243.	0.43
10		35.176	0.5	245.	0.48
24		35.176	0.5	244.	0.58
38		35.193	0.3	239.	0.56
48	15.48	35.230	1.1	225.	0.79
72	14.17	35.230	3.5	198.	0.93
96	13.67	35.175	4.6	184.	1.05
124	13.12	35.162	7.4	136.	1.54
153	12.41	35.102	6.8	157.	1.27
191	11.55	35.008	6.4	192.	1.22
239	10.47	34.878	8.1	186.	1.33
287	9.85	34.840	12.9	107.	1.98
335	8.80	34.750	15.0	103.	2.10
382	8.05	34.657	17.2	99.	2.30
430	7.19	34.588	18.9	113.	2.30

CHAIN 115 LEG 2 NIS 5 AT LVFS STNS
1440Z 22 36.65 12 05.9E 12/30/73

BOTTOM DEPTH = M

DEPTH	TEMPERATURE P.	SALINITY U.	SI (MICROMOLES/KG)	O2 (MICROMOLES/KG)	PC4
57				3.3	
86				5.0	
119				4.7	
209				8.9	
285				13.1	
380				17.4	
390	7.56	7.56		0.0	

CHAIN 115 LEG 2 NIS 5 AT LVFS STNS
0016Z 22 36.65 12 05.9E 12/31/73

BOTTOM DEPTH = M

DEPTH	TEMPERATURE P.	SALINITY U.	SI (MICROMOLES/KG)	O2 (MICROMOLES/KG)	PC4
20				0.6	
40				1.0	

CHAIN 115 LEG 2 HS1331 AT LVFS STN 6
 2315Z 25 11.95 09 59.3E 1/02/74

BOTTOM DEPTH = M

DEPTH	TEMPERATURE P.	SALINITY U.	SI (MICROMCLES/KG)	O2 (MICROMCLES/KG)	PC4
0	19.75	35.375	0.5	0.22	
10		35.383		0.22	
29		35.379	0.4	0.22	
48		35.419	0.6	0.21	
67	16.59	35.557	1.5	0.22	
86	16.01	35.506	2.0	0.27	
105	15.41	35.659		0.44	
134	14.71	35.339	2.9	0.52	
163	13.64	35.194	3.4	0.71	
191	12.96	35.135	4.0	0.80	
235	12.06	35.054	5.1	1.03	
287		34.928	6.7	1.18	
335	9.98	34.818	8.3	1.39	
382	9.09	34.712		1.46	
430	7.95	34.594	8.4	1.63	

CHAIN 115 LEG 2 NIS 7 AT LVFS STN 6
 0520Z 25 11.95 09 59.3E 1/03/74

BOTTOM DEPTH = M

DEPTH	TEMPERATURE P.	SALINITY U.	SI (MICROMCLES/KG)	O2 (MICROMCLES/KG)	PC4
24			0.5	235.	
58			0.6	247.	
121			2.6	236.	
193			3.9	211.	
289			6.2	202.	
366			8.4	202.	
376	9.13	9.13	9.0	204.	

CHAIN 115 LEG 2 HSI334 AT LVFS STN 7
1410Z 25 25.5S 07 58.6E 1/05/74

BOTTOM DEPTH =		M		
DEPTH	TEMPERATURE P.	SALINITY (O/CO)	SI O2 (MICROMCLES/KG)	PC4
0	20.62	35.782	1.4	232. 0.18
10		35.797	1.4	232. 0.17
29		35.770	1.4	234. 0.17
49		35.710	1.4	203. 0.18
68	17.67	35.627	1.5	253. 0.19
87	16.72	35.569	1.6	254. 0.18
107	16.45	35.569	1.8	242. 0.25
136	16.30	35.546	2.1	236. 0.33
165	15.95	35.488	2.3	234. 0.38
194	15.02	35.324	2.7	226. 0.54
243	13.66	35.199	3.6	210. 0.75
291	12.35	35.087	4.3	206. 0.93
341	11.37	34.976	6.5	198. 1.13
388	10.28	34.850	8.4	193. 1.29
437	9.24	34.745	12.4	163. 1.62

CHAIN 115 LEG 2 NIS 8 AT LVFS STN 7
2100Z 25 25.5S 07 58.6E 1/05/74

BOTTOM DEPTH =		M		
DEPTH	TEMPERATURE P.	SALINITY (O/CO)	SI O2 (MICROMCLES/KG)	PC4
19				
62	19.21	19.21	35.727	
72				
115	16.50		35.563	
125				
173	15.07	15.07	35.342	
182				
279	12.61	12.61	35.113	
288				
365				
375	10.44	10.45	35.047	

CHAIN 115 LEG 2 HS1335 AT LVFS STN 8
1604Z 33 20.35 17 38.6E 1/09/74

DEPTH	BOTTOM DEPTH = M			
	TEMPERATURE P.	TEMPERATURE U.	SALINITY (O/CO)	SI O2 (MICROMOLES/KG)
0	16.50		35.049	0.1 323. 0.16
5			35.052	0.1 323. 0.14
10			35.030	0.1 322. 0.16
20			35.167	5.0 211. 0.89
29	13.46	13.48	35.160	7.6 190. 1.07
49		12.01	33.565	8.1 190. 1.17
74	10.53	10.52	34.865	9.5 198. 1.35
98		10.25	34.854	9.6 195. 1.35
118	9.12	9.11	34.724	14.6 175. 1.65
137		8.87	34.700	15.2 179. 1.72
157	8.58	8.53	34.672	19.7 159. 1.96
176		8.40	34.656	22.6 152. 2.06
196		8.32	34.650	21.4 159. 2.02
211		8.26	34.642	22.0 159. 2.01
221	8.31	8.30	34.656	22.0 160. 0.00

CHAIN 115 LEG 2 NIS 9 AT LVFS STN 8
1420Z 33 20.35 17 38.6E 1/09/74

DEPTH	BOTTOM DEPTH = M			
	TEMPERATURE P.	TEMPERATURE U.	SALINITY (O/CO)	SI O2 (MICROMOLES/KG)
19			35.016	0.1 0.13
28	14.87	14.83	35.023	0.1 0.14
47			35.148	7.0 0.97
56	12.74	13.02	35.094	8.0 1.10
94			34.854	9.5 1.35
104	10.07	10.23	34.821	9.5 1.34
141			34.669	19.4 1.93
151	8.52	8.52	34.680	23.0 2.10
198			34.651	23.0 2.07
207	8.42	8.42	34.653	23.0 2.01

CHAIN 115 LEG 2 HS1330 DEEP CAST # 1
2207Z 22 30.05 12 08.4E 12/30/73

BOTTOM DEPTH = P

DEPTH	TEMPERATURE P.	SALINITY (C/CO)	SI (MICROMOLES/KG)	O2 (MICROMOLES/KG)	PC4
-------	-------------------	--------------------	-----------------------	-----------------------	-----

670	4.83	34.521	29.8		
867	3.95	34.524	36.8		
1079	3.52	34.607	40.8		
1262	3.40	34.738	40.7		
1447	3.35	34.914	37.7		
1634	3.43	34.891	34.0		
1832		34.997	33.6		
2035	3.14	35.006	34.1		
2206	3.00	35.028	35.4		
2265	2.97	35.000	35.3		
2275		0.000	35.5		
2326	2.85	34.899	35.9		
2336		0.000	36.1		
2361	2.90	34.931	36.1		
2371		34.821	36.8		
2386					
2429					

CHAIN 115 LEG 2 NIS 6 DEEP CAST # 2
2100Z 24 04.2S 12 39.9E 1/01/74

BOTTOM DEPTH = P

DEPTH	TEMPERATURE P.	SALINITY (C/CO)	SI (MICROMOLES/KG)	O2 (MICROMOLES/KG)	PC4
-------	-------------------	--------------------	-----------------------	-----------------------	-----

1954	3.09	35.035			
1965		34.915			
2025	3.02	34.908			
2035		34.975			
2061	3.02	34.931			
2071		34.934			
2086					

CHAIN 115 LEG 2 HS1333 DEEP CAST # 4
 1100Z 25 03.85 07 50.3E 1/05/73

BOTTOM DEPTH = M

DEPTH	TEMPERATURE P.	SALINITY (O/CO) U.	SI (MICROMOLES/KG)	O2 (MICROMOLES/KG)	PC4
3459	2.41	34.865	56.0		
3636	2.23	34.852	55.2		
3814	1.95	34.855	65.5		
3991	1.57	34.785	80.1		
4169	1.28	34.794	89.6		
4347	1.16	34.775	93.9		
4515	1.14	34.760	96.4		
4524		34.736	96.4		
4604	1.14	34.764	96.4		
4613					
4649	1.05	34.765	96.4		
4657		34.745	97.3		
4680	1.14	34.761	96.4		
4688		34.782	97.3		
4702					

CHAIN 115 LEG 2 HS1332 DEEP CAST # 3
 1600Z 25 12.7S 10 00.0E 1/03/74

BOTTOM DEPTH = M

DEPTH	TEMPERATURE P.	SALINITY (O/CO) U.	SI (MICROMOLES/KG)	O2 (MICROMOLES/KG)	PC4
3219	2.41	34.891	47.5		
3413	2.32	34.892	50.5		
3608	2.23	34.901	54.6		
3802	1.98	34.917	63.0		
3996	1.61	34.821	76.7		
4181	1.31	34.852	88.0		
4191		34.825	88.9		
4278	1.17	34.808	92.3		
4288		34.772	94.0		
4327	1.16	34.773	95.8		
4337		34.782	94.2		
4361		34.882	94.9		
4371		34.754	95.8		

BIOGRAPHICAL NOTE

The author was born on April 15, 1949, in Ottawa, Canada. He has lived in Washington, D.C., Sri Lanka, and Vancouver, B.C. and graduated from St. Georges School in June 1967. In September 1967, he entered the University of British Columbia, Vancouver, B.C., where he received a B.Sc. degree in chemistry (honors) in May 1971. In September 1971 he entered the Massachusetts Institute of Technology and Woods Hole Oceanographic Institution Joint Program in Oceanography as a candidate for the degree of Doctor of Science.

On December 30, 1976 he was married to Inez Fung.

Publications

Bishop J.K.B., W.R. Cullin, and M.C.L. Gerry (1971), ^{35}Cl Nuclear Quadrupole Resonance of some Phosphorus Chlorine Compounds, Canadian Journal of Chemistry, 49, 3910-3913.

Bishop J.K.B. and J.M. Edmond (1976), A New Large Volume in situ Filtration System for the sampling of Oceanic Particulate Matter, Journal of Marine Research, 34, 181 - 198.

Accepted for publication:

Bishop J.K.B., J.M. Edmond, D.R. Ketten, M.P. Bacon, and W.B. Silker, The Chemistry, Biology, and Vertical Flux of Particulate Matter from the upper 400 m of the equatorial Atlantic Ocean, Deep-Sea Research (in press).